c.1

DYNAMICS OF A LARGE CLASS OF SATELLITES WITH DEPLOYING FLEXIBLE APPENDAGES

by

KENNETH WAYNE LIPS

B.A.Sc. University of Toronto; Toronto, Canada 1967
M.A.Sc. University of Toronto (Institute for Aerospace Studies); Toronto, Canada 1971

A THESIS SUBMITTED IN PARTIAL FULFILLMENT OF
THE REQUIREMENTS FOR THE DEGREE OF

DOCTOR OF PHILOSOPHY

in

THE FACULTY OF GRADUATE STUDIES
(Department of Mechanical Engineering)

We accept this thesis as conforming to the required standard

THE UNIVERSITY OF BRITISH COLUMBIA
August 1980

In presenting this thesis in partial fulfilment of the requirements for an advanced degree at the University of British Columbia, I agree that the Library shall make it freely available for reference and study. I further agree that permission for extensive copying of this thesis for scholarly purposes may be granted by the Head of my Department or by his representatives. It is understood that copying or publication of this thesis for financial gain shall not be allowed without my written permission.

Kenneth Wayne Lips

Department of Mechanical Engineering

The University of British Columbia
2075 Wesbrook Place
Vancouver, Canada
V6T 1W5

Date September 4, 1980

ABSTRACT

A general formulation is presented for the librational dynamics of satellites having an arbitrary number, type, and orientation of flexible appendages, each capable of deploying independently. In particular, the case of beam-type appendages deploying from a satellite in an arbitrary orbit is considered. The governing nonlinear, nonautonomous, coupled system equations are not amenable to any closed form solution, hence are integrated numerically using a digital computer. Effect of important system parameters is assessed through illustrative configurations representing a large class of gravity gradient and spinning spacecraft. Rather than accumulation of a large amount of data, the emphasis is on evolution of a generalized and organized methodology for coping with such complex dynamical systems.

The analysis examines the degree of interaction between flexibility, deployment, and attitude motion through systematic variation of system parameters. A study of appendage vibration characteristics suggest that an orbiting beam cannot be treated simply as a rotating beam because of the presence of the gravitational field. Rate of rotation plays a dominant role in stiffening the beam as evidenced by the noticeable straightening of the eigenfunctions for even relatively low spin rates (2 rpm). Results also show that the deployment-related Coriolis force can play a major role in causing large in-plane deformations. This implies that, in some cases, deployment should be carried out in stages so as to limit the time available to build up large amplitude oscillations.

Investigation of librational response shows that the coupled character of the motion can significantly affect system dynamics, hence caution should be exercised in utilizing results based on simplified planar analyses. Depending on orbital parameters and physical properties of booms, there are critical values of appendage length and deployment rate for which the satellite can tumble over. On the other hand, in general, appendage offset and shifting center of mass were found to have insignificant effect on response for the cases considered. This may permit considerable simplification of the complex hybrid equations with associated saving in computational time and effort. Also, the small amplitude oscillations evident both with the gravity gradient and spin-stabilized configurations tends to substantiate the adoption of a linear vibration analysis. The simulation of such diverse classes of satellites with relative ease demonstrates the versatility of the formulation.

TABLE OF CONTENTS

Chapter Page

Appendix Page

III (continued)

LIST OF TABLES

LIST OF FIGURES

Figure Page

ACKNOWLEDGEMENT

The patience, guidance, and continued support provided by Dr. V.J. Modi have made this thesis possible.

A very special note of appreciation is also extended to Susann and our children (Vanessa, Hypatia, Ursula and Dartanion) for their cooperation and understanding.

For her expert typing of the final manuscript a note of thanks is offered to Maureen Skuce.

The investigation reported here was funded from the Natural Sciences and Engineering Research Council of Canada, Grant No. 67-2181.

LIST OF SYMBOLS

$A(x)$	area of beam cross section, $\int\int dy\, dz$
$\underline{A}_{O,i}$	acceleration of mass element dm_i due to vibration and deployment, $\frac{\partial \underline{V}_{O,i}}{\partial t} + (\underline{V}_i \cdot \nabla)\underline{V}_{O,i}$
$[B_j]$	modal integral coefficients as defined in Appendix VI.
$[B_{j,E}]$, $[B_{j,H}]$	modal integral coefficients found using admissible functions $E_n(\hat{x})$, $H_n(\hat{x})$ respectively; see section 4.2
$c(\ )$, $s(\ )$	cosine ( ), sine ( ), respectively
c_{jk}	coefficient identifying appendage orientation relative to the local vertical $\underline{R}_c$, equation (3.18)
cm	spacecraft center of mass, Figures 2-1 and 2-2
$\{C_j\}$	modal integral coefficients as defined in Appendix VI
$\{C_{j,E}\}$, $\{C_{j,H}\}$	modal integral coefficients found using admissible functions $E_n(x)$, $H_n(x)$, respectively; see section 4.2
CPU	a unit of computer time, Central Processing Unit
$\underline{d}_i$	vector locating dm_i for the undeformed appendage and measured with respect to O_i $(\underline{d}_i^a + \underline{d}_i^b)$; Figure 2-2
$\underline{d}_i^a$	vector $\underline{d}_i$ prior to deployment
$\underline{d}_i^b$	net change in $\underline{d}_i$ resulting from deployment
dD_i	infinitesimal element of spatial domain of i^{th} appendage, Figure 2-2
dm_i	elemental mass of i^{th} appendage, Figure 2-2
ds	elemental length as measured along neutral axis of the beam, Figure 3-1

dx_i	elemental length as measured along x_i direction
D_i	spatial domain of i^{th} appendage ($D_0 \equiv$ central rigid body)
e	orbital eccentricity
e_1	a function of e and θ defined for convenience in equation (4.3c)
$\underline{e}_{c,i}$	elastic displacement of dm_i relative to O_c, $u_{c,i}\ \underline{i}_i + v_{c,i}\ \underline{j}_i + w_{c,i}\ \underline{k}_i$; equation (2.5)
$\underline{e}_i$	elastic displacement of dm_i relative to O_0, $u_i\ \underline{i}_i + v_i\ \underline{j}_i + w_i\ \underline{k}_i$; see Figure 2-2 and equation (2.2a)
E_i	Young's modulus of elasticity, i^{th} appendage
{f}	effective load acting in transverse 'y' direction for beam-type appendage undergoing pitch librations only, equations (4.10c)
f(s)	an arbitrary function of s
$\{f_j\}$	effective load acting in the j direction for beam-type appendage undergoing general libration, equations (4.5c)
F_A	an effective axial load resulting from the inertial and gravitational force fields, equation (3.21d)
$g_n(\hat{x})$	n^{th} normal mode of a simple uniform cantilever beam, equation (4.7)
G	universal gravitation constant
{h}	local angular momentum resulting from vibration and deployment relative to O_c, equation (2.13a)
$\{h_s\}$	a constant (stored) contribution to the local angular momentum
h_θ	orbital angular momentum, equation (2.1a)
{H}	angular momentum associated with motion of the spacecraft relative to the instantaneous center of mass, equation (2.11)
H.O.T.	higher order terms
$\underline{i}$, $\underline{j}$, $\underline{k}$	unit vectors along the x, y, z axes respectively

$[I]$	overall system mass moments of inertia with respect to x, y, z axes, $[_uI]$, $[_eI] + [_{cm}I]$, equation (II.7)
$[_1I]$	contribution of rigid central 'core' body of the spacecraft to [I]
$[_2I]$	contribution to [I] resulting solely from the geometric offset of the undeformed appendage, equation (II.4a)
$[_3I]$	contribution of the undeformed appendage to [I] with $\underline{\sigma} = 0$, equations (II.3) and (II.4b)
$[_{cm}I]$	change in system mass moments of inertia due to a shift in location of satellite center of mass, equation (II.7)
$[_eI]$	change in system mass moments of inertia associated with flexibility, equations (II.7) and (II.9)
$[_uI]$	total contribution of the undeformed system to [I], $[_1I] + [_2I] + [_3I]$, equation (II.7)
$J_{jk,i}$	area moment of inertia for the i^{th} beam with respect to the local j, k axes
k_n	constant of proportionality relating the n^{th} eigenvalue to the spin parameter, equation (4.11)
$[K]$	stiffnes matrix associated with transverse vibrations of an arbiting, deploying, spinning, beam-type appendage, equation (4.10c)
$[K_j]$	stiffness matrix associated with vibration in the local j direction for a beam-type appendage under-doing general libration, equations (4.5c)
$\ell(t)$	instantaneous appendage length
ℓ_Δ	effective appendage length measured along the local x_i direction with foreshortening accounted for
ℓ_i^a	initial beam length prior to deployment
ℓ_i^b	net change in beam length as a result of deployment
L	fully deployed length
m_i	mass of i^{th} appendage

m_s — total mass of the satellite, $\sum_i m_i$, where i = 0 for the rigid central body

M — mass of attracting body located at focus O_I of the orbit

N — total number of second order equations governing system dynamics

O_c — instantaneous center of mass, Figures 2-1 and 2-2

O_i — point at which the i^{th} appendage is attached to the central body, Figure 2-2

O_I — center of force of the orbit

O_0 — center of mass of undeformed spacecraft

q, q_k — k^{th} generalized coordinate

Q_k — generalized force associated with k^{th} degree of freedom

$Q_{g,k}$ — generalized force resulting from the gravitational field and associated with the k^{th} degree of freedom

$\underline{r}_c$ — vector locating the instantaneous center of mass O_c with respect to the center of mass O_0 of the undeformed body, Figure 2-2

$\underline{r}_{d,i}$ — vector locating dm_i relative to O_c, Figure 2-2

$[\tilde{r}_{d,i}]$ — skew symmetric matrix constructed from vector $\underline{r}_{d,i}$,

$$\begin{bmatrix} 0 & -z_{d,i} & y_{d,i} \\ z_{d,i} & 0 & -x_{d,i} \\ -y_{d,i} & x_{d,i} & 0 \end{bmatrix}$$

$\underline{r}_i$ — vector locating dm_i of the undeformed appendage relative to O_0, see section 2.2.2

rpm — revolutions per minute

$\underline{R}_c$ — vector locating O_c relative to inertial reference X, Y, Z; Figures 2-1 and 2-2

$\underline{R}_{d,i}$	vector locating dm_i of the deformed spacecraft relative to inertial reference X, Y, Z; see equations (2.5) and Figure 2-2.
s	location of dm_i as measured along the neutral axis of the beam
SYSTM	subroutine used to define the first order state vector derivatives as derived from the second order system equations
t	'real' time
t_1, t_2	two different instants in time
tr[ ]	trace of matrix [ ]
u_i, v_i, w_i	elastic displacement of the mass element dm_i measured along the x_i, y_i, z_i directions, respectively, Figure 2-2
$u_{fs,i}$	shortening of the i^{th} appendage along the axial (x_i) direction due to transverse oscillations, equation (3.4)
U_i	deployment velocity in the x_i direction, Figure 2-2
V_i	general deployment velocity of dm_i relative to O_i
$V_{O,i}$	velocity of dm_i with respect to O_c due to vibration and deployment, equations (2.5)
x, y, z	body-fixed coordinate system with origin at O_c, Figures 2-1 and 2-2
x', y', z' x", y", z"	intermediate location of x,y,z axes undergoing a set of modified Eulerian rotations, Figure 2-1(b)
x_i, y_i, z_i	local appendage coordinate system with origin at O_i, Figure 2-2
x_0, y_0, z_0	body-fixed coordinate system with origin at O_0, Figure 2-2
X, Y, Z	inertial coordinate system with origin at focus O_I, Figures 2-1 and 2-2

X_O, Y_O, Z_O	orbiting reference frame with origin at O_c, X_O along local vertical, Y_O tangent to the orbit, and Z_O parallel to the orbit normal.
$E_n(x_i)$	n^{th} assumed admissible function associated with the v_i degree of freedom, equation (4.4)
F_j	external force applied to the beam along the j direction
$\mathcal{F}_\epsilon$	generalized force associated with the generalized coordinate ϵ
$H_n(x_i)$	n^{th} assumed admissible function associated with the w_i degree of freedom, equation (4.4)
$L, \mathcal{L}$	Lagrangian, $T-V$; equations (2.8), (3.20) and (V.2)
Q_n	coefficients as defined in equations (4.7)
$T, \mathcal{T}$	total system kinetic energy
T_i	kinetic energy of i^{th} appendage only
$V, \mathcal{V}$	total system potential energy
V_e	elastic potential energy, equations (2.6), (3.9), and (3.13)
V_g	gravitational potential, equations (2.6) and (3.16)
$\mathcal{W}$	generalized work function which can include nonconservative forces, equation (V.1)
α	dummy variable commonly used as a variable of integration
α_j	coefficients defined by equation (3.17)
β_n	frequency parameter for the n^{th} eigenfunction, $\rho\omega_n^2\ell^4/EJ$
$\beta_{n,IP}, \beta_{n,OP}$	frequency parameter associated with the 'v' and 'w' beam vibrations, respectively, equation (4.12)
γ_j	coefficients defined by equations (4.1c)
$\{\Gamma\}$	torque due to vibration and deployment relative to the center of mass, equation (2.13b)

$\delta( )$	variation of ( )
δ_{mn}	delta function $\int_0^1 g_m\, g_n\, d\hat{x}$, equation (4.7)
Δ	total foreshortening effect experienced by the beam, see p. 49
$\varepsilon, \boldsymbol{\epsilon}$	generalized coordinate representing continuous variables, i.e., $\boldsymbol{\epsilon} = u(x,t)$, $v(x,t)$, or $w(x,t)$; equation (2.8), (3.21) and (V.3)
$\varepsilon_{n,real}$	n^{th} real eigenfunction, Figure 4-7
$[\varepsilon_{s,i}]$	strain tensor of i^{th} appendage
ζ_n^i	generalized coordinate in the n^{th} mode for the 'v' degree of freedom of the i^{th} appendage, equation (4.4)
η	variable defined in equation (3.5), $x + u_{fs}$
θ	true anomaly of the orbit, Figure 2-1(a)
λ_a	dimensionless deployment acceleration parameter, $\rho\hat{\ell}\ell^4/EJ$
λ_r	dimensionless deployment rate parameter, $\rho\dot{\hat{\ell}}^2\ell^4/EJ$
λ_s	spin parameter, $\rho\omega_s^2\ell^4/EJ$
μ	gravitational constant, GM
μ_j	term appearing in the linear partial differential equations governing vibration along the j direction, equations (4.1c)
ξ_n^i	generalized coordinate in n^{th} mode for the 'v' degree of freedom of the i^{th} appendage, equation (4.4)
Ξ	that contribution to the system Lagrangian associated with the undeformed configuration only, equations (2.8) and (2.9)
$\underline{\pi}_i$	net offset of O_i from O_c, $(\underline{\sigma}_i - \underline{r}_c)$, Figure 2-2
$\rho_i(x_i)$	linear mass density for the i^{th} appendage

Σ	summation
σ^*	generalized stress tensor
$\underline{\sigma}_i$	geometric offset of O_i and O_0, Figure 2-2
T	that contribution to the system Lagrangian associated with system flexibility, equations (2.8) and (2.9)
$\{\chi_a\}$	matrix of direction cosines between $\underline{R}_c$ and x,y,z; equation (2.7)
$\{\chi_i\}$	matrix of direction cosines between x,y,z and x_i,y_i,z_i; equation (2.2c)
ψ_i,λ_i,ϕ_i	modified Eulerian rotations from x,y,z to x_i,y_i,z_i establishing appendage orientation
Ψ,Λ,Φ	modified Eulerian rotations defining librational motion of the body-fixed x,y,z axes relative to the orbiting reference X_O,Y_O,Z_O; Figure 2-1(b)
$\underline{\omega}$	inertial angular velocity of x,y,z axes; equations (2.5)
ω_s	effective spin rate as given in equations (4.10c)
Ω_n	natural frequency of the n^{th} eigenfunction
$\hat{\Omega}_n$	dimensionless frequency, $\Omega_n/\dot{\theta}$, equations (4.10c)
$\circ$	scalar product
$(\dot{})$, $(\,)'$	$d(\,)/dt$, $d(\,)/d\theta$
$(\,)_\alpha$	$\partial(\,)/\partial\alpha$
$(\,)^{(i)}$	$(\,)$ expressed in terms of local coordinates, x_i,y_i,z_i; see p. 32
$(\,)^{(0)}$	$(\,)$ expressed in terms of central coordinates x,y,z; see p. 32
$(\hat{})$	$(\,)$ nondimensionalized such that $(\hat{}) = (\,)/\ell$, except for $\hat{\Omega}_n = \Omega_n/\dot{\theta}$ and $\hat{\ell}' = \ell'/\ell$, $\ell'' = \ell''/\ell$; whereas $\hat{\pi}' = (\pi/\ell)'$, etc.

$(\tilde{})$	( )density, e.g. $\tilde{L}$ = Lagrangian density
{ }	column matrix
[ ]	square matrix
$[\tilde{}]$	skew symmetric matrix, see $[\tilde{r}_{d,i}]$ for example
$\{\ \}^T$, $[\ ]^T$	matrix transposed

Note that all symbols remain as described here unless specifically defined otherwise in the text. i,j,k are dummy indices with i being used exclusively to denote the i^{th} appendage and j,k generally identify vector/tensor components or reference axes (as referred to below). Also m,n identify the m^{th}, n^{th} assumed-mode. For clarity x,y,z are commonly replaced by subscripts 1,2,3 respectively. Finally, aside from 'rpm', MKS units and symbols are used throughout in the presentation of results.

1. INTRODUCTION

1.1 Preliminary Remarks

The study of satellite motion assumed practical importance with the launching of the Soviet Union's Sputnik I in October of 1957. A key component in this study is the angular rotation experienced with respect to an orbiting center of mass. Of course, it is the prediction and control of a spacecraft's orientation which ultimately determines its usefulness.

As a result of the relatively simple geometry of the early satellites, preliminary investigations of attitude behaviour were carried out using a rigid, single-body representation. In many instances this turned out to be a sufficiently accurate model. However, some of the satellites were neither entirely rigid nor could they be represented as a single body; for example, Explorer I had four flexible antennae radiating out from the main body. As the number and complexity of tasks grew, so too did the complexity of a spacecraft's configuration.

A general definition of a contemporary satellite would be: "any collection of orbiting, arbitrarily-shaped, interconnected bodies." Embedded in this concept are a number of characteristics rendering the process of mathematical modelling quite difficult. Overall, satellite configurations can assume quite irregular forms since they are not constrained by the aerodynamics to the same degree as an aircraft or a missile. Each spacecraft mission and

hence each configuration tends to be unique making it difficult to evolve a general analysis. The extent of flexibility may vary thus making the system a hybrid construction of the classical fully-rigid and fully-elastic parts. Considerable relative motion between components can occur as a result of articulation, deployment or vibration. Consequently, time-dependent inertias as well as a shifting center of mass are introduced, thus compounding the problem considerably.

Flexibility is a design choice dictated in part by a dichotomy of extremes in the force environment: very high accelerations during delivery to orbit followed by very low accelerations during most, if not all, of the operational life. Often structures having large dimensions are required to carry out experiments, provide stabilization, and generate power. However, configuration size and weight can be severely constrained as a result of launch vehicle limitations or structural strength of the satellite components. As a solution spacecraft are initially packaged as compact rigid bodies. Once in orbit various elements deploy to establish the desired configuration. Deployment, in many instances, accompanies the attitude acquisition phase during which large angle manoeuvres take place. An additional complication is contributed by the presence of such environmental forces as solar radiation pressure, the earth's magnetic field, free molecular forces, etc., capable of exciting elastic degrees of freedom.

The fact that flexibility is an important factor not to be overlooked was demonstrated quite convincingly by two incidents. Explorer I (1958) was initially spinning about the axis of minimum

moment of inertia. Four antennae located normal to the spin axis allowed for energy dissipation via dynamic coupling between precessional and vibrational degrees of freedom. The end result was a tumbling about the axis of maximum moment of inertia in a state of minimum kinetic energy - a result not previously recognized by classical rigid body stability theory. Canada's first satellite, Allouette I (1962), a spin-stabilized system with four booms up to about 23 m in length lying in the spin plane, experienced a premature decay in spin rate. Subsequent analysis suggested that a solar-thermal induced asymmetry in boom shape resulted in a net opposing moment from the radiation pressure. Thus, what was initially considered to be anomalous behaviour was attributed, by post-flight analysis, directly to flexibility effects. In this context it is relevant to mention the Orbiting Geophysical Observatory (OGO III), one of the more elaborate collections of rigid and elastic bodies. Launched in 1966, it demonstrated that interaction between control torques and elastic deformations could result in attitude instability.

With an increasing use of flexible appendages, the problem grows more critical as stationkeeping and pointing requirements become stringent. For example, the joint Canada/U.S.A. Communications Technology Satellite (CTS/Hermes) launched in 1976 carries two solar panels measuring 1.1 m by 7.3 m each to generate 1.2 kW. The 'Galileo', scheduled for launch in 1982, has articulated members with both spinning and nonspinning sections making up the main body. Attached to the spinning part are flexible booms up to 11 m long. In addition, wide variations are expected to occur

in the inertia properties over the life of the mission due to a relatively large ratio of propellant-to-spacecraft mass. Elastic members used in the construction of any future Solar Power Satellites (SPS) would have dimensions measurable in kilometers. With the advent of the Space Shuttle, tether-supported satellite systems extending to 100 km are anticipated.

As has been implied, predicting satellite attitude motion is by no means a simple proposition, even if the system is rigid. The time-bound character of most projects restricts attention to a given configuration with dynamic simulation confined to phases considered most important. It is therefore understandable why the majority of published papers discuss only steady state motion in the small. Transient behaviour associated with the critical phase of attitude acquisition and/or deployment related manoeuvres has been largely ignored. It should be mentioned that deployment effects, although of a transient nature, may be felt over a long period of time as a result of relatively small extension rates which can be associated with long appendages.* In addition, deployment affects the force field acting on the flexible members, thus influencing elastic response, structural integrity, and the libration itself.

As can be expected, the dynamics is strongly configuration dependent. Few investigations have been reported which apply to more than one type of spacecraft. As a rule the more general the formulation in terms of configuration the less developed is the

---

* For example, extension of a 200 m boom typically requires 2000 s.

analysis. Ultimately a specific case is chosen with its attendant simplifications.

An attempt is made in this thesis to demonstrate the use of a systematic methodology for dealing with complex orbiting dynamical systems. This is achieved by formulating and solving the equations of motion applicable to a large class of spacecraft configurations.

1.2 Literature Review

1.2.1 Background

Over the years the accumulated literature pertaining to the various aspects of satellite system response, stability, and control has indeed become enormous. Hence to review this literature in depth would present one with a formidable task not to mention the space required. Furthermore, several excellent review papers have been written covering specific areas of the subject [Noll et al. (1969),[1] Shrivastava et al. (1969),[2] Likins (1970, 1974, 1976, 1977),[3,4,5,6] Likins and Bouvier (1971),[7] Modi (1974),[8] Williams (1976),[9] Garg et al. (1978),[10] Stuhlinger (1979),[11] Roberson (1979)[12]]. Therefore, the objective here is to trace the general evolution of the subject, problems faced in modelling and analysis, achievements and shortcomings, and more importantly, to indicate the role of the present contribution within the overall scheme of progress to date. Only the more important contributions directly relevant to the thesis subject in hand are recorded here.

General spacecraft motion consists of: (i) translation of the center of mass (orbital), (ii) rotation with respect to the center of mass (librational), and (iii) relative motions between the constituent parts (e.g. vibration, deployment, fuel movement, etc.). To first order, the effect of libration and elastic deformation on orbital motion is negligible [Moran (1961),[13] Yu (1964),[14] Misra and Modi (1977)[15]]. Consequently, an a priori solution exists for the trajectory as represented by the classical Kepler relations.

According to Roberson (1979),[12] the first published paper devoted to attitude motion of an artificial earth satellite is by Klemperer and Baker (1956).[16] It discussed the planar motion of a rigid dumbbell configuration moving in a circular orbit. Following this, the model of a single rigid body travelling along a circular path was adopted for much of the early work [e.g. De Bra and Delp (1961)[17]]. Primarily, configurations were taken to be either symmetric (1963, 1964, 1962, 1966),[18-21] axisymmetric (1966),[22] or asymmetric (1965, 1963).[23,24] The libration itself was assumed to be coupled, linear (1961, 1965);[17,23] planar, nonlinear (1969);[25] etc. The various environmental influences considered (solar, magnetic, aerodynamic, gravitational, etc.) are discussed in reports such as those of Evans (1964),[26] Singer (1964),[27] and Roberson (1964).[28] In general, the effect of the earth's oblateness on attitude dynamics was found to be negligible. The literature suggests that even for the simplest of spacecraft, as represented by a single rigid body, the number of parameters involved in the problem is sufficiently large that analysts deal with a specific set of satellite parameters only. A welcome exception was the work of Beletskii (1965)[29] in which an axisymmetric body in an eccentric orbit is subjected to a variety of external torques.

The importance of configuration as a variable in the analysis increases with the use of multibody systems. One of the simpler concepts involves a relative motion within a main rigid body creating an 'effective' internal stiffness and/or damping. A planar case was examined by Brereton (1967)[30] and Tschann (1970).[31] Considered too were dampers with: (a) one degree of freedom parallel to the spin axis, i.e. a nutation damper [Kane and Levinson (1976)[32]]; (b) two degrees of freedom normal to the spin axis, i.e. a precession damper [Cloutier (1976)[33]]. Cochran et al. (1980)[34] compared the performance of nutation versus precession dampers for both axisymmetric and asymmetric satellites. Dampers have been applied to the dual spin concept as well by Vigneron (1971).[35] For control purposes two single-degree-of-freedom gyros were operated in a 'roll-vee' mode by Morrison (1969);[25] on the other hand, a single two-degree-of-freedom gyro was studied by Kane and Athel (1972).[36]

Frequently encountered in the literature are spacecraft made up of connected rigid masses. Both planar [Paul (1963)[37]] and coupled [Pringle (1968)[38]] librational behaviour has been studied for an orbiting dumbbell. Crist and Eisley (1969)[39] have presented linear as well as some nonlinear analysis for two spinning systems: (i) a flexible dumbbell; (ii) a small mass spring-connected to a large mass. Connell (1969)[40] sought to optimize pointing accuracy and attitude stability using a hinged two-body system. Also, considerable attention has been directed towards the analysis of cable-connected two-body systems. For example, Chobotov (1963)[41] and Bainum and Evans (1976)[42] have examined potential excitation of such a system by the gravity gradient. Tai and Loh (1965)[43] and

Stabekis and Bainum (1970)[44] dealt with planar response while Bainum and Evans (1975)[45] evaluated the use of a multiple cable design. The model of Modi and Sharma (1977)[47] allowed for both string-type as well as beam-type connection. Finally, Austin and Zetkov (1974)[48] have discussed simulations for a class of flexible two-body satellites.

A more general configuration is the articulated type, i.e. to the main body(ies) are appended secondary smaller bodies. Etkin (1962)[49] and Maeda (1963)[50] presented the linearized uncoupled equations together with some preliminary response data for a gravity-stabilized configuration in which a number of rods are symmetrically pinned to a central body with both stiffness and damping present at the joints. Hughes (1966)[51] added tip masses to the rods of this configuration and optimized both transient and steady state pointing performance with respect to system parameters. At synchronous altitude maximum pointing errors of the order of two degrees and damping times less than one orbit are achieved. Lips (1967)[52] derived the linearized planar equations for a similar system but augmented the gravity gradient effect by attaching the tip masses to the rods by means of long 'massless' strings. Later, the effectiveness of a number of different rod-string-tip-mass combinations in providing gravity gradient stabilization was investigated by Garg (1969).[53] Another series of complex configurations is typified by the gravity-stabilized Radio Astronomy Explorer (RAE) satellite studied by Dow et al. (1966).[54] In this case four long (228 m), flexible, deployable booms lie in the orbital plane and a set of rigid damper booms are skewed with respect to the orbital plane. The spin-stabilized Alouette I and II had four (11 m to 36 m) booms

attached to a central rigid body. Described by Charyk (1977)[56] is a series of communications satellites which have as appendages: antennae booms, antennae dishes, and/or solar panels. Janssens (1976)[57] discusses the dynamics of a spinning rigid body to which are attached appendages which act as spherical pendulums. Finally, it should be mentioned that the SPS of Glaser (1976) [58] could bring into question the role of the appendage as a secondary body.

In addition to rigid or hybrid rigid/elastic forms which a satellite might assume, there is also the prospect of a fully elastic system. Ashley (1967),[59] Modi and Brereton (1968),[60] Bainum et al. (1978, 1980)[61,62] have studied the dynamics of a beam-type satellite. Also Breakwell and Andeen (1977)[63] dealt with a chain of beads to be used for communications, while Chobotov (1977)[64] proposed a chain of solar arrays aligned along the local vertical as a method of collecting solar energy.

The introduction of flexibility into the design has proven to be a major source of complication. With respect to libration it acts as a dissipative feedback mechanism interacting with the control system and environmental forces. Provided structural integrity is maintained, large amplitude (or even unstable) vibrations are of concern only to the degree that they affect the librational behaviour.* Consequently, flexibility need be included in the analysis only if it is expected to interfere with the attitude motion. However, it is important to emphasize that a priori knowlege of flexibility effects is, in general, not available.

---

* Unless the flexible member must also satisfy some other design criteria, e.g., support a magnetometer.

Neglect of flexibility has produced a host of surprising dynamical behaviour, some of which was identified earlier. Among the first to review flexibility effects based on post-flight analysis were Noll et al. (1969).[1] Interaction problems are shown to manifest themselves as transient phenomena, limit cycle oscillations, or instabilities. Such unforeseen occurences are attributed to deficiencies in the structural dynamics analysis and/or knowledge of the flight environment. Similar findings are expressed by a NASA document (1969)[65] and by Likins and Bouvier (1971).[7] The survey was updated by Likins (1976, 1977)[5,6] who reported some successes as well as failures in treating flexible systems. Modi (1974)[8] offers a comprehensive state of the art assessment of efforts made in dealing with both the librational response and the appendage dynamics itself. Particularly helpful is the attempt to unify the problem by simultaneously bringing together different aspects of control system, structural, and librational dynamics.

1.2.2 Equations of motion

In general, time and effort involved in the derivation of governing equations of motion can be enormous hence, one seriously inquires about the most efficient procedure available. The fundamental choices range from D'Alembert's Principle and the Newton-Euler vector approach to the use of the Gibb's function[66] and the Hamilton-Lagrange variational model.[67] The issue will be reviewed only briefly here since it has been debated extensively in the literature by Russell (1969, 1976),[68,69] Hooker (1970),[70] Stichin et al. (1970, 1975),[74,75] Anand and Whisnant (1971),[73] Ho (1974, 1977),[74,75] Likins (1974, 1975),[4,76] Williams (1976),[9] McDonough

(1976),[77] Jerkovsky (1978),[78] and others. The most common objection raised regarding the Newton-Euler application is the need to include constraint forces even when they are not specifically sought. This difficulty is eliminated with the Lagrangian procedure but here the kinetic energy expression can become unwieldy to derive and even more so to differentiate, as indicated by Russell (1976)[69] and Lips (1978).[79] Overall, no one approach appears to be superior in all respects. Likins (1975),[76] for example, points out that any apparent advantage in structure of the Lagrange quasicoordinate equations over the Euler equations disappears when the issue is carefully examined. If any trend is discernable at all it is toward acceptance of a result similar to that of Kane et al. (1965, 1968)[80,81] and Jerkovsky (1978)[78] in which the variational application of D'Alembert's principle yields equations similar in forms to those of Newton and Euler. That is, for n rigid bodies having k degrees of freedom the governing equations of motion can be represented by [Likins (1977)[6]]:

$$\sum_{j=1}^{n} \left[(\underline{F}_j - m_j \ddot{\underline{R}}_j) \circ \frac{\partial \dot{\underline{R}}_j}{\partial \dot{q}_i} + (\underline{M}_j - \dot{\underline{H}}_j) \circ \frac{\partial \underline{\omega}_j}{\partial \dot{q}_i} \right] = 0; \; i,\ldots,k \qquad (1.1)$$

where,

$\underline{F}_j$ = force acting on j^{th} body,

$\underline{M}_j$ = moment acting about center of mass of j^{th} body,

$\underline{H}_j$ = angular momentum for the j^{th} body,

m_j = mass of j^{th} body,

$\underline{R}_j$ = inertial position vector,

q_i = i^{th} generalized coordinate,

$\underline{\omega}_j$ = angular velocity vector for the j^{th} body.

Constraints and redundant equations vanish as a result of the summed

dot multiplications. A recent paper by Kane and Levinson (1980)[82] suggests that such an approach involves the least effort. Levinson (1977)[83] has developed a computer program for constructing equations of motion for rigid systems via symbolic manipulation, based on equation (1.1).

The diversity with which the problem is approached is emphasized by the following collection of papers. Meirovitch et al.[84-89] have consistently adopted the variational approach to investigate stability of spacecraft having elastic appendages. A unique set of adiabatic invariants is provided by Mitchell and Lingerfelt (1970)[90] when studying the effects of 'slow' changes in material volume and elasticity. Keat (1970)[91] was among the first to outline a systematic method for deriving nonlinear equations, combining an Euler approach for attitude equations with a Lagrange approach for appendage dynamics. Alternatively, in applying the Lagrange equations, Samin and Willems (1975)[92] used quasicoordinates when dealing with the attitude dynamics while generalized coordinates describe the vibrations. Russell (1976)[69] preferred the use of first order momentum equations. A D'Alembert derivation is implemented by Bodley and Park (1972)[93] who employed projections of momentum as the dynamic variables, a choice first advanced by Vance and Stichin (1970).[71] Exact or 'global' equations of motion for an elastic body are offered by McDonough (1976)[77] as a check against approximate analyses. A number of studies have been carried out which consider the motion of a flexible system to be simply a perturbed form of the rigid body solution [Grote et al. (1971),[94] Huang and Das (1973),[95] Morton et al. (1973),[96] Kraige and Junkins (1976)[97]]. Pringle (1972)[98] has implemented a perturbation formal-

ism via canonical transformations.

Of course, one cannot over-emphasize the importance of choice of reference coordinates in any formulation procedure, as it can have a profound effect in either simplifying or complicating the resultant governing equations. Williams (1976)[9] has recommended a satellite attitude reference frame fixed to the centerbody. Naturally, this may not be useful for spacecraft which are not all-flexible, as pointed out by Veubeke (1976)[99] and Canavin and Likins (1977).[100] Also, an array of variables such as the Euler angles, direction cosines, Euler parameters, quaternions, Cayley-Klein and Euler-Rodriguez parameters can be used to identify vehicle attitude. Recently, many authors such as Davenport (1973),[101] Ohkami (1976),[102] and Nazaroff (1979)[103] have reexamined the general problem of transformation between reference frames in a three dimensional space. Wilkes (1979)[104] derives an expression in which the elements of the transformation are expressed explicitly as functions of any three rotation angles and the corresponding rotation axes. What has become common for spacecraft navigation applications is the use of the Hamilton quaternions because of their relative compactness - four elements versus nine for direction cosines [Garg (1978),[10] Mayo (1979)[105]]. Ickes (1970)[106] integrated the concept of quaternions into a digital attitude control system. Also helpful is the work of Klumpp (1976),[107] Spurrier (1978),[108] Sheppard (1978),[109] and Grubin (1979)[110] in enabling one to efficiently extract a quaternion from a direction cosine matrix.

1.2.3 Appendage dynamics

A critical step in completing the development of the governing equations for a satellite is the dynamical modelling of any flexible elements present. Much of the background to the problem is presented by Modi (1974).[8] Because of its importance, some of the main features and conclusions are discussed here along with a review of the more recent literature. Pioneering contributions to the field may be attributed to Vigneron (1968),[111] Likins (1970),[3] Hughes and Garg (1973),[112] and Meirovitch.[84-89] Basically, elastic members are treated either as a series of interconnected rigid bodies whose dynamics is governed by a set of ordinary differential equations, or as a continuum generating a system of partial differential equations. The continuum set can be 'discretized' in a mathematical sense by means of an assumed-mode solution, thus providing a set of 'distributed' or 'modal' coordinates* governed by ordinary differential equations. Likins (1970)[3] encouraged the adoption of a hybrid system combining the attitude variables describing libration with the distributed coordinates defining flexible behaviour. Depending on the accuracy required, one can truncate the modal series representation appropriately, thus signficantly reducing the number of degrees of freedom while at the same time avoiding troublesome high frequency interactions in the simulation. Truncation is rationalized by Hughes and Garg (1973).[112] More quantitative criteria are prescribed by Russell (1976),[69] and Likins et al. (1976).[113] No truncation is needed if one works in the

---

* Coordinates representing the shape or motion of a continuum at particular instant.

frequency domain as suggested by Kulla (1972),[114] Larsen and Likins (1976),[115] and Poelart (1977);[116] however, this is not possible for a nonlinear system.

Determination of spacecraft vibration characteristics can consume a large proportion of the analysis effort. Ideally the assumed-modes chosen in solving for distributed coordinates would be the exact eigenfunctions. The approach taken by Likins (1970)[3] is to derive modal characteristics based on the assumption of a constant average angular motion. On the other hand, Hughes and Garg (1973)[112] carried out an ambitious and detailed study for flexible solar array characteristics, both 'constrained' (no libration) and 'unconstrained' (libration fully integrated into the vibration equations). Nguyen and Hughes (1976)[117] and Gupta (1976)[118] applied the finite element method to the same end. Structural dynamics associated with the CTS is also studied by Vigneron (1975)[119] who examined 'free' vibration characteristics at one-g (ground level) and zero-g (in-orbit) states, and by Sincarsin (1977)[120] who includes the gravity gradient effect. Hughes and Sharpe (1975)[121] generalized the model somewhat by including a source of internal angular momentum when deriving appendage characteristics. Meirovitch (1974, 1975, 1976)[122,123,124] has presented a general eigenvalue approach for arriving at overall spacecraft modes. In effect, this represents an extension of the normal coordinate method to any hybrid representation which can be modelled as a linear gyroscopic system. The second order system is replaced by a set of first order equations expressed in terms of the state variables. As pointed out by Nelson and Glasgow (1979),[125] one could work with second order eigenrelations. Still another alternative is to construct vehicle

modes by synthesis of the modes of the constituent elements as suggested by Rubin (1975)[126] and Hintz (1975).[127]

One of the more common spacecraft appendages is the boom used in communications and in providing gravitational stability. Because of its long slender nature it can, in general, be modelled as a beam. For this reason the problem of rotating beams is of particular interest and has been studied extensively.[128-135] In particular, Kaza and Kvaternik (1977)[136] have surveyed several methods for linear as well as second degree nonlinear representations of the problem. Independent of this result, Lips and Modi (1977, 1978)[137,138] worked out second degree equations for the more general case of a deploying rotating beam. Nguyen (1978)[139] derived and attempted to solve (not always successfully) the fully nonlinear equations. It is useful to recognize that it is not always necessary to deal with nonlinear equations. If, for example, the nonlinearity is a result of large steady state deformations (as might be the case with high spin rates), the nontrivial equilibrium shape can be established together with linear equations describing oscillations with respect to it [Flatley (1966),[140] Meirovitch et al. (1976),[141] Kisselbach (1976),[142] Hablani et al. (1978)[143]].

A number of authors have focused attention on investigating the dynamics of 'large' flexible spacecraft.[144-146] Canavin and Meirovitch (1979)[147] have pointed out that with an increase in significance of flexibility, its effects can no longer always be considered as simply a perturbation on the rigid body response. Veubeke (1976)[99] has presented a method for dealing with the nonlinear dynamics of completely flexible spacecraft.

As a final point, one should bear in mind that flexible elements in space are susceptible to environmental excitation. Modi (1974)[8] has reviewed most of the significant investigations reported in the literature. In addition, thermal effects on appendage dynamics have been studied by Lorenz (1975),[144] Tsuchiya (1977),[148] Farrell (1977),[149] and Frisch (1980).[150] Also more recently, Kumar (1976),[151] making use of quasi-steady assumptions about elastic response, has assessed thermal and radiation pressure effects on librational stability. Joshi and Kumar (1980)[152] make direct use of solar radiation pressure to offset the effect of orbital eccentricity on attitude performance.

1.2.4 Stability and control of flexible spacecraft

Perhaps a good indicator as to just how important flexibility effects have become is the large body of literature devoted to stability analysis alone for non-rigid satellites. Classical results based on rigid body inertias proved inadequate. Many studies deal specifically with systems having long, flexible, beam-type appendages; for example: Vigneron et al. (1976, 1970),[153-155] Hughes et al. (1971),[156] Dong et al. (1974),[157] etc.[142,158,159] Typically it is found that: (i) the 'major-axis' theorem is a necessary but not a sufficient condition for stability of a flexible system;[156] (ii) necessary conditions for stability can also be derived using such approaches as that of Lyapunov; (iii) assuming the spacecraft to be rigid could lead directly to erroneous results; for example, the effect of elasticity is to destabilize 'crossed-dipole' configurations which are stable when considered to be rigid bodies.[154] How far booms can be extended without

causing attitude instability was discussed by Meirovitch (1974)[160] for spinning systems. Barbera and Likins (1973)[161] and Meirovitch et al.[84-89] have developed stability criteria for a large class of continuum systems using the Lyapunov method. Very general criteria are developed also by Likins (1972)[162] and are applicable to any linear dynamical system including that represented by spacecraft. The Lyapunov technique was put in a state variable format by Smith and Gill (1974).[163] Nonzero products of inertia associated with flexibility were found to assist in stabilizing the dual-spin configuration studied by Tseng and Phillips (1976).[164] During the stability study of a gyrostat having flexible appendages, Calico (1976)[165] found it sufficient to represent each elastic displacement by a single discrete coordinate. Boland et al. (1974)[166] dealt quite generally with stability of a system of interconnected deformable bodies. Although brief, such an outline should convince the reader of the need to include flexibility when carrying out any stability studies.

Even when flexibility does not upset the intrinsic stability of a configuration it can, nonetheless, interefere with the ability to control attitude to the desired degree. Several alternatives exist if one has to deal with unwanted vibrations. The control system can be modified. Also, the elastic behaviour itself may be controlled. Specific examples of interaction between a spacecraft's control system and its structural degrees of freedom have been documented by Likins et al. (1970),[167] Millar (1970),[168] Malich (1975),[169] Loesch et al. (1976),[170] and others. More recently, Yocum and Slafer (1978),[171] during their study of 'severe' interactions , observed the possibility of a 'beating' phenomenon in a

multi-boom satellite system. Hughes (1976)[172] has discussed the use of a passive damper to reduce such interactions. With respect to control, Hughes has also considered the implications of flexibility for the pitch attitude control of the CTS[173] and for flexible spacecraft in general.[174] Basically a continuum mechanics representation is adopted followed by a truncated modal series approximation which results in additional degrees of freedom forming a feedback loop relative to the attitude response. Zach (1970)[175] attempted optimal control of a distributed gravity-stabilized system. Also, a design approach based on pole allocation has been advanced by Tseng and Mahn (1978).[176] Millar et al. (1979)[177] and Hughes et al. (1979)[178] have suggested various types of control system logic one might apply. Methods for providing control torque include the use of a flexible boom actuator [Gatlin et al. (1969)[179]], a double-gimbaled momentum wheel [Hillard (1976)[180]], and the use of environmental forces [Pande et al. (1974, 1976),[181,182,183] etc.].

As a means of reducing flexibility effects, Hughes (1975)[184] and Gething et al. (1975)[185] suggest increased damping of structural modes. More direct is the vibration isolation adopted by Cretcher and Mingori (1971)[186] and the vibration suppression of Balas (1979).[187] Smith and Gill (1977)[188] introduced the concept of state parameter control in which elastic degrees of freedom are included in the state vector to be controlled. Somewhat more sophisticated versions of this procedure are described as appendage modal control by Beysens (1976),[189] Jonckhere (1976),[190] Sellappan et al. (1978),[61] and Meirovitch et al. (1978, 1979).[191-193] Martin and Bryson (1980)[194] discuss a possible low order controller which

provides near optimal attitude regulation but is not as sensitive to modelling error in the appendage dynamics as is the full-order controller.

Indications as to trends in the control of present and future spacecraft are provided by the discrete-time approach of Folgate (1976)[195] and Kuo (1976)[196] along with the appearance of digital onboard computers [Kuo et al. (1974),[197] Kawato et al. (1976),[198] Van Landingham et al. (1978)[199]]. De Bra (1979)[200] suggests that the added sophistication of modelling error compensation via the control system itself [Skelton and Likins (1978)[201]] may become a prerequisite for coping with future challenges.

1.2.5 Transient response and deployment dynamics

By now we have gained some appreciation as to the complexities associated with configuration geometry and vehicle elasticity. Analysis becomes even more involved during extension or retraction of flexible appendages. The deployment introduces a variable mass distribution (and hence variable moments of inertia) together with relative velocities and accelerations. Perhaps because of its inherent complexity the problem has received relatively little attention. In general, available investigations tend to be more limited in scope than those dealing with nondeploying flexible structures.

Lang and Honeycutt (1967)[202] approximated spinning flexible deploying rods to point masses located at the radius of gyration. Cloutier (1968)[203] has considered spinning systems with tip masses extended by means of weightless rigid rods. On the other hand, Bowers and Williams (1970)[204] employed rigid booms and synchronized their deployment intervals with pitch attitude so as to ensure

capture by the gravity gradient. The assumption of rigid booms permitted Hughes (1972)[205] to obtain an approximate closed form solution for attitude behaviour of a spin-stabilized satellite, during appendage deployment. A series of deployment-related situations ranging from spacecraft detumbling to a study of stability during asymmetric deployment were examined by Bainum et al.[206-211] for some specific configurations. The elements deployed in these studies were either rigid rods having a uniformly distributed mass or point masses - no flexibility was taken into account. Dow et al. (1966),[54] however, did consider flexible boom deployment as it applied to the RAE. As described by the authors the model developed is quite extensive in that it includes such factors as structural damping, a rigid damper-boom model, solar radiation pressures, gravitational effects, and 3-axis attitude motion with both analog and digital simulations. Although interesting results were presented in the form of pitch/yaw displacement, maximum libration angles attained under different deployment and pitch initial conditions, and energy variation in orbit; no governing equations are given. Cherchas (1971)[212] investigated maximum nutation, precession, bending moments, and deflections occuring for a specific spinning configuration with booms extending normal to the nominal spin axis. However, when evaluating vibration characteristics deployment rate effects were ignored and a constant spin rate was assumed. A similar approach is adopted for the case of solar array deployment perpendicular to the major spin axis [Cherchas and Gossain (1974)[213]]. In both the previous presentations, the so-called 'quasi-modal' approach is used in which eigenfunctions associated with the instantaneous appendage configuration are used when forming the

series representation for the elastic deformations. The difficult issue of differentiating the quasi-modes is not addressed.

A somewhat different class of deploying systems is represented by the cable configuration of Ebner (1970)[214] and Stuvier et al. (1973).[215] In this case, attitude motion is determined without analyzing cable oscillations. Such effects are fully accounted for, however, by Modi et al. (1978, 1979).[216,217] Kane and Levinson (1977)[218] have presented an initial analysis of the dynamics related to a payload undergoing free-flight deployment from an orbiting spacecraft at the end of a massless cable. Simulations indicate the possibility of retrieving a payload from 100 m in less than 78 minutes for a spacecraft moving in a 90 minute orbit.

Significant progress has been made toward generating analyses applicable to deploying systems but still retaining some degree of generality. In the form of a progress report on the CTS, Hughes (1976)[219] deals with the effect of deployment when formulating equations for a nonrotating rigid body with an arbitrary number of deployable appendages capable of small deformations. A set of general equations are developed for the case in which deployment occurs at a constant rate along the rectilinear directions of the appendage. Also, the view is expressed that the use of a modal analysis[212,213] can be expected to yield good results if rates of deployment are gradual enough, i.e. $\dot{\ell} < \Omega_1 \ell$. Lips and Modi (1978)[138] presented a more general formulation allowing for three dimensional nonlinear attitude motion, gravitational effects, an arbitrary number/type/orientation of appendages, shifting center of mass and independent deployment rates and accelerations of arbitrary magnitude and direction for each appendage. In addition, second degree nonlinear equations were de-

rived which govern the vibration of deploying beam-type appendages of arbitrary cross-section. Preliminary results suggested the existence of critical combinations of flexibility, deployment, and spin which can give rise to large amplitude, and even unstable, vibrations and hence librations. A linear form of the Newton-Euler equations governing translation and rotation are formulated (but not applied) by Jankovic (1980),[220] for a single deformable body having a time variable (deploying) configuration.

An important aspect, and a major area of study in its own right, is the effect of deployment on appendage vibration characteristics. Leech (1970),[221] Tabarrok et al. (1974),[222] and Jankovic (1976)[223] have studied the behaviour of a uniform beam extending along the axial direction. For example, an analytic solution exists for deployment at a constant rate since the equations can then be expressed as a Bessel equation.[222] A solution for the case of arbitrary deployment history was obtained using a series of admissible functions. As opposed to this case, the second degree vibration equations of Lips and Modi (1978),[138] account for the effect of deployment acceleration, spin rate and spin acceleration. 'Free' vibration characteristics obtained with a linearized form of these equations have been used to assess the influence of spin, deployment rate, deployment acceleration, and Coriolis effects arising from coupling of deployment and spin velocities [Lips and Modi (1978)[224]]. Jankovic (1980)[220] worked out vibration equations for the CTS solar panels modelled as a nonspinning boom, rigid pressure plate, and membrane. No gravity gradient or deployment acceleration effects were considered. Governing equations were solved using both the quasi-modal approach and Galerkin polynomials. Good agreement was

obtained between measured and simulated acceleration at the array tip for the CTS. However, the tremendous effort involved in generating response via the quasi-modal approach suggests the progress can be made only by means of some other approximate procedures, such as through the use of admissible functions.

1.3 Purpose and Scope of the Investigation

The literature review illustrates the large number of factors with which the analyst is faced when modelling the dynamical behaviour of a modern day spacecraft. Equations of motion can be formulated by means of the Eulerian, D'Alembert, or Lagrangian principle using generalized coordinates or quasicoordinates. Elastic members are treated as a series of interconnected rigid bodies as in the finite element procedure, or as a continuum. Mathematically, the governing equations range from a finite set of partial differential equations to an infinite set of ordinary differential equations. In general, investigators have dealt extensively with the linear steady state response for a well-defined configuration. Very little attention has been directed toward the transient phase which is of considerable interest and importance because of the possibility of large angle motions during deployment of appendages. There are only scattered attempts which consider flexibility and deployment for a general configuration.

This thesis presents a general nonlinear formulation for librational dynamics (Chapter 2) of a spacecraft in an eccentric orbit with an arbitrary number, type, and orientation of deploying flexible appendages. Both shifts in the center of mass location and geometric offset of the point of attachment of the appendage

from the center of mass are provided for.

The beam-type appendage which is chosen here is typical of what one actually finds in use. Note that even solar panels of the CTS were supported by a dominant central boom. Second degree nonlinear vibration equations for such flexible appendages, derived in Chapter 3, are based on a variational approach. Taken into account are such features as variable sectional properties and axial 'foreshortening'. Of course, the general equations account for coupling with the three attitude degrees of freedom. The conjugate character of the system with the librational motion affecting the vibratory displacement and vice-versa, renders the problem quite challenging.

Evaluation of exact appendage modal characteristics can be expensive and time consuming. Improvements in librational predictions may not always justify the effort. The situation is further obscured during deployment since the system is then nonautonomous. Hence it is helpful to examine the vibration characteristics for models more accurate than the simple Euler-Bernoulli beam and yet not as involved as the nonlinear case. For this reason a linearized analysis of the vibratory motion is carried out over a range of spin and deployment parameters, assuming only pitch attitude motion, i.e. librational motion, in the orbital plane (Chapter 4).

However, from design considerations, the main aspect of interest would be the transient librational response over a range of system parameters and initial conditions. Thus, having formulated general librational equations, one seeks their solution. Results of direct numerical integration on a digital computer are given in Chapter 5 for the case of planar motions and in Chapter 6

for the case of 3-axis attitude response. The system is so programmed as to isolate the effect of flexibility, spin, shifting center of mass, etc., and to assess their significance in a given situation.

To summarize, the objective here is to evolve a formulation of a general character applicable to a large class of spacecraft. Rather than the accumulation of a large amount of data, the intent has been to establish a systematic methodology for coping with complex dynamical systems.

Figure 1.1 provides an overview of the research effort.

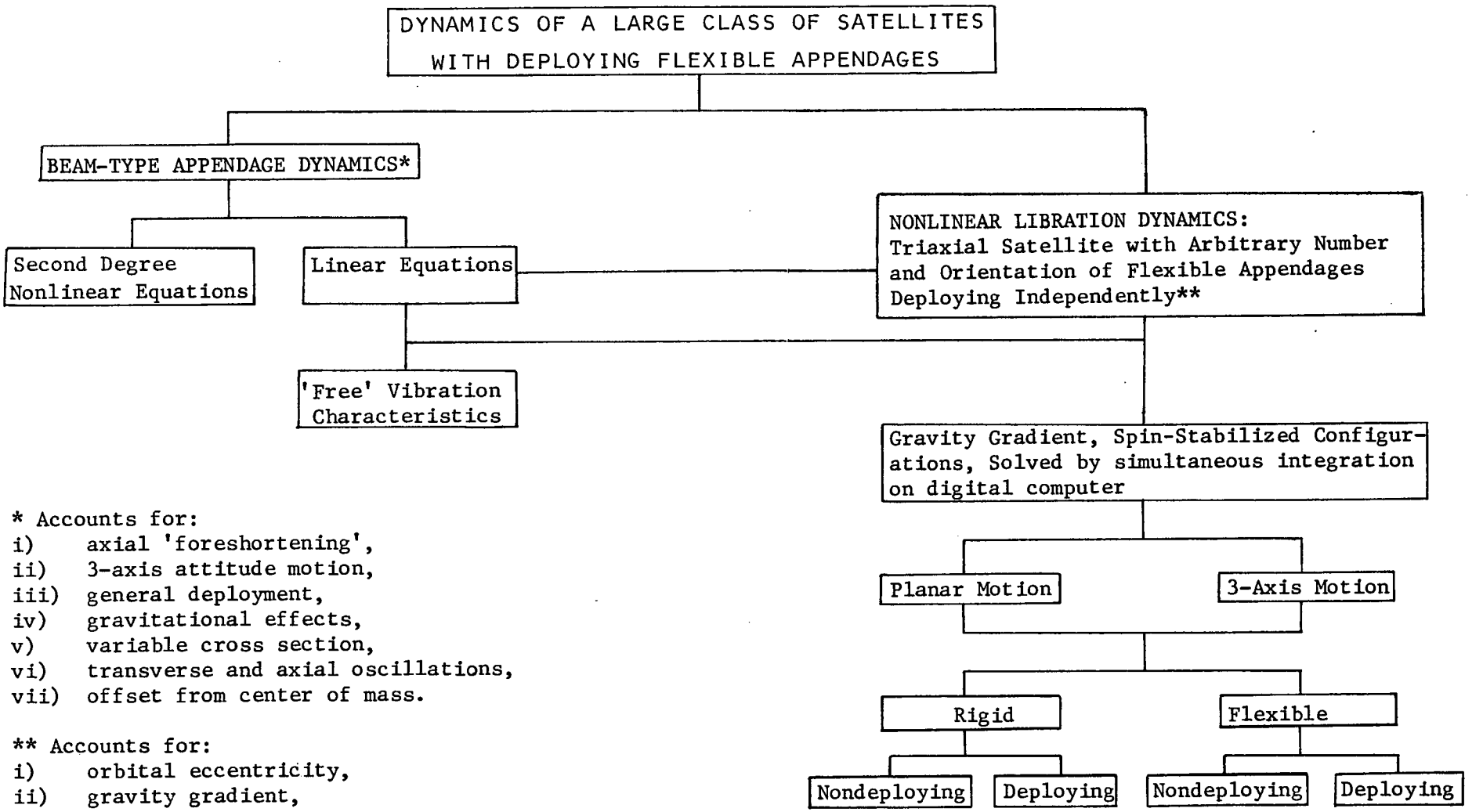

* Accounts for:
i) axial 'foreshortening',
ii) 3-axis attitude motion,
iii) general deployment,
iv) gravitational effects,
v) variable cross section,
vi) transverse and axial oscillations,
vii) offset from center of mass.

** Accounts for:
i) orbital eccentricity,
ii) gravity gradient,
iii) shifting center of mass,
iv) geometric offset of appendages.

Figure 1-1 Outline of the research program

2. GENERAL ATTITUDE EQUATIONS OF MOTION

Recognizing that orbital perturbations due to either spacecraft libration or appendage vibration are in general negligible,[15] one can describe the motion of the center of mass according to the following Keplerian relations:

$$h_\theta = R_c^2\dot{\theta} = \text{constant}; \tag{2.1a}$$

$$R_c = h_\theta^2/\mu(1+ec\theta). \tag{2.1b}$$

Of course, it has been tacitly assumed that deployment will not alter this finding. Thus, in almost all missions of practical importance, librational dynamics can be studied independently of the orbital motion. This chapter derives, using the Lagrangian procedure, governing nonlinear librational equations valid for a large class of flexible satellite systems.

2.1 Configuration and Reference Coordinate Systems

Consider a spacecraft with its instantaneous center of mass O_c negotiating an arbitrary trajectory with respect to the center of force at O_I [Figure 2-1(a)]. Position vector $\underline{R}_c$ and true anomaly θ define the location of O_c with respect to the inertial reference X, Y, Z centered at O_I. X_O, Y_O, Z_O represent an orthogonal orbiting reference frame with its origin fixed at O_c where X_O and Y_O are the local outward vertical and horizontal respectively, and Z_O is aligned with the orbit normal.

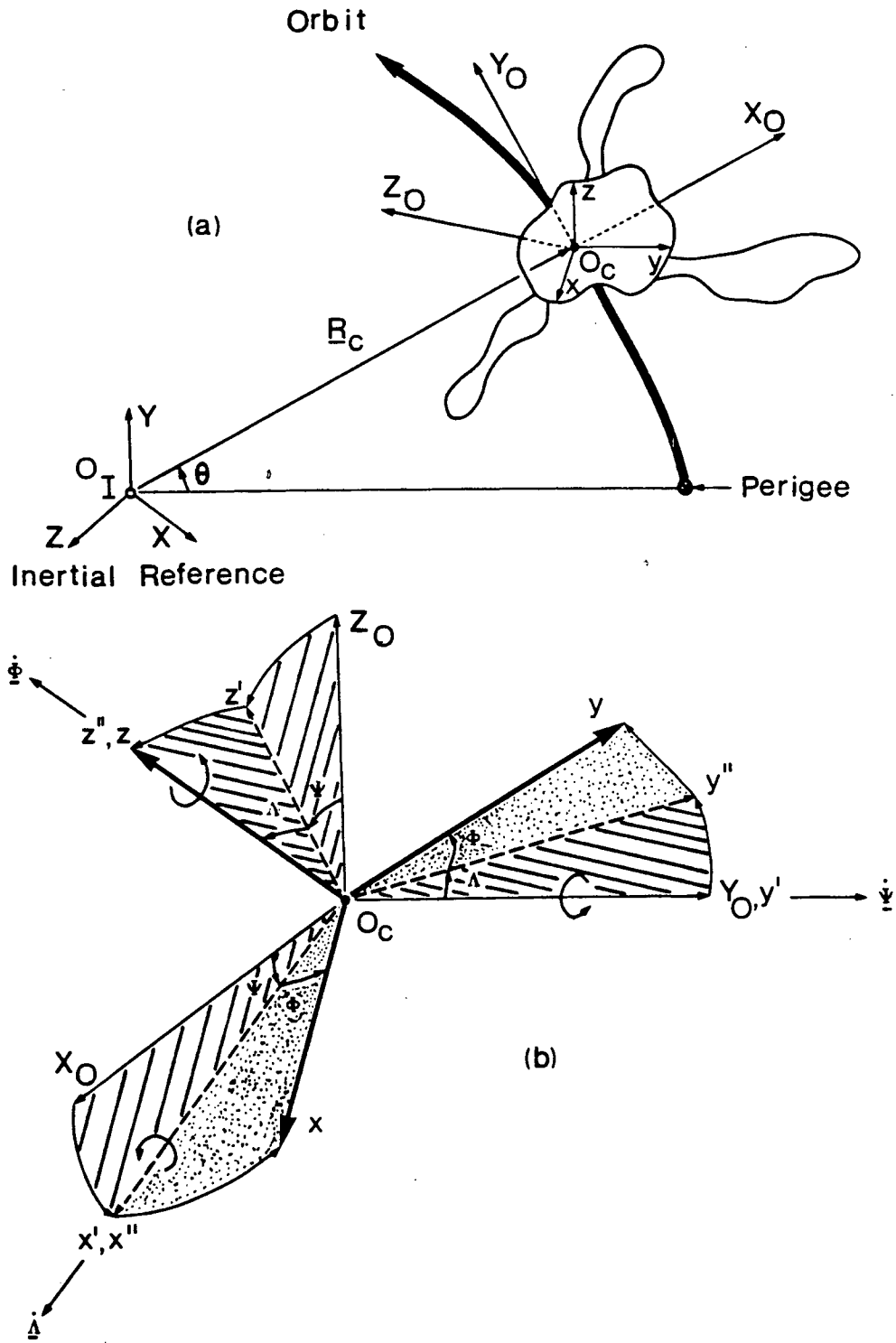

Figure 2-1 Geometry of satellite motion: (a) inertial, rotating, and body-fixed coordinate systems; (b) modified Eulerian rotations Ψ,Λ,Φ defining arbitrary orientation of the central rigid body during librations.

The librational response is defined by the modified Eulerian rotations Ψ, Λ, Φ of the body-fixed axes x, y, z with respect to the orbiting reference X_O, Y_O, Z_O [Figure 2-1(b)]. Note that this sequence is synonomous with the Bryant and Kardan angles referred to by Wittenburg.[225] Axes x_0, y_0, z_0 are parallel to the x, y, z coordinates at all times, but have a different origin, O_0, representing center of mass location in the absence of any flexibility effects (Figure 2-2).

The literature survey suggests that the class of configurations represented by an arbitrarily-shaped central rigid body to which are attached an arbitrary number of deploying appendages has a wide range of application. The appendages can be rigid or flexible and are to be cantilevered to the main body forming a simplified topological tree* [Meirovitch (1972)[85]]. Note both the orientation and the shape of the appendages vary.

The presence of a rigid main body allows one to describe the rotational dynamics relative to a set of axes x, y, z fixed to this main body. Such a reference is still a 'floating' system by virtue of the orbital and the attitude motions of the central body. As with the orbiting axes, the origin in this case is taken to be coincident with the instantaneous center of mass. Consequently, in such a case the linear momentum is zero at all times resulting in the simplification of kinetic energy, gravitational potential, and angular momentum expressions.[100]

---

* i.e., no closed loops and no secondary branches occur in the topology of the structure.

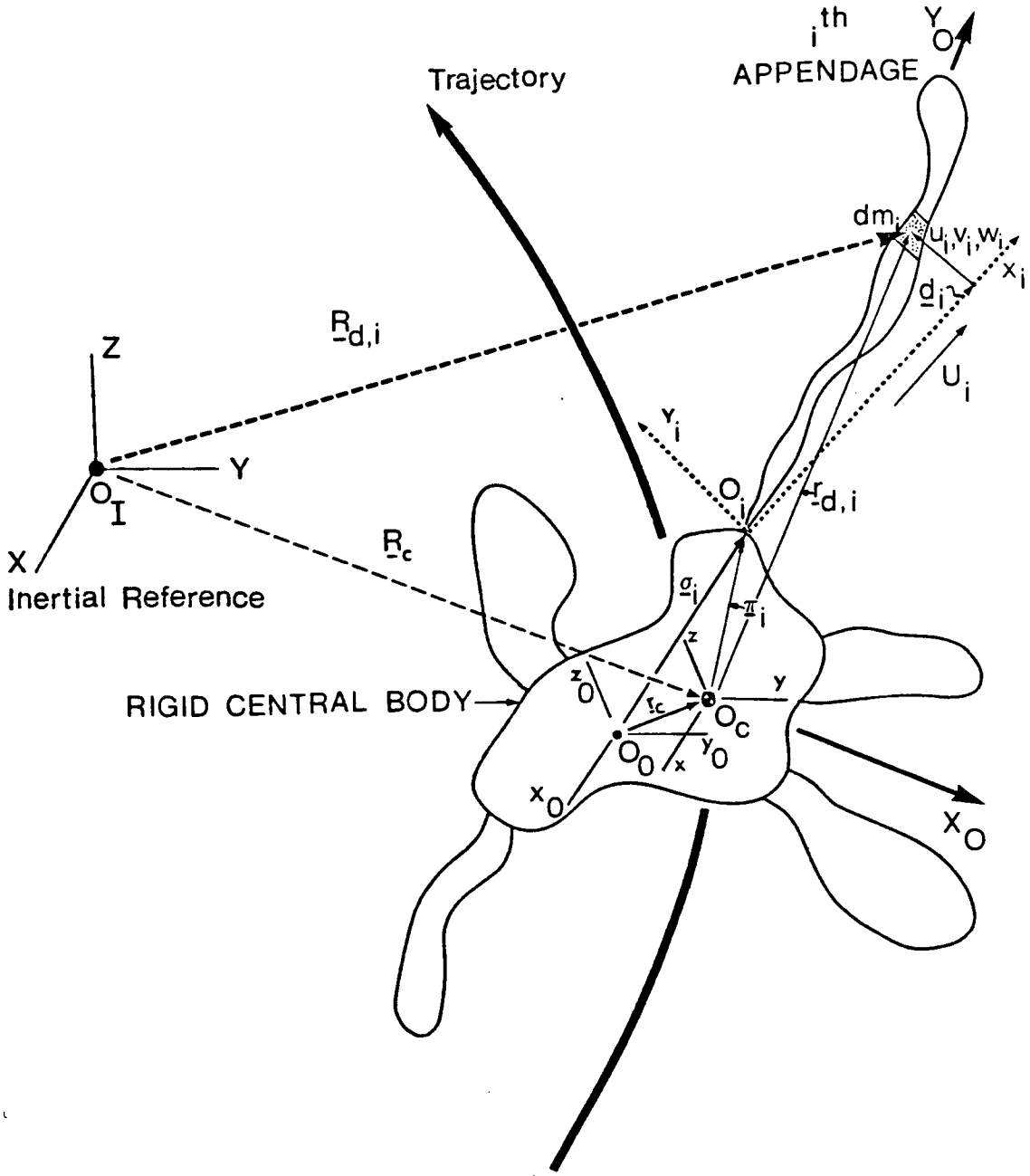

Figure 2-2 A general spacecraft configuration showing shifting center of mass, appendage offset, deployment, and deformations.

The practical significance of the above choice for a reference frame becomes apparent when one recognizes that attitude sensors too are fixed to the main body. This fact provides some guidance also when one is selecting coordinates to be used in monitoring spacecraft attitude. Ideally, the same coordinates should be capable of representing both the gravity gradient and spin-stabilized configurations. Such considerations lead one to choose the Euler angles as defined in Figure 2-1(b).

Elastic deflections u_i, v_i, w_i of the i^{th} appendage are measured with respect to their undeformed configuration as specified by the x_i, y_i, z_i system of coordinate axes which, in turn, are obtained through the modified Euler rotations ψ_i, λ_i, ϕ_i relative to the x_0, y_0, z_0 coordinates. These rotations are used to construct the transformation matrix $[\chi_i]$, allowing conversion between local appendage coordinates $\underline{e}_i^{(i)}$ and central coordinates $e_i^{(0)}$:

$$\underline{e}_i^{(i)} = u_i \underline{i}_i + v_i \underline{j}_i + w_i \underline{k}_i; \tag{2.2a}$$

$$\underline{e}_i^{(i)} = [\chi_i] \quad \underline{e}_i^{(0)}; \tag{2.2b}$$

$$[\chi_i] = \begin{bmatrix} (c\phi_i c\psi_i + s\phi_i s\lambda_i s\psi_i) & s\phi_i c\lambda_i & (-c\phi_i s\psi_i + s\phi_i s\lambda_i c\psi_i) \\ (-s\phi_i c\psi_i + c\phi_i s\lambda_i s\psi_i) & c\phi_i c\lambda_i & (s\phi_i s\psi_i + c\phi_i s\lambda_i c\psi_i) \\ c\lambda_i s\psi_i & -s\lambda_i & c\lambda_i c\psi_i \end{bmatrix}; \tag{2.2c}$$

where:

s( ) = sine ( );

c( ) = cosine ( ).

The origin of the local appendage coordinate system, O_i, has a net offset $\underline{\pi}_i$ from the instantaneous mass center as a result of flexibility and deployment, as given by $\underline{r}_c$, and due to geometric offset $\underline{\sigma}_i$. Each appendage is shown deploying independently with velocity U_i along the x_i axis (Figure 2-2). Note that the center of mass shift is measured from O_0 to O_c and allows for asymmetric deployment. That is

$$\underline{r}_c = \frac{1}{m_s} \sum_i \int_{m_i} (\underline{d}_i^a + \underline{d}_i^b + \underline{\sigma}_i + \underline{e}_i)\, dm_i, \tag{2.3a}$$

where:

$\underline{d}_i$ vector locating dm_i for the undeformed appendage and is measured with respect to O_i, $\underline{d}_i^a + \underline{d}_i^b$;

$\underline{d}_i^a$ vector $\underline{d}_i$ prior to deployment;

$\underline{d}_i^b$ net change in $\underline{d}^i$ as a result of deployment;

But,

$$\sum_i \int_{m_i} (\underline{d}_i^a + \underline{\sigma}_i) dm_i = 0, \tag{2.3b}$$

hence, in general,

$$\underline{r}_c = \frac{1}{m_s} \sum_i \int_{m_i} (\underline{d}_i^b + \underline{e}_i) dm_i. \tag{2.3c}$$

2.2 Lagrangian Formulation

2.2.1 Background

Principle methods of formulating equations of motion were outlined in Chapter 1. Use of the Lagrangian equations were pre-

ferred here since the objective is to study overall vehicle motions, not forces of interaction. The degrees of freedom associated with such a holonomic system can be represented by the quaternions in conjunction with quasicoordinates or momentum variables to arrive at relatively simpler sets of relations. However, the quantities which physically describe the motion become more deeply buried in an escalating number of equations. They may permit more rapid numerical analysis, however, at the cost of lost physical understanding of the true nature of the motion.

2.2.2 System kinetic and potential energies

Figure 2-2 identifies the undeformed ($\underline{r}_i = \underline{d}_i + \underline{\sigma}_i$) and deformed ($\underline{r}_{d,i} = \underline{r}_i - \underline{r}_c + \underline{e}_i$) spacecraft configuration. Such a system undergoing general libration together with appendage vibration and deployment at velocity $\underline{V}_i$ has a kinetic energy which can be expressed, relative to the inertial reference, in the matrix form:

$$
\begin{aligned}
T &= \frac{1}{2} \sum_i \int_{m_i} \{\frac{d\underline{R}_{d,i}}{dt}\}^T \cdot \{\frac{d\underline{R}_{d,i}}{dt}\} \, dm_i \\
&= \frac{1}{2} m_s \{\frac{d\underline{R}_c}{dt}\}^T \cdot \{\frac{d\underline{R}_c}{dt}\} \\
&+ \frac{1}{2} \sum_i \{\omega\}^T [\chi_i]^T [I_i^{(i)}] [\chi_i] \{\omega\} \\
&+ \{\omega\}^T \sum_i \int_{m_i} [r_{d,i}] \{V_{O,i}\} \, dm_i \\
&+ \frac{1}{2} \sum_i \int_{m_i} \{V_{O,i}\}^T \{V_{O,i}\} \, dm_i ; \qquad (2.4)
\end{aligned}
$$

where:

$$\underline{R}_{d,i} = \underline{R}_c + \underline{r}_{d,i} = \underline{R}_c + \underline{r}_i + \underline{e}_{c,i}$$

$$= \underline{R}_c + \underline{r}_i + \underline{e}_i - \underline{r}_c;$$

$\underline{V}_{O,i}$ = relative velocity of mass element dm_i, due to vibration and deployment only, as measured with respect to the x_i, y_i, z_i axes; $\frac{\partial \underline{e}_{c,i}}{\partial t} + (\underline{V}_i \cdot \nabla)(\underline{r}_i + \underline{e}_{c,i})$;

$[I_i^{(i)}]$ = instantaneous moment of inertia matrix for the i^{th} appendage, expressed in 'local' coordinates;

$$\{\omega\} = \begin{Bmatrix} \omega_1 \\ \omega_2 \\ \omega_3 \end{Bmatrix} = \begin{Bmatrix} \dot{\Lambda}c\Phi + \dot{\theta}(c\Psi s\Lambda s\Phi - s\Psi c\Phi) + \dot{\Psi}c\Lambda s\Phi \\ -\dot{\Lambda}s\Phi + \dot{\theta}(c\Psi s\Lambda c\Phi + s\Psi s\Phi) + \dot{\Psi}c\Phi c\Phi \\ \dot{\Phi} + \dot{\theta}c\Psi c\Lambda - \dot{\Psi}s\Lambda \end{Bmatrix} . \qquad (2.5)$$

It is easy to recognize distinct contributions from:

(i) orbital motion associated with a translating mass center;

(ii) rotational motion due to overall attitude librations;

(iii) relative motion due to appendage oscillation and deployment.

Total potential energy (V) consists of a gravitational (V_g) and an elastic (V_e) contribution. Neglecting terms of third and higher order in the variable (r_i/R_c), one can write [Etkin (1962),[49] England (1969),[226] Meirovitch (1972),[85] etc.]:

$$V = V_g + V_e$$

$$= -\frac{\mu m_s}{R_c} - \left(\frac{\mu}{2R_c^3}\right) \sum_i \text{tr}\left([\chi_i]^T [I_i^{(i)}][\chi_i]\right)$$

$$+ \frac{3}{2}\left(\frac{\mu}{R_c^3}\right) \sum_i \{\chi_a\}^T [\chi_i]^T [I_i^{(i)}] [\chi_i] \{\chi_a\}$$

$$+ V_e \left(\frac{\partial u_{c,i}}{\partial x_i}, \ldots, \frac{\partial^2 u_{c,i}}{\partial x_i^2}, \frac{\partial^2 u_{c,i}}{\partial x_i \partial y_i}, \ldots, \frac{\partial^2 w_{c,i}}{\partial z_i^2}\right); \quad (2.6)$$

where:

μ = gravitational constant, GM;

m_s = total combined mass of the satellite;

$\{\chi_a\}$ = vector of direction cosines between $\underline{R}_c$ and x, y, z;

$$= \begin{Bmatrix} c\Psi c\Phi + s\Psi s\Lambda s\Phi \\ -c\Psi s\Phi + s\Psi s\Lambda c\Phi \\ s\Psi c\Lambda \end{Bmatrix} = \begin{Bmatrix} \chi_{a,1} \\ \chi_{a,2} \\ \chi_{a,3} \end{Bmatrix}. \quad (2.7)$$

2.2.3 The Lagrange equations and an alternative momentum formulation

The Lagrangian for the hybrid configuration of Figure 2-2 can be separated into two parts: one associated with the undeformed configuration (Ξ) and one with the deformed appendages ($\sum_i \int_{D_i} T \, dD_i$):[156]

$$L = T - V = \Xi(q, \dot{q}, t) + \sum_i \int_{D_i} T(q, \dot{q}, \varepsilon, \varepsilon, \varepsilon_x, \ldots, t) \, dD_i. \quad (2.8)$$

Application of Hamilton's principle to such a holonomic system (Appendix V) yields the following form of the Lagrange equations for the attitude degrees of freedom $q_k = \Psi, \Lambda, \Phi$:

$$\frac{d}{dt}\left(\frac{\partial L}{\partial \dot{q}_k}\right) - \frac{\partial L}{\partial q_k} = Q_k, \quad (2.9a)$$

or,

$$\frac{d}{dt}\left(\frac{\partial \Xi}{\partial \dot{q}_k}\right) - \frac{\partial \Xi}{\partial q_k} + \sum_i \int_{D_i} \left[\frac{\partial}{\partial t}\left(\frac{\partial T}{\partial \dot{q}_k}\right) - \frac{\partial T}{\partial q_k}\right] dDi = Q_k \qquad (2.9b)$$

where,

Q_k = generalized force associated with q_k.

Note, the equations are amenable to a control system study since prescribed control forces can be introduced directly as generalized forces in conjunction with a suitable control strategy.

Applying equation (2.9) to the multibody configuration under consideration here, can be extremely involved. In fact, at this point it is not particularly advantageous to evaluate the Lagrangian in detail. Rather, one can take advantage of the following relations for the kinetic energy:

$$\frac{\partial T}{\partial q_k} = \frac{\partial T}{\partial \underline{\omega}} \circ \frac{\partial \underline{\omega}}{\partial q_k};$$

$$\frac{\partial T}{\partial \dot{q}_k} = \frac{\partial T}{\partial \underline{\omega}} \circ \frac{\partial \underline{\omega}}{\partial \dot{q}_k};$$

$$\frac{d}{dt}\left(\frac{\partial T}{\partial \dot{q}_k}\right) = \frac{\partial T}{\partial \underline{\omega}} \circ \frac{d}{dt}\left(\frac{\partial \underline{\omega}}{\partial \dot{q}_k}\right) + \frac{d}{dt}\left(\frac{\partial T}{\partial \underline{\omega}}\right) \circ \frac{\partial \underline{\omega}}{\partial \dot{q}_k};$$

where [Samin and Willems (1975),[92] Likins (1975)[76]]:

$$\frac{\partial T}{\partial \underline{\omega}} = \underline{H}. \quad \text{(angular momentum)} \qquad (2.10)$$

Substituting the above relations into equation (2.9a) provides an alternative form for the governing equations in a momentum format

which can be expressed in matrix notation as [79]

$$\{\frac{\partial \omega}{\partial \dot{q}_k}\}^T \circ \{\frac{dH}{dt}\} + (\frac{d}{dt}\{\frac{\partial \omega}{\partial \dot{q}_k}\} - \{\frac{\partial \omega}{\partial q_k}\})^T \circ \{H\} + \frac{\partial V}{\partial q_k} = Q_k, \qquad (2.11)$$

where:

$\{H\}$ = angular momentum vector associated with motion relative to the system mass center, $[I]\{\omega\} + \sum_i \int_{m_i} [\tilde{r}_{d,i}]\{V_{O,i}\}\, dm_i$;

$[I]$ = overall system moments of inertia with respect to x, y, z, axes, presented in such a way as to isolate flexibility effects (Appendix II);

and, note for example,

$Q_{g,k} = \frac{\partial V_g}{\partial q_k}$ = generalized force associated with the gravitational field, $3(\frac{\mu}{R_c^3})\{\frac{\partial \chi_a}{\partial q_k}\}^T [I] \{\chi_a\}$.

The formulation presents several advantages, particularly when one is faced with complex rotating systems. It results in considerable saving in the amount of algebra involved. As a rule, the more complex the system the greater the saving. This is because rather than differentiating the kinetic energy twice, one carries out a single differentiation of the simpler momentum function together with with some relatively straightforward differentiations of the angular velocity vector $\underline{\omega}$. In addition to reducing the algebraic effort such a method can be applied systematically; as a result it should prove less error prone. System kinematics, configuration, and flexibility effects are not intertwined to the degree that they are with the Lagrange generalized coordinate equations. Consequently, digital simulations can be set up to more easily accommodate changes in either configuration or choice of coordinates.

2.3 Governing Nonlinear Three-Axis Equations

In such a matrix form the equations (2.11) appear rather compact. However, in actual application they can be expanded resulting in governing second order equations for roll (Ψ), yaw (Λ), and pitch (spin, Φ) as follows:

Ψ, Roll degree of freedom

$$[c^2\Lambda(s^2\Phi I_{11}+c^2\Phi I_{22}-s2\Phi I_{12}) + s^2\Lambda I_{33} + s2\Lambda(s\Phi I_{13}+c\Phi I_{23})]\ddot{\Psi}$$

$$+ c^2\Lambda(s^2\Phi \dot{I}_{11}+c^2\Phi \dot{I}_{22}-s2\Phi \dot{I}_{12}) + s^2\Lambda \dot{I}_{33} + s2\Lambda(s\Phi \dot{I}_{13}+c\Phi \dot{I}_{23})]\dot{\Psi}$$

$$- s\Psi s\Lambda c\Lambda(2s^2\Phi I_{11}-s2\Phi I_{12}+2s^2\Lambda s\Phi I_{13})\dot{\theta}\dot{\Psi} + [s2\Lambda(I_{33}-s^2\Phi I_{11}-c^2\Phi I_{22}$$

$$+ s2\Phi I_{12}) + 2c2\Lambda(s\Phi I_{13}+c\Phi I_{23})]\dot{\Lambda}\dot{\Psi} + \{c^2\Lambda[s2\Phi(I_{11}-I_{22})$$

$$+ (1-c2\Phi)I_{12}] + s2\Lambda(c\Phi I_{13}-s\Phi I_{23})\dot{\Phi}\dot{\Psi} + (3\mu/R_c^3)\{[(s^2\Lambda s^2\Phi-c^2\Phi)I_{11}$$

$$+ (s^2\Lambda c^2\Phi-s^2\Phi)I_{22} + c^2\Lambda I_{33} - (1+s^2\Lambda)s2\Phi I_{12} - s2\Lambda(s\Phi I_{13}+c\Phi I_{23})]s\Psi c\Psi$$

$$+ c2\Psi s\Lambda[s\Phi c\Phi(I_{11}-I_{22}) - c2\Phi I_{12}] - c2\Psi c\Lambda\ (c\Phi I_{13}-s\Phi I_{23})\}$$

$$+ c\Lambda(s\Phi\Gamma_1+c\Phi\Gamma_2) - s\Lambda\Gamma_3 + \{[c\Lambda(s\Phi c\Phi(I_{11}-I_{22}) - c2\Phi I_{12}]$$

$$+ s\Lambda(c\Phi I_{13}-s\Phi I_{23}\}\ddot{\Lambda} + \{s\Lambda[s\Phi c\Phi(I_{22}-I_{11}) + c2\Phi I_{12}]$$

$$+ c\Lambda(c\Phi I_{13}-s\Phi I_{23})\}\dot{\Lambda}^2 + \{c\Lambda(s\Phi c\Phi(\dot{I}_{11}-\dot{I}_{22}) - c2\Phi \dot{I}_{12}-h_3]$$

$$+ s\Lambda[-s\Phi(\dot{I}_{23}+h_1) + c\Phi(\dot{I}_{13}-h_2)]\}\dot{\Lambda} + \{c\Psi(c2\Lambda s^2\Phi+c^2\Phi)\ I_{11}$$

$$+ [c\Psi(s^2\Phi+c2\Lambda c^2\Phi) - s\Psi s\Lambda s2\Phi]\ I_{22} - c\Psi c2\Lambda I_{33} + [c\Psi s2\Phi(1-c2\Lambda)$$

$$- 2s\Psi s\Lambda c^2\Phi]I_{12} + 2c\Lambda[(2c\Psi s\Lambda s\Phi - s\Psi c\Phi)I_{13} + (2c\Psi s\Lambda c\Phi$$

$$+ s\Psi c\Phi)I_{23}]\}\dot{\theta}\dot{\Lambda} + c\Lambda[c2\Phi(I_{11}-I_{22}) + s2\Phi I_{12}-I_{33}]\dot{\Phi}\dot{\Lambda} - [c\Lambda(s\Phi I_{13}$$

$$+ c\Phi I_{23}) - s\Lambda I_{33}]\ddot{\Phi} + c\Lambda(s\Phi I_{23}-c\Phi I_{13})\dot{\Phi}^2 - \{c\Lambda[s\Phi(\dot{I}_{13}+h_2)$$

$$+ c\Phi(\dot{I}_{23}-h_1)] + s\Lambda\dot{I}_{33}\}\dot{\Phi} + \{c\Lambda[c\Psi s\Lambda s2\Phi - s\Psi c2\Phi)(I_{11}-I_{22})$$

$$+ s\Psi I_{33}] - 2c\Lambda(s\Psi s2\Phi + c\Psi s\Lambda c2\Phi)I_{12} + 2(s\Psi s\Lambda s\Phi - c\Psi c^2\Lambda c\Phi)\ I_{13}$$

$$+ 2c\Psi c^2\Lambda s\Phi I_{23}\}\dot{\theta}\dot{\Phi} + [c\Psi s\Lambda c\Lambda(s^2\Phi I_{11} + c^2\Phi I_{22}-I_{33}) + s\Psi c\Lambda s\Phi c\Phi(I_{22}$$

$$- I_{11}) + c\Lambda(s\Psi c2\Phi - c\Psi s\Lambda s2\Phi)I_{12} - (c\Psi c2\Lambda s\Phi + s\Psi s\Lambda c\Phi)I_{13}$$

$$+ (s\Psi s\Lambda s\Phi - c\Psi c2\Lambda c\Phi)I_{23}]\ddot{\theta} + \{s\Psi c\Psi[(s^2\Lambda c^2\Phi - s^2\Phi)I_{22}$$

$$- (s^2\Lambda s^2\Phi + c^2\Phi)I_{11} + c^2\Lambda I_{33}] + c2\Psi s\Lambda s\Phi c\Phi\ (I_{11}-I_{22})$$

$$- [s\Lambda(c^2\Psi c2\Phi - s^2\Psi) + s\Psi c\Psi s2\Phi]I_{12} - c2\Psi c\Lambda c\Phi I_{13} - c\Lambda(s2\Psi s\Lambda c\Phi$$

$$- c2\Psi s\Phi)I_{23}\}\dot{\theta}^2 + \{c\Psi s\Lambda c\Lambda\ (s^2\Phi\dot{I}_{11} + c^2\Phi\dot{I}_{22} - \dot{I}_{33})$$

$$+ s\Psi c\Lambda s\Phi c\Phi\ (\dot{I}_{22}-\dot{I}_{11}) - c\Lambda(c\Psi s\Lambda s2\Phi - s\Psi c2\Phi)\dot{I}_{12}-c\Psi[s\Phi(c2\Lambda\dot{I}_{13}$$

$$+ h_2) + c\Phi(c2\Lambda\dot{I}_{23}-h_1)] - s\Psi s\Lambda[c\Phi(\dot{I}_{13}-h_2) - s\Phi(\dot{I}_{23}-h_1)]$$

$$+ s\Psi c\Lambda h_3\}\dot{\theta} = Q_\Psi; \qquad (2.12a)$$

Λ, Yaw degree of freedom

$$(c^2\Phi I_{11} + s^2\Phi I_{22} + s2\Phi I_{12})\ddot{\Lambda} + (c^2\Phi \dot{I}_{11} + s^2\Phi \dot{I}_{22} + s2\Phi \dot{I}_{12})\dot{\Lambda}$$

$$+ [s2\Phi(I_{22} - I_{11}) + 2c2\Phi I_{12}]\dot{\Phi}\dot{\Lambda} + (3\mu/R_c^3)\{s^2\Psi s\Lambda c\Lambda(s^2\Phi I_{11}$$

$$+ c^2\Phi I_{22} - I_{33} - s2\Phi I_{12}) - s\Psi c2\Lambda(s\Phi I_{13} + c\Phi I_{23})$$

$$+ s\Psi c\Psi c\Lambda\,[s\Phi c\Phi(I_{11} - I_{22}) - c2\Phi I_{12}] + s\Psi c\Psi s\Lambda\,(c\Phi I_{13} - s\Phi I_{23})\}$$

$$+ (c\Phi\Gamma_1 - s\Phi\Gamma_2) - (c\Phi I_{13} - s\Phi I_{23})\ddot{\Phi} + (s\Phi I_{13} + c\Phi I_{23})\dot{\Phi}^2$$

$$- [c\Phi(\dot{I}_{13} + h_2) - s\Phi(\dot{I}_{23} - h_1)]\dot{\Phi} + [(c\Psi s\Lambda c2\Phi + s\Psi s2\Phi)(I_{11} - I_{22})$$

$$+ c\Psi s\Lambda I_{33} - 2(s\Psi c2\Phi - c\Psi s\Lambda s2\Phi)I_{12} + 2c\Psi c\Lambda(s\Phi I_{13} + c\Phi I_{23})]\dot{\theta}\dot{\Phi}$$

$$+ \{c\Lambda[c2\Phi(I_{11} - I_{22}) + I_{33} + 2s2\Phi I_{12}] - 2s\Lambda(s\Phi I_{13} + c\Phi I_{23})\}\dot{\Psi}\dot{\Phi}$$

$$+ \{c\Lambda[s\Phi c\Phi(I_{11} - I_{22}) - c2\Phi I_{12}] + s\Lambda(c\Phi I_{13} - s\Phi I_{23})\}\ddot{\Psi}$$

$$+ [s\Lambda c\Lambda(s^2\Phi I_{11} + c^2\Phi I_{22} - I_{33} - s2\Phi I_{12}) - c2\Lambda(s\Phi I_{13} + c\Phi I_{23})]\dot{\Psi}^2$$

$$+ \{c\Lambda[s\Phi c\Phi(\dot{I}_{11} - \dot{I}_{22}) - c2\Phi\dot{I}_{12} + h_3] + s\Lambda[s\Phi(-\dot{I}_{23} + h_1)$$

$$+ c\Phi(\dot{I}_{13} + h_2)\}\dot{\Psi} + \{c\Psi[c2\Lambda(I_{33} - 3^2\Phi I_{11} - c^2\Phi I_{22})$$

$$- (c^2\Phi I_{11} + s^2\Phi I_{22})] - [c\Psi s2\Phi(1 + s^2\Lambda) - 2s\Psi s\Lambda c2\Phi]I_{12}$$

$$+ s\Psi s\Lambda s2\Phi(I_{22} - I_{11}) - 2c\Psi s2\Lambda(s\Phi I_{13} + c\Phi I_{23}) + 2s\Psi c\Lambda(c\Phi I_{13}$$

$$- s\Phi I_{23})\}\dot{\theta}\dot{\Phi} + \{c\Psi s\Lambda[s\Phi c\Phi(I_{11} - I_{22}) - c2\Phi I_{12} - s\Psi(c^2\Phi I_{11}$$

$$+ s^2\Phi I_{22} + s2\Phi I_{12}) - c\Psi c\Lambda(c\Phi I_{13} - s\Phi I_{23})\}\dot{\theta} + \{s\Psi c\Psi c\Lambda[s\Phi c\Phi(I_{11}$$

$$- I_{22}) - c2\Phi I_{12}] - c^2\Psi s\Lambda c\Lambda(s^2\Phi I_{11} + c^2\Phi I_{22} + I_{33} - s2\Phi I_{12})$$

$$+ c^2\Psi c2\Lambda(s\Phi I_{13} + c\Phi I_{23}) + s\Psi c\Psi s\Lambda(c\Phi I_{13} - s\Phi I_{23})\}\dot{\theta}^2$$

$$+ \{c\Psi s\Lambda[s\Phi c\Phi(\dot{I}_{11} - \dot{I}_{22}) - c2\Phi\dot{I}_{12} + h_3] - s\Psi(c^2\Phi\dot{I}_{11} + s^2\Phi\dot{I}_{22}$$

$$+ s2\Phi\dot{I}_{12} - c\Psi c\Lambda[c\Phi(\dot{I}_{13} + h_2) - s\Phi(\dot{I}_{23} - h_1)\}\dot{\theta} = Q_\Lambda; \qquad (2.12b)$$

Φ, Pitch (spin) degree of freedom

$$I_{33}\ddot{\Phi} + \dot{I}_{33}\dot{\Phi} + (3\mu/R_c^3)\{c2\Phi[s\Psi c\Psi s\Lambda(I_{11} - I_{22}) + (c^2\Psi - s^2\Psi s^2\Lambda)I_{12}$$

$$+ s\Phi c\Phi[(c^2\Psi - s^2\Psi s^2\Lambda)(I_{22} - I_{11}) + 2s2\Psi s\Lambda I_{12}] - s\Psi c\Lambda c\Phi(s\Psi s\Lambda I_{13}$$

$$- c\Psi I_{23}) + s\Psi c\Lambda s\Phi(c\Psi I_{13} + s\Psi s\Lambda I_{23})\} + \Gamma_3 - [s\Lambda I_{33} + c\Lambda(s\Phi I_{13}$$

$$+ c\Phi I_{23})]\ddot{\Psi} + \{c^2\Lambda[s\Phi c\Phi(I_{22} - I_{11}) + c2\Phi I_{12}] - s\Lambda c\Lambda(c\Phi I_{13}$$

$$- s\Phi I_{23})\}\dot{\Psi}^2 - \{c\Lambda[s\Phi(\dot{I}_{13} - h_2) + c\Phi(\dot{I}_{23} + h_1) + s\Lambda\dot{I}_{33}\}\dot{\Psi}$$

$$+ \{c\Lambda[(c\Psi s\Lambda s2\Phi - s\Psi c2\Phi)(I_{22} - I_{11}) - s\Psi I_{33}] + (c\Psi s2\Lambda c2\Phi$$

$$+ 2s\Psi c\Lambda s2\Phi)I_{12} + 2c\Psi c^2\Lambda(c\Phi I_{13} - s\Phi I_{23})\}\dot{\theta}\dot{\Psi} + \{c\Lambda[c2\Phi(I_{22} - I_{11})$$

$$- I_{33} - 2s2\Phi I_{12}] + 2s\Lambda(s\Phi I_{13} + c\Phi I_{23})\dot{\Lambda}\dot{\Psi} - (c\Phi I_{13} - s\Phi I_{23})\ddot{\Lambda}$$

$$- [s\Phi c\Phi(I_{22} - I_{11}) + c2\Phi I_{12}]\dot{\Lambda}^2 + [s\Phi(\dot{I}_{23} - h_1) - c\Phi(\dot{I}_{13} - h_2)]\dot{\Lambda}$$

$$+ \{c\Psi s\Lambda[c2\Phi(I_{22} - I_{11}) - I_{33} - 2(c\Psi s\Lambda s2\Phi - s\Psi c2\Phi)I_{12}$$

$$- 2c\Psi c\Lambda(s\Phi I_{13} + c\Phi I_{23})\} + \{c\Psi[c\Lambda I_{33} - s\Lambda(s\Phi I_{13} + c\Phi I_{23})]$$

$$+ s\Psi(c\Phi I_{13} - s\Phi I_{23})\}\ddot{\theta} + \{-(s^2\Psi - c^2\Psi s^2\Lambda)[s\Phi c\Phi(I_{22} - I_{11})$$

$$+ c2\Phi I_{12}] - s\Psi c\Psi s\Lambda(c2\Phi(I_{22} - I_{11}) - 2s2\Phi I_{12} + c\Lambda[c^2\Psi s\,(c\Phi I_{13}$$

$$- s\Phi I_{23}) + s\Psi c\Psi(s\Phi I_{13} + c\Phi I_{23})]\}\dot{\theta}^2 + \{-(c\Psi s\Lambda s\Phi - s\Psi c\Phi)(\dot{I}_{13} - h_2)$$

$$- (c\Psi s\Lambda c\Phi + s\Psi s\Phi)(\dot{I}_{23} + h_1) + c\Psi c\Lambda\dot{I}_{33}\}\dot{\theta} = Q_\Phi \; ; \qquad (2.12c)$$

Aside from instantaneous moments of inertia and the value of $\underline{r}_c$, the influence of flexibility and deployment extends to the terms:

$$\{h\} = \begin{Bmatrix} h_1 \\ h_2 \\ h_3 \end{Bmatrix} = \sum_i \int_{m_i} [\tilde{r}_{d,i}]\,\{V_{O,i}\}\,dm_i ; \qquad (2.13a)$$

= a local angular momentum resulting from the relative velocities associated with vibration and deployment;

$$\{\Gamma\} = \begin{Bmatrix} \Gamma_1 \\ \Gamma_2 \\ \Gamma_3 \end{Bmatrix} = \sum_i \int_{m_i} [\tilde{r}_{d,i}]\,\{A_{O,i}\}\,dm_i ; \qquad (2.13b)$$

= a locally applied inertia torque resulting from the relative accelerations associated with vibration and deployment.

The expressions are worked out in detail in Appendix III.

With the equations in this form, one appreciates the complex nonlinear, nonautonomous, and coupled character of the system. Even the simplest of the equations (2.12c) contains more than

seventy terms! The problem is further aggravated by the fact that deformations u_i, v_i, w_i appearing in the above expressions are themselves functions of librational motion. Obviously, even for relatively simple situations, one can hope to search for a general solution only through numerical methods. Even that is a formidable task!

Finally, the range of application can be indicated by summarizing essential features of the formulation:

- arbitrary satellite geometry;
- arbitrary number/type/orientation of flexible appendages;
- independently deploying appendages;
- appendage offset with respect to the center of mass;
- system center of mass moves along an arbitrary trajectory;
- three degrees of freedom are associated with both attitude behaviour and appendage deformation;
- nonlinear attitude motion;
- both spin-stabilized and gravity-stabilized orientations are described by the modified Eulerian rotations chosen;
- generalized force terms are retained.

3. NONLINEAR APPENDAGE DYNAMICS

3.1 Background

In the derivation so far, the physical characteristics of the appendages have been left unspecified; for example, one could be dealing with a string, beam, membrane, shell, etc. As found in Chapter 2, the attitude equations require a description of the elastic displacement field [$\underline{e}_i$ ($\underline{r}_i$, t)] only and are not directly dependent on the <u>type</u> of appendages involved. Ultimately, however, to obtain a solution of the librational dynamics one must specify the type of appendage and solve the associated equations governing flexibility. This can involve even greater effort than the attitude equations themselves.

In the following development the spacecraft is assumed to have beam-type appendages. They are representative of antennae, stabilizing booms, and the supporting bars associated with experimental packages and solar arrays. Furthermore, one would expect long truss-like structures to display an overall beam-type behaviour. Taking the beam to be of the Euler-Bernoulli type makes it essentially one dimensional. Hence, its characteristics are specified by only one spatial variable (x_i). Such a 'slender' system is assumed to experience simple flexure only, i.e., effects of rotary inertia and shear deformation are considered negligible. Furthermore, torsion is not dealt with here. England (1969)[226] states that the fundamental frequency of boom in torsion is separated from the bending frequency and, as such, these oscilla-

ations may be considered uncoupled. The signficance of twist is further reduced for contemporary space booms which tend to be zippered thus ensuring a high torsional stiffness [Nguyen (1978)[139]].

An important aspect of the beam-type appendages is their relatively low flexural rigidity which makes them quite susceptible to large amplitude oscillations when exposed to environmental disturbances and control manoeuvres. Ideally, one would like to analyze the appendage nonlinear dynamics with the utmost accuracy; however, in general, this would be quite a challenging task even with the help of a computer [Nguyen (1978),[139] Almroth et al. (1978),[227] Helliwell (1978),[228] Jankovic (1980)[220]]. Also it can be expensive and often may not be quite necessary. In most situations one can obtain results of adequate accuracy by including only the more important nonlinear contributions. With this in mind, general vibration equations are derived which retain terms only up to 2^{nd} degree. This is consistent with the use of 2^{nd} degree vibration-related terms as found in the inertia, momentum, and torque calculations for the attitude equations.

3.2 Kinetic and Potential Energy of a Deploying Beam Undergoing General Librations

In derivation of equations of motion for a continua the methods of analytical dynamics have an intuitive appeal in that they apply to any 'system' - rigid, flexible, or a hybrid collection of such bodies. For example, the application of Hamilton's Principle to the beam-type appendage under consideration here, can yield a complete set of boundary conditions in addition to the governing equations.

3.2.1 Beam configuration and coordinates

Consider the i^{th} appendage to be a beam deploying with local velocity U_i along the x_i direction, where the x_i axis coincides with the undeformed neutral axis of the appendage (Figure 2-2). Note the appendage attachment position is offset from the overall system center of mass. The linear density ρ_i, stiffness E_i, and cross sectional inertia $J_{jk,i}$ are allowed to vary along the length of the boom. Also, the appendage is permitted to have any arbitrary initial orientation in space and is free to undergo transverse as well as axial deformations. Fang (1975)[134] points out the need for considering axial and transverse degrees of freedom simultaneously when dealing with large amplitude problems. Neglecting appendage thickness in the y_i, z_i directions, the general displacement of elemental mass dm_i located at x_i with respect to the instantaneous mass center of the overall spacecraft is:

$$\underline{r}_{d,i} = [x_i + \sigma_{1,i} - x_c + u_i(x_i,t) - u_{fs,i}(x_i,t)]\,\underline{i}_i + [\sigma_{2,i} - y_c + v_i(x_i,t)]\,\underline{j}_i + [\sigma_{3,i} - z_c + w_i(x_i,t)]\,\underline{k}_i \quad . \tag{3.1}$$

where axial foreshortening ($-u_{fs,i}$) due to transverse displacements has been included explicitly.

3.2.2 Treatment of axial foreshortening

Assessment of the foreshortening effect has presented several problems in the past [Vigneron (1975),[133] Kaza and Kvaternik (1977)[136]]. The approach adopted in this thesis unifies some of

the earlier procedures.

Consider a beam of undeformed length ℓ as measured along the x axis (Figure 3-1). In the presence of transverse displacement v, w the effective length at any instant becomes ℓ_Δ. That $\ell_\Delta < \ell$ can be established by noting that any deformed beam element of length ds has a projected length dx and:

$$ds = (1 + v_x^2 + w_x^2)^{1/2} dx \tag{3.2}$$

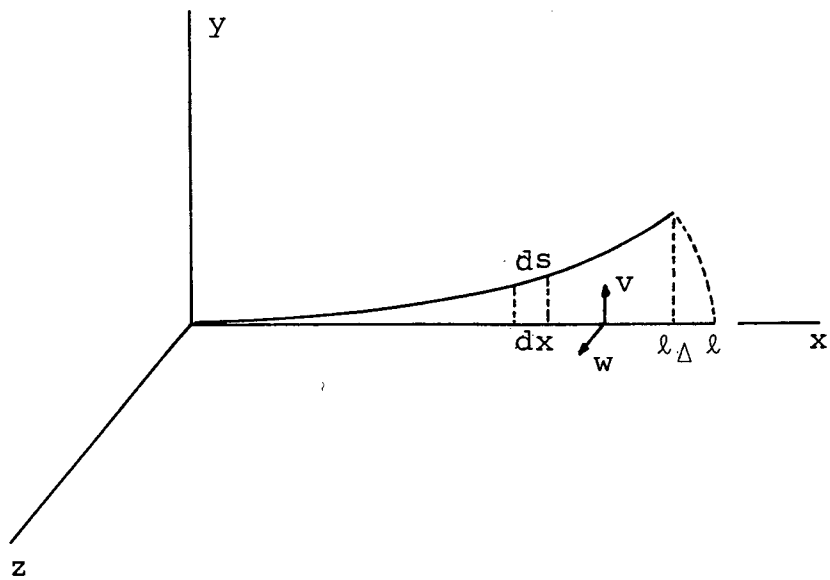

Figure 3-1 Beam axial foreshortening caused by transverse deformations v, w.

As indicated, a number of different methods have been devised to deal with this difference. For the problem of rotating beam vibration Hurty et al. (1964)[229] and Meirovitch (1967)[230] consider the effect as a working axial displacement (ds - dx) acting on the centrifugal loading. It is introduced through the limits of inte-

gration by Hughes and Fung (1971)[156] as:

$$\int_0^{\ell} f(s)\, ds = \int_0^{\ell_\Delta} f(x)\, [1 + \tfrac{1}{2}(v_x^2 + w_x^2)]\, dx + H.O.T.; \quad (3.3)$$

where:

$f(s)$ = any arbitrary function of location (s) along the neutral axis at any instant;

ℓ_Δ = instantaneous beam length as measured along the x axis, $\ell - \Delta$;

$\Delta \simeq \frac{1}{2} \int_0^{\ell} (v_x^2 + w_x^2)\, dx; \quad v_x = \frac{\partial v}{\partial x}, \quad w_x = \frac{\partial w}{\partial x};$

H.O.T.= higher order terms.

Vigneron (1975),[133] on the other hand, includes it directly as a contribution to the assumed axial displacement field equal to:

$$u_{fs} \simeq \frac{1}{2} \int_0^{x} (v_\alpha^2 + w_\alpha^2)\, d\alpha. \quad (3.4)$$

The differing approaches suggested by equations (3.3) and (3.4) can be shown to yield identical results. Defining

$$\eta = x + u_{fs}, \quad (3.5)$$

it follows that

at $x = 0$; $u_{fs} = 0$, $\eta = 0$;

and at $x = \ell - \Delta$; $u_{fs} = \Delta$; $\eta = \ell$.

Therefore:

$$d\eta = dx + du_{fs} = [1 + \tfrac{1}{2}(v_x^2 + w_x^2)]\, dx.$$

Substituting in (3.3) gives the following relation valid to 2nd degree in v, w,

$$\int_0^{\ell} f(s)ds = \int_0^{\ell-\Delta} f(x)[1 + \frac{1}{2}(v_x^2 + w_x^2)]dx = \int_0^{\ell} f(\eta - u_{fs})d\eta . \tag{3.6}$$

Clearly the foreshortening can be dealt with by considering it to be an additional displacement $-u_{fs}$, thus justifying the assumption of Vigneron.[133] Kaza and Kvaternik (1977)[136] point out that this effect can be dealt with implicitly by working with nonlinear strain-displacement relations but a linear displacement field. This latter approach requires that one retain terms through fourth degree in the energy expressions in order to obtain the 2^{nd} degree equations. For the purpose of this thesis the use of a modified displacement is preferred as terms only up to 3^{rd} degree are necessary.[136] However, in order to apply this method to a beam of variable cross-section, the theorem of Appendix (IV) is required as well.

It is worth noting that to obtain even the linear vibration equations for a rotating beam, one must take into account geometric nonlinearities[136] thus again emphasizing the significance of foreshortening terms. The implicit approach of using nonlinear strain-displacement relations was demonstrated by Likins (1973)[130] and Samin and Willems (1975).[92]

3.2.3 Kinetic energy density

Kinetic energy terms associated with appendage oscillations are already implicit in equation (2.4). Here they are expanded for a beam-type appendage. As the formulation is with respect to the overall system center of mass the vibrations are unaffected by the orbital motion.

Consequently, kinetic energy associated with the flexible behaviour of the i^{th} appendage can be expressed as

$$T_i = \{\omega\}^T \int_{m_i} [\tilde{r}_{d,i}] \{V_{O,i}\} \, dm_i + \frac{1}{2} \int_{m_i} \{V_{O,i}\}^T \{V_{O,i}\} \, dm_i . \tag{3.7}$$

Substituting for the angular velocity, deployment velocity, position vector, etc. in terms of local coordinates, expanding, and omitting the subscript i which denotes the i^{th} appendage; the kinetic energy to 3^{rd} degree can be written as

$$\begin{aligned}
T = \frac{1}{2} \int_0^{\ell} \rho \{ & (\pi_{1,t} + u_t + Uu_x)^2 \\
& + (\pi_{2,t} + v_t + Uv_x)^2 + (\pi_{3,t} + w_t + Uw_x)^2 \\
& + U[2(\pi_{1,t} + u_t) + U(1 + 2u_x)] \\
& - 2[\pi_{1,t} + u_t + U(1+u_x)] \, (u_{fs,t} + Uu_{fs,x}) \\
& + [(\pi_2 + v)^2 + (\pi_3 + w)^2] \, \omega_1^2 \\
& + [(\pi_1 + x + u)^2 + (\pi_3 + w)^2 - 2(\pi_1 + x + u) \, u_{fs}] \, \omega_2^2 \\
& + [(\pi_1 + x + u)^2 + (\pi_2 + v)^2 - 2(\pi_1 + x + u) \, u_{fs}] \, \omega_3^2 \\
& - 2[(\pi_1 + x + u - u_{fs})(\pi_2 + v) \, \omega_1\omega_2 + (\pi_3 + w) \, \omega_2\omega_3 \\
& \qquad + (\pi_1 + x + u - u_{fs})(\pi_3 + w) \, \omega_1\omega_3]
\end{aligned}$$

$$+ \; 2[\pi_{1,t} + (u_t + Uu_x) - (u_{fs,t} + Uu_{fs,x}) + U][\pi_3$$

$$+ \; w)\omega_2 - (\pi_2 + v)\omega_3]$$

$$+ \; 2(\pi_{2,t} + v_t + Uv_x)[(\pi_1 + x + u - u_{fs})\omega_3 - (\pi_3 + w)\omega_1]$$

$$+ \; 2(\pi_{3,t} + w_t + Uwx)[(\pi_2 + v)\omega_1 - (\pi_1 + x + u - u_{fs})\omega_2]\}dx$$

$$= \int_m \tilde{T}\,(x, \varepsilon, \varepsilon_x, \varepsilon_{xx}, \varepsilon_t, \varepsilon_{xt}, t)\, dm, \qquad (3.8)$$

where

ε = generalized coordinate of the continuum, u, v, or w in this case.

3.2.4 Potential energy density

The appendage being studied is under the influence of two conservative force fields: one the result of a variation in strength of the gravitational force distributed over the body, the other a consequence of the elastic restoring moments present during bending.

3.2.4.1 Strain energy

A general expression for the elastic strain energy for a homogeneous isotropic continuum with no dissipative elements but experiencing large strains is:

$$V_e = \frac{1}{2}\iiint \sigma^{*T}\ \varepsilon_s\ dxdydz; \qquad (3.9)$$

where:

σ^{*T} = transpose of generalized stress tensor;

ε_s = strain tensor.

Strain can be taken small while still allowing for large relative deflection and rotation within the system. For the case of small strains, Hooke's Law can be introduced into equation (3.9) giving [Likins et al. (1973)[130]]:

$$V_e = \frac{1}{2}\iiint \varepsilon_s^T E \varepsilon_s \, dxdydz; \tag{3.10}$$

where:

E = Young's modulus for the material.

Green's strain tensor is developed for a slender one-dimensional Euler-Bernoulli beam by Kaza and Kvaternik (1977)[136], giving strain as a function of displacement. Only the axial strain is relevant here. Foreshortening is introduced explicitly as in the evaluation of kinetic energy so that, using the beam coordinates of Figure 2-2:

$$\varepsilon_{s,11} = (u-u_{fs})_x + \frac{1}{2}\left[(u-u_{fs})_x^2 + v_x^2 + w_x^2\right];$$

$$= u_x - yv_{xx} - zw_{xx} + \frac{1}{2}(u_x - yv_{xx} - zw_{xx})^2; \tag{3.11}$$

and

$$\varepsilon_{s,22} = \varepsilon_{s,33} = \varepsilon_{s,12} = \varepsilon_{s,13} = \varepsilon_{s,23} = 0.$$

Squaring (3.11),

$$\varepsilon_{s,11}^2 = u_x^2 + y^2 v_{xx} + z^2 w^2_{xx} - 2u_x (yv_{xx} + zw_{xx})$$

$$+ 2yzv_{xx}w_{xx} + u_x^3 - 3u_x^2 (yv_{xx} + zw_{xx})$$

$$+ \quad 3u_x \left(y^2 v_{xx}^2 + z^2 w_{xx}^2 + 2yz v_{xx} w_{xx}\right)$$

$$- \quad y^3 v_{xx}^3 - z^3 w_{xx}^3 - 3yz^2 v_{xx} w_{xx}^2 - 3y^2 z v_{xx}^2 w_{xx}$$

$$+ \quad \text{H.O.T.} \tag{3.12}$$

Substituting this result into (3.10), integrating, and taking advantage of the one-dimensional character of the system

$$\iint y\,dydz = \iint z\,dydz = \iint yz\,dydz \simeq 0,$$

gives the potential due to flexure to the 3rd degree

$$V_e \simeq \frac{1}{2} \int_0^{\ell} E\left[A\left(u_x^2 + u_x^3\right) + \left(1 + 3u_x\right)\left(J_{22} w_{xx}^2 + J_{33} v_{xx}^2\right)\right] dx, \tag{3.13}$$

where:

$E = E(x)$;

$A(x)$ = beam cross sectional area, $\iint dydz$;

$J_{22} = \iint z^2\,dydz$;
$J_{33} = \iint y^2\,dydz$;
} cross sectional area moments of inertia.

3.2.4.2 Gravitational potential

To the 2nd degree in (r_i/R_c), the gravitational potential of any body with finite dimensions is given by equation (2.6) as:

$$V_g = -\frac{\mu m_s}{R_c}$$

$$+ \frac{\mu}{2R_c^3}\left\{3\{\chi_a\}^T [\chi_i]^T [I_i^{(i)}] [\chi_i] \{\chi_a\}\right.$$

$$- \text{tr}\left([\chi_i]^T\,[I_i^{(i)}]\,[\chi_i]\right)\Big\}. \qquad (3.14)$$

In order to derive governing appendage equations of motion this expression is expanded using local appendage coordinates. Axial foreshortening is introduced explicitly in the displacement field as discussed in the previous sections. Also, use is made of the integral theorem from Appendix (IV). The potential related to motion of the center of mass is uncoupled from flexibility and thus is ignored. Extending the energy density concept to moments of inertia, one can write, for a given appendage:

$$I_{jk} = \int_{D_i} \tilde{I}_{jk}\, dDi. \qquad (3.15)$$

Using this definition one is provided with a concise description of the vibration-related gravitational potential,

$$\tilde{V}_g = \left(\frac{\mu}{2R_c^3}\right)\left(c_{11}\tilde{I}_{11} + c_{22}\tilde{I}_{22} + c_{33}\tilde{I}_{33} + c_{12}\tilde{I}_{12} + c_{13}\tilde{I}_{13} + c_{23}\tilde{I}_{23}\right), \qquad (3.16)$$

where, for clarity the subscript i is omitted for the i^{th} appendage, and j, k are dummy indices referring to the local x_i, y_i, z_i axes of any given appendage as 1, 2, 3, respectively. Also

c_{jk} = coefficient identifying appendage orientation relative to the local vertical $\underline{R}_c$.

For convenience let:

$$\alpha_1 = (3\chi_{a,1}^2 - 1);$$

$$\alpha_2 = (3\chi_{a,2}^2 - 1);$$

$$\alpha_3 = (3\chi_{a,3}^2 - 1);$$

$$\alpha_4 = \chi_{a,1}\,\chi_{a,2};$$

$$\alpha_5 = \chi_{a,1}\,\chi_{a,3};$$

$$\alpha_6 = \chi_{a,2}\,\chi_{a,3}. \qquad (3.17)$$

Then:

$$c_{jj} = \alpha_1\chi_{j1}^2 + \alpha_2\chi_{j2}^2 + \alpha_3\chi_{j3}^2 + 6(\alpha_4\chi_{j1}\chi_{j2} + \alpha_5\chi_{j1}\chi_{j3} + \alpha_6\chi_{j2}\chi_{j3}), \qquad (3.18a)$$

$$j = 1, 2, 3;$$

$$c_{12} = -2(\alpha_1\chi_{11}\chi_{21} + \alpha_2\chi_{12}\chi_{22} + \alpha_3\chi_{13}\chi_{23})$$

$$-6[\alpha_4(\chi_{11}\chi_{22} + \chi_{12}\chi_{21}) + \alpha_5(\chi_{11}\chi_{23} + \chi_{13}\chi_{21}) + \alpha_6(\chi_{12}\chi_{23} + \chi_{13}\chi_{22})];$$

$$c_{13} = -2(\alpha_1\chi_{11}\chi_{31} + \alpha_2\chi_{12}\chi_{32} + \alpha_3\chi_{13}\chi_{33})$$

$$-6[\alpha_4(\chi_{11}\chi_{32} + \chi_{12}\chi_{31}) + \alpha_5(\chi_{11}\chi_{33} + \chi_{13}\chi_{31}) + \alpha_6(\chi_{12}\chi_{33} + \chi_{13}\chi_{32});$$

$$c_{23} = -2(\alpha_1\chi_{23}\chi_{31} + \alpha_2\chi_{22}\chi_{32} + \alpha_3\chi_{23}\chi_{33})$$

$$-6[\alpha_4(\chi_{21}\chi_{32} + \chi_{22}\chi_{31}) + \alpha_5(\chi_{21}\chi_{33} + \chi_{23}\chi_{31})$$

$$+ \alpha_6(\chi_{22}\chi_{33} + \chi_{23}\chi_{32}). \qquad (3.18b)$$

Substituting the inertia densities from Appendix II, equation (II.6), into (3.16) yields the following expression for gravitational potential applicable to a beam-type appendage having an arbitrary orientation in space:

$$\begin{aligned}\tilde{V}_g = {} & \left(\frac{\rho\mu}{2R_c^3}\right) \{(c_{22} + c_{33})\ (x + u)^2 \\ & + [2(c_{22}+c_{33})\pi_1 + c_{12}(\pi_2+v) + c_{13}(\pi_3+w)]\ (x+u) \\ & + [c_{12}\pi_1 + (c_{11}+c_{23})\ (2\pi_2+v) + c_{23}\pi_3]v \\ & + [c_{13}\pi_1 + c_{23}(\pi_2+v) + (c_{11}+c_{22})(2\pi_3+w)]w\} \\ & - \left\{\left(\frac{\mu}{2R_c^3}\right) \int_x^{\ell} \rho[2(c_{22}+c_{33})(\pi_1+\alpha+u) + c_{12}(\pi_2+v) \right. \\ & \left. + c_{13}(\pi_3+w)]\, d\alpha\right\} \left(\frac{v_x^2+w_x^2}{2}\right). \qquad (3.19)\end{aligned}$$

By inspection one appreciates the considerable simplifications possible if general orientation and offset terms are not present. Of course, the complexity is further reduced if the equation is carried just to the 2nd degree.

3.3 Nonlinear Equations Governing Transverse and Axial Vibrations

To start with, applying Hamilton's Principle (Appendix V) leads to an equivalent set of Lagrange equations appropriate for this system. Making use of the energy expressions developed for

such a beam-type appendage, together with the theorem of Appendix IV, one can establish the Lagrangian density of the beam. That is, in this case:

$\tilde{L}$ = the difference between the kinetic and potential energy per unit length;

$$= \tilde{T} - \tilde{V} = \tilde{L}\,(x, \varepsilon, \varepsilon_x, \varepsilon_{xx}, \varepsilon_{xt}, \varepsilon_t, t). \tag{3.20}$$

Substituting (3.20) into the Lagrange equations discussed above yields the 2nd degree equations for vibration:

axial oscillation ($\varepsilon = u$)

$$\begin{aligned}
&\rho\{u_{tt} - u_{fs,tt} + 2U(u_{xt} - u_{fs,xt}) + \dot{U}(u_x - u_{fs,x}) \\
&\quad + U^2(u_{xx} - u_{fs,xx}) + \dot{U} + \pi_{1,tt} \\
&\quad - [\omega_2^2 + \omega_3^2 - 2(c_{22} + c_{33})(\mu/2R_c^3)]\,(\pi_1 + x + u - u_{fs}) \\
&\quad + [-\omega_{3,t} + \omega_1\omega_2 + c_{12}\,(\mu/2R_c^3)](\pi_2 + v) \\
&\quad + [\omega_{2,t} + \omega_1\omega_3 + c_{13}(\mu/2R_c^3)](\pi_3 + w) - 2\,\omega_3(\pi_{2,t} + v_t \\
&\quad + Uv_x) + 2\omega_2\,(\pi_{3,t} + w_t + Uw_x)\} \\
&\quad + \rho_x U\,[u_t - u_{fs,t} + U(u_x - u_{fs,x}) + U + \pi_{1,t} \\
&\qquad\qquad - \omega_3(\pi_2 + v) + \omega_2(\pi_3 + w)] \\
&\quad - \tfrac{1}{2}\{(EA)_x(2 + 3u_x)u_x + 3[(EJ_{33})_x v_{xx}^2 + (EJ_{22})_x w_{xx}^2]\}
\end{aligned}$$

$$- E[A(1 + 3u_x)u_{xx} + 3(J_{33}v_{xx}v_{xxx} + J_{22}w_{xx}w_{xxx})] = F_1; \tag{3.21a}$$

transverse oscillation ($\varepsilon = v$)

$$\rho\{v_{tt} + 2Uv_{xt} + \dot{U}v_x + U^2v_{xx} + \pi_{2,tt}$$

$$+ [\omega_{3,t} + \omega_1\omega_2 + c_{12}(\mu/2R_c^3)](\pi_1 + x + u - u_{fs})$$

$$- [\omega_1^2 + \omega_3^2 - 2(c_{11} + c_{33})(\mu/2R_c^3)](\pi_2 + v)$$

$$+ [-\omega_{1,t} + \omega_2\omega_3 + c_{23}(\mu/2R_c^3)](\pi_3 + w)$$

$$+ 2\omega_3 [\pi_{1,t} + u_t - u_{fs,t} + U(u_x - u_{fs,x}) + U]$$

$$- 2\omega_1 (\pi_{3,t} + w_t + Uw_x)\}$$

$$+ \rho_x U [v_t + Uv_x + \pi_{2,t} + \omega_3(\pi_1 + x + u - u_{fs}) - \omega_1(\pi_3 + w)]$$

$$- (F_A v_x)_x + (EJ_{33}v_{xx})_{xx} (1 + 3u_x)$$

$$+ 3[2 (EJ_{33}v_{xx})_x u_{xx} + EJ_{33}v_{xx}u_{xxx}] = F_2; \tag{3.21b}$$

transverse oscillation ($\varepsilon = w$)

$$\rho\{w_{tt} + 2Uw_{xt} + \dot{U}w_x + U^2w_{xx} + \pi_{3,tt}$$

$$+ [-\omega_{2,t} + \omega_1\omega_3 + c_{13}(\mu/2R_c^3)](\pi_1 + x + u - u_{fs})$$

$$+ [\omega_{1,t} + \omega_2\omega_3 + c_{23}(\mu/2R_c^3)](\pi_2 + v)$$

$$- [\omega_1^2 + \omega_2^2 - 2(c_{11} + c_{22})(\mu/2R_c^3)](\pi_3 + w)$$

$$- \; 2\omega_2[\pi_{1,t} + u_t - u_{fs,t} + U(u_x - u_{fs,x}) + U]$$

$$+ \; 2\omega_1(\pi_{2,t} + v_t + Uv_x)\}$$

$$+ \; \rho_x U[\pi_{3,t} + w_t + Uw_x - \omega_2(\pi_1 + x + u - u_{fs}) + \omega_1(\pi_2 + v)]$$

$$- \; (F_A W_x)_x + (EJ_{22} w_{xx})_{xx} \; (1 + 3u_x)$$

$$+ \; 3[2(EJ_{22} w_{xx})_x u_{xx} + EJ_{22} w_{xx} u_{xxx}] = F_3; \qquad (3.21c)$$

where:

F_A = an effective axial load resulting from the inertial and gravitational force field

$$= \int_x^{\ell} \Big\{ \rho \{-\pi_{1,tt} - u_{tt} - 2Uu_{\alpha t} - \dot{U}u_\alpha$$

$$- \; U^2 u_{\alpha\alpha} - \dot{U}$$

$$+ \; [\omega_2{}^2 + \omega_3{}^2 - 2(c_{22} + c_{33})(\mu/2R_c{}^3)](\pi_1 + \alpha + u)$$

$$+ \; [\omega_{3,t} - \omega_1\omega_2 - c_{12}(\mu/2R_c{}^3)](\pi_2 + v)$$

$$- \; [\omega_{2,t} + \omega_1\omega_3 + c_{13}(\mu/2R_c{}^3)](\pi_3 + w)$$

$$+ \; 2\omega_3(\pi_{2,t} + v_t + Uv_\alpha) - 2\omega_2(\pi_{3,t} + w_t + Uw_\alpha)\}$$

$$- \; \rho_\alpha U[\pi_{1,t} + u_t + Uu_\alpha + U - \omega_3(\pi_2 + v) + \omega_2(\pi_3 + w)]\Big\} d\alpha.$$

(3.21d)

Here $(\dot{})$ = total time rate of change as measured in local coordinates, $\frac{\partial()}{\partial t} + U\frac{\partial()}{\partial x}$.

All components are derived with respect to the local x_i, y_i, z_i axes as indicated by subscripts 1, 2, 3, respectively.

As in the case of general librational motion, the equations governing translational oscillations of the elastic appendages are also seen to be nonlinear, nonautonomous, and coupled. Together, the librational and vibrational degrees of freedom form a conjugate system hence, they must be solved simultaneously. As can be expected, the overall system is too complex to be amenable to any closed-form solution.

The essential features included when modelling the oscillations of a beam-type appendage are summarized below:

- arbitrary trajectory;
- gravitational effects;
- 3-axis librations;
- shifting center of mass;
- geometric offset of appendage point of attachment from the mass center;
- transverse as well as axial oscillations;
- nonlinear (2^{nd} degree) effects;
- variable mass density, flexural rigidity, and area of the beam cross-section;
- arbitrary deployment velocity and deployment acceleration;
- arbitrary appendage orientation.

4. SIMPLIFIED APPENDAGE DYNAMICS

4.1 Linearized Equations for Transverse Vibrations of a Deploying, Orbiting Beam-Type Appendage

The second degree vibration equations of Chapter 3 are extremely involved making even a numerical solution elusive in the general case.[227,228] Through linearization and considering the appendage to be uniform the problem becomes somewhat more tractable. This, together with the realistic assumption of axial rigidity as well as continuity considerations, result in the deployment velocity being uniform along the length of the appendage [Tabarrok et al. (1974)[222]], i.e. $U(x,t) = U(t) = \dot{\ell}(t)$ and $\frac{dU(x,t)}{dt} = \dot{U}(t) = \ddot{\ell}(t)$. Application of such considerations to equation (3.21) leads to the governing first degree equations for the i^{th} appendage in the v and w degrees of freedom

$$\rho\{v_{tt} + 2\dot{\ell}v_{xt} + \ddot{\ell}v_x + \dot{\ell}^2 v_{xx} + \pi_{2,tt}$$

$$+ \gamma_1 (x + \pi_1) - \gamma_2 (v + \pi_2) + \gamma_3 (w + \pi_3)$$

$$+ 2\omega_3 (\pi_{1,t} + \dot{\ell}) - 2\omega_1 (\pi_{3,t} + w_t + \dot{\ell}w_x)\}$$

$$- (F_A v_x)_x + EJ_{33} v_{xxxx} = F_2; \qquad (4.1a)$$

$$\rho\{w_{tt} + 2\dot{\ell}w_{xt} + \ddot{\ell}w_x + \dot{\ell}^2 w_{xx} + \pi_{3,tt}$$

$$+ \gamma_4 (x + \pi_1) + \gamma_5 (v + \pi_2) - \gamma_6 (w + \pi_3)$$

$$- 2\omega_2 (\pi_{1,t} + \dot{\ell}) + 2\omega_1 (\pi_{2,t} + v_t + \dot{\ell}v_x)\}$$

$$- (F_A w_x)_x + EJ_{22} w_{xxxx} = F_3. \tag{4.1b}$$

Here:

$$\gamma_0 = \mu/2R_c^3;$$

$$\gamma_1 = \dot{\omega}_3 + \omega_1\omega_2 + c_{12}\gamma_0;$$

$$\gamma_2 = \omega_1^2 + \omega_3^2 - 2(c_{11} + c_{33})\gamma_0;$$

$$\gamma_3 = -\dot{\omega}_1 + \omega_2\omega_3 + c_{23}\gamma_0;$$

$$\gamma_4 = -\dot{\omega}_2 + \omega_1\omega_3 + c_{13}\gamma_0;$$

$$\gamma_5 = \dot{\omega}_1 + \omega_2\omega_3 + c_{23}\gamma_0;$$

$$\gamma_6 = \omega_1^2 + \omega_2^2 - 2(c_{11} + c_{22})\gamma_0;$$

$$\gamma_7 = \omega_2^2 + \omega_3^2 - 2(c_{22} + c_{33})\gamma_0;$$

$$\gamma_8 = \dot{\omega}_3 - \omega_1\omega_2 - c_{12}\gamma_0;$$

$$\gamma_9 = \dot{\omega}_1 + \omega_1\omega_3 + c_{13}\gamma_0;$$

$$\gamma_{10} = -\pi_{1,tt} - \ddot{\ell} + \gamma_7\pi_1 + \gamma_8\pi_2 + \gamma_9\pi_3 + 2\omega_3\pi_{2,t} - 2\omega_2\pi_{3,t};$$

$$\gamma_{11} = \gamma_{10} + \ddot{\ell};$$

$$F_A = \rho[\gamma_{10}(\ell - x) + (\tfrac{1}{2})\gamma_7 (\ell^2 - x^2)]. \tag{4.1c}$$

The number of parameters can be reduced by use of a nondimensional form of the equations. Defining:

$$\hat{x} = x/\ell; \qquad \hat{t} = \dot{\theta}t;$$
$$\hat{v} = v/\ell; \qquad \hat{w} = w/\ell;$$
$$\dot{\theta} = h_\theta/R_c^2; \qquad \ddot{\theta} = -2\dot{\theta}^2 es\theta/(1 + ec\theta); \tag{4.2}$$

and substituting into (4.1) yields:

$$\begin{aligned}
&\hat{v}_{\theta\theta} + 2(\hat{\ell}' - e_1)\hat{v}_\theta + 2\hat{\ell}'\hat{v}_{\hat{x}\theta} \\
&\quad + (\hat{\ell}'' - 2e_1\hat{\ell}' - \gamma_2)\hat{v} \\
&\quad + (\hat{\ell}'' - 2e_1\hat{\ell}' + 2\hat{\ell}'^2 + \gamma_7\hat{x} + \gamma_{10})\hat{v}_{\hat{x}} \\
&\quad + [\hat{\ell}'^2 - \gamma_{10}(1 - \hat{x}) - \tfrac{1}{2}\gamma_7(1 - \hat{x}^2)]\hat{v}_{\hat{x}\hat{x}} \\
&\quad + (EJ_{33}/\rho\dot{\theta}^2\ell^4)\hat{v}_{\hat{x}\hat{x}\hat{x}\hat{x}} \\
&\quad - 2\omega_1\hat{w}_\theta - (2\hat{\ell}'\omega_1 - \gamma_3)\hat{w} - 2\hat{\ell}'\omega_1\hat{w}_{\hat{x}} \\
&\quad + \gamma_1\hat{x} + \mu_2 = F_2/\rho\dot{\theta}^2\ell;
\end{aligned} \tag{4.3a}$$

$$\begin{aligned}
&\hat{w}_{\theta\theta} + 2(\hat{\ell}' - e_1)\hat{w}_\theta + 2\hat{\ell}'\hat{w}_{\hat{x}\theta} \\
&\quad + (\hat{\ell}'' - 2e_1\hat{\ell}' - \gamma_6)\hat{w} \\
&\quad + (\hat{\ell}'' - 2e_1\hat{\ell}' + 2\hat{\ell}'^2 + \gamma_7\hat{x} + \gamma_{10})\hat{w}_{\hat{x}} \\
&\quad + [\hat{\ell}'^2 - \gamma_{10}(1 - \hat{x}) - \tfrac{1}{2}\gamma_7(1 - \hat{x}^2)]\hat{w}_{\hat{x}\hat{x}} \\
&\quad + (EJ_{22}/\rho\dot{\theta}^2\ell^4)\hat{w}_{\hat{x}\hat{x}\hat{x}\hat{x}}
\end{aligned}$$

$$+ \quad 2\omega_1\hat{v}_\theta + (2\omega_1\hat{\ell}' + \gamma_5)\hat{v} + 2\omega_1\hat{\ell}'\hat{v}_{\hat{x}}$$

$$+ \quad \gamma_4\hat{x} + \mu_3 = (F_3/\rho\dot{\theta}^2\ell); \qquad (4.3b)$$

where γ_j, ω_j (j = 0, ... , (11)) expressed using 'θ' as a measure of time are based on equations 2.5, 4.1c, 4.2; and:

$(\dot{\ })$ = d( )/dt;

$(\ )'$ = d( )/dθ;

$(\ )_{\hat{x}}$ = ∂( )/$\partial\hat{x}$;

$(\hat{\ })$ = ( )/ℓ, except note $\hat{\ell}' = \ell'/\ell$, $\hat{\ell}'' = \ell''/\ell$;

e_1 = esθ/(1 + ecθ);

$$\mu_2(\theta) = \hat{\pi}_2'' + 2(\hat{\ell}' - e_1)\hat{\pi}_2' - 2e_1\hat{\ell}'\hat{\pi}_2 + 2\omega_3(\hat{\pi}_1' + \hat{\ell}' - \hat{\pi}_1 + \hat{\ell}')$$

$$- 2\omega_3(\hat{\pi}_3' + \hat{\ell}'\hat{\pi}_3) + \gamma_1\hat{\pi}_1 + (\hat{\ell}'' - \gamma_2)\hat{\pi}_2 + \gamma_3\hat{\pi}_3;$$

$$\mu_3(\theta) = \hat{\pi}_3'' + 2(\hat{\ell}' - e_1)\hat{\pi}_3'' - 2e_1\hat{\ell}'\hat{\pi}_3 - 2\omega_2(\hat{\pi}_1' + \hat{\ell}'\hat{\pi}_1 + \hat{\ell}')$$

$$+ 2\omega_1(\hat{\pi}_2' + \hat{\ell}'\hat{\pi}_2) + \gamma_4\hat{\pi}_1 + \gamma_5\hat{\pi}_2 - \gamma_6\hat{\pi}_3. \qquad (4.3c)$$

4.2 Solution of the Linearized Vibration Equations

The assumed-mode approach is adopted to solve equations (4.3) as explained by Meirovitch (1967).[230] A careful truncation of the number of modes used can effect a considerable reduction in the order of the system without sacrificing essential dynamical characteristics. Elastic displacements are represented here by a linear combination of known functions of the spatial variable $\hat{x}$ multiplied by time-dependent generalized coordinates as follows:

$$\hat{v}(\hat{x},\theta) = \sum_n E_n(\hat{x})\xi_n(\theta);$$

$$\hat{w}(\hat{x},\theta) = \sum_n H_n(\hat{x})\zeta_n(\theta) \qquad (4.4)$$

Care must be exercised when evaluating such derivatives as

$$\frac{\partial \hat{v}}{\partial \theta} = \left.\frac{\partial \hat{v}}{\partial \theta}\right|_{x \text{ fixed}} = \left.\frac{\partial \hat{v}}{\partial \theta}\right|_{\hat{x} \text{ fixed}} + \frac{\partial \hat{v}}{\partial \hat{x}} \frac{\partial \hat{x}}{\partial \theta},$$

since for a deploying system

$$\frac{\partial \hat{x}}{\partial \theta} = -\hat{\ell}'\hat{x} \neq 0 ;$$

in general.

Spatial dependence of the coefficients in the equations can be replaced by constant coefficients dependent only on the selected E_n, H_n. The procedure involves multiplying throughout by the m^{th} assumed mode shape and integrating the equation for the v_i, w_i degrees of freedom over the domain $\hat{x} = 0\text{-}1$. The resulting equations can be expressed in the following matrix form;

$$\{\xi''\} + 2([B_{20,E}]\hat{\ell}' - [B_{1,E}]e_1)\{\xi'\} + [K_2]\{\xi\} - 2\omega_1[B_{1,H}]\{\zeta'\}$$

$$+ (\gamma_3[B_{1,H}] - 2\omega_1\hat{\ell}'[B_{20,H}])\{\zeta\} = \{f_2\}; \qquad (4.5a)$$

$$\{\zeta''\} + 2([B_{20,H}]\hat{\ell}' - [B_{1,H}]e_1)\{\zeta'\} + [K_3]\{\zeta\} + 2\omega_1[B_{1,H}]\{\xi'\}$$

$$+ (\gamma_5[B_{1,E}] + 2\omega_1\hat{\ell}'[B_{20,E}])\{\xi\} = \{f_3\}; \qquad (4.5b)$$

where:

$$[K_2] = \hat{\ell}''[B_{31,E}] + \hat{\ell}'^2[B_{29,E}] + 2e_1\hat{\ell}'[B_{32,E}] + \gamma_{11}[B_{10,E}] + \tfrac{1}{2}\gamma_7[B_{11,E}] - \gamma_2[B_{1,E}] + \left(\frac{EJ_{33}}{\rho\dot{\theta}^2\ell^4}\right)[B_{0,E}];$$

$$[K_3] = \hat{\ell}''[B_{31,H}] + \hat{\ell}'^2[B_{29,H}] + 2e_1\hat{\ell}'[B_{32,H}] + \gamma_{11}[B_{10,H}] + \tfrac{1}{2}\gamma_7[B_{11,H}] - \gamma_6[B_{1,H}] + \left(\frac{EJ_{22}}{\rho\dot{\theta}^2\ell^4}\right)[B_{0,H}];$$

$$\{f_2\} = -\gamma_1\{C_{4,E}\} + (F_2/\rho\dot{\theta}^2\ell - \mu_2)\{C_{1,E}\};$$

$$\{f_3\} = -\gamma_4\{C_{4,H}\} + (F_3/\rho\dot{\theta}^2\ell - \mu_3)\{C_{1,H}\}; \qquad (4.5c)$$

with γ_j and μ_2, μ_3 given in equations (4.1c) and (4.3c), respectively. Modal coefficients $[B_j]$, $\{C_j\}$ are as defined in Appendix VI.

The analysis is simplified by taking the beam cross-section to be symmetric, i.e., $J_{22,i} = J_{33,i}$. Since the appendage is uniform as well, it is reasonable to assume similar shape functions in both the y_i and z_i directions. Ideally one would use the exact eigenfunctions for each boom in a manner similar to that employed in the component-mode synthesis technique.[126,127] However, as indicated in the introduction, the evaluation of such characteristics can be quite difficult and expensive for complex systems even if the eigenvalue problem can be clearly defined. The problem is further complicated by the fact that during deployment, system characteristics vary with time. Meirovitch et al. (1979)[193] have concluded that for any linear gyroscopic system it is sufficient to use a set of admissible functions provided they are complete. For a function to be considered admissible it must satisfy the geometric boundary conditions and be differentiable to order p for

a system of order 2p. In the particular case studied here a convenient set of modes are provided by the eigenfunctions of a simple uniform cantilevered beam $g_n(\hat{x})$,[231,232] which satisfy the following equation and boundary conditions.

$$g_{n,\hat{x}\hat{x}\hat{x}\hat{x}} - \beta_n^4 g_n = 0;$$

$$\beta_n^4 = \rho\Omega_n^2\ell^4/EJ;$$

$$g_n(0) = g_{n,\hat{x}}(0) = g_{n,\hat{x}\hat{x}}(1) = g_{n,\hat{x}\hat{x}\hat{x}}(1) = 0. \tag{4.6}$$

The solution of (4.6) and some of its properties are:

$$g_n(\hat{x}) = \cosh\beta_n\hat{x} - \cos\beta_n\hat{x} - \varrho_n(\sinh\beta_n\hat{x} - \sin\beta_n\hat{x});$$

$$\varrho_n = (\cosh\beta_n + \cos\beta_n)/(\sinh\beta_n + \sin\beta_n);$$

$$1 + \cosh\beta_n \cos\beta_n = 0;$$

$$\int_0^1 g_m g_n d\hat{x} = [B_1] = 0, \quad m \neq n;$$

$$= 1, \quad m = n. \tag{4.7}$$

Note,

$$E_n(\hat{x}) = H_n(\hat{x}) = g_n(\hat{x});$$

so that,

$$[B_{j,E}] = [B_{j,H}] = [B_j],$$

$$\{C_{j,E}\} = \{C_{j,H}\} = \{C_j\}. \tag{4.8}$$

The net result of this approach is to eliminate the spatial dependence transforming each partial differential equation into a time-dependent set of coupled ordinary differential equations for the discrete generalized coordinates.

Also, the following relations are useful when evaluating $\{r_c\}$, $\{h\}$, $\{\Gamma\}$, $[\dot{I}]$:

$$\hat{v}_t = \sum_n (g_n\dot{\xi}_n - \hat{x}\dot{\hat{\ell}}g_{n,\hat{x}}\xi_n);$$

$$\hat{v}_{\hat{x}t} = \sum_n [g_{n,\hat{x}}\dot{\xi}_n - \dot{\hat{\ell}}(g_{n,\hat{x}} + \hat{x}g_{n,\hat{x}\hat{x}})\xi_n];$$

$$\hat{v}_{tt} = \sum_n \{g_n\ddot{\xi}_n - 2\hat{x}\dot{\hat{\ell}}g_{n,\hat{x}}\dot{\xi}_n + [(2\dot{\hat{\ell}}^2 - \ddot{\hat{\ell}})\hat{x}g_{n,\hat{x}} + \hat{x}^2\dot{\hat{\ell}}^2 g_{n,\hat{x}\hat{x}}]\xi_n\};$$

$$v_t = \ell(\hat{v}_t + \dot{\hat{\ell}}\hat{v}) = \sum_n \ell[g_n\dot{\xi}_n + \dot{\hat{\ell}}(g_n - \hat{x}g_{n,\hat{x}})\xi_n];$$

$$v_{xt} = \dot{\hat{v}}_{\hat{x}t} + \dot{\hat{\ell}}\hat{v}_{\hat{x}} = \sum_n (g_{n,\hat{x}}\dot{\xi}_n - \hat{x}\dot{\hat{\ell}}g_{n,\hat{x}\hat{x}}\xi_n);$$

$$v_{tt} = (\hat{v}_{tt} + 2\dot{\hat{\ell}}\hat{v}_t + \ddot{\hat{\ell}}\hat{v});$$

$$= \sum_n \ell\{g_n\ddot{\xi}_n + 2\dot{\hat{\ell}}(g_n - \hat{x}g_{n,\hat{x}})\dot{\xi}_n + [\ddot{\hat{\ell}}(g_n - \hat{x}g_{n,\hat{x}}) + \hat{x}^2\dot{\hat{\ell}}^2 g_{n,\hat{x}\hat{x}}]\zeta_n\};$$

$$v_{xtt} = \hat{v}_{\hat{x}tt} + 2\dot{\hat{\ell}}\hat{v}_{\hat{x}t} + \ddot{\hat{\ell}}v_{\hat{x}};$$

$$= \sum_n \{g_{n,\hat{x}}\ddot{\xi}_n - 2\hat{x}\dot{\hat{\ell}}g_{n,\hat{x}\hat{x}}\dot{\xi}_n + [\dot{\hat{\ell}}^2(\hat{x}^2 g_{n,\hat{x}\hat{x}\hat{x}} + 2\hat{x}g_{n,\hat{x}\hat{x}})$$

$$- \hat{x}\ddot{\hat{\ell}}g_{n,\hat{x}\hat{x}}]\xi_n\}. \qquad (4.9)$$

4.3 'Free' Vibration Characteristics of Spinning, Deploying, Orbiting, Beam-Type Appendages

4.3.1 Governing equations

As discussed, both in section 4.2 and by Hughes and Garg (1973),[112] the use of 'exact' appendage modal characteristics may not be necessary when assessing potential interaction effects such as resonance, between the structural dynamics and the orbital, attitude, or control dynamics [Hughes and Sharpe (1975)[121]].

The high degree of coupling makes even a parametric numerical study difficult for equations (4.5). In order to obtain some appreciation as to the fundamental character of the vibrations, the simpler system of Figure 4-1 is examined. Here planar (pitch only) attitude motion is allowed. Neglecting offset and considering the vibrations to be free ($F_2 = F_3 = 0$), equations (4.5) can be expressed, for boom orientations $\phi_i = 0, \pi$ as:

$$\{\xi''\} + 2(\hat{\ell}'[B_{20}] - e_1[B_1])\{\xi'\} + ([K] - \omega_s^2[B_1])\{\xi\} = \{f\}; \tag{4.10a}$$

$$\{\zeta''\} + 2(\hat{\ell}'[B_{20}] - e_1[B_1])\{\zeta'\} + [K]\{\zeta\} = \{0\}; \tag{4.10b}$$

where:

$$[K] = \hat{\ell}''[B_{31}] + \hat{\ell}'^2[B_{29}] - 2e_1\hat{\ell}'[B_{32}] + \tfrac{1}{2}[(1 + \Phi')^2 + (\tfrac{1}{2} + \tfrac{3}{2}\,c2\Phi)][B_{11}] + (\hat{\Omega}_n^2 - 1)[B_1];$$

$$\omega_s^2 = (1 + \Phi')^2 + (\tfrac{1}{2} - \tfrac{3}{2}\,c2\Phi);$$

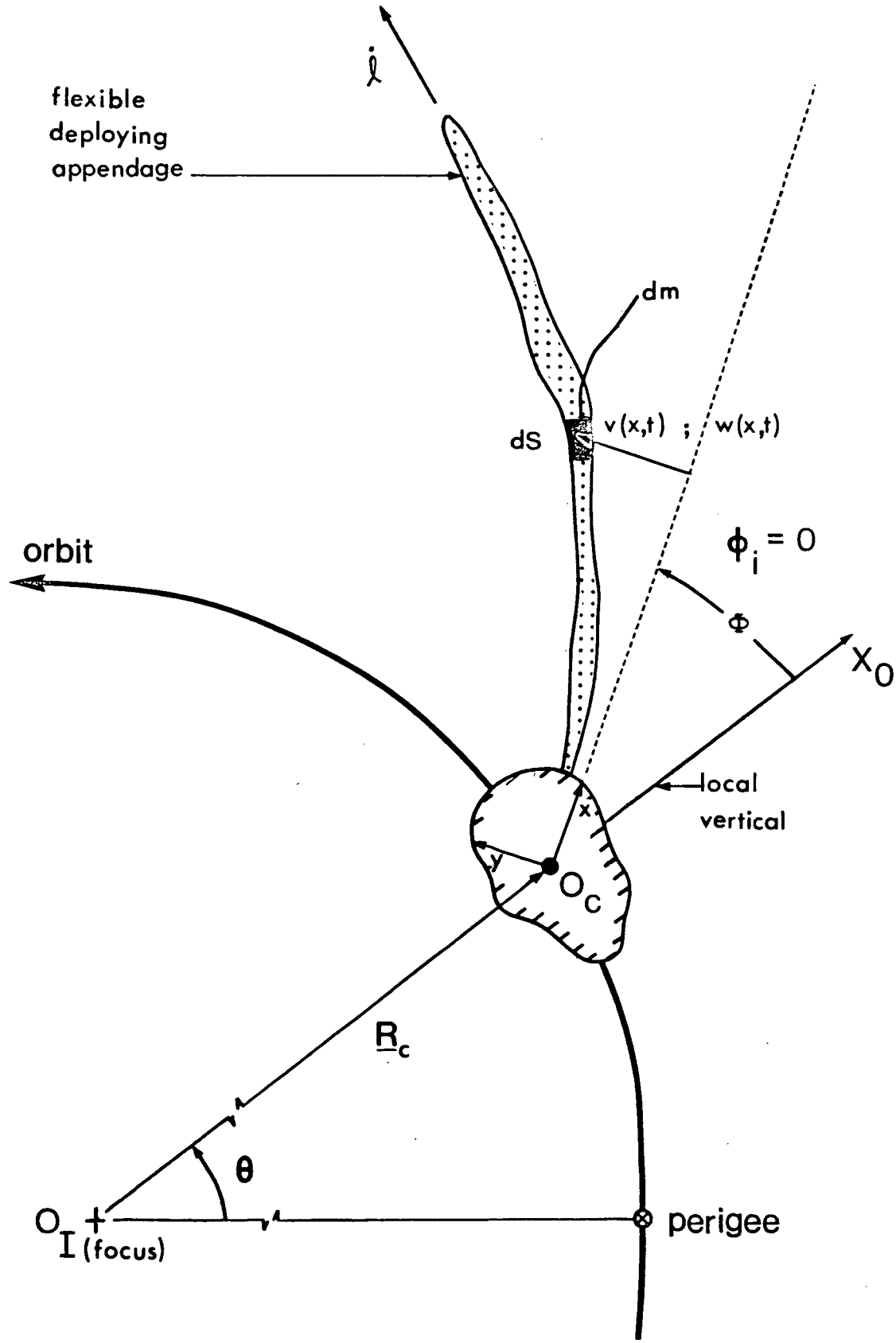

Figure 4-1 Model of deploying, orbiting, librating, beam-type appendage experiencing flexural oscillation both in [v(x,t)] and out [w(x,t)] of the orbital plane.

$$\hat{\Omega}_n^2 = (\Omega_n/\dot{\theta})^2;$$

$$\{f\} = -[\Phi'' - 2e_1(1 + \Phi') + \frac{3}{2} s2\Phi]\{C_4\} - 2(1 + \Phi')\hat{\ell}'\{C_1\}. \quad (4.10c)$$

Equations (4.10a, 4.10b), being coupled and non-autonomous are, in general, not amenable to any simple closed form solution. It is interesting to note that the equations are essentially similar in form. Effective spin (ω_s) resulting from orbital motion, pitch, and the gravity gradient serves to reduce stiffness for the in-plane coordinate ξ relative to out-of-plane motion ζ. Also, the in-plane degree of freedom experiences an additional loading resulting from the Coriolis force associated with deployment and rotation, forces due to spin acceleration, and those of the gravitational field. Deployment alters stiffness while introducing an effective negative damping into the system. Type of trajectory is specified through e_1.

A truncated set of the equations (4.10a, 4.10b) is treated as a discrete eigenvalue problem at any given instant in time. The right hand side is taken to be zero when solving for the 'free' eigenvalues and eigenfunctions. The analysis is carried out over a large range of parameter values. Of course, the characteristics found in this way are valid only over that period of time for which the coefficients can be considered constant [Lips and Modi (1978)[224]]. This technique also forms the basis for the 'quasi-modal' approach of Cherchas (1971).[212] A similar concept was presented by Worden (1980)[233] during a study of ship motions. The approach adopted here makes use of the eigenvalue analysis only to assess fundamental vibration characteristics and their parametric variation. Response is then based on a direct numerical integration.

4.3.2 Results and discussion

From the time of orbital injection until steady state attitude equilibrium is achieved, a satellite can experience high rates of spin resulting in a very significant influence on flexible appendage characteristics. Figure 4-2 demonstrates this effect, for in-plane vibration, in an efficient and compact manner by plotting frequency parameter $\beta_n^4 = \rho\Omega_n^2\ell^4/EJ$ over a large range of spin parameter values $\lambda_s^4 = \rho\omega_s^2\ell^4/EJ$. Note that with newer generation spacecraft increasingly employing longer members, spin parameter values will also tend to be larger than in the past. Equations 4.10 are truncated so as to include only the first three modes. The relationship between the eigenvalue and the spin parameter is essentially linear, i.e.,

$$\beta_n = k_n\lambda_s . \tag{4.11}$$

There is no need to plot the out-of-plane result since, comparing equations for the case of 'free' vibration and spin only:

$$\beta_{n,OP}^4 = \beta_{n,IP}^4 + \lambda_s^4 ; \tag{4.12}$$

as indicated in Table 4.1. The results allow one to assess the effect of variations in the natural vibration frequency (Ω_n), physical characteristics of the beam (ρ, EJ, ℓ), and spin rate. Note the dramatic changes which could occur in characteristic vibration frequencies and spin-up/spin-down.

For booms aligned along the local radius vector, $\underline{R}_c$, variations of the in-plane frequency parameter are not linear for small values of the spin parameter ($0 < \lambda_s < 6$), as indicated in Figure 4-3. Also, when the spin parameter results solely from

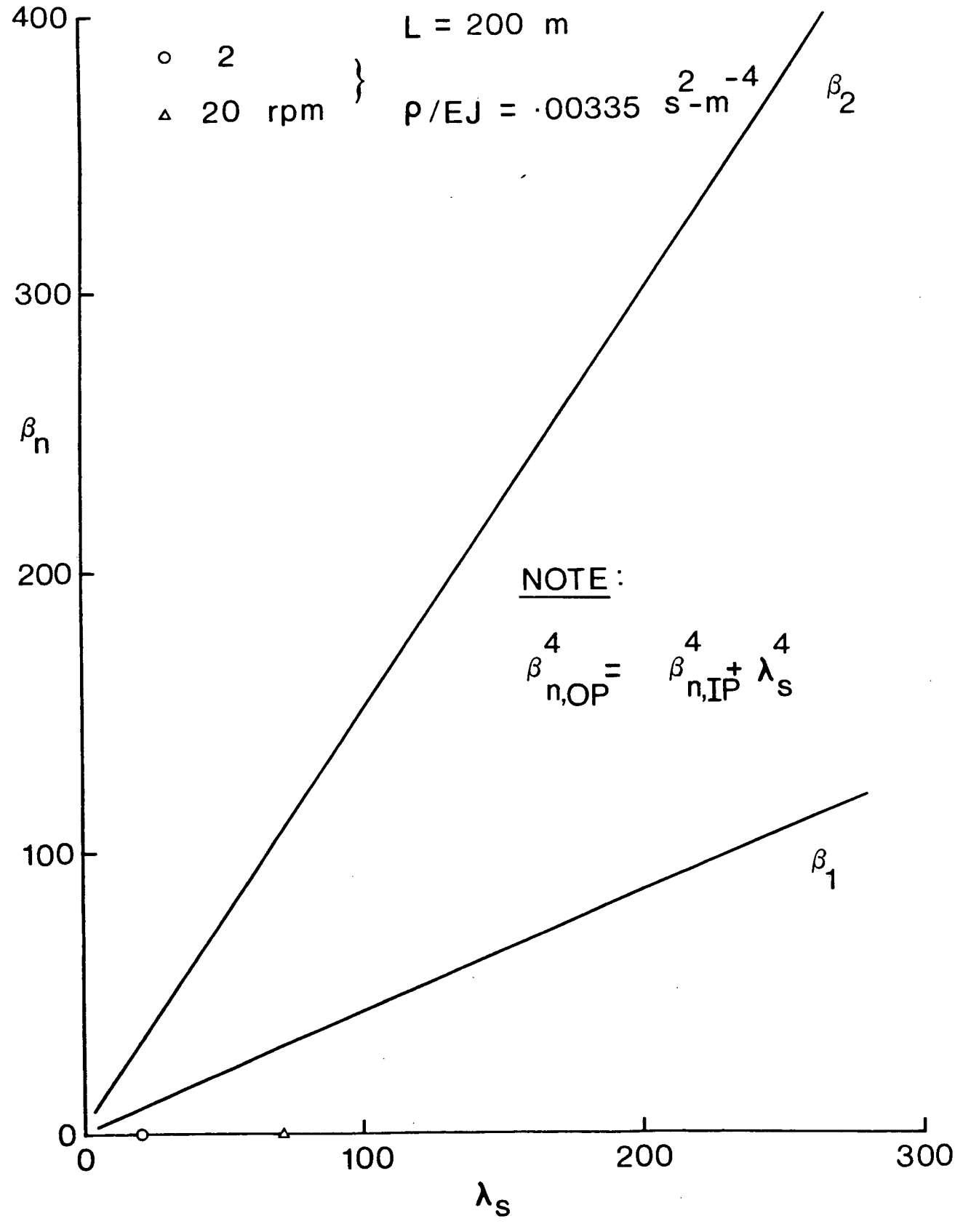

Figure 4-2 Frequency parameter for in-plane vibrations covering a wide range of spin parameter values - no deployment.

Table 4.1 System Eigenvalues Demonstrating Individual and Combined Influences of Orbital Motion, Spin and Deployment.†

SYSTEM	VIBRATION*	ϕ	$(\dot{\phi}+\dot{\theta})$ rpm	$\dot{\ell}$, m/s	$\ddot{\ell}$, $_2$ m/s^2	EIGENVALUE REAL PART, 1/s 1st	EIGENVALUE REAL PART, 1/s 2nd	β_n (BASED ON IMAGINARY PART OF EIGENVALUES) 1st	β_n (BASED ON IMAGINARY PART OF EIGENVALUES) 2nd
Flexure Only	Both	-	0	0	0	0	0	1.875	4.694
Deploying	Both	-	0	0.05	0	0.7499×10^{-3} $_1$	0.7500×10^{-3} $_2$	1.869	4.693
	Both	-	0	0.50	0	0.1021×10^{-1}	0.7506×10^{-2}	0	4.594
	Both	-	0	0	0.005	0	0	1.837	4.416
	Both	-	0	0	-0.005	0	0	1.914	4.928
Orbiting (no libration, $\phi = 0$)	In-Plane	0	$\dot{\theta}$	0	0	0	0	1.884	4.697
	In-Plane	$\pi/2$	$\dot{\theta}$	0	0	0	0	1.867	4.693
	Out-of-Plane	0	$\dot{\theta}$	0	0	0	0	1.887	4.697
	Out-of-Plane	$\pi/2$	$\dot{\theta}$	0	0	0	0	1.870	4.694
Spinning (non-orbiting, $\dot{\theta} = 0$)	In-Plane	0	0.2	0	0	0	0	2.336	5.991
	In-Plane	0	2.0	0	0	0	0	4.894	16.66
	In-Plane	0	20.0	0	0	0	0	15.15	52.58
	Out-of-Plane	0	0.2	0	0	0	0	3.647	6.155
	Out-of-Plane	0	2.0	0	0	0	0	11.12	17.41
	Out-of-Plane	0	20.0	0	0	0	0	35.14	54.95
Deploying	Both	-	0	0.05	0.005	0.7676×10^{-3}	0.7462×10^{-3}	1.831	4.415
	Both	-	0	0.05	-0.005	0.739 x10^{-3}	0.7492x10	1.909	4.927
Deploying + Orbiting (no libration, $\dot{\phi} = 0$)	In-Plane	0	$\dot{\theta}$	0.05	0	0.7499×10^{-3} $_1$	0.7500×10^{-3} $_2$	1.878	4.696
	In-Plane	0	$\dot{\theta}$	0.05	0	0.1007×10^{-1}	0.7500×10^{-2}	0	4.597
	In-Plane	0	$\dot{\theta}$	0	0.005	0	0	1.846	4.419
	In-Plane	0	$\dot{\theta}$	0	-0.005	0	0	1.922	4.931
	In-Plane	0	$\dot{\theta}$	0.05	0.005	0.7676×10^{-3} $_3$	0.7463×10^{-3} $_3$	1.840	4.418
	In-Plane	0	$\dot{\theta}$	0.05	-0.005	0.7390×10^{-1}	0.7492×10^{-2}	1.916	4.930
	In-Plane	0	$\dot{\theta}$	0.50	0	0.1012×10^{-1}	0.7506×10^{-2}	0	4.596
	Out-of-Plane	0	$\dot{\theta}$	0.50	0				
Deploying + Spinning (non-orbiting, $\dot{\theta} = 0$)	In-Plane	0	2.0	0.05	0	0.7498×10^{-3} $_2$	0.7498×10^{-3} $_2$	4.746	16.12
	In-Plane	0	2.0	0.50	0	0.7498×10^{-3} $_3$	0.7497×10^{-3} $_3$	4.708	16.12
	In-Plane	0	2.0	0.05	0.005	0.7499×10^{-3} $_3$	0.7499×10^{-3} $_3$	4.745	16.11
	In-Plane	0	2.0	0.05	-0.005	0.7497×10^{-2}	0.7497×10^{-2}	4.747	16.12
	Out-of-Plane	0	2.0	0.50	0	0.7498x10^{-2}	0.7497x10	10.750	16.83

*In-Plane, Out-of-Plane, or Both.
†R_C = 12,378 Km; e = 0; ℓ = 100 m; $\rho/EJ = 0.00335 \frac{s^2}{m^4}$.

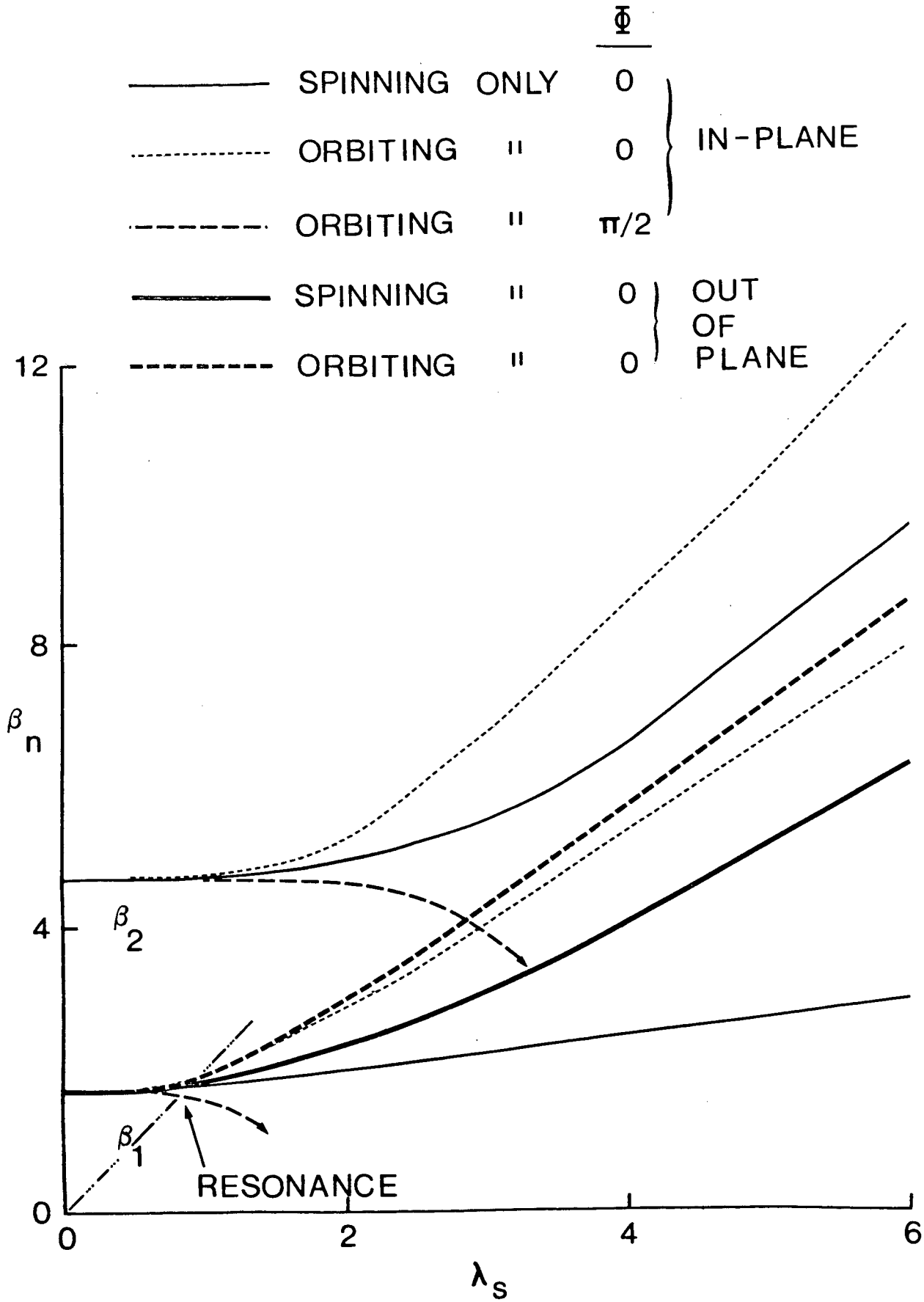

Figure 4-3 Frequency parameter during orbital motion only or spinning only, at small values of spin parameter - no deployment.

orbital motion, boom frequencies are significantly higher than those for the case of pure spin in the region $\lambda_s > 1$. The reason for this is the additional stiffening provided by the gravitational field (Equation 4.10). A similar phenomenon exists for out-of-plane oscillations. Note, resonance is indicated when spin rate equals the natural frequency for the case of in-plane vibrations. This finding was also discussed by Nguyen (1978).[139] The inherently unstable nature of a beam pointing along a tangent to the orbit is also displayed in Figure 4-3.

Isolated in Figure 4-4 is the influence of deployment rate and deployment acceleration. Regardless of whether the beam is extending or retracting, a decrease occurs in the vibration frequency with an increase in the magnitude of ℓ. For a given deployment velocity the tendency toward non-oscillatory behaviour increases for longer booms. The trend is similar for booms accelerating out from the spacecraft. However, the system becomes stiffer during deceleration. Note that although deployment is itself capable of a significant influence, in practical application, its effect can be nullified by orbital effects alone.

Much of the information contained in Figure 4-5 is implicit in earlier results, nevertheless, it will serve to emphasize some of the major factors affecting frequency as the beam extends. For the nonspinning case, $\Omega_n^2 \alpha 1/\ell^4$ hence large variations occur up to about 200 meters (Figure 4-5). However, spin stiffens the system considerably such that these large variations in frequency last only up to 100 meters at 2.0 rpm. During deployment, but in the absence of spin and/or orbital effects beam behaviour becomes non-oscillatory. The greater the rate of deployment the shorter the

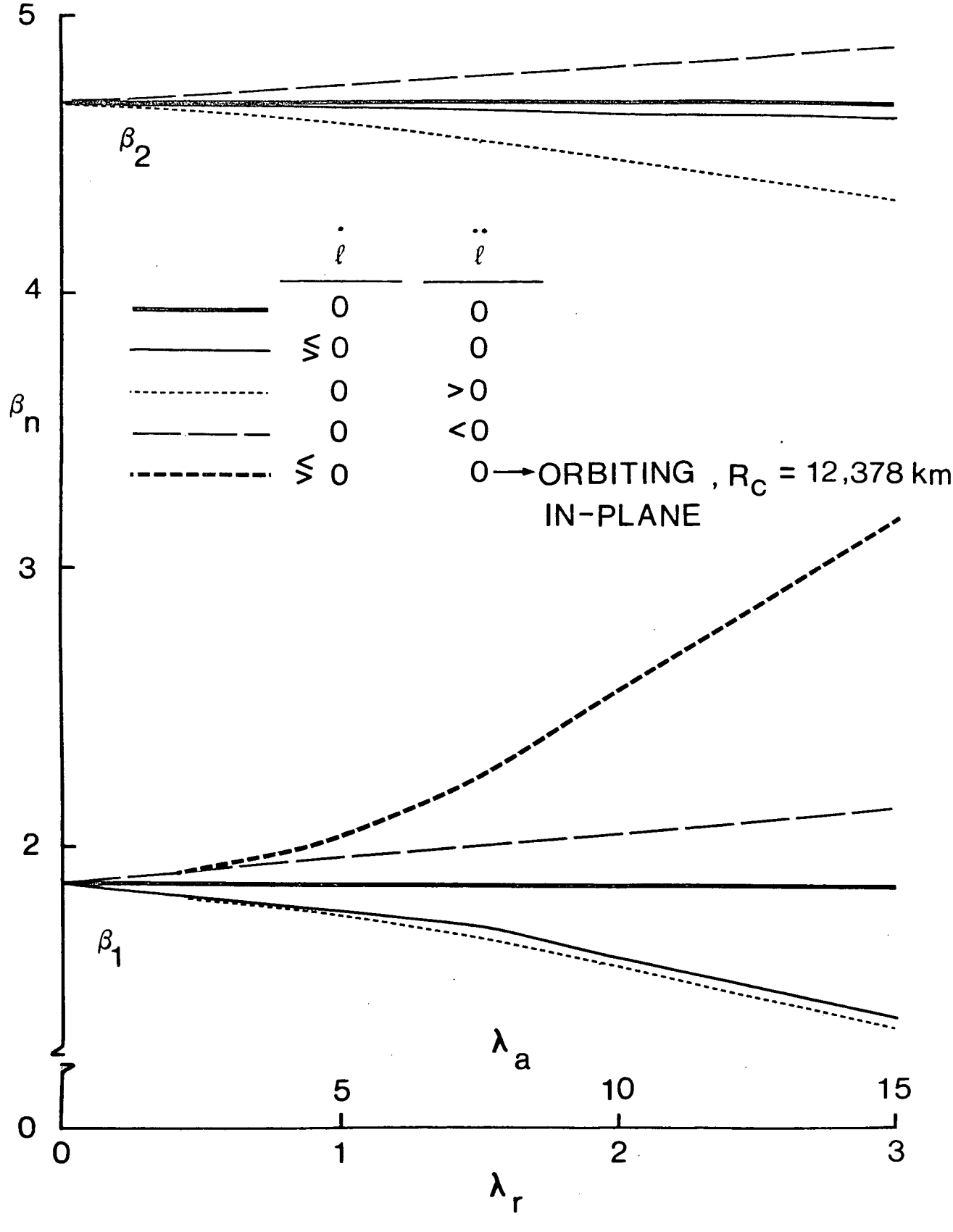

Figure 4-4 Isolation of deployment rate and deployment acceleration effects on frequency parameter.

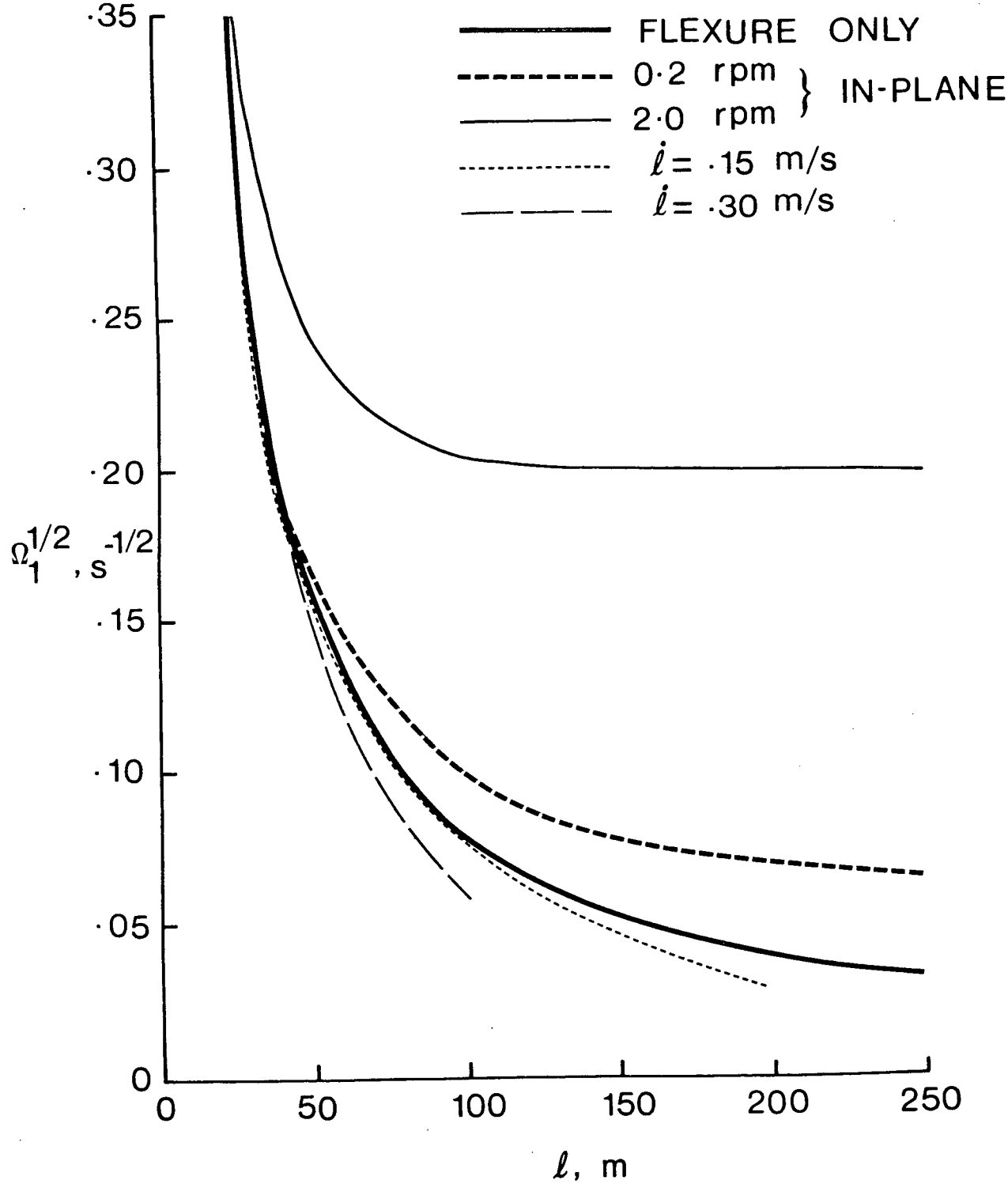

Figure 4-5 Influence of changes in length, deployment rate, or spin rate on (in-plane) frequency.

length at which this occurs.

The natural frequency of vibration, associated with the imaginary part of the system eigenvalue, is of prime importance. However, Table 4.1 demonstrates that the real part can also prove to be of interest during deployment. In this case it is nontrivial and, in fact, can be greater than zero implying instability or, by analogy, a negative damping thus helping to explain some of the previous results (Figure 4-5). Increasing the deployment velocity can decrease frequency (or eliminate it altogether) while increasing the magnitude of the real part. On the other hand, spin improves stability as implied, for example, by a beam deploying at 2 rpm. In this case all real parts of the eigenvalue become negative. Additional results contained in the table allow one to judge combined effects of deployment velocity, deployment acceleration, and spin.

Figure 4-6 clearly demonstrates that the stiffening effect of spin rate on eigenvalues also extends to the eigenfunctions. Even at 2 rpm the effect is substantial with a limiting shape being reached by 10 rpm.

The stiffening behaviour of the eigenfunctions in Figure 4-7 is clearly due to an increase in length only and is not affected by deployment rate. However, eigenfunctions have been altered by higher deployment rates (e.g., $\dot{\ell}$ = 1.0 m/s). Another effect of deployment is to produce complex sets of eigenfunctions. When evaluating the results contained in Figures 4-6 and 4-7 one should bear in mind that for a simple nondeploying, nonrotating beam, the shape of the eigenfunctions remains invariant with length.

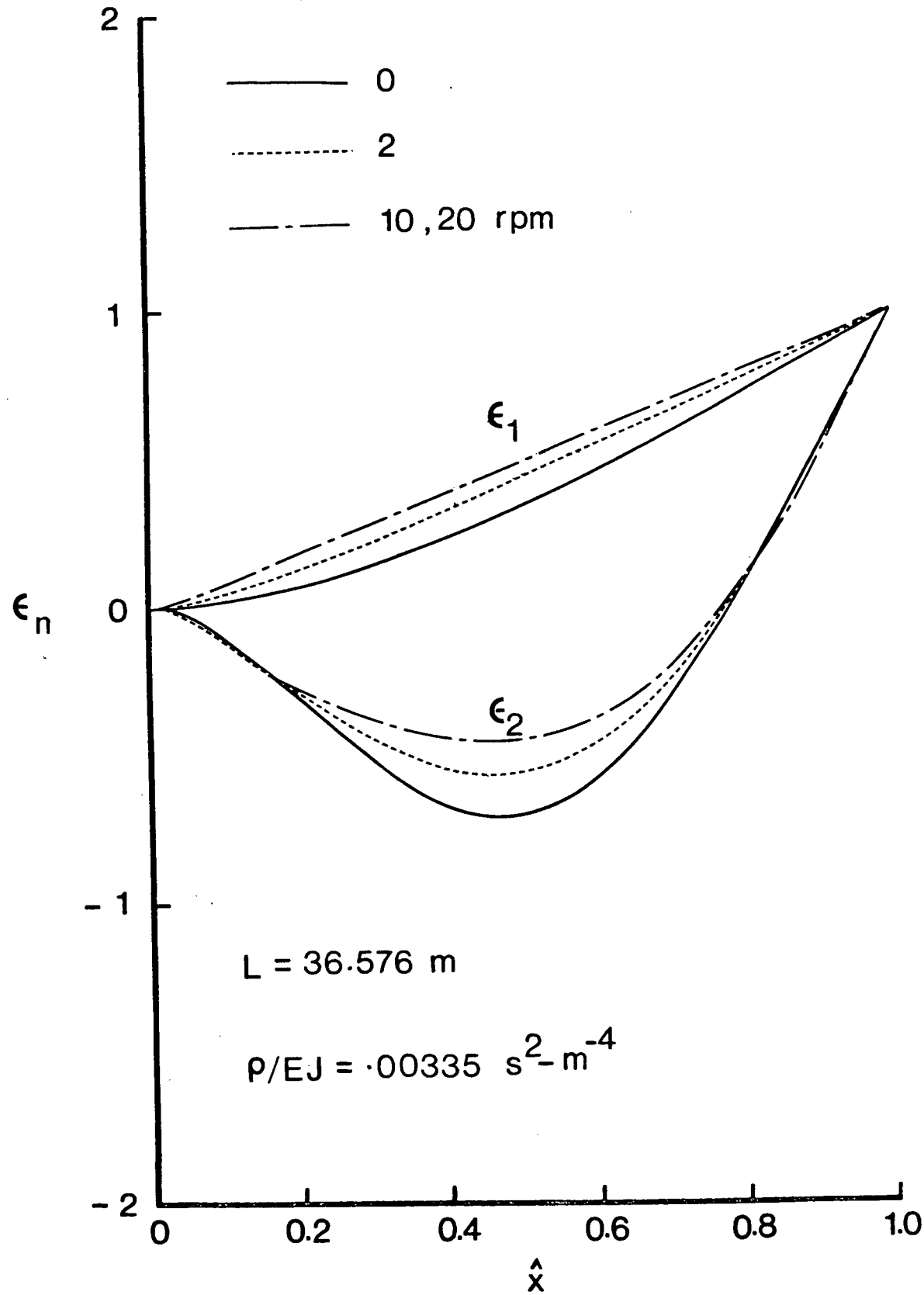

Figure 4-6 Spin rate and its influence on system eigenfunctions in the absence of deployment.

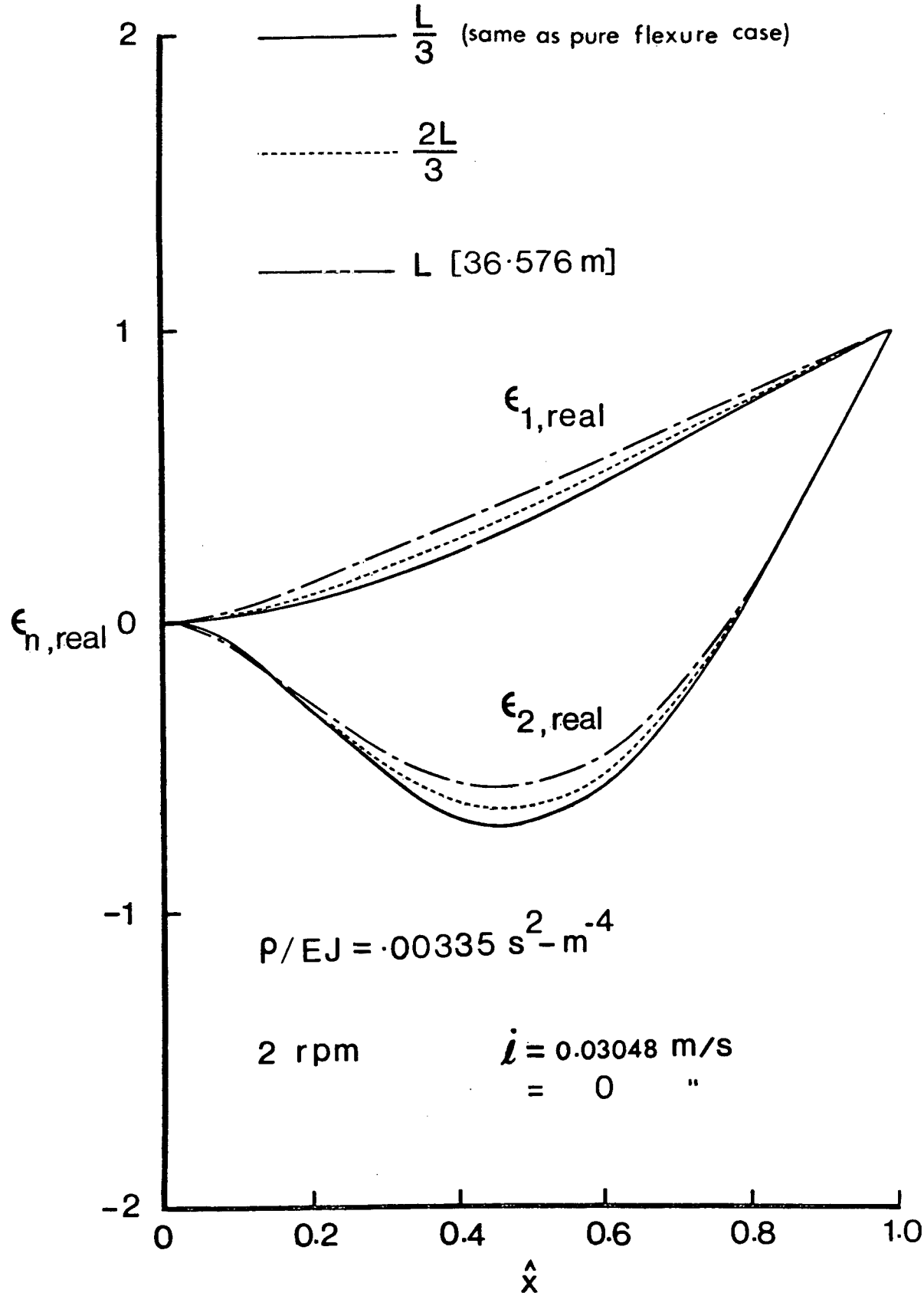

Figure 4-7 Mode changes associated with length of a spinning deploying beam.

Boom response to an initial tip displacement equal to 5% of the length is displayed in Figure 4-8 by a plot of the generalized coordinate associated with the first admissible function (i.e., $n = 1$). The contribution of the second assumed mode was found to be $<<5\%$ in all situations. This is in part expected because of the nature of the initial condition, but it does support the conclusion stated by Jankovic (1976),[233] that modal coupling is negligible between the first two modes for deployment velocities of this order. Stiffening caused by spin is reflected by an increase in the oscillation frequency. No amplitude change occurs for such a conservative system. The deploying beam operates at a small amplitude because of the smaller initial length and hence smaller initial condition. It is deployment rate itself which shifts the frequency of the response. Despite the smaller initial condition the deploying, orbiting beam still experiences an increase in amplitude. This is a conseqence of the Coriolis force contained in the $\{f\}$ matrix (Equation 4.10c). In fact, this amplitude increase is a prelude to the case of the deploying beam rotating at 0.2 rpm and experiencing nonlinear displacement. An order of magnitude check reveals that the $\hat{\ell}$-related term is capable of severely loading the boom. Although not shown here, this effect could be either augmented or reduced by spin accelerations. Misra and Modi (1979)[217] also describe the possible build up of deflections due to Coriolis effect on an orbiting flexible tether system. Out-of-plane vibrations occur at a higher frequency, but do not experience the Coriolis effect which caused the excessive in-plane displacements.

Finally, it should be emphasized that the presence of this additional load during deployment makes the duration time associated

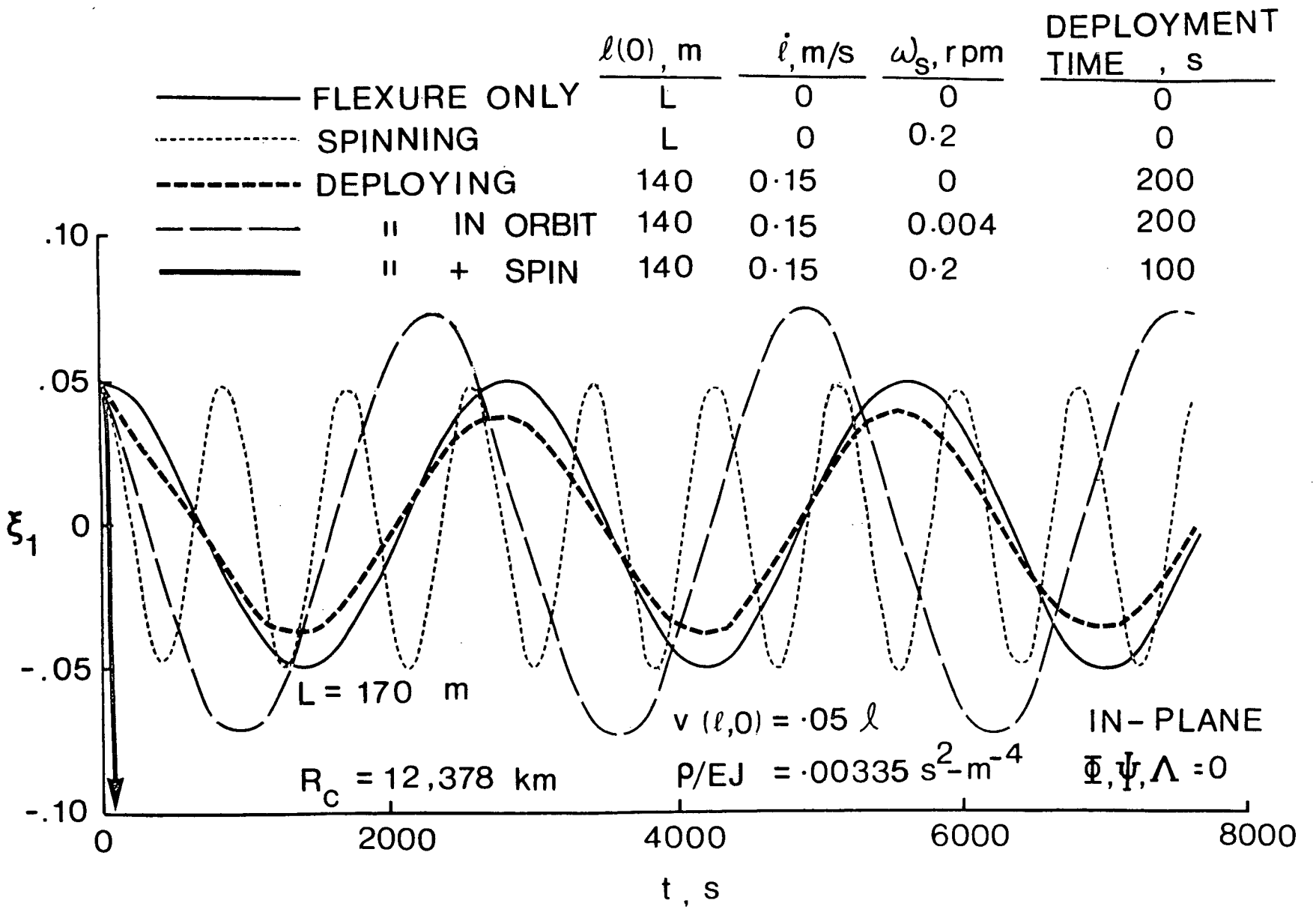

Figure 4-8 Planar response of a deploying, rotating beam-type appendage to initial tip displacement, $\Psi=\Lambda=0$.

with the deployment process an important parameter. In a practical situation, should vibrations become excessive, the deployment process could be terminated until amplitudes return to acceptable levels.

4.4 Concluding Remarks

In summary, presented is a method of solution for a deploying, orbiting, librating, beam-type spacecraft appendage capable of transverse oscillation both in and out of the plane of rotation. The object is to provide some appreciation as to the influence deployment and rotation parameters have either separately, or when combined. The more salient observations are:

(i) An orbiting beam cannot be treated simply as a rotating beam because of the presence of the gravitational field which can contribute to higher frequencies, depending on the relative magnitude of the spin parameter.

(ii) The 'free' vibration characteristics of out-of-plane motion during spin are identical with in-plane motion except that it occurs at a higher frequency (Equation 4.10).

(iii) Resonance can occur between in-plane appendage vibrations and the spin degree of freedom.

(iv) In the absence of rotation, deployment rate introduces instability regardless of the direction of extension. On the other hand, acceleration effects are dependent on direction (extension or retraction).

(v) The change in length itself, as opposed to deployment rate or deployment acceleration, remains one of the strongest factors influencing frequency variations (spin or no-spin).

(vi) Spin accelerations do not affect system eigenvalues or eigenfunction but, rather, contribute an additional transverse loading to the beam.

(vii) Rate of rotation plays a dominant role in stiffening the system as evidenced by the straightening of the eigenfunctions (Table 4.1, Figures 4-5 to 4-8).

(viii) Deployment related Coriolis forces can play a major role in causing large in-plane deformations. This implies in some cases that deployment should be carried out in stages so as to limit the time available to build up a large amplitude response. Once the deployment has been turned off the oscillations can be damped out.

Note, results given here apply to both spinning and gravity-gradient spacecraft during and after attitude acquisition. The frequency parameter data should be particularly useful in dealing with problems of interaction between the structural, control system, and vehicle dynamics.

5. PLANAR LIBRATIONS OF A TYPICAL GRAVITY GRADIENT CONFIGURATION

Having obtained rather general equations for both librational and vibrational motions the next logical step would be to apply them to a class of representative systems. However, the problem in its utmost generality is so complex that the physical character of the system is likely to get lost in the immense amount of algebra involved. As a first step in assessing the significance of system parameters and in order to establish some of the basic characteristics of the motion a simple yet realistic configuration consisting of a rigid central body having two long flexible booms free to librate and deform in the orbital plane was considered. Although this results in some simplification of the governing equations, they still remain nonlinear, nonautonomous, and coupled and hence quite challenging. The main objective is to get some appreciation as to the interaction between flexibility and librational motion during the steady state as well as transient phases as represented by deploying appendages.

5.1 Simplified Spacecraft Configuration and System Equations

Figure 5-1 illustrates the specific spacecraft studied here which is a simplified form of the general configuration presented in Figure 2-2. Cantilevered to a central rigid body are two diametrically opposed uniform flexible beam-type appendages, which can be deployed independently. In the nominal equilibrium con-

dition the undeformed appendages are aligned along the local vertical ($\underline{R}_c$) with boom number 1 pointing in the outward direction ($\phi_1 = 0$) relative to the center of force O_I. If attitude motion is restricted such that roll and yaw remain unexcited then pitch motion (Φ) takes place in the orbital plane only, the condition referred to as 'planar' motion. Furthermore, the boom vibrations are also assumed to be confined to the orbital plane. This type of configuration is typical of the many gravity-stabilized concepts. Although this represents a degree of approximation it provides a starting point in the analysis of such a complex system.

Governing equations are arrived at by applying the general results of Chapter 2 and 4 to the specific configuration represented in Figure 5-1. Note the use of a hybrid system of coordinates with nonlinear attitude equations (so important during the transient attitude acquisition stage) together with linear appendage equations. The simplified expressions here omit the effect of offset ($\underline{\pi}$) of the appendage attachment point.

Considering $\Psi = \Lambda = u = w = 0$, evaluating appendage coordinate transformation matrices $[\chi_1]$ and $[\chi_2]$, expanding out $[I]$, $[\dot{I}]$, $\{h\}$, $\{\Gamma\}$ as in Appendices II and III and substituting into equation (2.12c) yield the following equation for pitch attitude motion:

$$I_{33}\,(\ddot{\theta} + \ddot{\Phi}) + \dot{I}_{33}\,(\dot{\theta} + \dot{\Phi}) + \frac{3}{2}\left(\frac{\mu}{R_c^3}\right)[(I_{22} - I_{11})s2\Phi + 2I_{12}c2\Phi]$$

$$+ \sum_i \rho_i \int_0^{\ell_i} \{x_i\,(v_{i,tt} + 2\dot{\ell}_i v_{i,xt} + \dot{\ell}_i^2 v_{i,xx} + \ddot{\ell}_i v_{i,x})$$

$$- \ddot{\ell}_i v_i\,[1 + \tfrac{1}{2}\,(\ell_i - x_i)c\phi_i v_i]\}\,dx_i = 0; \quad i = 1,2 \qquad (5.1a)$$

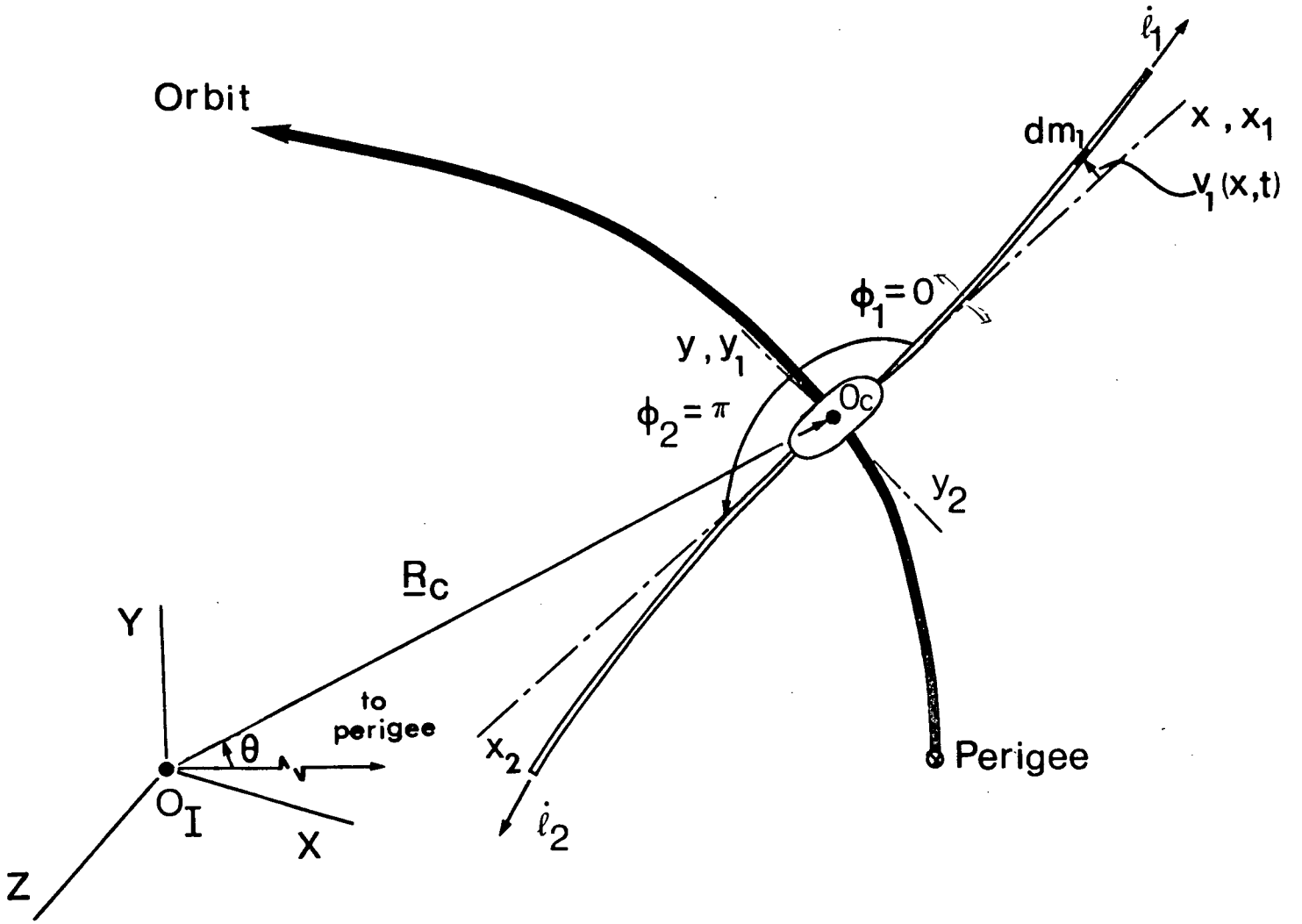

Figure 5-1 Configuration of a representative gravity gradient satellite, with two in-plane flexible deploying uniform booms, undergoing planar deformation.

where:

$$\phi_i = 0, \pi;$$

$$I_{33} = {}_1I_{33} + \sum_i \{\rho_i [\tfrac{1}{3} \ell_i^3 + \int_0^{\ell_i} (v_i^2 - 2x_i u_{fs,i})\, dx_i]\};$$

$$(I_{22}-I_{11}) = ({}_1I_{22}-{}_1I_{11}) + \sum_i \{\rho_i [\tfrac{1}{3}\ell_i^3 - \int_0^{\ell_i} (v_i^2 + 2x_i u_{fs,i})\, dx_i]\};$$

$$I_{12} = {}_1I_{12} + \sum_i [\rho_i \int_0^{\ell_i} (x_i - u_{fs,i})\, v_i dx_i].$$

Also with $\omega_1 = \omega_2 = 0$, equations (4.1a) for linear in-plane vibrations become:

$$\rho_i [v_{i,tt} + 2\dot{\ell}_i [(\dot{\theta} + \dot{\Phi}) + v_{i,xt}] + [(\dot{\theta} + \dot{\Phi})^2 + (\frac{\mu}{R_c^3}) (\tfrac{1}{2} - \tfrac{3}{2} c2\Phi)]v_i + [(\dot{\theta} + \dot{\Phi})^2 + (\frac{\mu}{R_c^3})(\tfrac{1}{2} + \tfrac{3}{2} c2\Phi)]x_i v_{i,x} + [(\ddot{\theta} + \ddot{\Phi}) + \tfrac{3}{2}(\frac{\mu}{R_c^3}) s2\Phi]x_i + \{\dot{\ell}_i^2 + \ddot{\ell}_i(\ell_i - x_i) - \tfrac{1}{2} [(\dot{\theta} + \dot{\Phi})^2 + (\frac{\mu}{R_c^3})(\tfrac{1}{2} + \tfrac{3}{2} c2\Phi)(\ell_i^2 - x_i^2)]\} v_{i,xx} + E_i J_{33,i} v_{i,xxxx} = 0. \qquad (5.1b)$$

5.2 Equations Based on 'Discrete' Deformation Coordinates and 'Orbital' Time

The solution of equations (5.1) is obtained using the assumed-mode procedure for representing elastic deformations, as established in Chapter 4. In terms of orbital time and using the nondimensional form of the vibration equations (4.3a), the equation governing pitch can be expressed as:

$$I_{33}\Phi'' + (I'_{33} - 2e_1 I_{33})(1 + \Phi') + \frac{3}{2}(1 + ec\theta)$$

$$[(I_{22} - I_{11})s2\Phi + 2I_{12}c2\Phi] + \Gamma_3 - 2e_1 h_3 = 0; \qquad (5.2)$$

where:

$$I_{33} = {}_1I_{33} + \sum_i \{\rho_i \ell_i^3 [\frac{1}{3} + \sum\sum_{mn} (B_{mn,1} - \frac{1}{2}B_{mn,11})\xi_m^i \xi_n^i]\};$$

$$(I_{22}-I_{11}) = ({}_1I_{22} - {}_1I_{11}) + \sum_i \{\rho_i \ell_i^3 [\frac{1}{3} - \sum\sum_{mn} (B_{mn,1} + \frac{1}{2} B_{mn,11})\xi_m^i \xi_m^i]\};$$

$$I_{12} = {}_1I_{12} + \sum_i [\rho_i \ell_i^3 (\sum_m C_{m,4}\xi_m^i)];$$

$$I'_{33} = \sum_i \{\rho_i \ell_i^2 \sum\sum_{mn} (B_{mn,1} - \frac{1}{2} B_{mn,11})(2\ell_i \xi_m^{i'} \xi_n^i + 3\ell' \xi_m^i \xi_n^i)\};$$

$$h_3 = \sum_i [\rho_i \ell_i^2 \sum_m (C_{m,4}\ell_i \xi_m^{i'} + C_{m,12}\ell'_i \xi_m^i)];$$

$$\Gamma_3 = \sum_i \rho_i \ell_i \{\sum\sum_{mn} (-\frac{1}{2} B_{mn,10} c\phi_i \ell_i \ell''_i \xi_m^i \xi_n^i) + \sum_m [C_{m,4}\ell_i^2 \xi_m^{i''} + 2C_{m,11}\ell_i \ell'_i \xi_m^{i'} + (C_{m,12}\ell_i \ell''_i + C_{m,14}\ell_i'^2)\xi_m^i]\};$$

$i \doteq 1, 2;$

$\phi_i = 0, \pi.$

Both appendages are governed by equation (4.10a). Consequently pitch excitation can generate asymmetric oscillations only. This is not the case, however, for differing boom initial conditions. Also differences in boom physical properties or deployment will alter the response.

System equations governing the planar dynamics (4.10a and 5.2) were solved simultaneously with the help of an AMDAHL 470/V6-II digital computer. The numerical integration routine was based on the implicit Adam's method with built-in error control. Vigneron[111] has pointed out several difficulties encountered in the numerical treatment of this class of problems. Flanagan (1969)[234] also refers to deficiencies related to digital computation. Fortunately, with advances in computer technology and better integration routines available today, no such difficulties were encountered.

5.3 Results and Discussion

Calculations were carried out for the two-boom gravity gradient configuration at an orbital altitude of 6000 km. The physical characteristics of the appendages coincide with those of the RAE antennas (ρ=0.023024 kg/m, EJ_{33} = 7.85 Nm^2). Principal inertias and mass for the central rigid body are 18 Nm^2 and 150 kg respectively. Through a systematic variation of the large number of variables inherent to the system one can generate extensive amounts of information. However, for conciseness, only typical results suggesting trends are recorded here.

Recognizing that the flexibility effects are likely to increase with length of the appendages, Figure 5-2 studies pitch and vibrational response of a satellite with two gravity gradient booms

$R_c = 12{,}378$ km , $e = 0$, $\dot{\Phi}(0) = \dot{\theta}$.

$EJ_{33} = 7.85$ Nm^2 . $\ell(0) = 0$.

$\varrho = 0.023024$ kg /m . $\dot{\ell} = 0.2$ m/s.

L = 50 m ——————

= 200 m ----------

= 250 m — — — —

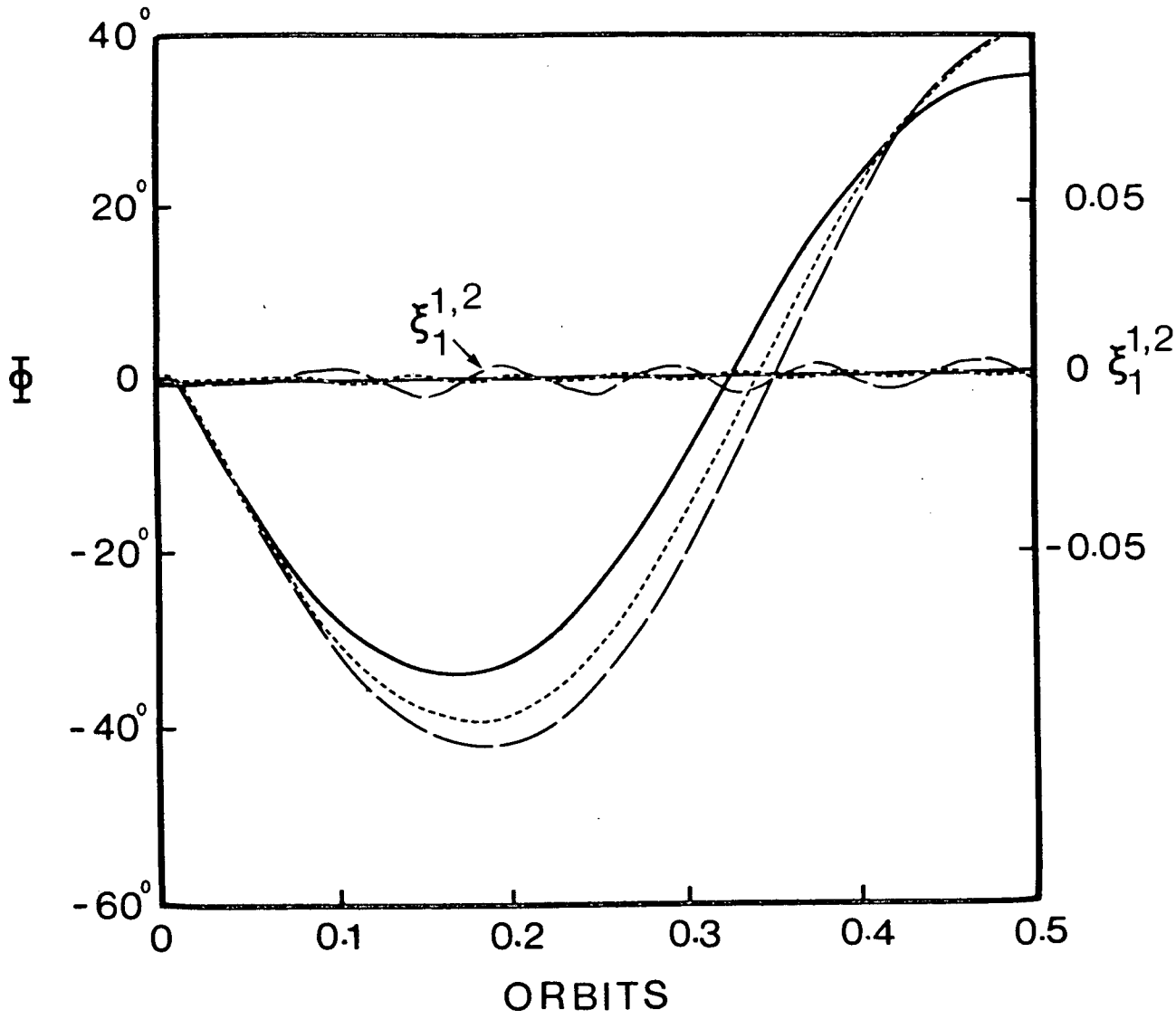

Figure 5-2 Effect of the flexible boom length on system response for the planar case.

extending to 50, 200 and 250 m. The satellite is in a circular orbit with the booms extending at a rate of 0.2 m/s. It is subjected to an impulsive disturbance of $\dot{\Phi}(0) = \dot{\theta}$. In addition to the very large amplitude experienced by the pitch response the figure shows three points of interest:

(i) There is a quick reversal in the direction of pitch motion due to increase in the moment of inertia about the pitch axis (conservation of momentum) brought about by deployment.

(ii) Amplitude of pitch oscillations tends to increase with an increase in the final deployment length, L. This appears to be a direct consequence of the vibratory motion which sets in at larger lengths.

(iii) Flexible appendages undergo small amplitude antisymmetric motion.

Figure 5-3 compares the response of rigid and flexible satellites during appendage deployment from 180 to 200 m. Corresponding performance with the appendage length fixed at 200 m is also included. It is of interest to recognize that for the nondeploying condition, flexible appendages remain virtually unexcited resulting in a pitch response that is identical to the rigid case. However, the effect of deployment of rigid appendages is to reduce the maximum amplitude from 35° to 30°. The influence of flexibility is to further accentuate this trend with the amplitude reduced to around 20°. Note also the high frequency modulation of the librational response due to vibratory motion of the flexible appendages. This is a direct result of the flexibility interaction, that is,

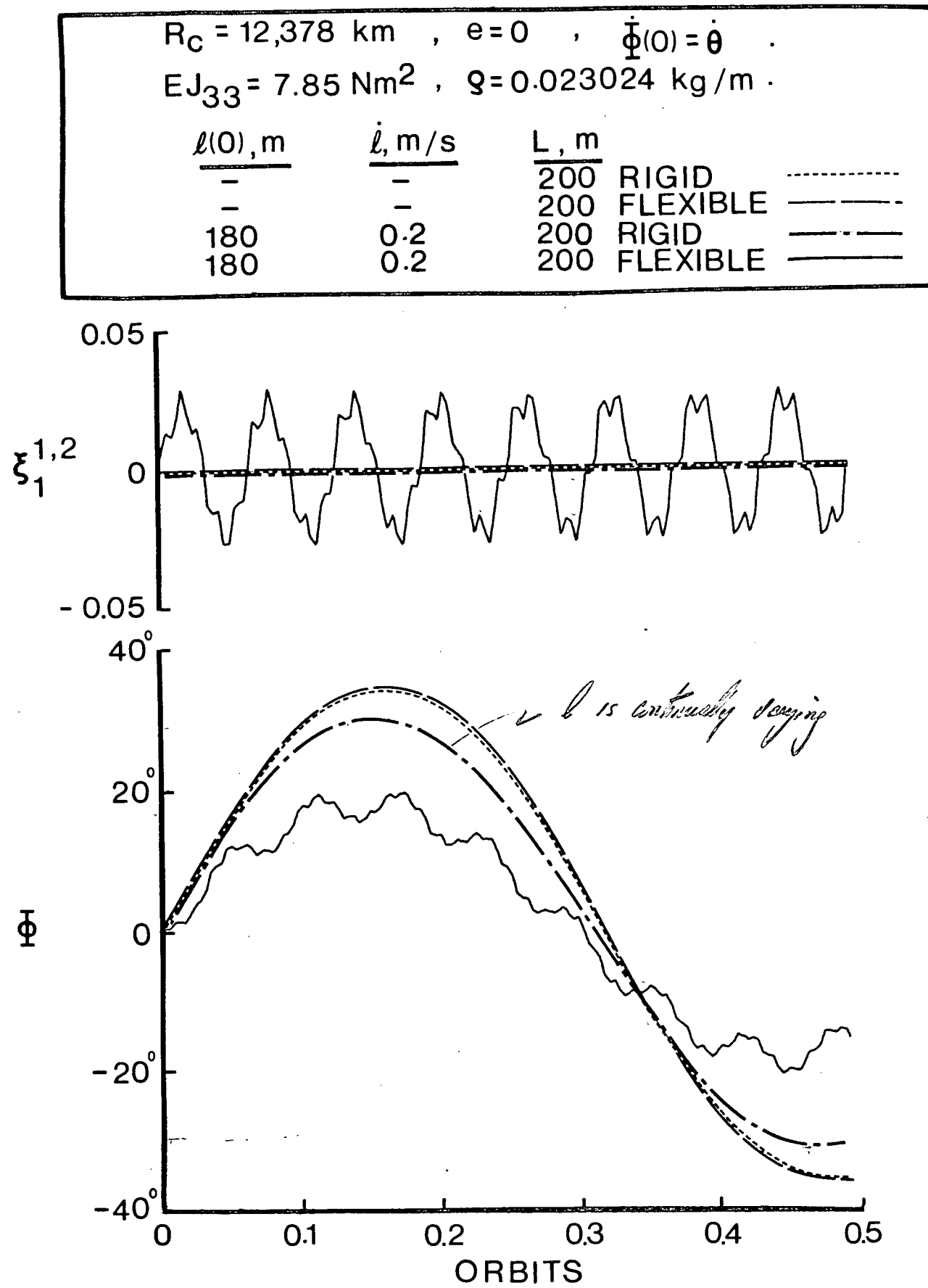

Figure 5-3 Transient response of a gravity gradient satellite showing the effect of flexibility and deployment, $\Psi=\Lambda=0$.

the booms serve as a feedback mechanism for the attitude motion.

Effect of the deployment rate on the system dynamics is indicated in Figure 5-4 where the appendages are deployed from the initial length of 200 m to a fully deployed value of 250 m. Increasing the deployment rate from 0.1 m/s to 0.2 m/s does not seem to affect the pitch response substantially except for a distinct shift in phase, however, the vibrational response becomes quite sensitive to the deployment rate and at a critical value of around 0.22 m/s the vibrational motion becomes unbounded leading to instability of the pitch vibrations.

Boom response to an initial tip displacement equal to 5% of the length is displayed in Figure 5-5 by a plot of the generalized coordinate associated with the first admissible function of boom number 1 and the corresponding pitch libration. Symmetric initial displacements of the booms produce no pitching while antisymmetric initial conditions (tip displacement = 5% of boom length) result in a pitch $\simeq 9°$. Disturbing only one boom initially yields librations less than 5°. A considerable difference exists in the frequency of vibrational response for the symmetric case as opposed to the other two. The high frequency behaviour is eliminated along with the pitch response for the symmetric case. This is because the high frequency modulation is a direct result of coupling with the pitch motion, which is not excited during the symmetric case.

During the formulation of the governing equations it was recognized that inclusion of the shifting center of mass and/or geometric offset of the appendages considerably adds to the complexity of the problem. Hence it was considered desirable to assess their effects on the general response. This is examined in Figure

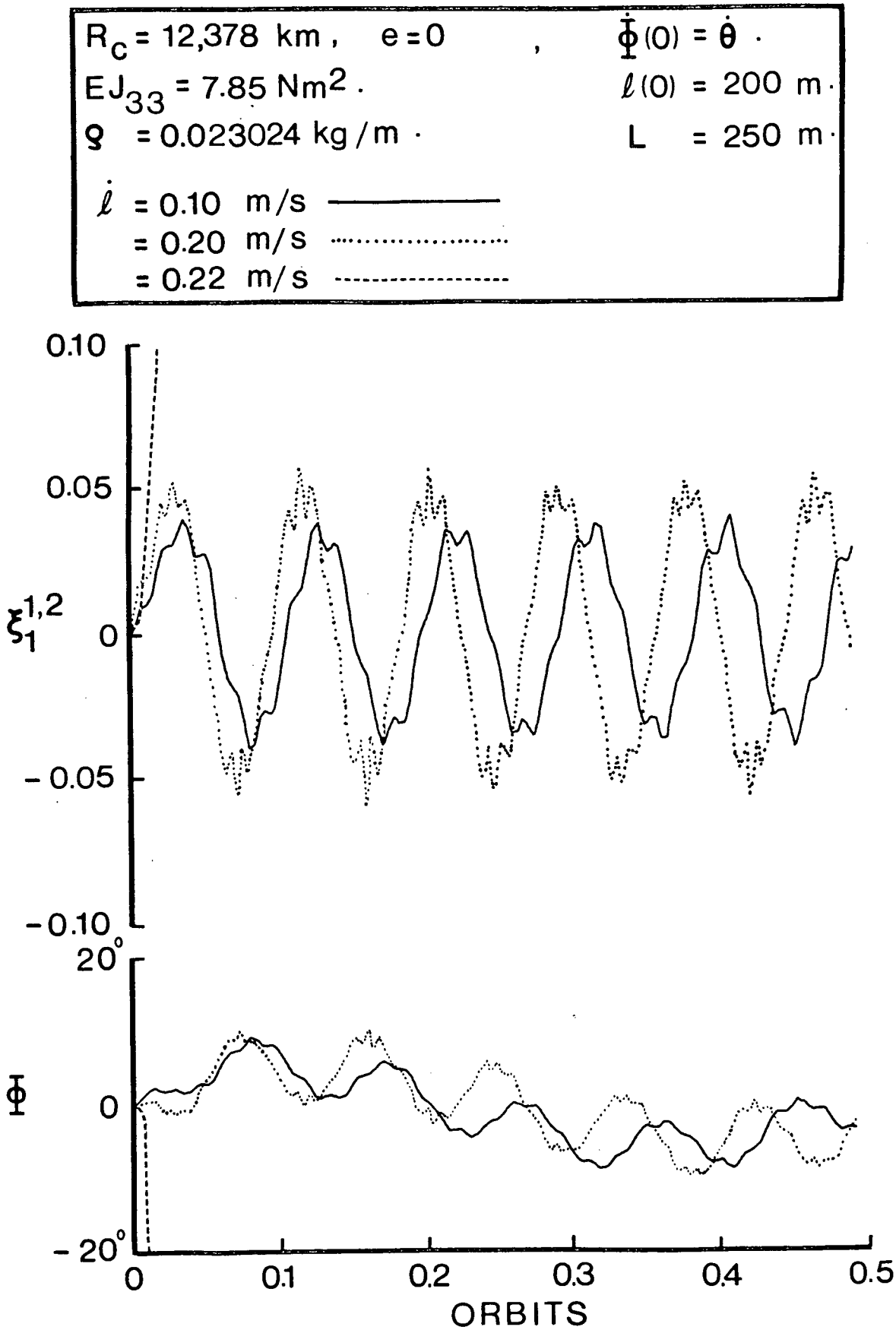

Figure 5-4 Effect of the deployment rate on pitch and vibrational response of a gravity gradient satellite.

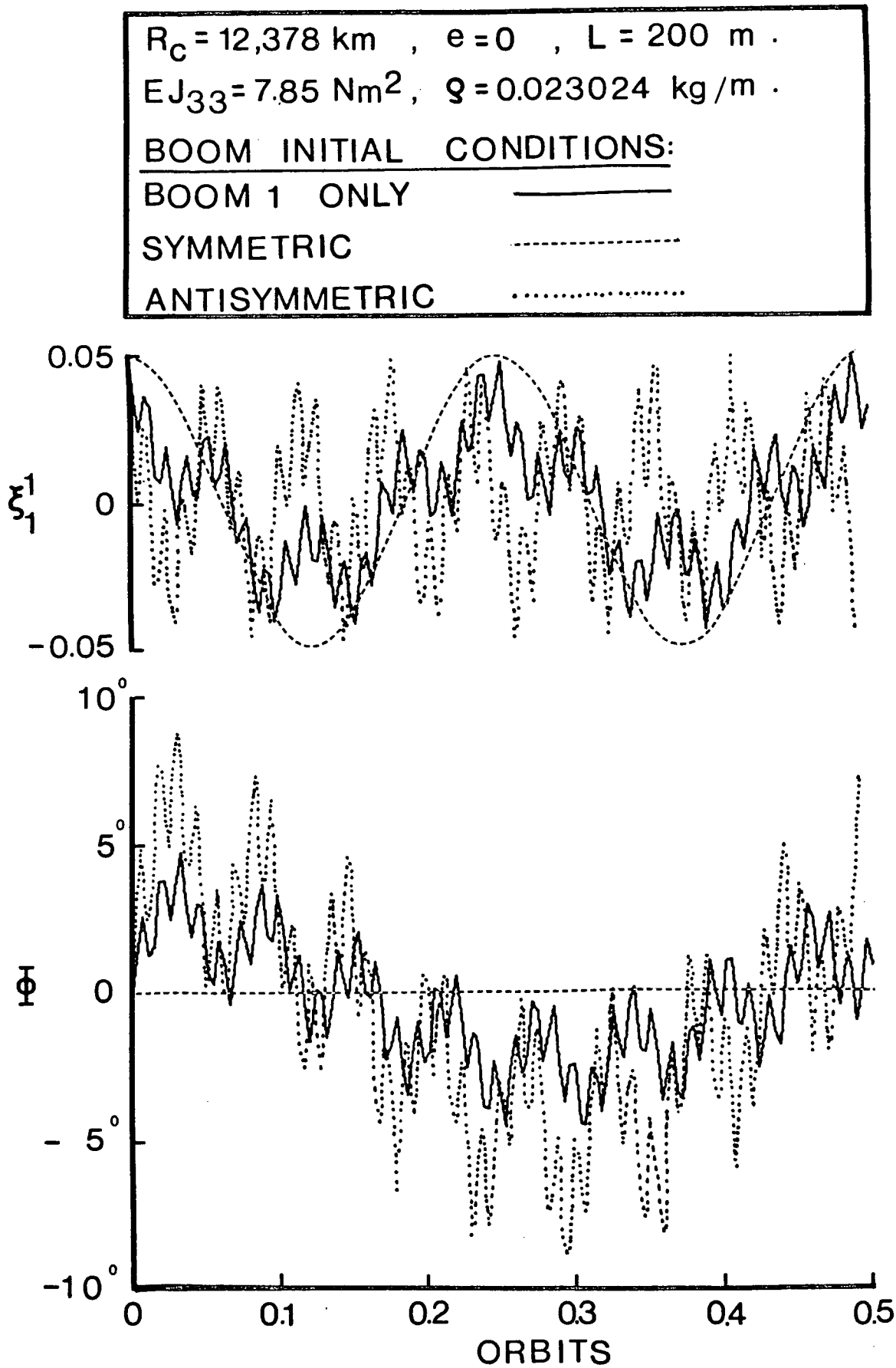

Figure 5-5 Effect of initial elastic deformations on system response for three different initial conditions, $\Psi=\Lambda=0$.

5-6 which shows the effect to be minimal for the case considered. This is quite important as considerable simplification of the equations and subsequent saving in the computational effort can be achieved without sacrificing accuracy.

5.4 Concluding Remarks

The planar dynamics reveals some important features associated with the motion of gravity gradient systems having flexible deploying appendages:

(i) Digital computation now permits solution of attitude dynamics problems previously intractable with such an approach.

(ii) Pitch motion excites antisymmetric boom deformations only.

(iii) The results indicate that even large amplitude librational motion fails to excite substantial appendage deformations. On the other hand, appendage deformations, caused by initial conditions or otherwise, can have substantial effects on response as evidenced by the considerable modulation of pitch amplitude together with a significant increase in frequency of appendage oscillation when compared with the uncoupled case.

(iv) Deployment can result in a significant increase in vibration amplitude. In fact, depending on the orbital parameters and physical properties of the booms, there exists critical combinations of boom length and deployment rate for which the satellite can tumble over.

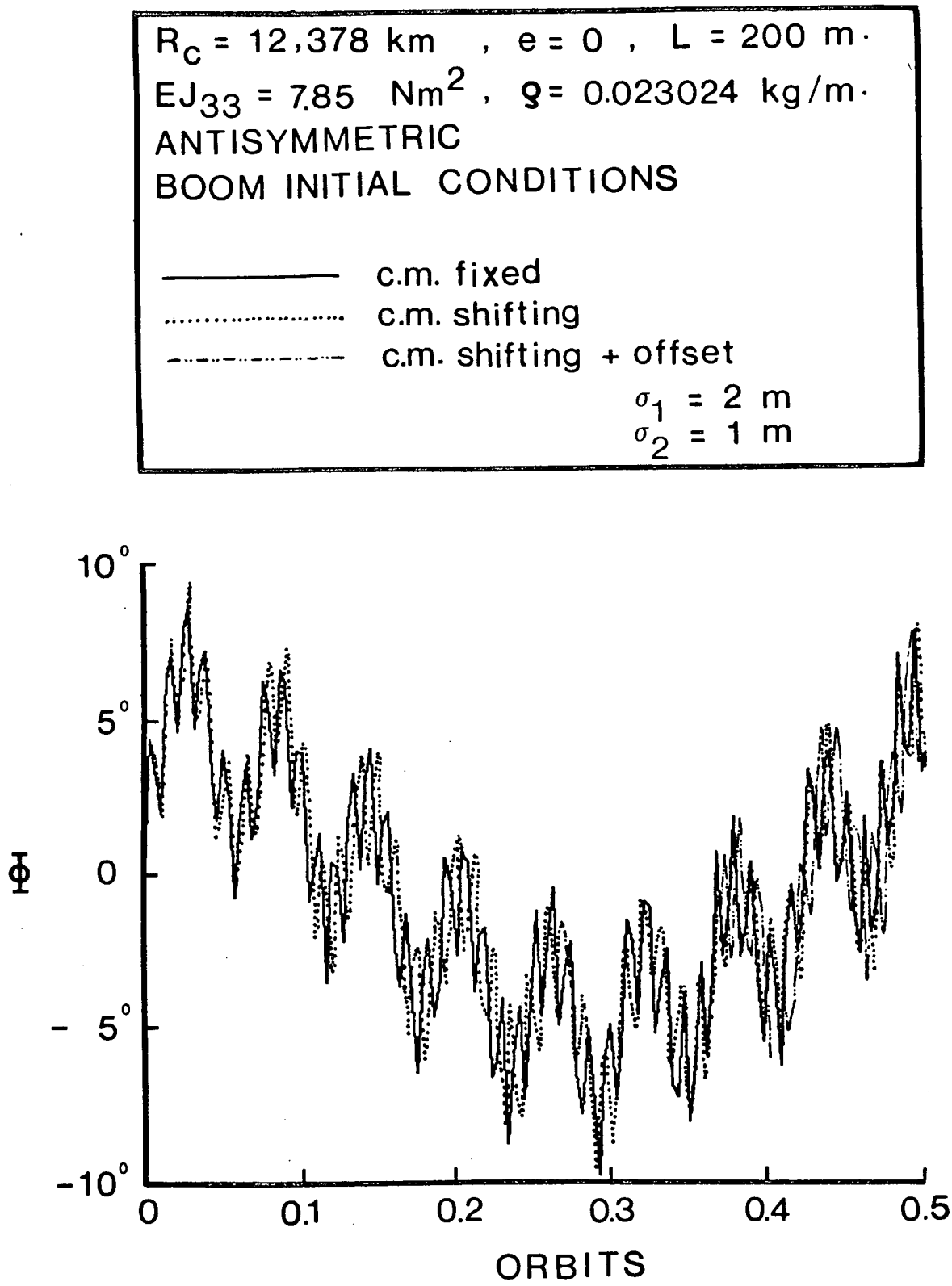

Figure 5-6 Typical planar response as affected by the shifting center of mass and appendage offset.

(v) Deployment increases the degree of coupling between the attitude and vibrational degrees of freedom.

(vi) In certain cases the effect of shifts in center of mass and offset can be negligible.

6. GENERAL THREE-AXIS ATTITUDE MOTION

The planar dynamical study though useful should be considered approximate and provides merely preliminary information concerning the system behaviour. To an extent, it gives a mechanism for checking the enormous amount of algebra and also involves a simplified version of the general computer program. With this as background, the present chapter applies the analysis to the case of general three-axis attitude motion.

6.1 Spacecraft Configuration and System Equations

The two-boom gravity gradient configuration of Chapter 5 is but one particular case of that class of spacecraft depicted in Figure 6-1. The equilibrium attitude is taken to be such that the x-y plane coincides with the orbital plane. Also, any pitch or spin motion occurs in the x-y plane hence it is referred to as the 'spin' plane and contains booms numbered 1 through 4 having the arbitrary orientation ϕ_p as indicated (Figure 6-1). Booms 5 and 6 lie in the x-z plane. Although a maximum of six appendages are illustrated, the governing equations considered in this section apply to a configuration having an arbitrary number of booms in each of these planes. Coordinate transformation matrices required to relate local appendage coordinates to the central axes include:

$$[\chi_p] = \begin{bmatrix} c\phi_p & s\phi_p & 0 \\ -s\phi_p & c\phi_p & 0 \\ 0 & 0 & 1 \end{bmatrix} \quad \text{(for a planar boom);}$$

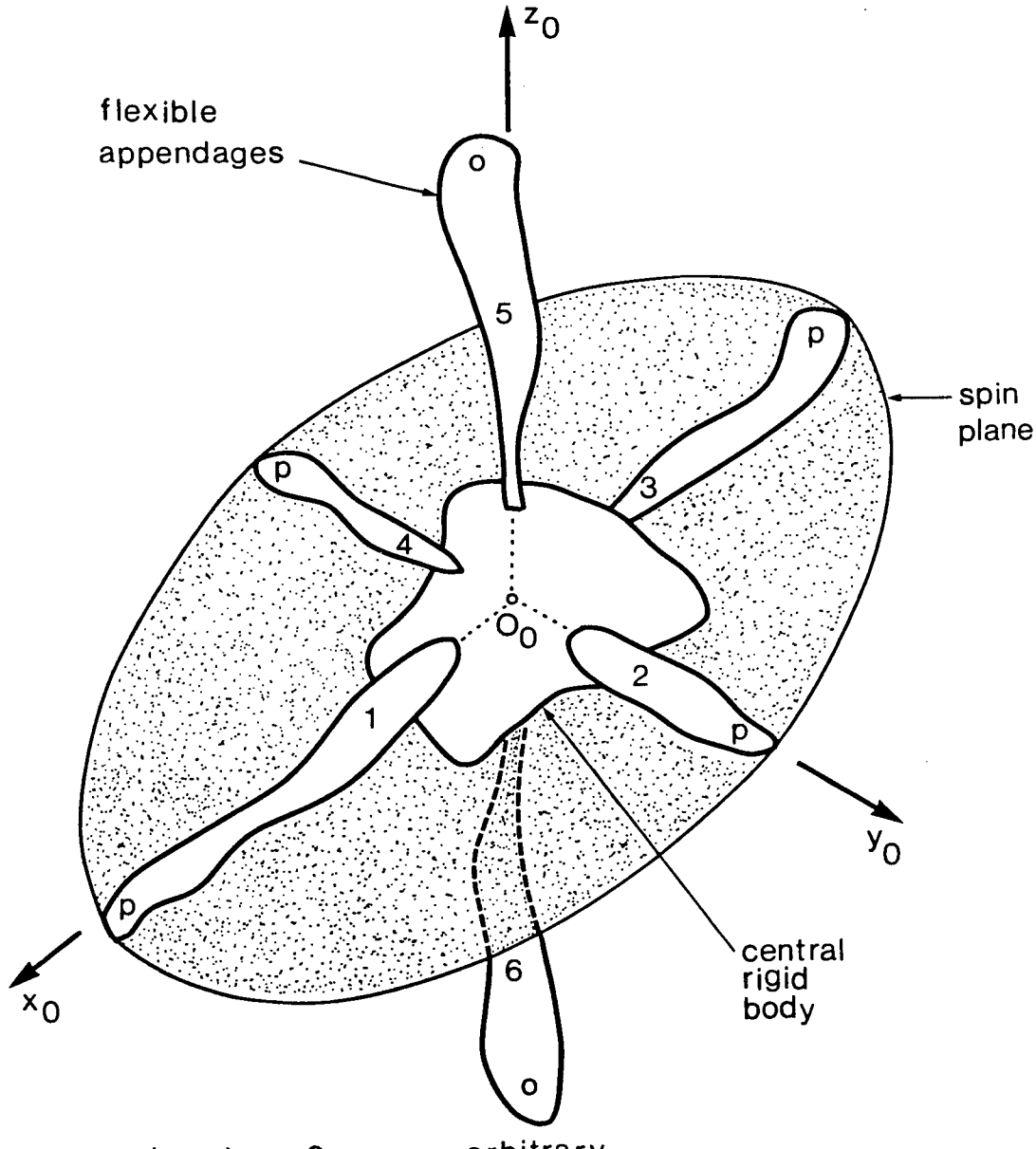

Figure 6-1 Configuration representing a large class of spacecraft chosen for detailed study. Note the arrangement shows appendages in the x-y plane coinciding with the pitch plane (p) and in the x-z plane perpendicular to the pitch plane (o).

$$[\chi_o] = \begin{bmatrix} c\psi_o & 0 & -s\psi_o \\ 0 & 1 & 0 \\ s\psi_o & 0 & c\psi_o \end{bmatrix}$$ (for a boom in the x-z plane). (6.1)

Possible gravity gradient configurations represented by Figure 6-1 include that of two diametrically opposed appendages in the spin plane (Figure 5-1), an RAE-type arrangement involving four booms symmetrically placed in the spin plane, or perhaps a set of six mutually perpendicular booms. Similarly, one could identify configurations applicable to spin-stabilized spacecraft such as the Alouette series having two sets of antennae of different lengths lying in the spin plane. On the other hand, a CTS-type configuration could be modelled using just two booms (numbers 5 and 6) perpendicular to the spin plane. Of course, rigid unsymmetrical satellites with no appendages can also be included within this class.

Obviously the representation of Figure 6-1 has a wide range of applicability. However, it is but one particular case of the more general configuration originally presented in Figure 2-2, thus emphasizing the versatility offered by that formulation.

Appropriate equations governing librational and vibrational behaviour can be arrived at by applying the more general results of Chapters 2 through 4 to the configuration under study here. The main assumption made is that an arbitrary number of flexible, deploying, uniform booms lie in the x-y and the x-z planes. As in Chapters 4 and 5, appendage motion is governed by a set of partial differential equations and advantage is taken of the assumed-mode procedure in arriving at a final solution. Again, axial oscil-

lations are neglected. With a description available for the appendage motion one can proceed as in Chapter 5 to evaluate those terms in the libration equations dependent on flexibility and deployment. Consequently, the system equations of motion consist of equation (2.12) for the attitude dynamics and the set of equations (4.5) for each boom.

A study of these equations reveals how an already complex system becomes more complicated when one takes into account such factors as shifting center of mass, appendage offset, axial foreshortening and deployment.

6.1.1 Computational considerations

As before the solution was sought by direct numerical integration on a digital computer. It is perhaps of interest to outline the basic programming approach adopted for dealing with such an involved system.

The motion is governed by 3 librational and N-3 vibrational second order ordinary differential equations which are transformed to 2N first order equations by constructing a state vector of the N zeroth order (displacement) and the N first order (velocity) terms. In this form, all degrees of freedom are solved for simultaneously as a first order initial value problem. Used is an integration routine provided by the UBC Computing Services which is based on an implicit Adam's method. For the procedure to succeed one must use the latest data available when updating derivatives. Consequently, the second order derivative associated with each degree of freedom must be expressed as a function of the lower order derivatives only [Conte (1965)[235]]. This presents one with a considerable challenge

for the complex highly coupled system at hand. The amount of algebra involved is minimized by taking advantage of the numerical technique outlined in Appendix VII.

Organization of the computer program centered on a series of subroutines. A main program directed the integration process calling the system-supplied routines as desired and provided the needed input/output services. The integration package required a routine (SYSTM) to define the system dynamics in terms of explicit expressions for the first order derivative of the state vector. The governing equations are employed directly in SYSTM in two distinct stages to deal with the librational and vibrational contributions. In addition, a separate subroutine was written for each of the quantities $\{r_c\}$, $\{h\}$, $\{\Gamma\}$, $[I]$, $[I']$ required by SYSTM. In each case first degree, second degree, and foreshortening effects due to flexibility were grouped in separate blocks. Overall the modular approach adopted was intended to permit easy extension of the program to include additional appendage equations and to allow for isolation of the effects indicated above.

The 3-axis program was set up to accommodate an arbitrary number of assumed modes and six booms, four in the x-y plane and two in the x-z plane. Assuming a two mode representation results in a system of fifty-four first order equations. Modal integration coefficients were determined independently by numerical quadrature. Where possible, these integrals were evaluated analytically as well. Accompanied by a liberal use of comment cards the program exceeded three thousand five hundred lines. However, no storage limitations were encountered; although execution times could not be ignored as CPU values of 50-100 were not uncommon. Particularly time consum-

ing are integrations involving small appendage lengths. A similar finding was pointed out by Misra and Modi (1979).[236] To cope with the relatively small step size demanded by the high frequency oscillations a two-stage integration procedure is established thus allowing for a complete change in such parameters once during the course of the integration. The program was coded in FORTRAN using double precision variables throughout.

6.2 Results and Discussion

The endeavour here has aimed at developing a model which tests the transient and steady state effects of flexibility and deployment in a relatively general manner, the ultimate objective being to assess their interaction with the attitude dynamics. Practical difficulties arise if one wishes to simulate the behaviour of an actual spacecraft. Firstly, only limited response data is available in the open literature and what there is rarely applies to nonlinear deploying situations. Even for the existing data one tends to find but an incomplete identification of those parameters needed for carrying out a meaningful comparative simulation. Secondly, additional refinements to the model developed here may have to be made in order to include characteristics unique only to the system under consideration. In many cases the effort required to take into account new features may not be great since dynamic simulation of the flexibility effects has already been carried out.

For example, introduction of momentum biasing as used on the CTS would simply mean the adding of a constant term to the h_3 component of the local momentum vector. Similarly, it is relatively

straightforward to introduce damping into the study. However, this injects a degree of uncertainty into the simulation since no single theory has emerged which adequately describes the damping characteristics; a point emphasized by the recent findings of Garg et al. (1979).[237] This is one reason it has not been dealt with in the current investigation. Also it was considered unnecessary to further complicate an already complicated task when one could be reasonably certain as to the effect of the phenomenon - energy dissipation along with attenuation of the amplitude of vibration.

Although comparisons of simulations with actual flight conditions is the ideal, there exist, nonetheless, alternative measures one can take to establish confidence in the working of the program. A check on the algebra exists, to some extent at least, during application of the assumed-mode solution to such terms as $\{h\}$, $\{\Gamma\}$, etc. Aside from the usual symmetry one expects of the expressions for the general three dimensional case, one also finds the grouping of coefficients falling into a familiar pattern so that any deviation leads one to again review the derivation. Actual response can be checked by pursuing such trivial cases as response to zero initial conditions. The program can be run in the vibration or pitch modes only so that amplitudes and periods can be precisely checked. Planar nonlinear response of a rigid configuration in an eccentric orbit was compared with that by Brereton (1978).[30] Comparison of simultaneous response of both librational and vibrational motions is possible using a planar program derived independently of the general program. Also, peak pitch displacement and pitch reversal predicted for the RAE by Dow et al. (1966)[54] and Bowers et al. (1970)[204] are similar to the response generated here.

6.2.1 Two boom gravity gradient configuration

Having gained some familiarity with the planar response of a two-boom gravity gradient system, a logical step was to examine its fully coupled attitude behaviour. Representative results presented here assume the same orbit, configuration, and boom characteristics as described in section 5.3.

Figure 6-2 compares the response of rigid and flexible satellites during appendage deployment from 0-100 m. Corresponding response with the appendage length fixed at 100 m is also included. In all the cases, the system is subjected to the initial impulsive pitch (planar) excitation of $\dot{\Phi}(0) = \dot{\theta}$ with roll and yaw degrees of freedom left undisturbed. As can be expected, large amplitude pitch motion results, however, it is of interest to recognize that there are virtually no coupling effects as roll and yaw motions are essentially absent, so is the vibratory response of the flexible appendages. Note that for the nondeploying condition, near absence of the flexible appendage vibration results in pitch response that is identical to the rigid case. However, during deployment, slight vibration of the flexible members in the early stage does bring about a noticeable difference in the resulting pitch response. This is analogous to the behaviour observed earlier during the planar motion (Figures 5-2, 5-3).

Just how strong coupling effects can be is demonstrated by applying an impulsive initial condition of $\dot{\Psi}(0) = \dot{\theta}$ to the roll degree of freedom only, Figure (6-3). Large amplitudes result in both yaw and pitch as well as for vibrations. In fact, the overall motion becomes unstable within half an orbit. This is in marked

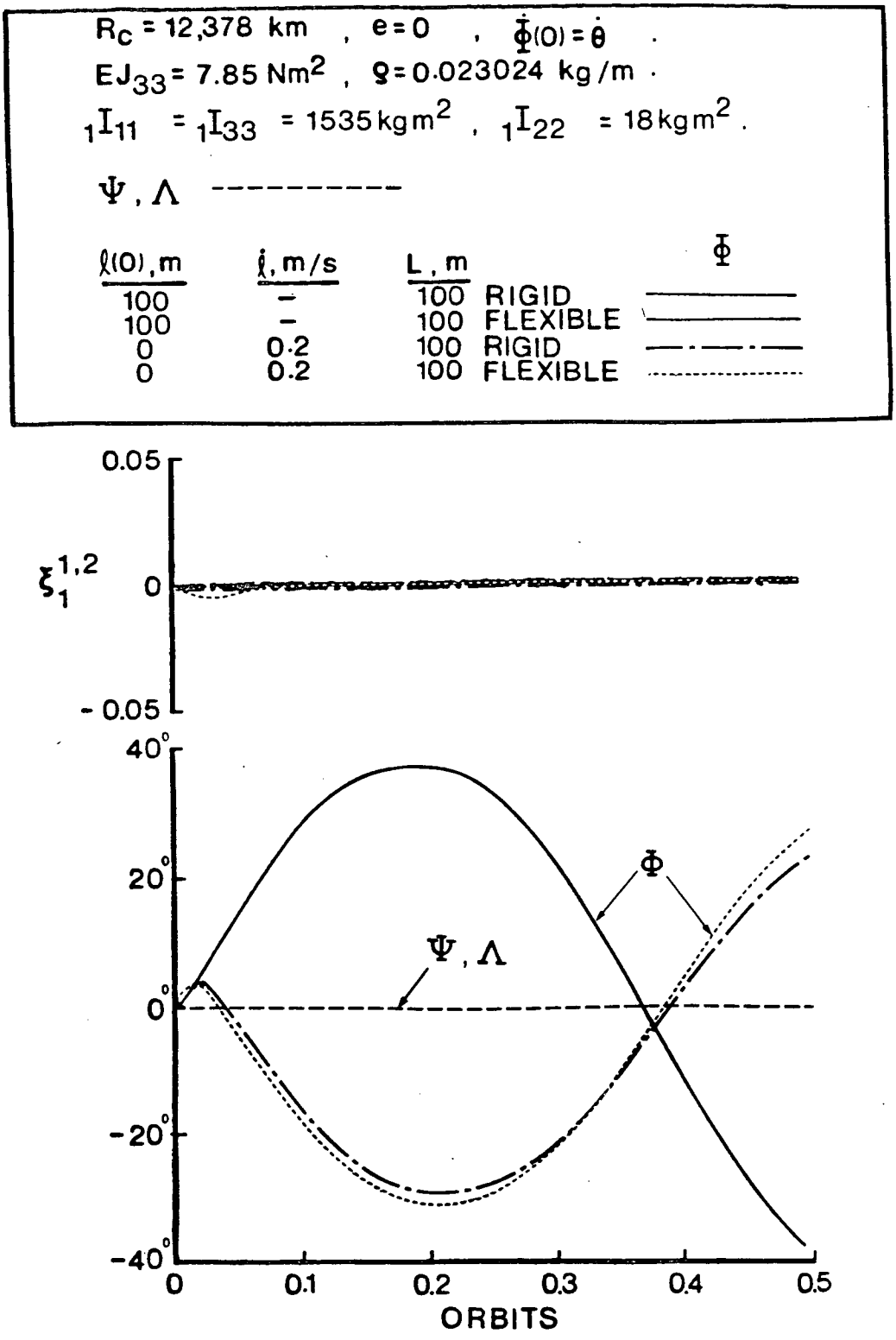

Figure 6-2 Three-axis response of a satellite to an impulsive pitch disturbance.

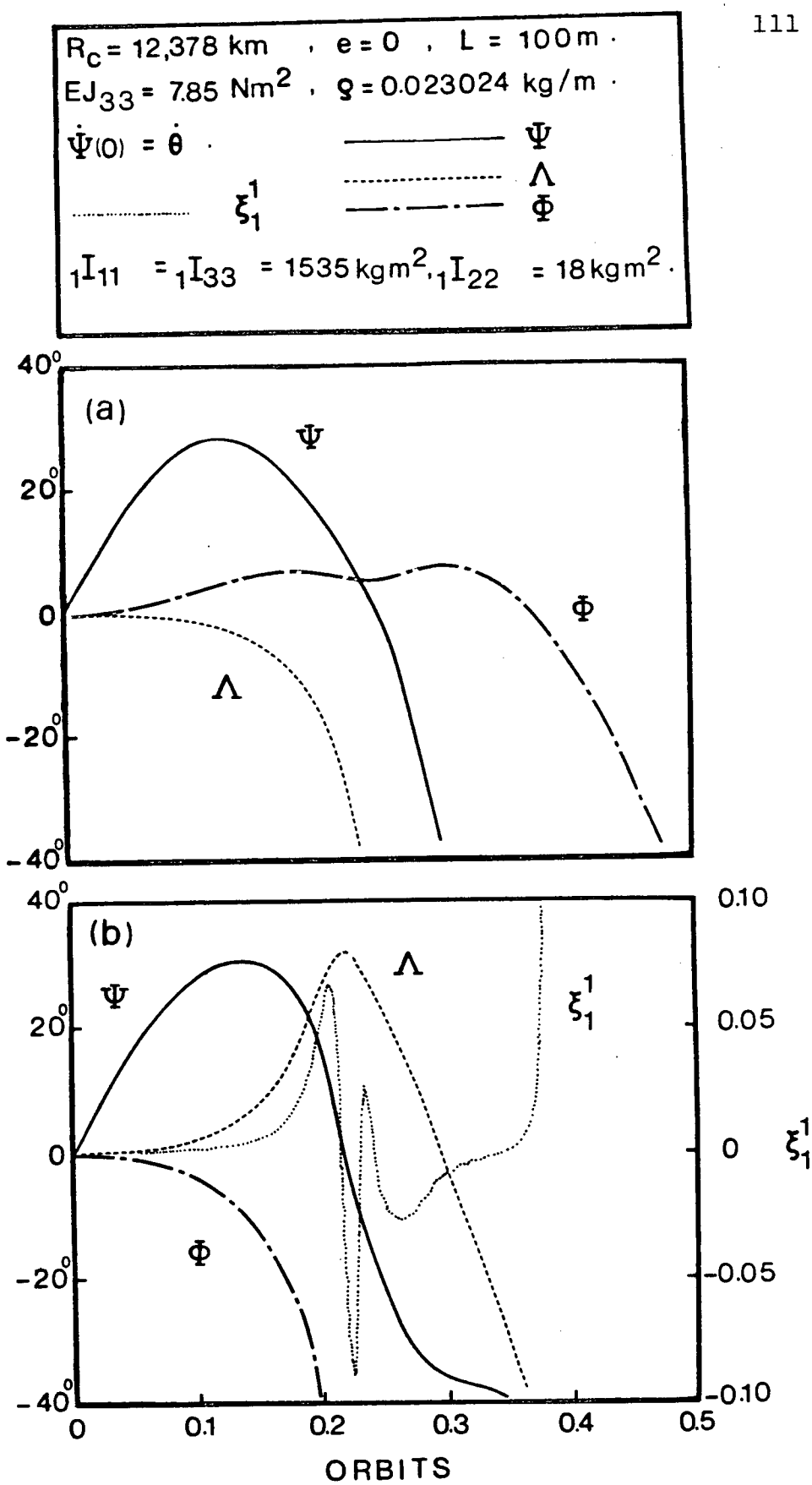

Figure 6-3 Three-axis response of a satellite with fully deployed appendages to an impulsive out-of-plane disturbance: (a) rigid booms; (b) flexible booms.

contrast to the stable response associated with the planar initial condition of the same magnitude. Note also the significant effect of deployment on the nature of the coupled response (Figure 6-4). Large displacements are also experienced in this case within less than 0.5 orbit. Flexibility, however, has minimal effect except near the point of instability where it alters pitch response quite dramatically.

Having considered two very different types of attitude disturbances, the next logical step was to assess system sensitivity to a given disturbance. To this end the system was subjected to a set of three impulsive roll velocities of increasing magnitude (Figure 6-5). Note the strong coupling effects continue to persist even in the presence of a small disturbance. The larger the roll rate, the earlier the instability sets in. The results also suggest that large displacements in librational and vibrational degrees of freedom are closely related.

Boom response to an initial tip displacement equal to 5% of the length is displayed in Figure 6-6 by a plot of the generalized coordinate associated with the first admissible function and the corresponding pitch libration. Symmetric initial displacements of the booms produce no pitching while antisymmetric initial conditions result in a peak pitch $\approx 8°$. Disturbing only one boom initially yields librations less than 5°. Note a considerable difference in frequency between the vibrational response for the symmetric case as opposed to the other two situations. Such high frequeney behaviour is eliminated during symmetric oscillation since pitch itself is not excited.

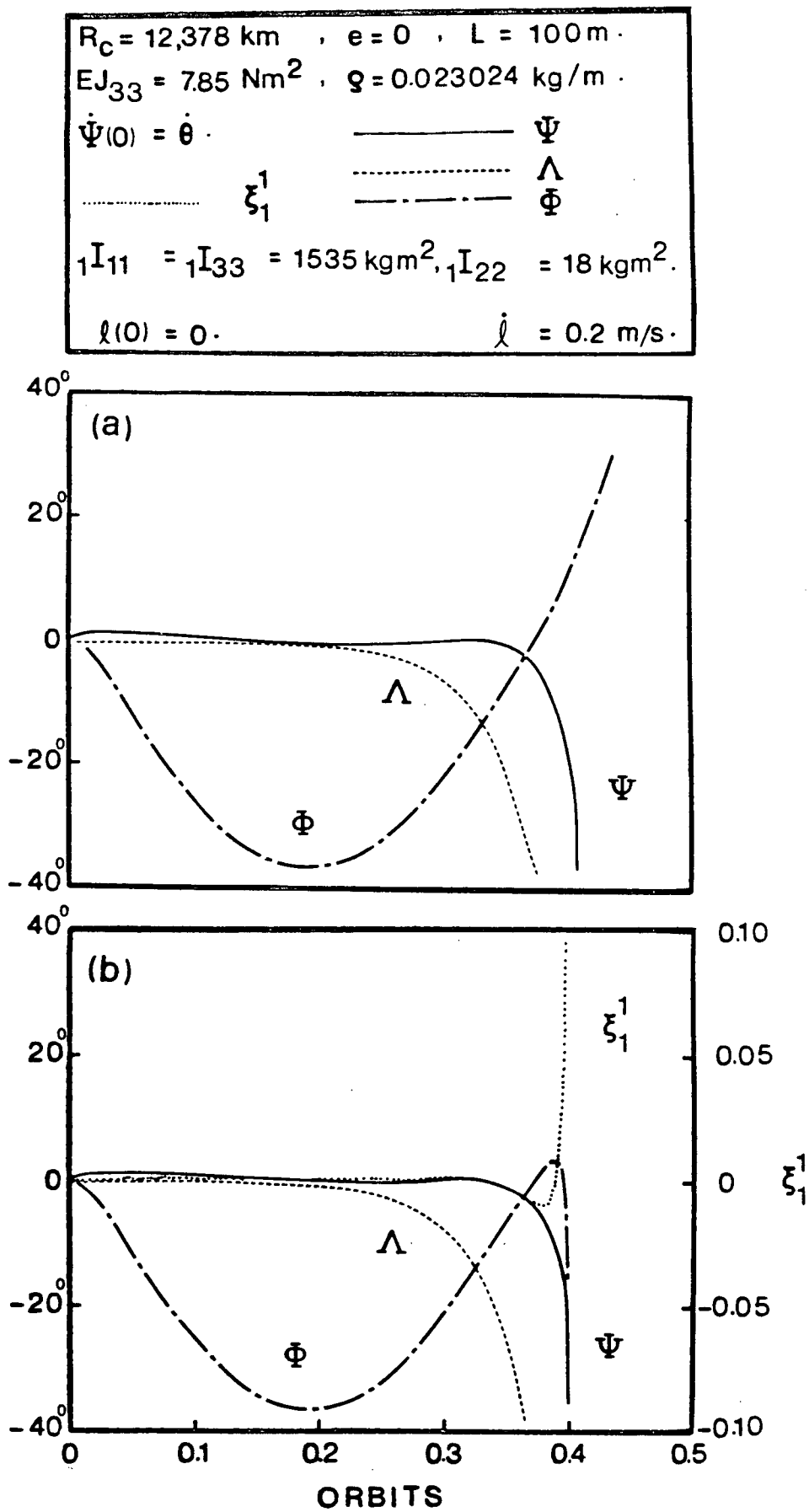

Figure 6-4 Effect of boom deployment on the three-axis response of a satellite to an impulsive out-of-plane disturbance: (a) rigid booms; (b) flexible booms.

R_c = 12,378 km, e = 0, L = 100 m , ϱ/EJ = 0.00293 $s^2 m^{-4}$.

$_1I_{11} = {}_1I_{33}$ = 1535 kgm^2 , $_1I_{22}$ = 18 kgm^2.

$\dot{\Psi}(0)$ = (a) 0.01 $\dot{\theta}$, (b) 0.10 $\dot{\theta}$, (c) $\dot{\theta}$.

——— Ψ ····· Λ — — Φ ····· ξ_1^1

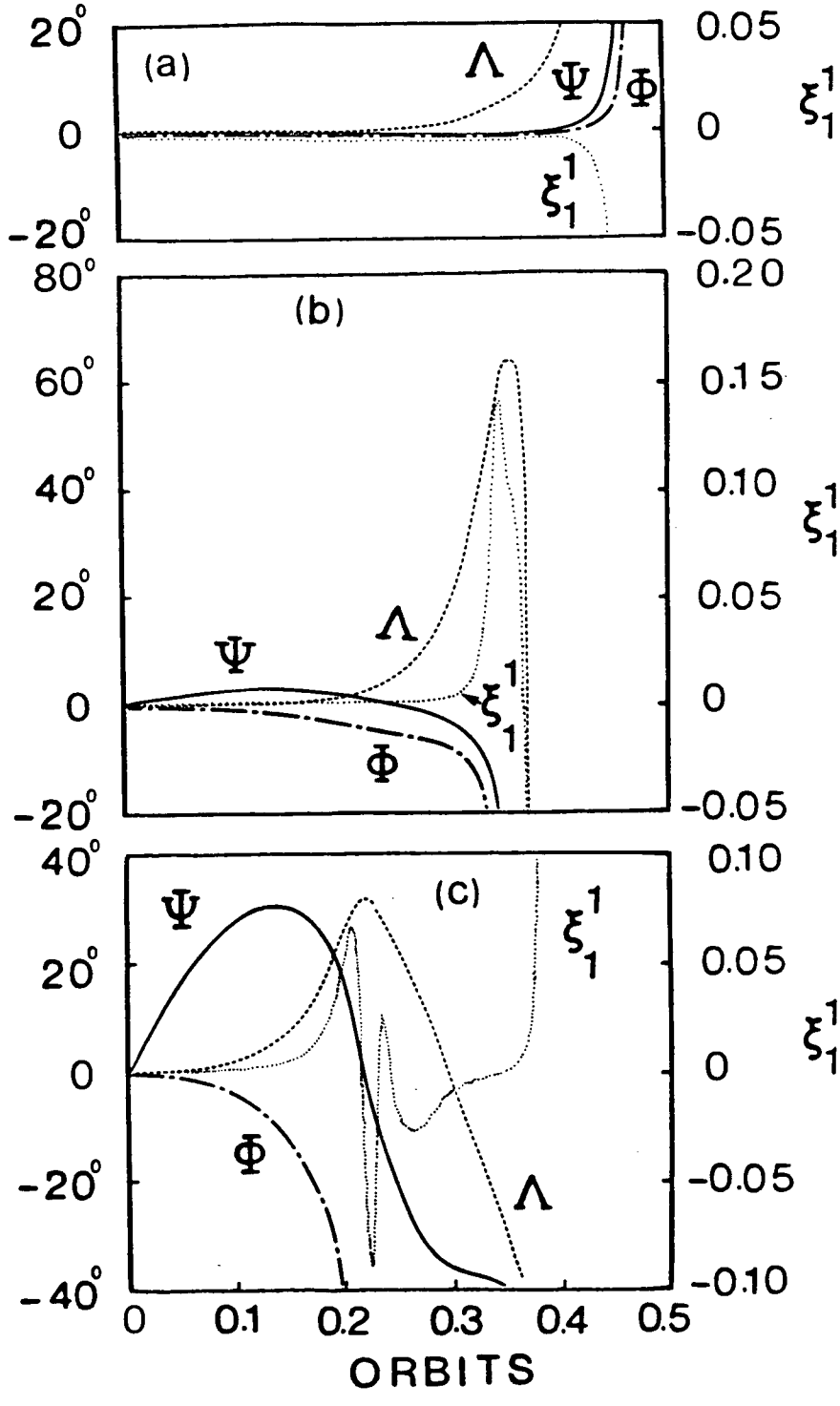

Figure 6-5 Effect of magnitude of an impulsive out-of-plane disturbance on three-axis response.

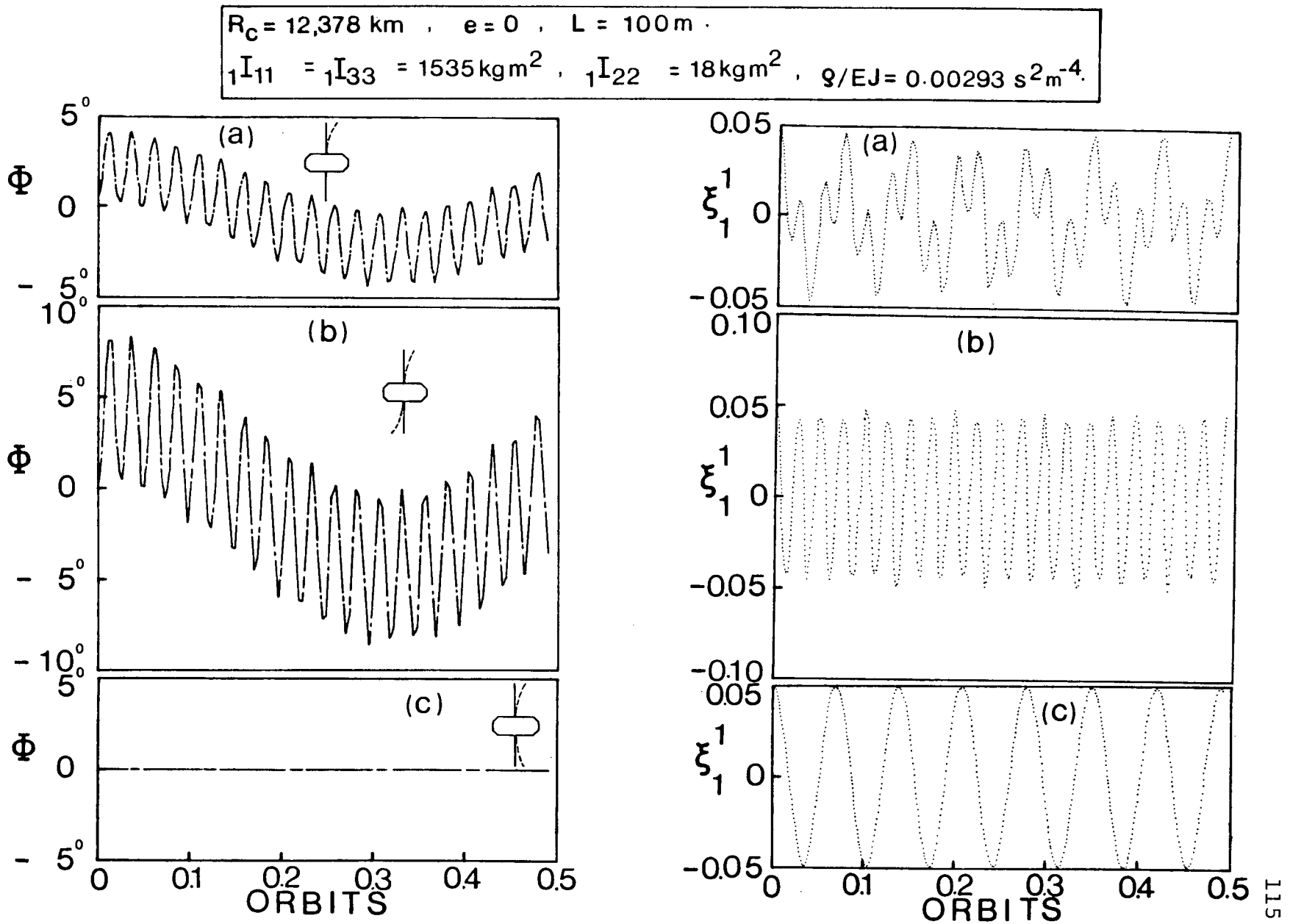

Figure 6-6 Planar response of the gravity gradient configuration to different initial elastic deformations.

Figure 6-7 describes three-dimensional librational response when tip of the appendage is displaced (in the orbital plane) by an amount equal to one per cent of its length. As expected, the case of symmetric appendage disturbance closely resembles the planar response data given earlier in Figure 6-6(c). There is, however, approximately one degree of yaw apparent after half an orbit. This is in contrast to the antisymmetric case where both roll and yaw remain unexcited [Figure 6-7(b)]. Pitch responds in a manner analogous to that in the planar case except that now the peak amplitude is only around 1.5°. However, a strikingly dramatic effect of coupling is revealed when the system is subjected to a disturbance in the form of tip displacement of one of the booms [Figure 6-7(a)]. Initially, up to around a quarter of an orbit, only a small amplitude pitch librational motion is unexcited. However, subsequently both yaw and roll appear, grow in magnitude monotonically and in turn cause large amplitude vibration driving the system unstable within half an orbit! This is in marked contrast to the apparently stable behaviour in the planar case, even with more severe initial conditions, as given in Figure 6-6(a). This emphasizes significance of coupling effects in a study of the class of spacecraft with flexible appendages.

Although not shown here, results were also obtained to assess effects of several other parameters on dynamics of the two boom gravity gradient configuration free to undergo three-axis librations. The use of higher modes to represent appendage vibration showed only minor difference in amplitude without affecting general character of the response. Similarly, the effect of shifting center of mass, off-set of the appendage attachment, and the appendage foreshortening

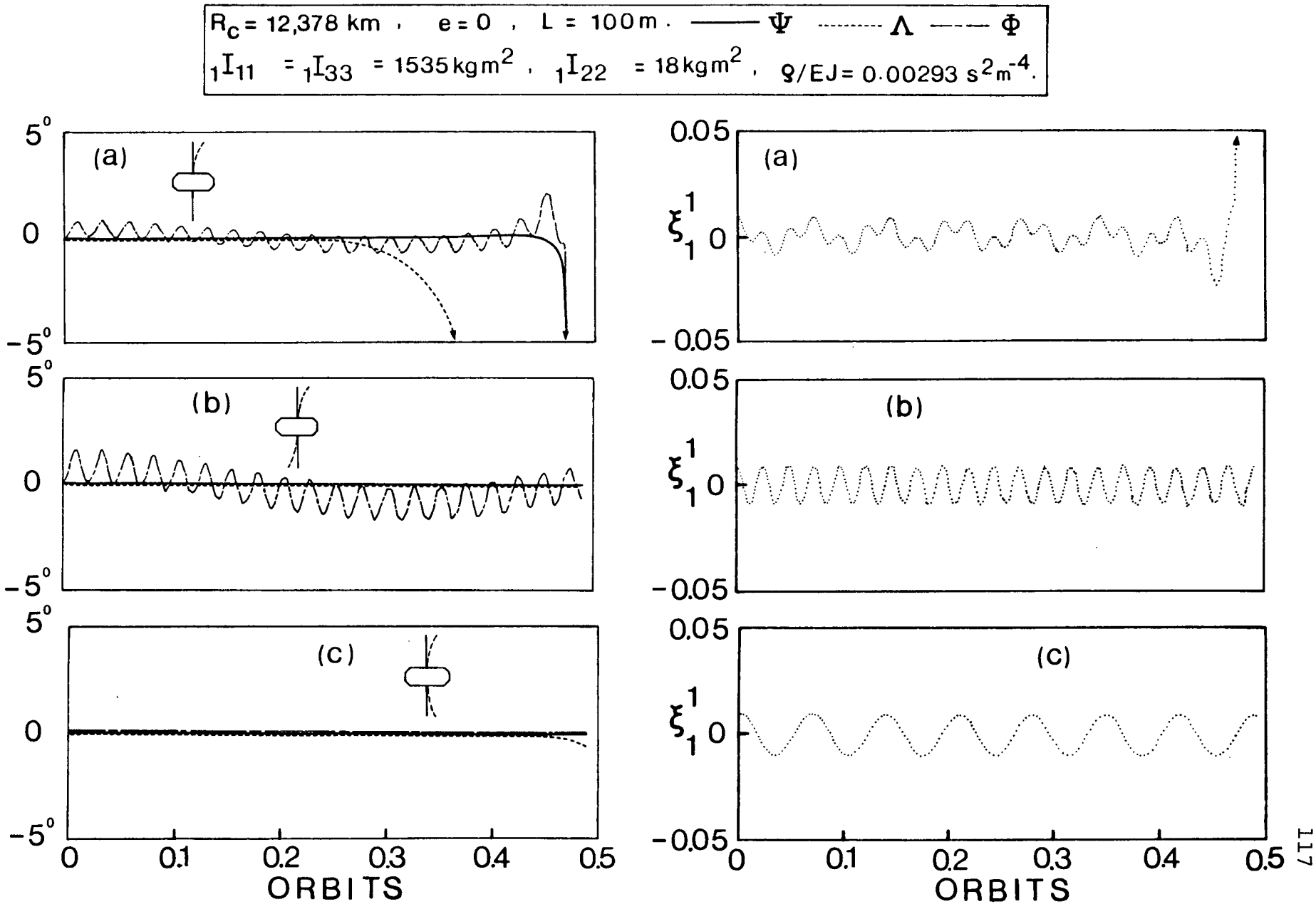

Figure 6-7 Three-axis response of the gravity gradient configuration to different initial elastic deformations.

during transverse oscillations was found to be negligible on librational response (amplitude change less than 5%). More noticeable was the shift in the phase which was also present during deployment of the appendage. Also, as found in Chapter 5, deployment can affect the system response substantially and under certain critical combination of parameters can drive it unstable.

6.2.2 Four-boom spin-stabilized configuration

In addition to the gravity-stabilized concept, another equilibrium orientation involves a satellite spinning at a rate much greater than the orbital rate, with the axis of spin normal to the orbital plane. Using coordinates as defined in Figure 2-2, the x, y body-fixed axes lie in the spin plane (orbital plane). This section studies dynamics of a system having four mutually orthogonal, flexible, deploying, uniform beam-type appendages numbered 1 through 4 lying in the spin plane (Figure 6-1). Orbital characteristics together with boom properties ρ, EJ_{33} are the same as in the gravity-stabilized case. The length of each pair of diametrically opposed booms is similar to that of the Allouette II satellite.

Presented in Figure 6-8 is the three-axis attitude response of the system (initially spinning at 0.1 rad s^{-1}) during deployment of appendages at 0.10 ms^{-1}. Although all booms have the same starting length and deploy at the same rate, booms numbered 2 and 4 stop deploying at 10 m whereas 1 and 3 extend to 35 m. Results for rigid appendages are also included for comparison. Despin of the pitch degree of freedom is according to the conservation of angular momentum. The configuration is highly stable with the pitch rate attaining a constant value following deployment, and there is no

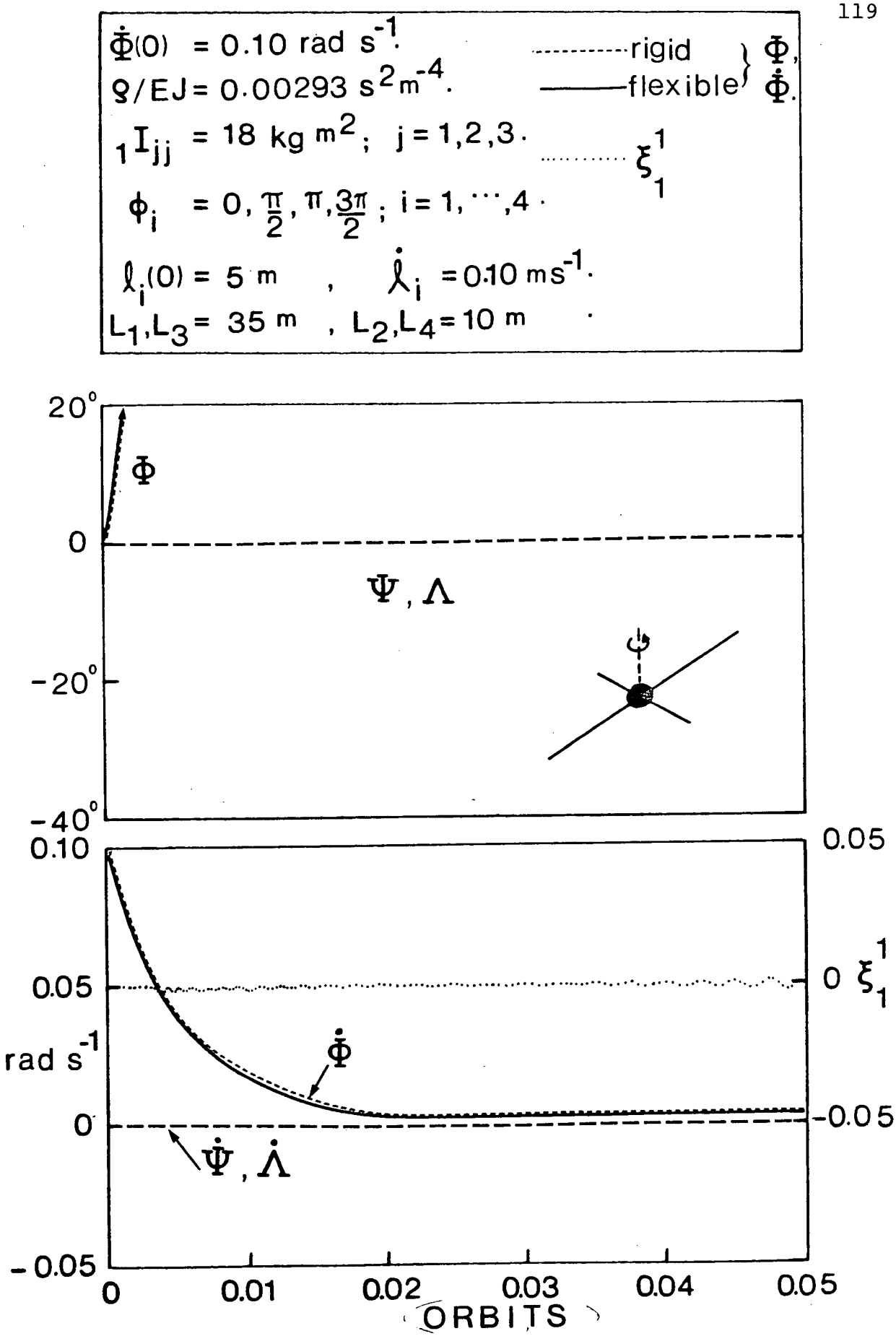

Figure 6-8 Three-axis response of a spinning spacecraft during deployment of rigid or flexible appendages.

out-of-plane librations. Note the effect of flexibility is essentially negligible. This is consistent with the low level of vibrations. In fact, the appendage vibration is virtually absent until the first set of booms stop deploying. Even after 0.05 orbit (685 s) oscillations at the tip stay much less than 1% of the boom length.

Displacing boom 1 [$\phi_1 = 0, \ell_1(0) = 5$m] by 0.25 m at the tip in the spin plane at the start of deployment still fails to excite any roll/yaw motion (Figure 6-9). However, considerable interaction between the pitch and the flexible appendages leads to high frequency modulation of the pitch rate, a result similar to that observed in the gravity gradient case.

Figure 6-10 presents response of the system to an impulsive roll/yaw disturbance equal to 10% of the nominal initial spin rate. Large amplitude displacements result leading to tumbling motion in less than eleven minutes. Furthermore, not only the pitch rate but also the yaw rate decreases significantly. On the other hand, the roll rate appears to grow. Note that the strong roll coupling effects experienced in the gravity gradient case are not dominant here. Also the appendage oscillations are minimal.

6.2.3 CTS-type configuration

A completely different class of satellites is represented by the CTS-type configuration briefly referred to in Chapter 1. It is characterized by two flexible appendages (numbered 5 and 6, Figure 6-1) and a momentum wheel perpendicular to the orbital plane. The general formulation of Chapter 2 is readily adapted to this configuration as well by simply adding the momentum wheel effect to the {h} vector.

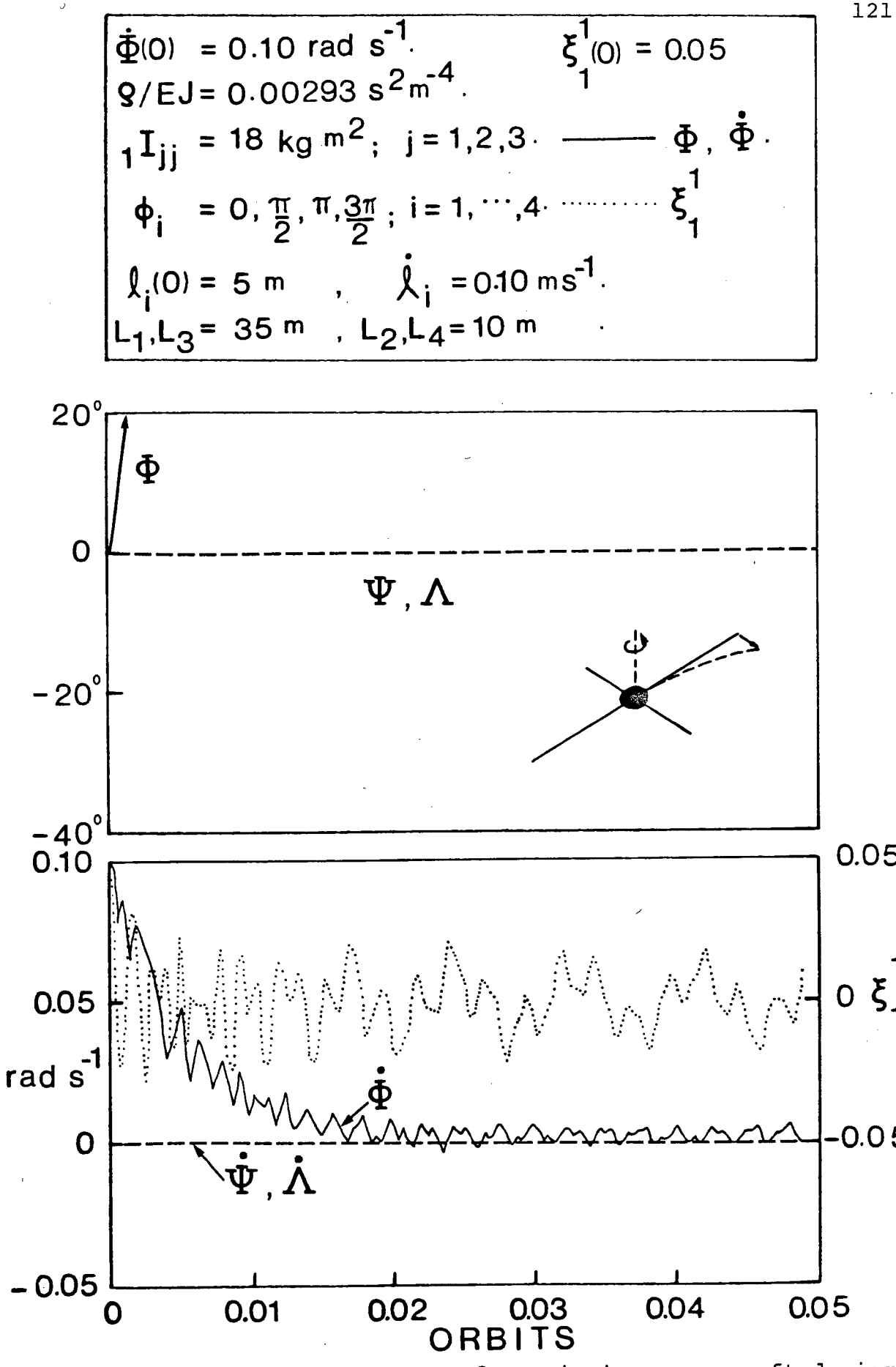

Figure 6-9 Three-axis response of a spinning spacecraft during deployment of flexible appendages with one boom initially deformed.

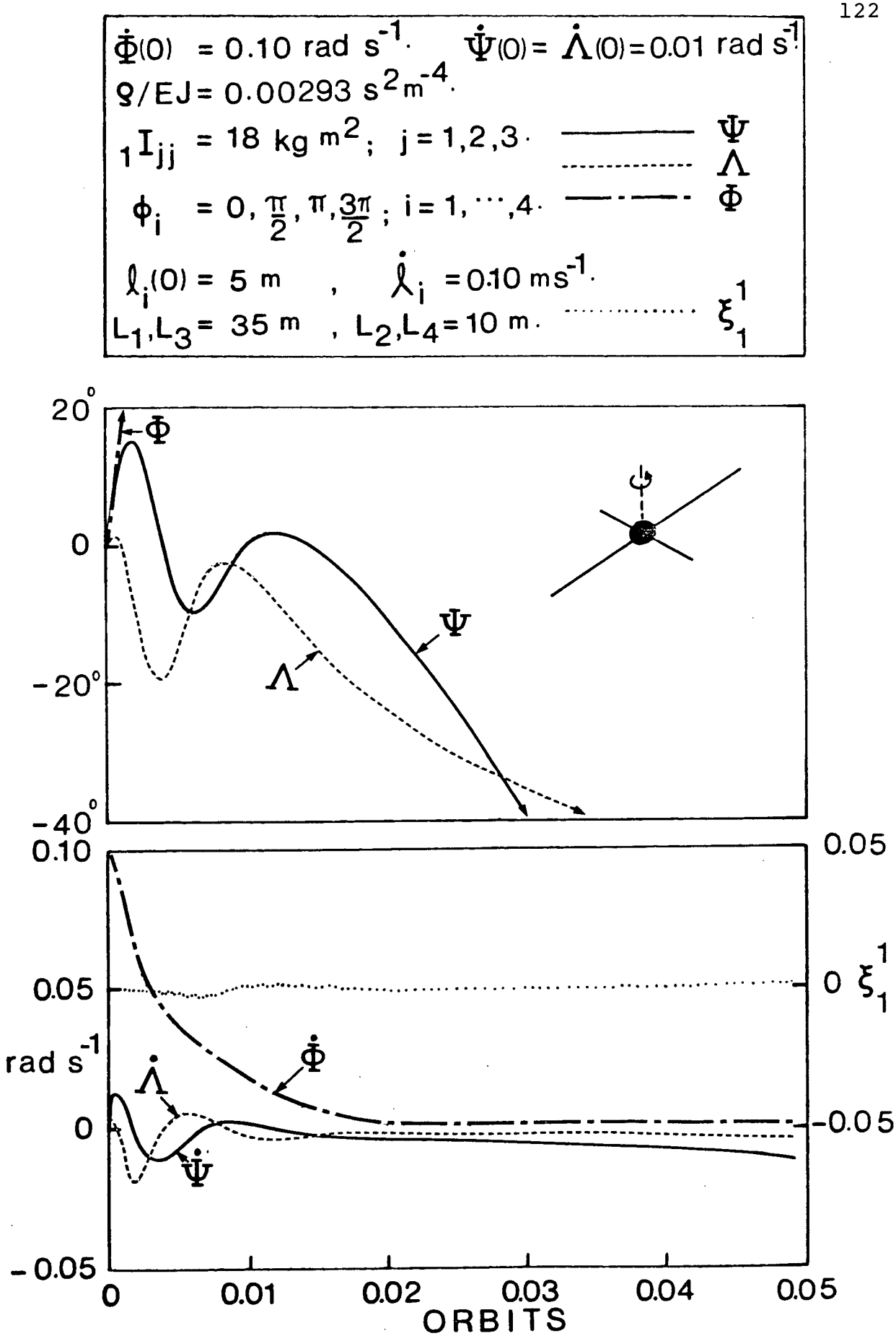

Figure 6-10 Three-axis response of a spinning spacecraft with flexible deploying appendages when subjected to out-of-plane attitude disturbances.

Some representative response data is given by Figures 6-11, 6-12. The effect of including a stored momentum and of flexibility, in the absence of deployment, is emphasized in Figure 6-11. As expected, the additional momentum has a stabilizing effect [compare Figures 6-11(a), (b)]. On the other hand, flexibility tends to make the system unstable [Figure 6-11(c)].

Deployment effects are illustrated by Figure 6-12. Note a marked difference in the pitch behaviour due to interaction with the boom vibrations. Furthermore, the instability appears to set in somewhat earlier compared to the rigid case.

6.2.4 Asymmetric deployment of appendages

Also of interest is the case of asymmetry introduced by the appendages. This could occur in the event of failure of a boom to deploy fully or if the fully-deployed configuration of the overall spacecraft is itself asymmetric (e.g. Pioneer IV). An equivalent effect would be present during modular construction of very large space structures such as the SPS. Also, asymmetric deployment has been proposed as a useful means of attitude control.[179,208]

Figures 6-13 and 6-14 compare response of rigid and flexible asymmetric configurations to planar excitation for the two-boom gravity gradient satellite studied in sections 5.3 and 6.2.1.

Figure 6-14 involves appendage deployment from 0-100 m for the boom aligned along the outward-pointing vertical, and from 0-50 m for the second boom located 180 degrees with respect to the first. Corresponding performance with the appendage length fixed at 100 m and 50 m respectively, is also included, (Figure 6-13). It is

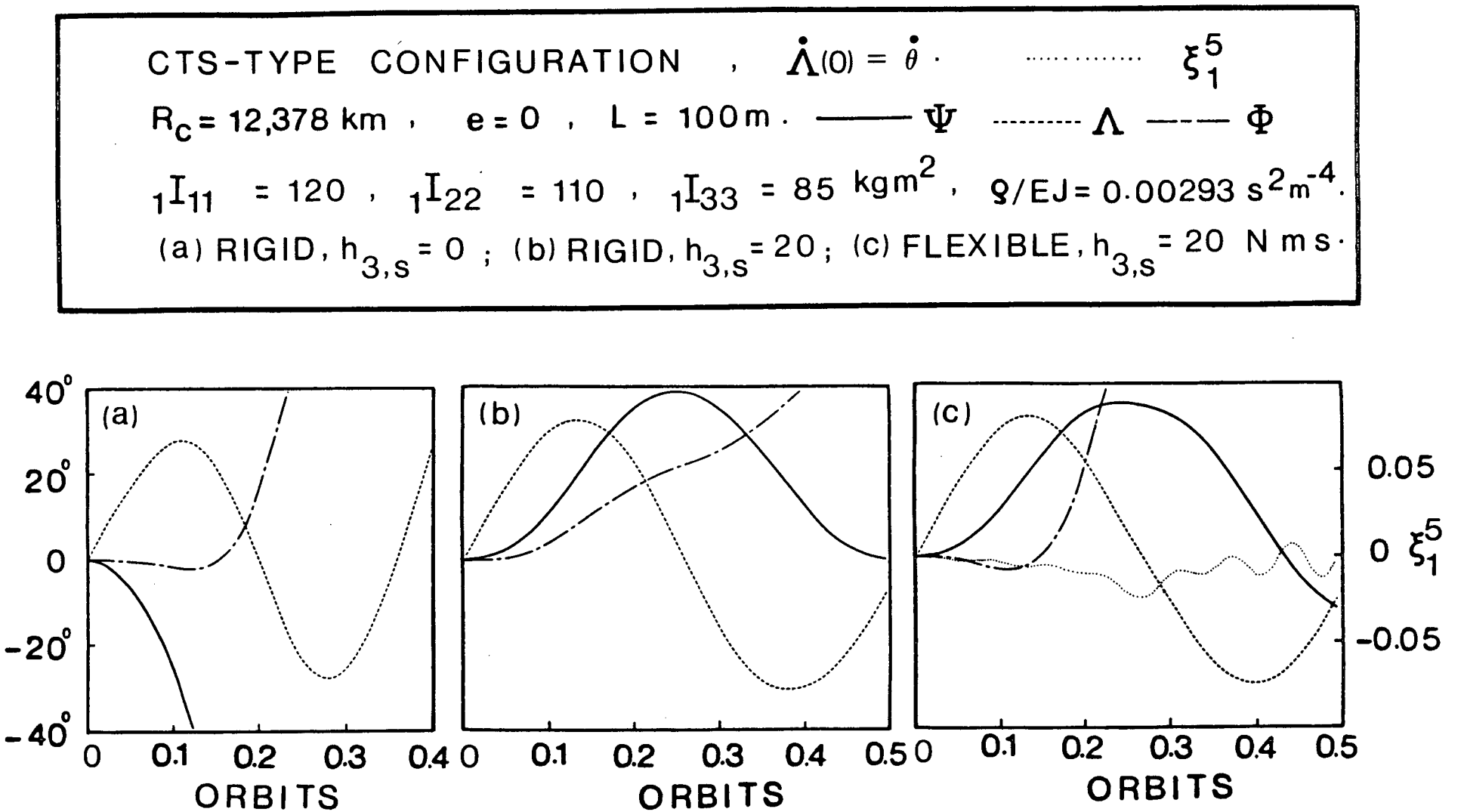

Figure 6-11 Effect of stored momentum and flexibility for: (a) rigid appendages, no momentum wheel; (b) rigid appendages with added momentum; (c) flexible appendages with added momentum.

CTS-TYPE CONFIGURATION , $\dot{\Lambda}(0) = \dot{\theta}$.

R_c = 12,378 km , e = 0 , L = 100 m . ..... ξ_1^5

$\varrho/EJ = 0.00293\ s^2 m^{-4}$. —— Ψ ..... Λ —·— Φ

${}_1I_{11}$ = 120 , ${}_1I_{22}$ = 110 , ${}_1I_{33}$ = 85 kgm^2.

$\ell(0)$ = 50 m , $\dot{\ell}$ = 0.10 ms^{-1} , $h_{3,s}$ = 20 N m s .

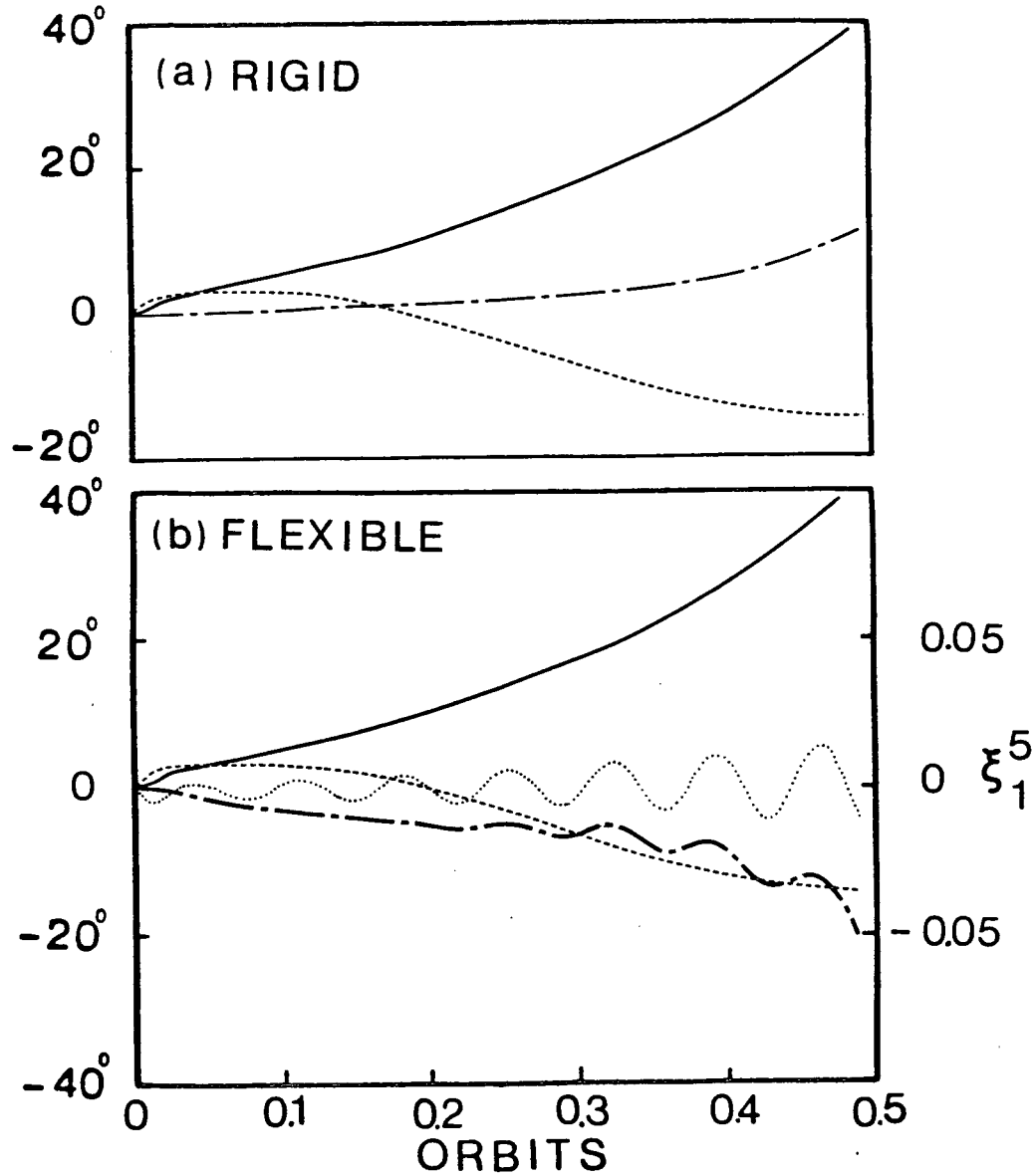

Figure 6-12 Response of a CTS-type spacecraft to an initial yaw rate disturbance during deployment of: (a) rigid booms; and (b) flexible booms.

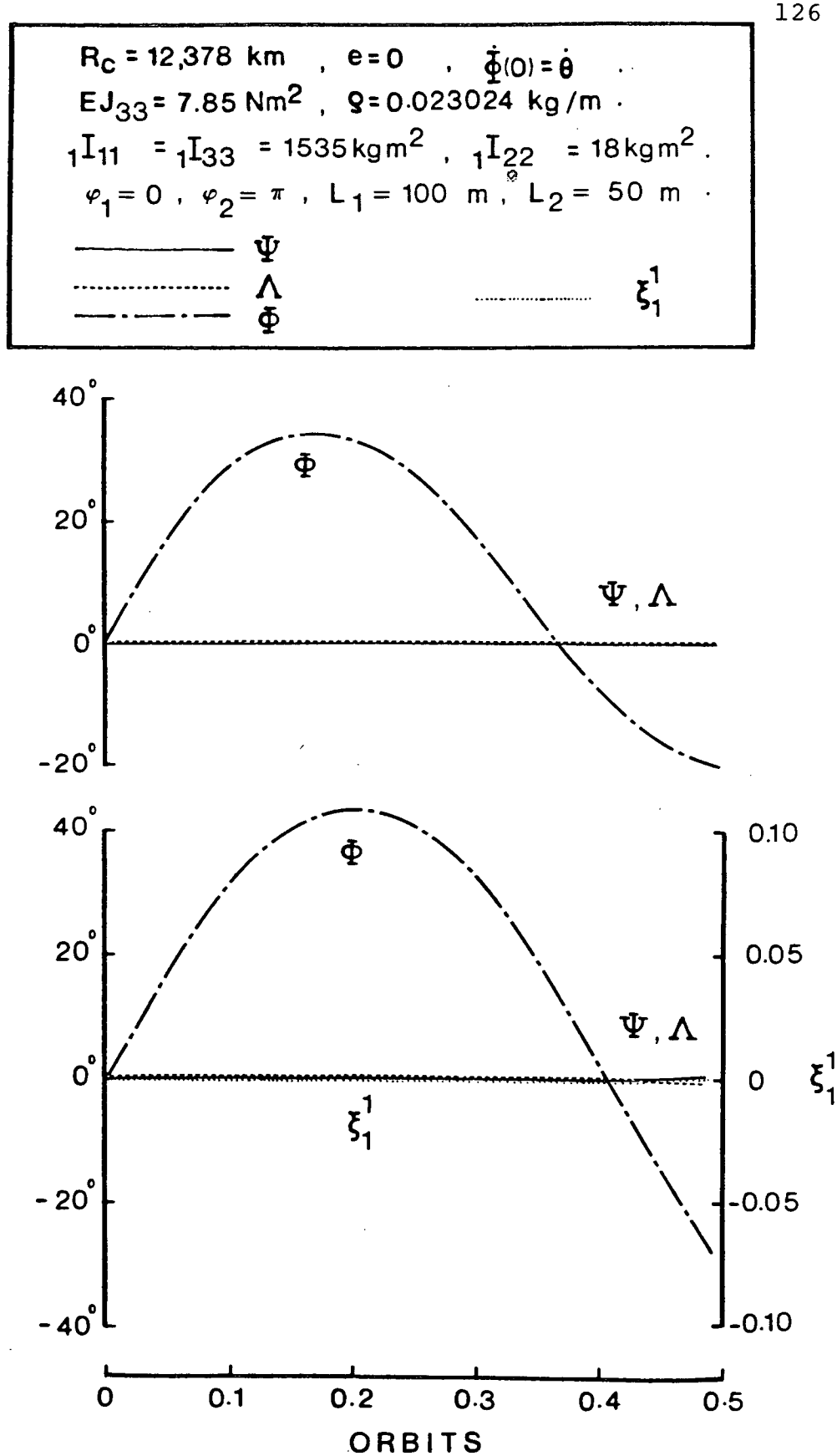

Figure 6-13 Three-axis response of a two-boom gravity gradient satellite with asymmetrically deployed appendages: (a) rigid booms; (b) flexible booms.

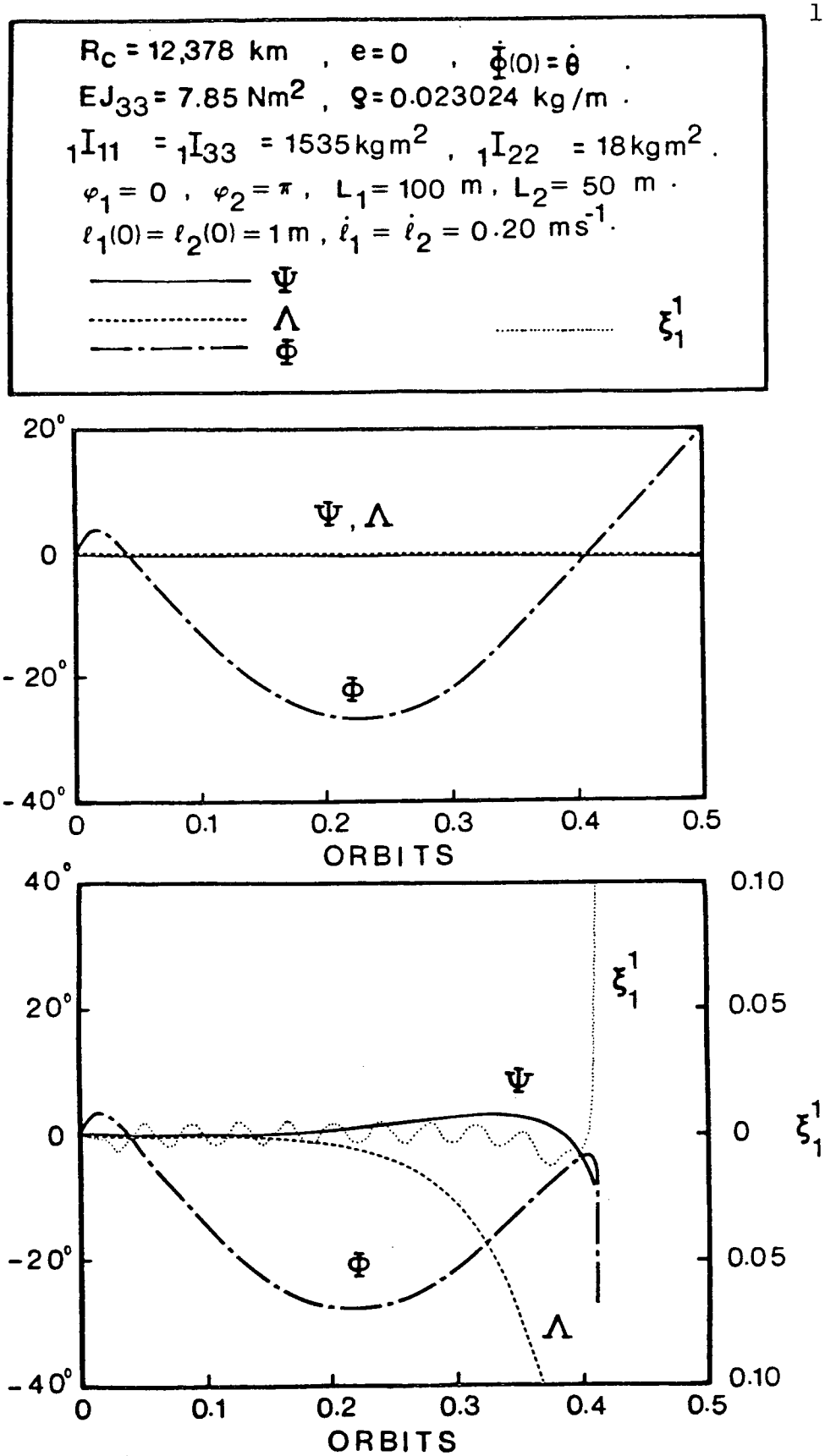

Figure 6-14 Effect of asymmetric boom deployment on three-axis response of a two-boom gradient satellite: (a) rigid booms; (b) flexible booms.

demonstrated that flexibility can result in a pitch response of up to 10 degrees larger for a nondeploying asymmetric configuration as opposed to the symmetric case (Figure 6-13). Also, a weak coupling of the roll/yaw motions becomes apparent after 0.5 orbits. Comparisons based on flexible deploying booms are even more dramatic. The asymmetric condition (Figure 6-14) produces significant vibrations which eventually become unstable as a result of the large amplitude roll/yaw behaviour induced by coupling effects.

6.3 Concluding Remarks

Examination of the governing system equations together with some typical three dimensional simulations presented in this chapter leads to the following conclusions:

(i) The ease with which such diverse classes of satellite configurations have been simulated demonstrates the versatility of the general formulation.

(ii) Coupled character of the motion significantly affects the system dynamics, hence caution should be exercised in utilizing results based on the planar analysis.

(iii) Significant simplification in the equations can occur with appendages having a specific orientation or, if one can ignore such factors as appendage offset, foreshortening, shifts in the center of mass location, flexibility, deployment, or higher modes used in the assumed vibration solution. Elimination of even one of these parameters such as π effects considerable savings in algebra with associated reduction in computational time and effort.

(iv) Pitch and associated in-plane vibrations do not excite roll/yaw degrees of freedom. On the other hand, a roll disturbance can excite the yaw/pitch motion.

(v) Stable librations do not excite significant appendage motion whereas initial boom displacements can result in very noticeable changes in attitude.

(vi) Interaction between flexibility and libration leads to an increase in the frequency of appendage oscillation together with a high frequency modulation of the attitude response.

(vii) The small amplitude oscillations evident both with the gravity gradient and spin-stabilized response justify a linear vibration analysis.

(viii) There are combinations of flexibility, deployment, and initial conditions for which a satellite can tumble over.

(ix) Flexibility considerations can be particularly significant in the study of asymmetric deployment as it can greatly increase the magnitude of attitude response and the degree of coupling to the point of causing tumbling.

7. CLOSING COMMENTS

Overall, the thesis presents a unified procedure, based on the methods of analytical dynamics, for deriving and solving system equations governing general spacecraft librational motion, which includes the effects of flexibility and deployment. Application of the method is illustrated through a generalized configuration representative of an important class of problems. This is particularly helpful to a design engineer as there is no need to continually rederive a complete set of equations for each new spacecraft. Rather than the accumulation of a large amount of data, the emphasis is on evolution of a generalized and organized methodology for coping with such complex nonlinear, nonautonomous, and coupled dynamical systems. Effectiveness of the approach is illustrated through an extensive response evaluation of gravity gradient, spin-stabilized and CTS-type configurations. Important features of the formulation procedure and conclusions based on the response results are presented in the following sections.

7.1 On Formulating System Equations of Motion

Although several studies have been carried out on the formulation alone for flexible satellite attitude dynamics, none has attacked the problem to this degree of generality. It should be emphasized that the momentum formulation of Chapter 2 need not be restricted to the study of satellite dynamics alone, but is a general result of particular value in analyzing any complex rotating system. Note also that the attitude equations ultimately involve only the

generalized coordinates associated with the appendage degrees of freedom. Consequently, for any satellite configuration, governing librational equations remain the same. However, the vibration equations change to reflect the character of the appendage. Developing appendage equations in terms of 'local' coordinates means that they can be analyzed directly, the point emphasized also by Laurenson (1976)[135] and Gupta (1978).[118] Overall, the formulation related to appendage vibrations presented in this thesis represents a significant extension to the Euler-Bernoulli beam theory.

In the analysis of such involved systems the key element which makes a solution feasible is adoption of a continuum representation in conjunction with an assumed-mode solution. Note, in general, any approximate shape functions satisfying geometric boundary conditions can be used, including ones found by means of a finite element method.

7.2 Characteristics Associated with a Deploying, Orbiting, Spinning Beam-Type Appendage

The dominant influences on system eigenvalues for most practical applications are the spin parameter and appendage length. Changes in spin rate itself however do not affect the natural vibration characteristics but act as an additional external boom loading. Also of importance is the fact that resonance can occur between the spin degree of freedom and in-plane oscillations.

Deployment rate and changes in deployment rate alter effective stiffness of the boom. In addition, deployment rate introduces a term into the equations which can be viewed as a negative damping.

Specifically, deployment-related Coriolis forces can result in large amplitude deformations in the spin plane and hence must be considered when arriving at any deployment strategy.

Out-of-plane eigenfrequencies become shifted by an amount proportional to the spin parameter. This result is modified for an orbiting beam since, in general, the characteristics of an orbiting beam can vary significantly from those for a beam rotating in the absence of the gravity gradient influence.

7.3 Overall System Response

Results suggest that large amplitude attitude behaviour can occur simultaneously with small amplitude oscillations thus justifying a linear vibration analysis in such cases.

The planar study carried out in Chapter 5 demonstrates that large amplitude pitch motion does not necessarily excite the appendage vibrations; the reverse, however, is not true. In fact, once the appendages are excited, significant coupling between vibrational and librational motion results in a high frequency modulation of the pitch response together with a shift in the expected frequency of the appendage vibration. In general, planar motions do not cause out-of-plane rotations whereas, for example, a roll disturbance results in a three-axis attitude response. Hence care must be taken when interpreting data based on a planar analysis only since the coupling effects can become quite significant, to the point of dominating the response.

Three-axis analysis suggests that, in general, parameters such as shifting center of mass, appendage offset, and the use of a larger

number of modes (all of which substantially complicate the formulation) have little effect on the magnitude of the response. Hence one can neglect them, at least during the preliminary design stage, with considerable saving in computational time and effort. Also, it was found that libration during asymmetric deployment of appendages can become unstable when flexibility is taken into account, even though no such instability may exist for the rigid configuration.

Depending on orbital parameters and physical properties of booms, results show that there exist critical values of appendage length and deployment rate for which a satellite can tumble over. Application of the analysis to three distinctly different classes of satellites (gravity gradient, spin-stabilized, CTS-type) demonstrates the versatility of the general formulation. It is of interest to note that the size, speed, and accuracy of the modern day digital computer permits dynamical simulations which would not have been possible a decade earlier.

7.4 Recommendations for Future Work

(i) A comprehensive numerical investigation could be carried out varying initial conditions and major spacecraft characteristics in a systematic manner. Using such a matrix of conditions one could generate a parameter map identifying essential response features for a family of configurations, e.g., gravity gradient, spinning, CTS and RAE classes of satellites, etc.

(ii) The forced response of the system can be readily examined by introducing the appropriate generalized forces. Of primary concern would be the effect of environmental forces such as those resulting from solar radiation pressure, aerodynamic and, perhaps, control forces.

(iii) Governing equations can be formulated for additional types of appendages.

(iv) A significant extension to the modelling of appendages would be to relax constraints at the root so as to allow for cantilevered and/or hinged connections with/without stiffness and discrete damping. Structural damping could also be allowed for. In addition, the analysis could be extended to include appendages undergoing a controlled variation in orientation with time - a feature of potential military importance.

(v) An interesting study would be to create a computer-generated visualization of the spacecraft response. For instance, one might wish to look at a simulated dynamical history starting with the initial undeployed high-spin state at orbital injection, through the attitude acquisition phase involving deployment of appendages, to the steady state equilibrium condition. Also, it could prove rewarding to visualize the effect of attitude control manoeuvres made using extension and retraction of the appendages.

(vi) Having such a general formulation at hand, the next logical step to fully exploit its potential would be to devise an appropriate control strategy and seek the optimal design.

BIBLIOGRAPHY

1. Noll, R.B. et al. (1969) A survey of structural flexbility effects on spacecraft control systems. AIAA 7th Aerospace Sciences Meeting, New York, New York, AIAA Paper No. 69-116.

2. Shrivastava, S.K. et al. (1969) Librational dynamics of earth orbiting satellites. Proc. 14th Congress on Theoretical and Applied Mechanics, Kurukshetra, 284-306.

3. Likins, P.W. (1970) Dynamics and control of flexible space vehicles. National Aeronautics and Space Administration, Tech. Report No. 32-1329.

4. Likins, P.W. (1974) Analytical dynamics and nonrigid spacecraft simulation. National Aeronautics and Space Administration, Report No. 32-1593.

5. Likins, P.W. (1976) Interaction problems between the dynamics and control system for nonrigid spacecraft. Proc. ESA Symp. on Dynamics and Control of Non-Rigid Spacecraft, ESA SP 117, 265-271.

6. Likins, P.W. (1977) The influence on dynamics and control theory of the spacecraft attitude control problem. Invited Lecture, Proc. Sixth Canadian Congress of Applied Mechanics, Vancouver, May 30 - June 3, I, 321-335.

7. Likins, P.W. and Bouvier, H.K. (1971) Attitude control of nonrigid spacecraft. AIAA Astronautics and Aeronautics J. 9 (5), 64-71.

8. Modi, V.J. (1974) Attitude dynamics of satellites with flexible appendages - A brief review. J. Spacecraft and Rockets, 11 (11), 743-751.

9. Williams, C.J.H. (1976) Dynamics modelling and formulation techniques for non-rigid spacecraft. Proc. ESA Symp. on Dynamics and Control of Non-Rigid Spacecraft, ESA SP 117, 53-70.

10. Garg, S.C. et al. (1978) Strapdown navigation technology: A literature survey. AIAA J. Guidance and Control, 1 (3), 161-172.

11. Stuhlinger, E. (1979) First steps into space, 1946-1978. AIAA J. Spacecraft and Rockets, 16(1), 3-9.

12. Roberson, R.E. (1979) Two decades of spacecraft attitude control. AIAA J. Guidance and Control, 2(1), 3-8.

13. Moran, J.P. (1961) Effects of plane librations on the orbital motion of a dumbell satellite. ARS J. 1089-1096.

14. Yu, E.Y. (1964) Long-term coupling effects between the librational and orbital motions of a satellite. AIAA J. 2(3), 553-555.

15. Misra, A.K. and Modi, V.J. (1977) The influence of satellite flexibility on orbital motion. Proc. AIAA Symp. on Large Flexible Satellites, Blacksburg, Virginia, 59-74.

16. Klemperer, W.B. and Baker, Jr., R.M.L. (1956) Satellite librations. Proc. 7th International Astronautical Congress, Rome, 3-21.

17. De Bra, D.B. and Delp, R.H. (1961) Rigid body attitude stability and natural frequencies in a circular orbit. J. Astronautical Sciences, 8, 14-17.

18. Auelmann, R.R. (1963) Regions of libration for a symmetrical satellite. AIAA J. 1(6), 1445-1447.

19. Pringle, Jr., R. (1964) Bounds on the librations of a symmetrical satellite. AIAA J. 2(5), 908-912.

20. Thomson, W.T. (1962) Spin stabilization of attitude against gravity torque. J. Astronautical Sciences, 9, 31-33.

21. Kane, T.R. and Barba, P.M. (1966) Attitude stability of a spinning symmetrical satellite in an elliptic orbit. Trans. ASME J. of Applied Mech. 402-405.

22. Likins, P.W. and Columbus, R.L. (1966) Effects of eddy-current damping on satellite attitude stability. AIAA J. 4(6), 1123-1125.

23. Kane, T.R. (1965) Attitude stability of earth-pointing satellites. AIAA J. 3(4), 726-731.

24. Kane, T.R. and Shippy, D.J. (1963) Attitude stability of a spinning unsymmetrical satellite in a circular orbit. J. Astronautical Sciences, 10(4), 114-119.

25. Morrison, J.A. (1969) Stationary resonant pitching motions of a controlled satellite. AIAA J. 7(6), 1032-1038.

26. Evans, W.J. (1964) Aerodynamic and radiation disturbance torques on satellites having complex geometry. Reported in: Torques and Attitude Sensing in Earth Satellites, edited by S.F. Singer, Academic Press, 83-98.

27. Singer, S.F. (1964) Forces and torques due to Coulomb interaction with the magnetosphere. Reported in: Torques and Attitude Sensing in Earth Satellites, edited by S.F. Singer, Academic Press, 99-105.

28. Roberson, R.E. (1964) Generalized gravity-gradient torques. Reported in: Torques and Attitude Sensing in Earth Satellites, edited by S.F. Singer, Academic Press, 7382.

29. Beletskii, V.V. (1965) Motion of an artificial satellite about its center of mass. Moscow Technical Publishing House of Physical-Mathematical Literature, (in Russian). English translation in NASA TT F-429, TT 67-51366.

30. Brereton, R.C. (1967) A stability study of gravity oriented satellites. Vol. I & II. Ph.D. dissertation, University of British Columbia.

31. Tschann, C.A. (1970) On the librational dynamics of damped satellites. Ph.D. dissertation, University of British Columbia.

32. Kane, T.R. and Levinson, D.A. (1976) Stability, instability, and terminal attitude motion of a spinning, dissipative spacecraft. AIAA J. 14(1), 39-42.

33. Cloutier, G.J. (1976) Resonances of a two-DOF system on a spin stabilized spacecraft. AIAA J. 14(1), 107-109.

34. Cochran, J.E. and Thomspon, J.A. (1980) Nutation dampers vs. precession dampers for asymmetric spacecraft. AIAA J. Guidance and Control, 3(1), 22-28.

35. Vigneron, F.R. (1971) Stability of a dual-spin satellite with two dampers. J. Spacecraft and Rockets, 8(4), 386-389.

36. Kane, T.R. and Athel, S. (1972) Behaviour of a two degree-of-freedom gyroscope in a rotating satellite. J. Spacecraft and Rockets, 9(4), 253-259.

37. Paul, B. (1963) Planar librations of an extensible dumbell satellite. AAIA J. 1(2), 411-418.

38. Pringle, Jr., R (1968) Exploitation of nonlinear resonance in damping an elastic dumbbell satellite. AIAA J. 6(7), 1217-1222.

39. Crist, S.A. and Eisley, J.G. (1969) Motion and stability of a spinning spring-mass system in orbit. J. Spacecraft and Rockets, 6(7), 819-824.

40. Connell, G.M. (1969) Optimal configuration for hinged, two body satellites. J. Spacecraft and Rockets, 6(9), 1024-1030.

41. Chobotov, V. (1963) Gravity gradient excitation of a rotating cable-counterweight space station in orbit. J. Applied Mech. 30, 547-561.

42. Bainum, P.M. and Evans, K.S. (1976) Gravity-gradient effects on the motion of two rotating cable-connected bodies. AIAA J. 14(1), 26-32.

43. Tai, C.L. and Loh, M.M.H. (1965) Planar motion of a rotating cable-connected space station in orbit. J. Spacecraft and Rockets, 2(6), 889-894.

44. Stabekis, P. and Bainum, P.M. (1970) Motion and stability of a rotating space station-cable-counterweight configuration. J. Spacecraft and Rockets, 7(8), 912-918.

45. Bainum, P.M. and Evans, K.S. (1975) Three-dimensional motion and stability of two rotating cable-connected bodies. J. Spacecraft and Rockets, 12(4), 242-250.

46. Nixon, D.D. (1972) Dynamics of a spinning space station with a counterweight connected by multiple cables. J. Spacecraft and Rockets, 9(12), 896-902.

47. Modi, V.J. and Sharma, S.C. (1977) Structural dynamics and configuration control of spinning and gravity oriented multibody systems. IUTAM Symp. Munich.

48. Austin, F. and Zetkov, G. (1974) Simulation capability for dynamics of two-body flexible satellites. J. Spacecraft and Rockets, 11 (3), 129-130.

49. Etkin, B. (1962) Attitude stability of articulated gravity-oriented satellites. Part I - General theory and motion in orbital plane. University of Toronto Institute of Aerophysics, Report No. 89.

50. Maeda, H. (1963) Attitude stability of articulated gravity-oriented satellites. Part II - Lateral motion. University of Toronto Institute of Aerophysics, Report No. 93.

51. Hughes, P.C. (1966) Optimized performance of an articulated gravity gradient satellite at synchronous altitude. University of Toronto Institute for Aerospace Studies, Report No. 118.

52. Lips, K.W. (1967) A proposed high altitude passive satellite design. B.A.Sc. dissertation, University of Toronto Institute for Aerospace Studies.

53. Garg, S.C. (1969) On the use of flexible strings in gravity-gradient stabilization systems. University of Toronto Institute for Aerospace Studies, Tech. Note No. 135.

54. Dow, P.C. et al. (1966) Dynamic stability of a gravity gradient stabilized satellite having long flexible antennas. AIAA/JACC Guidance and Control Conf., AIAA, New York, 285-303.

55. Hughes, P.C. (1973) Recent advances in the attitude dynamics of spacecraft with flexible solar arrays. Canadian Aeronautics and Space J. 19(4), 165-171.

56. Charyk, J.V. (1977) Communications satellites. J. Spacecraft and Rockets, 14(7), 385-394.

57. Janssens, F. (1976) Dynamics of spinning satellites modelled as a rigid central body and spherical pendulums as appendages. Proc. ESA Symp. on Dynamics and Control of Non-Rigid Spacecraft, ESA SP 117, 39-49.

58. Glaser, P.E. (1976) Evolution of the satellite solar power station (SSPS) concept. J. Spacecraft and Rockets, 13(9), 573-576.

59. Ashley, H. (1967) Observations on the dynamic behaviour of large flexible bodies in orbit. AIAA J. 5(3), 460-469.

60. Modi, V.J. and Brereton, R.C. (1968) Planar librational stability of a flexible satellite. AIAA J. 6(3), 511-517.

61. Sellappan, R. and Bainum, P.M. (1978) Modal control of the planar motion of a long flexible beam in orbit. Presentation at the 29th Congress of the International Astronautical Federation, Dubrovnik, Yugoslavia.

62. Kumar, V.K. and Bainum, P.M. (1980) Dynamics of a flexible body in orbit. AIAA J. Guidance and Control, 3(1), 90-92.

63. Breakwell, J.V. and Andeen, G.B. (1977) Dynamics of a flexible passive space array. J. Spacecraft and Rockets, 14(9), 556-561.

64. Chobotov, V.A. (1977) Gravitationally stabilized satellite solar power station in orbit. J. Spacecraft and Rockets, 14(4), 249-251.

65. (1969) Effects of structural flexibility on spacecraft control systems. NASA sp-8016.

66. Liégeois, A. and Simon, J.P. (1976) The controllability of multi-body mechanisms. Proc. ESA Symp. on Dynamics and Control of Non-Rigid Spacecraft, ESA SP 117, 227-236.

67. Meirovitch, L. (1970) Methods of analytical dynamics. McGraw-Hill Book Co.

68. Russell, W.J. (1969) On the formulations of equations of rotational motion for an n-body spacecraft. Space and Missle Systems Organization, Air Force Systems Command. Air Force Report No. SAMSO-TR-69-202.

69. Russell, W.J. (1976) Dynamic analysis of the communication satellites of the future. AIAA/CASI 6th Communication Satellite Systems Conf., Montreal, Canada, Paper No. 76-261.

70. Hooker, W.W. (1970) A set of r dynamical attitude equations for an n-body satellite having r rotational degrees of freedom. AIAA J. 8(7), 1205-1207.

71. Vance, J.M. and Stichin, A. (1970) Derivation of first-order difference equations for dynamical systems by direction application of Hamilton's Principle. J. Applied Mech. 276-278.

72. Stichin, A. (1975) On the use of the canonical equations of motion for the numerical solution of dynamical systems. Proc. 14th Midwestern Mech. Conf. University of Oklahoma, 241-250.

73. Anand, D.K. and Whisnant, J.M. (1971) Generalized equations for the position and attitude of a multiply connected spacecraft I. The dynamical equations. John Hopkins University Applied Physics Lab. Tech. Memorandum TG 1163-1.

74. Ho, J.Y.L. (1974) The direct path method for deriving the dynamic equations of motion of a multibody flexible spacecraft with topological tree configuration. AIAA Mech. and Control of Flight Conf. Anaheim, California, AIAA Paper No. 74-786.

75. Ho, J.Y.L. (1977) Direct path method for flexible multibody spacecraft dynamics. J. Spacecraft and Rockets, 14(2), 102-110.

76. Likins, P.W. (1975) Quasicoordinate equations for flexible spacecraft. AIAA J. 13(4), 524-526.

77. McDonough, T.B. (1976) Formulation of the global equations of motion of a deformable body. AIAA J. 14(5), 656-660.

78. Jerkovsky, W. (1978) The structure of multibody dynamics equations. AIAA J. Guidance and Control, 1(3), 173-182.

79. Lips, K.W. (1978) A 'compact' momentum formulation of equations of motion for complex rotating systems. 8th U.S. National Congress of Applied Mech., Los Angeles, June 26-30.

80. Kane, T.R. and Wang, C.F. (1965) On the derivation of equations of motion. J. Soc. Ind. App. Math. 13(2), 524-526.

81. Kane, T.R. (1968) Dynamics. Holt, Rinehart, and Winston, New York, U.S.A.

82. Kane, T.R. and Levinson, D.A. (1980) Formulation of equations of motion for complex spacecraft. AIAA J. Guidance and Control, 3(2), 99-112.

83. Levinson, D.A. (1977) Equations of motion for multiple-rigid-body systems via symbolic manipulation. J. Spacecraft and Rockets, 14(8), 479-487.

84. Meirovitch, L. (1970) Stability of a spinning body containing elastic parts via Liapunov's direct method. AIAA J. 8(7), 1193-1200.

85. Meirovitch, L. (1972) Liapunov stability analysis of hybrid dynamical systems with multi-elastic domains. Int. J. Non-Linear Mech. 7, 425-443.

86. Meirovitch, L. and Calico, R.A. (1972) Stability of motion of force-free spinning satellites with flexible appendages. J. Spacecraft and Rockets, 9(4), 237-245.

87. Meirovitch, L. and Calico, R.A. (1973) A comparative study of stability methods for flexible satellites. AIAA J. 11(1), 91-98.

88. Meirovitch, L. (1973) Liapunov stability analysis of hybrid dynamical systems in the neighbourhood of nontrivial equilibrium. Presented at the AAS/AIAA Astrodynamics Conf., Vail, Colorado.

89. Meirovitch, L. and Calico, R.A. (1975) Stability analysis of flexible spacecraft via the method of integral coordinates. AIAA J. 13(5), 653-658.

90. Mitchell, T.P. and Lingerfelt, J. (1970) The librational dynamics of deformable bodies. J. Celestial Mech. 1, 289-296.

91. Keat, J.E. (1970) Dynamical equations of nonrigid satellites. AIAA J. 8(7), 1344-1345.

92. Samin, J.C. and Willems, P.V. (1975) On the attitude dynamics of spinning deformable systems. AIAA J. 13(6), 812-817.

93. Bodley, C.S. and Park, A.C. (1972) The influence of structural flexibility on the dynamic response of spinning spacecraft. AIAA/ASME/SAE 13th Structures, Structural Dynamics, and Materials Conf. San Antonio, Texas, April 10-12.

94. Grote, P.B. et al. (1971) Equations of motion of flexible spacecraft. J. Spacecraft and Rockets, 8(60, 561-567.

95. Huang, T.C. and Das, A. (1973) Singular perturbation equations for flexible satellites. 24th International Astronautical Congress, Baku, U.S.S.R.

96. Morton, Jr., H.S. et al. (1973) Analytical solutions for Euler parameters. AAS/AIAA Astrodynamic Conf., Vail, Colorado.

97. Kraige, L.G. and Junkins, J.L. (1976) Perturbation formulations for satellite attitude dynamics. J. Celestial Mech. 13, 39-64.

98. Pringle, Jr., R. (1972) Satellite vibration-rotation motion studied via canonical transformations. AIAA/AAS Astrodynamics Conf. Palo Alto, Calif. AIAA Paper No. 72-919.

99. Fraeijs de Veubeke, B. (1976) Nonlinear dynamics of flexible bodies. Proc. ESA Symp. on Dynamics and Control of Non-Rigid Spacecraft, ESA SP 117, 11-19.

100. Canavin, J.R. and Likins, P.W. (1977) Floating reference frames for flexible spacecraft. J. Spacecraft and Rockets, 14(12), 724-732.

101. Davenport, P.B. (1973) Rotations about nonorthogonal axes. AIAA J. 11(6), 853-857.

102. Ohkami, Y. (1976) Computer algorithms for computation of kinematical relations for three attitude angle systems. AIAA J. 14(8), 1135-1137.

103. Nazaroff, G.J. (1979) The orientation vector differential equation. AIAA J. Guidance and Control, 2(4), 351-352.

104. Wilkes, J.M. (1979) General expression for a three-angle rotation matrix. AIAA J. Guidance and Control, 2(2), 156-158.

105. Mayo, R.A. (1979) Relative quaternion station transition relation. AIAA J. Guidance and Control, 2(1), 44-48.

106. Ickes, B.P. (1970) A new method for performing digital control system attitude computations using quaternions. AIAA J. 8(1), 13-17.

107. Klumpp, A.R. (1976) Singularity-free extraction of a quaternion for a direction-cosine matrix. J. Spacecraft and Rockets 13(12), 754-755.

108. Spurrier, R.A. (1978) Comment on "singularity-free extraction of a quaternion from a direction-cosine matrix." J. Spacecraft and Rockets, 15(4), 255-256.

109. Sheppard, S.W. (1978) Quaternion from rotation matrix. AIAA J. Guidance and Control, 1(3), 223-224.

110. Grubin, C. (1979) Quaternion singularity revisited. AIAA J. Guidance and Control, 2(3), 255-256.

111. Vigneron, F.R. (1968) Configuration instability and despin of crossed-dipole satellites due to the earth's gravity field. Ph.D. dissertation, University of Illinois.

112. Hughes, P.C. and Garg, S.C. (1973) Dynamics of large flexible solar arrays and application to spacecraft attitude control system design. University of Toronto Institute for Aerospace Studies, Report No. 179.

113. Likins, P. et al. (1976) Appendage modal coordinate truncation criteria in hybrid coordinate dynamic analysis. J. Spacecraft and Rockets, 13(10), 611-617.

114. Kulla, P. (1972) Dynamics of spinning bodies containing elastic rods. J. Spacecraft and Rockets, 9(4), 246-253.

115. Larsen, V. and Likins, P. (1976) Frequency domain approach for evaluation of stochastic control of elastic spacecraft. XXVIIth Congress, International Astronautical Federation, Anaheim, California, Paper No. 76-021.

116. Poelaert, D. (1976) Exact modal analysis for spinning flexible spacecraft. Proc. ESA Symp. on Dynamics and Control of Non-Rigid Spacecraft, ESA SP 117, 31-38.

117. Nguyen, P.K. and Hughes, P.C. (1976) Finite-element analysis of CTS-like flexible spacecraft. University of Toronto Institute for Aerospace Studies, Report No. 205.

118. Gupta, K.K. (1976) Free vibration analysis of spinning flexible space structures. J. Astronautical Sciences, XXIV (3), 273-380.

119. Vigneron, F. (1975) A structural dynamics model for flexible solar arrays of the Communications Technology Satellite. Communication Research Center, Ottawa, Canada, Report No. 1268.

120. Sincarsin, G.B. (1977) Dynamical model for the CTS development model solar array under the influence of gravity. University of Toronto Institute for Aerospace Studies, Tech. Note No. 206.

121. Hughes, P.C. and Sharpe, H.N. (1975) Influence of stored angular momentum on the modal characteristics of spacecraft with flexible appendages. ASME Trans. J. Applied Mech. 785-788.

122. Meirovitch, L. (1974) A new method of solution of the eigenvalue problem for gyroscopic systems. AIAA J. 12(10), 1337-1342.

123. Meirovitch, L. (1975) A new modal method for the response of structures rotating in space. Acta Astronautica, 2, 563-576.

124. Meirovitch, L. (1976) A stationarity principle for the eigenvalue problem for rotating structures. AIAA J., 14(10), 1387-1394.

125. Nelson, H.D. and Glasgow, D.A. (1979) Eigenrelations for general second-order systems. AIAA J. 17(7), 795-797.

126. Rubin, S. (1975) Improved component-mode representation for structural dynamic analysis. AIAA J. 13(8), 995-1006.

127. Hintz, R.M. (1975) Analytical methods in component modal synthesis. AIAA J. 13(8), 1007-1016.

128. Etkin, B. and Hughes, P.C. (1965) Spin decay of a class of satellites caused by solar radiation. University of Toronto Institute for Aerospace Studies, Report No. 107.

129. Austin, F. (1970) Planar dynamics of free rotating flexible beams with tip masses. AIAA J. 8(4), 726-733.

130. Likins, P.W. et al. (1973) Mathematical modelling of spinning elastic bodies for modal analysis. AIAA J. 11(9), 1251-1258.

131. Kumar, R. (1974) Vibrations of space booms under centrifugal force field. Trans. Canadian Aeronautics and Space Institute, 7(1), 1-5.

132. Nguyen, P.K. and Hughes, P.C. (1975) Approximate mode shapes and frequencies for rotating cantilever beams and application to flexible spinning spacecraft. Trans. Canadian Aeronautics and Space Institute, 8(1), 10-19.

133. Vigneron, F.R. (1975) Comment on "Mathematical modeling of spinning elastic bodies for modal analysis." AIAA J. 13(1), 126-127.

134. Fang, B.T. (1975) Further comment on "Mathematical modeling of spinning elastic bodies for modal analysis." AIAA J. 13(11), 1541-1542.

135. Laurensen, R.M. (1976) Modal analysis of rotating flexible structures. AIAA J. 14(10), 1444-1450.

136. Kaza, K.R.V. and Kvaternik, R.G. (1977) Nonlinear flap-lag-axial equations of a rotating beam. AIAA J. 15(6), 871-874.

137. Lips, K.W. and Modi, V.J. (1977) Flexible appendage deployment dynamics as applied to satellite attitude control. Proc. Sixth Canadian Congress of Applied Mechanics, Vancouver, May 30-June 3, 365.

138. Lips, K.W. and Modi, V.J. (1978) Transient attitude dynamics of satellites with deploying flexible appendages. Acta Astronautica, 5(10), 797-815.

139. Nguyen, P.K. (1978) Dynamics of spinning spacecraft with tubular appendages including large amplitude deflections. University of Toronto Institute for Aerospace Studies, Report No. 223.

140. Flatley, T.W. (1966) Equilibrium shape of an array of long elastic structural members in circular orbit. NASA TN D-3173.

141. Meirovitch, L. and Juang, J. (1976) Natural modes of oscillation of rotating flexible structures about nontrivial equilibrium. J. Spacecraft and Rockets, 13(1), 37-44.

142. Kiesselbach, G. (1976) Attitude stability of satellites with flexible appendages. Proc. ESA Symp. on Dynamics and Control of Non-Rigid Spacecraft, ESA SP 117, 137-145.

143. Hablani, H.B. and Shrivastava, S.K. (1978) Nontrivial equilibrium and Liapunov stability of flexible damped gravity satellite as a hybrid dynamical system. Presented at AIAA XVI Aerospace Sciences Meeting, Huntsville, Alabama, Paper No. 78-53.

144. Lorenz, W. (1975) Thermal simulation of large rotating solar arrays. J. Spacecraft and Rockets, 12(6), 342-345.

145. Juang, J.N. and Balas, M. (1978) Dynamics and control of large spinning spacecraft. AIAA/AAS Astrodynamics Conference, Palo Alto, California.

146. Nayfeh, A.H. and Hefzy, M.S. (1978) Continuum modelling of three-dimensional truss-like space structures. AIAA J. 16(8), 779-787.

147. Canavin, J.R. and Meirovitch, L. (1979) Eigensolution for large flexible spacecraft with singular gyroscopic matrices. AIAA J. Guidance and Control, 2(1), 88-90.

148. Tsuchiya, K. (1977) Thermally induced vibrations of a flexible appendage attached to the spacecraft. AIAA J. 15(4), 505-510.

149. Farrell, J.L. (1977) Thermal curvature of satellite booms. AIAA J. 15(9), 1331-1333.

150. Frisch, H.P. (1980) Thermally induced response of flexible structures: a method for analysis. AIAA J. Guidance and Control, 3(1), 92-94.

151. Kumar, K. (1976) Librational dynamics of satellites with thermally flexed appendages. XXVII Congress International Astronautical Federation, Anaheim, Calif. Paper No. IAF-76-025.

152. Joshi, V.K. and Kumar, K. (1980) New solar attitude control approach for satellites in elliptic orbits. AIAA J. Guidance and Control, 3(1), 42-47.

153. Vigneron, F.R. (1967) Elastic stability and equilibrium configuration of earth pointing non-rigid satellites. (draft), Defence Research Board, Ottawa, Canada.

154. Vigneron, F.R. (1970) Stability of a freely spinning satellite of crossed-dipole configuration. Trans. Canadian Aeronautics and Space Institute, 3(1), 8-19.

155. Vigneron, F.R. and Boresi, A.P. (1970) Effect of the earth's gravitational forces on the flexible crossed-dipole satellite configuration Part 1 - Configuration stability and despin. Part 2 - Attitude stability. Trans. Canadian Aeronautics and Space Institute, 3(2), 115-134.

156. Hughes, P.C. and Fung, J.C. (1971) Liapunov stability of spinning satellites with long flexible appendages. J. Celestial Mech. 4, 295-308.

157. Dong, W.N. and Schlack, Jr., A.L. (1974) Stability of a spinning satellite with flexible antennas. AIAA J. 12(12), 1737-1739.

158. Longman, R.W. and Fedor, J.V. (1973) Dynamics of flexible spinning satellites with radial wire antennas. Goddard Space Flight Center, X-732-73-233.

159. Levinson, D.A. and Kane, T.R. (1976) Explicit attitude stability of a satellite equipped with four booms. J. Spacecraft and Rockets, 13(4), 208-213.

160. Meirovitch, L. (1974) Bounds on the extension of antennas for stable spinning satellites. J. Spacecraft and Rockets, 11(3), 202-204.

161. Barbera, F.J. and Likins, P. (1973) Liapunov stability analysis of spinning flexible spacecraft. AIAA J. 11(4), 457-466.

162. Likins, P.W. (1972) Linearization and Liapunov stability analysis of a class of dynamical differential equations. AIAA J. 10(4), 453-455.

163. Smith, E.H. and Gill, K.F. (1976) Flexible space vehicle control based on state observation and Lyapunov's method. Proc. ESA Symp. on Dynamics and Control of Non-Rigid Spacecraft, ESA SP 117, 213-220.

164. Tseng, G.T. and Phillips, K.J. (1976) Attitude stability of a flexible dual spin spacecraft with active nutation damping using products of inertia. J. Astronautical Sciences, XXIV (3), 257-272.

165. Calico, R. (1976) Stability of a gyrostat satellite with flexible appendages. J. Spacecraft and Rockets, 13(8), 505-508.

166. Boland, P. et al. (1974) Stability analysis of interconnected deformable bodies in a topological tree. AIAA J. 12(8), 1025-1030.

167. Likins, P.W. and Fleischer, G.E. (1970) Results of flexible spacecraft attitude control studies utilizing hybrid coordinates. AIAA 8th Aerospace Sciences Meeting, New York, New York, AIAA Paper No. 70-20.

168. Millar, R.A. (1971) Effect of antisymmetric array-bending motion (excited by thruster control torques) on satellite attitude. Memorandum, Government of Canada. File No. CRC 6666-9-8 (NSTL) program.

169. Malich, G. (1975) Effects of structural flexibility on a reaction jet satellite attitude control system. University of Toronto Institute for Aerospace Studies, Tech. Note No. 199.

170. Loesch, F.C. and Hecht, C. (1976) Work/energy analysis of bending limit cycles in a deadband attitude control system. J. Spacecraft and Rockets, 13(7), 406-415.

171. Yocum, J.F. and Slafer, L.I. (1978) Control system design in the presence of severe structural dynamics interactions. AIAA J. Guidance and Control. 1 (2), 109-116.

172. Hughes, P.C. (1976) Passive damper analysis for reducing attitude control/flexibility interaction. J. Spacecraft and Rockets, 13(5), 271-274.

173. Hughes, P.C. (1972) Flexibility considerations for the pitch attitude control of the Communications Technology Satellite. Trans. Canadian Aeronautics and Space Institute, 5(1).

174. Hughes, P.C. (1973) Dynamics of flexible space vehicles with active attitude control. Celestial Mech. 9, 21-39.

175. Zach, C. (1970) Time-optimal control of gravity-gradient satellites with disturbances. J. Spacecraft and Rockets, 7 (12), 1434-1440.

176. Tseng, G.T. and Mahn, Jr., R.H. (1978) Flexible spacecraft control design using pole allocation technique. AIAA J. Guidance and Control, 1(4), 279-281.

177. Millar, R.A. and Vigneron, F.R. (1979) Attitude stability of a pseudorate jet-controlled flexible spacecraft. AIAA J. Guidance and Control, 2(2), 111-118.

178. Hughes, P.C. and Abdel-Rahman, T.M. (1979) Stability of proportional-plus-derivative-plus-integral control of flexible spacecraft. AIAA J. Guidance and Control, 2(6), 499-503.

179. Gatlin, J.A. et al. (1969) Satellite attitude control using a torqued, 2-axis-gimbaled boom as the actuator. J. Spacecraft and Rockets, 6(9), 1013-1018.

180. Hillard, S.E. (1976) Attitude control of synchronous satellites possessing flexible solar arrays using a double-gimbaled momentum wheel. Proc. ESA Symp. on Dynamics and Control of Non-Rigid Spacecraft, ESA SP 117, 113-124.

181. Pande, K.C. et al. (1974) Time-optimal pitch control of satellites using solar radiation pressure. J. Spacecraft and Rockets, 11(8), 601-603.

182. Modi, V.J. and Pande, K.C. (1974) Magnetic-solar hybrid attitude control of satellites in near-equatorial orbits. J. Spacecraft and Rockets, 11(12), 845-851.

183. Pande, K.C. (1976) Attitude control of spinning spacecraft by radiation pressure. J. Spacecraft and Rockets, 13(12), 765-768.

184. Hughes, P.C. (1974) Analysis of two dampers on the flexible appendage of a three-axis controlled satellite. CASI/AIAA Joint Meeting, Toronto, Canada, Paper No. 74-1268.

185. Gething, J.M. and Gill, K.F. (1975) An attitude control system for a flexible satellite providing active damping of flexural motion. Aeronautical J. 134-139.

186. Cretcher, C.K. and Mingori, D.L. (1971) Nutation damping and vibration isolation in a flexible coupled dual-spin spacecraft. J. Spacecraft and Rockets, 8(8), 817-823.

187. Balas, M.J. (1979) Direct velocity feedback control of large space structures. AIAA J. Guidance and Control, 2(3), 252-253.

188. Smith, E.H. and Gill, K.F. (1977) Controlling the attitude and two flexure-modes of a flexible satellite. Astronautical J. 41-44.

189. Beysens, A. (1976) Design of a control loop with flexibility and in-flight identification of the flexible modes. Proc. ESA Symp. on Dynamics and Control of Non-Rigid Spacecraft, ESA SP 117, 273-283.

190. Jonckheere, E. (1976) On the observability of the deformable modes in a class of non-rigid satellites. Proc. ESA Symp. on Dynamics and Control of Non-Rigid Spacecraft, ESA SP 117, 251-262.

191. Meirovitch, L. and Oz, H. (1978) Modal control of distributed gyroscopic systems. AIAA/AAS Astrodynamics Conf. Palo Alto, California, Paper No. 78-1421.

192. Meirovitch, L. and Oz, H. (1979) Observer modal control of a dual-spin flexible spacecraft. AIAA J. Guidance and Control, 2(2), 101-110.

193. Meirovitch, L. et al. (1979) Distributed control of spinning flexible spacecraft. AIAA J. Guidance and Control, 2(5), 407-415.

194. Martin, G.D. and Bryson, Jr., A.E. (1980) Attitude control of a flexible spacecraft. AIAA J. Guidance and Control, 3(1), 37-41.

195. Folgate, K. (1976) Discrete time attitude control of spacecraft containing low frequency lightly damped structural modes. AIAA/CASI Communications Satellite Conf. Montreal, Canada, AIAA Paper No. 76-262.

196. Kuo, B.C. et al. (1976) Stability analysis of the discrete data Large-Space-Telescope system. J. Spacecraft and Rockets, 13(6), 332-339.

197. Kuo, B.C. et al. (1974) Design of a digital controller for spinning flexible spacecraft. J. Spacecraft and Rockets, 11(8), 584-589.

198. Kawato, N. et al. (1976) Accuracy improvement of a 3-axis stabilization by the use of an onboard computer and the modern control theory. XXVIIth Congress International Astrnautical Federation, Anaheim, Calif. Paper No. IAF-76-017.

199. Van Landingham, H.F. and Meirovitch, L. (1978) Digital control of spinning flexible spacecraft. AIAA J. Guidance and Control, 1(5), 347-351.

200. De Bra, D.B. (1979) Control technology challenges for gravitational physics experiments in space. AIAA J. Guidance and Control, 2(2), 147-151.

201. Skelton, R.E. and Likins, P.W. (1978) Orthogonal filters for model error compensation in the control of nonrigid spacecraft. AIAA J. Guidance and Control, 1(1), 41-49.

202. Lang, W. and Honeycutt, G.H. (1967) Simulation of deployment dynamics of spinning spacecraft. NASA-TN-D-4074.

203. Cloutier, G.J. (1968) Dynamics of deployment of extendible booms from spinning space vehicles. J. Spacecraft and Rockets, 5(5), 547-552.

204. Bowers, Jr., E.J. and Williams, C.E. (1970) Optimization of RAE satellite boom deployment timing. J. Spacecraft and Rockets, 7(9), 1057-1062.

205. Hughes, P.C. (1972) Dynamics of a spin-stabilized satellite during extension of rigid booms. Trans. Canadian Aeronautics and Space Institute, 5(1), 11-14.

206. Puri, V. and Bainum, P.M. (1971) Planar librational motion of a gravity-gradient satellite during deployment. Presented at the 22nd International Astronautical Congress, Brussels, Belgium.

207. Bainum, P.M. and Sellappan, R. (1976) Spacecraft detumbling using movable telescoping appendages. Acta Astronautica, 3, 953-969.

208. Bainum, P.M. and Sellappan, R. (1976) Optimal control of spin-stabilized spacecraft with telescoping appendages. J. Astronautical Sciences, XXIV (4), 329-346.

209. Rajan, M. and Bainum, P.M. (1977) Effect of gravity-gradient toruqes on the dynamics of a spinning spacecraft with telescoping appendages. To be presented at the AIAA Symp. on Dynamics and Control of Large Flexible Spacecraft, Blacksburg, Virginia.

210. Bainum, P.M. and Sellappan, R. (1977) The use of a movable telescoping end mass system for the time-optimal control of spinning spacecraft. International Astronautical Federation XXVIIIth Congress, Prague, Paper No. 77-227.

211. Sellappan, R. and Bainum, P.M. (1976) Dynamics of spin-stabilized spacecraft during deployment of telescopic appendages. J. Spacecraft and Rockets, 13(10), 605-610.

212. Cherchas, D.B. (1971) Dynamics of spin-stabilized satellites during extension of long flexible booms. J. Spacecraft and Rockets, 8(7), 802-804.

213. Cherchas, D.B. and Gossain, D.M. (1974) Dynamics of a flexible solar array during deployment from a spinning spacecraft. Trans. Canadian Aeronautics and Space Institute, 7(1), 10-18.

214. Ebner, S.G. (1970) Deployment dynamics of rotating cable-connected space stations. J. Spacecraft and Rockets, 7(10), 1274-1275.

215. Stuiver, W. and Bainum, P.M. (1973) A study of planar deployment control and libration damping of a Tethered Orbiting Interferometer satellite. J. Astronautical Sciences. XX(6), 321-346.

216. Modi, V.J. and Misra, A.K. (1978) Deployment dynamics and control of tethered satellite systems. AIAA/AAS Astrodynamics Conf. Palo Alto, Calif. Paper No. 78-1398.

217. Misra, A.K. and Modi, V.J. (1979) Dynamics of a tether connected payload deploying from the space shuttle. 2nd VPI & SU/AIAA Symp. On Dynamics and Control of Large Flexible Spacecraft, Blacksburg, Virginia. June 21-23, 591-609.

218. Kane, T.R. and Levinson, D.A. (1977) Deployment of a cable supported payload from an orbiting spacecraft. J. Spacecraft and Rockets, 14(7), 409-413.

219. Hughes, P.C. (1976) Deployment dynamics of the Communications Technology Satellite - a progress report. Proc. ESA Symp. on Dynamics and Control of Non-Rigid Spacecraft, ESA SP 117, 335-340.

220. Jankovic, M.S. (1980) Deployment dynamics of flexible spacecraft. Ph.D. dissertation, University of Toronto Institute for Aerospace Studies.

221. Leech, C.M. (1970) The dynamics of beam under the influence of convecting inertial forces. Ph.D. dissertation, University of Toronto.

222. Tabarrok, B. et al. (1974) On the dynamics of an axially moving beam. J. Franklin Institute, 297(3), 201-220.

223. Jankovic, M.S. (1976) Lateral vibrations of an extending rod. University of Toronto Institute for Aerospace Studies, Tech. Note No. 202.

224. Lips, K.W. and Modi, V.J. (1978) Dynamical characteristics associated with deploying, orbiting, beam-type appendages. AIAA/AAS Astrodynamics Conf. Palo Alto, Calif. Paper No. 78-1399.

225. Wittenburg, J. (1977) Dynamics of systems of rigid bodies. B.G. Teubner, Stuttgart, W. Germany.

226. England, F.E. (1969) A normal mode analysis of a satellite employing long flexible booms. Ph.D. dissertation, University of Maryland.

227. Almroth, B.D., et al. (1978) Automatic choice of global shape functions in structural analysis. AIAA J. 16(5) 525-528.

228. Helliwell, W.S. (1978) A fast implicit iterative numerical method for solving multi-dimensional partial differential equations. AIAA J. 16(7), 663-666.

229. Hurty, W.C. and Rubinstein, M.F. (1964) Dynamics of structures. Prentice-Hall.

230. Meirovitch, L. (1967) Analytical methods in vibrations. MacMillan Co.

231. Young, D. and Felgar, Jr., R.P. (1949) Tables of characteristic functions representing normal modes of vibration of a beam. Bureau of Engineering Research, University of Texas, Publication No. 4913.

232. Felgar, R.P., Jr. (1950) Formulas for integrals containing characteristic functions of a vibrating beam. Bureau of Engineering Research, University of Texas, Austin, Texas, Circular No. 14.

233. Worden, D. (1979) Slamming motions of a rectangular-section barge model in harmonic waves. M.A.Sc. dissertation, University of British Columbia.

234. Flanagan, R.C. (1969) Effect of environmental forces on the attitude dynamics of gravity oriented systems. Ph.D. dissertation, University of British Columbia, p. 8.

235. Conte, S.D. (1965) Elementary numerical analysis. McGraw-Hill.

236. Modi, V.J. and Misra, A.K. (1979) On the deployment dynamics of tether connected two-body systems. Acta Astronautica, 6(9), 1183-1197.

237. Garg, S.C., et al. (1979) Flight results on structural dynamics from Hermes. J. Spacecraft and Rockets, 16(2), 81-87.

APPENDIX I

GENERAL EQUATIONS OF LIBRATION ON TRUE ANOMALY

The equations of Chapter 2 can be expressed in a somewhat more elegant manner if one takes advantage of the Kepler relations to describe the orbital variables while also taking the orbital anomaly as a measure of time as in Chapter 4.

Ψ Degree of Freedom (Roll)

$$
\begin{aligned}
&[c^2\Lambda\,(s^2\Phi\, I_{11} + c^2\Phi\, I_{22} - s2\Phi\, I_{12} + s^2\Lambda\, I_{33} + s2\Lambda \\
&(s\Phi\, I_{13} + c\Phi\, I_{23})]\,\Psi'' + \{c^2\Lambda\,[s^2\Phi\,(I_{11}' - 2e_1 I_{11}) \\
&+ c^2\Phi\,(I_{22}' - 2e_1 I_{22})] + s^2\Lambda\,(I_{33}' - 2e_1 I_{33}) \\
&+ s2\Lambda\,[s\Phi\,(I_{13}' - 2e_1 I_{13}) + c\Phi\,(I_{23}' - 2e_1 I_{23})] \\
&- s\Psi s\Lambda c\Lambda\,(2s^2\Phi\, I_{11} - s2\Phi\, I_{12} + 2s^2\Lambda\, s\Phi\, I_{13})\}\,\Psi' \\
&+ [s2\Lambda\,(I_{33} - s^2\Phi\, I_{11} - c^2\Phi\, I_{22} + s2\Phi\, I_{12}) + 2c2\Lambda \\
&(s\Phi\, I_{13} + c\Phi\, I_{23})]\,\Lambda'\Psi' + \{c^2\Lambda\,[s2\Phi\,(I_{11} - I_{22}) \\
&+ (1 - c2\Phi)\, I_{12}] + s2\Lambda\,(c\Phi\, I_{13} - s\Phi\, I_{23})\}\,\Phi'\Psi' \\
&+ [3/(1 + e\,c\theta)]\{[(s^2\Lambda\, s^2\Phi - c^2\Phi)\, I_{11} + (s^2\Lambda\, c^2\Phi \\
&- s^2\Phi)\, I_{22} + c^2\Lambda\, I_{33} - (1 + s^2\Lambda)\, s2\Phi\, I_{12} - s2\Lambda
\end{aligned}
$$

$$(s\Phi I_{13} + c\Phi I_{23})] s\Psi c\Psi + c2\Psi s\Lambda [s\Phi c\Phi (I_{11} - I_{22})$$

$$- c2\Phi I_{12}] - c2\Psi c\Lambda (c\Phi I_{13} - s\Phi I_{23})\} + c\Lambda [s\Phi$$

$$(f_1' - 2e_1 h_1) + c\Phi (f_2' - 2e_1 h_1)] - s\Lambda (f_3' - 2e_1 h_3)$$

$$+ \{ c\Lambda [s\Phi c\Phi (I_{11} - I_{22}) - c2\Phi I_{12}] + s\Lambda (c\Phi I_{13}$$

$$- s\Phi I_{23}) \} \Lambda'' + \{ s\Lambda [s\Phi c\Phi (I_{22} - I_{11}) + c2\Phi$$

$$I_{12}] + c\Lambda (c\Phi I_{13} - s\Phi I_{23})\} (\Lambda')^2 + \{ c\Lambda s\Phi c\Phi$$

$$[(I_{11}' - 2e_1 I_{11}) - (I_{22}' - 2e_1 I_{22}) - c\Lambda c2\Phi (I_{12}'$$

$$- 2e_1 I_{12}) - c\Lambda h_3 + s\Lambda [c\Phi (I_{13}' - 2e_1 I_{13} - h_2)$$

$$- s\Phi (I_{23}' - 2e_1 I_{23} + h_1)] + c\Psi (c2\Lambda s^2\Phi + c^2\Phi) I_{11}$$

$$+ [c\Psi (s^2\Phi + c2\Lambda c^2\Phi) - s\Psi s\Lambda s2\Phi] I_{22} - c\Psi c2\Lambda I_{33}$$

$$+ [c\Psi s2\Phi (1 - c2\Lambda) - 2 s\Psi s\Lambda c^2\Phi] I_{12} + 2 c\Lambda [(2 c\Psi$$

$$s\Lambda s\Phi - s\Psi c\Phi) I_{13} + (2 c\Psi s\Lambda c\Phi + s\Psi c\Phi) I_{23}]\} \Lambda'$$

$$+ c\Lambda [c2\Phi (I_{11} - I_{22}) + s2\Phi I_{12} - I_{33}] \Phi' \Lambda'$$

$$- [s\Lambda I_{33} - c\Lambda (s\Phi I_{13} + c\Phi I_{23})] \Phi'' + c\Lambda (s\Phi$$

$$I_{23} - c\Phi I_{13}) (\Phi')^2 + \{ - s\Lambda (I_{33}' - 2e_1 I_{33})$$

$$- c\Lambda [s\Phi (I_{13}' - 2e_1 I_{13} + h_2) + c\Phi (I_{23}' - 2e_1 I_{23} - h_1)]$$

$$+ c\Lambda\,[s\Psi\, I_{33} + (c\Psi s\Lambda s2\Phi - s\Psi c2\Phi)(I_{11} - I_{22})]$$

$$- 2\,c\Lambda\,(s\Psi s2\Phi + c\Psi s\Lambda c2\Phi)\,I_{12} + 2\,(s\Psi s\Lambda s\Phi - c\Psi$$

$$c^2\Lambda\, c\Phi)\,I_{13} + 2\,c\Psi c^2\Lambda\, s\Phi\, I_{23}\}\,\Phi' + \{c\Psi s\Lambda c\Lambda$$

$$[s^2\Phi\,(I_{11}' - 2\,e_1 I_{11}) + c^2\Phi\,(I_{22}' - 2e_1 I_{22}) - (I_{33}'$$

$$- 2\,e_1\, I_{33})] + s\Psi c\Lambda s\Phi c\Phi\,[(I_{22}' - 2e_1 I_{22}) - (I_{11}'$$

$$- 2\,e_1\, I_{11})] - c\Lambda\,(c\Psi s\Lambda s2\Phi - s\Psi c2\Phi)(I_{12}' - 2e_1 I_{12})$$

$$- (c\Psi c2\Lambda s\Phi + s\Psi s\Lambda c\Phi)(I_{13}' - 2e_1 I_{13}) - (c\Psi c2\Lambda\, c\Phi$$

$$- s\Psi s\Lambda\, s\Phi)\,(I_{23}' - 2\,e_1\, I_{23}) + (c\Psi c\Phi - s\Psi s\Lambda\, s\Phi)\,h_1$$

$$- (c\Psi s\Phi - s\Psi s\Lambda\, c\Phi)\,h_2 + s\Psi c\Lambda\, h_3 + s\Psi c\Psi\,[(s^2\Lambda\, c^2\Phi$$

$$- s^2\Phi)\,I_{22} - (s^2\Lambda s^2\Phi + c^2\Phi)\,I_{11} + c^2\Lambda\, I_{33} + c2\Psi$$

$$s\Lambda\, s\Phi c\Phi\,(I_{11} - I_{22}) - [s\Lambda\,(c^2\Psi c2\Phi - s^2\Psi)$$

$$+ s\Psi c\Psi s2\Phi\,]\,I_{12} - c2\Psi c\Lambda\, c\Phi\, I_{13} - c\Lambda$$

$$(s2\Psi s\Lambda\, c\Phi - c2\Psi s\Phi)\,I_{23}\} = \mathcal{O}_\Psi(\theta)\;;$$

(I.1a)

Λ Degree of Freedom (Yaw)

$$(c^2\Phi\, I_{11} + s^2\Phi\, I_{22} + s2\Phi\, I_{12})\,\Lambda'' + [c^2\Phi\,(I_{11}' - 2e_1 I_{11}) + s^2\Phi\,(I_{22}' - 2e_1 I_{22}) + s2\Phi\,(I_{12}' - 2e_1 I_{12})]\,\Lambda' + [-s2\Phi\,(I_{11} - I_{22}) + 2c2\Phi\, I_{12}]\,\Phi'\Lambda' + [3/(1 + e\,c\theta)]\{s^2\Psi s\Lambda c\Lambda\,(s^2\Phi\, I_{11} + c^2\Phi\, I_{22} - I_{33} - s2\Phi\, I_{12}) - s\Psi c2\Lambda\,(s\Phi\, I_{13} + c\Phi\, I_{23}) + s\Psi c\Psi c\Lambda\,[s\Phi c\Phi\,(I_{11} - I_{22}) - c2\Phi\, I_{12}] + s\Psi c\Psi s\Lambda\,(c\Phi\, I_{13} - s\Phi\, I_{23})\} + c\Phi\,(\Gamma_1 - 2e_1 h_1) - s\Phi\,(\Gamma_2 - 2e_1 h_2) - (c\Phi\, I_{13} - s\Phi\, I_{23})\,\Phi'' + (s\Phi\, I_{13} + c\Phi\, I_{23})(\Phi')^2 + [-c\Phi\,(I_{13}' - 2e_1 I_{13} + h_2) + s\Phi\,(I_{23}' - 2e_1 I_{23} - h_1) + (c\Psi s\Lambda c2\Phi + s\Psi s2\Phi)(I_{11} - I_{22}) + c\Psi s\Lambda\, I_{33} - 2(s\Psi c2\Phi - c\Psi s\Lambda s2\Phi)\, I_{12} + 2c\Psi c\Lambda\,(s\Phi\, I_{13} + c\Phi\, I_{23})]\,\Phi' + \{c\Lambda\,[c2\Phi\,(I_{11} - I_{22}) + I_{33} + s2\Phi\, I_{12}] - 2s\Lambda\,(s\Phi\, I_{13} + c\Phi\, I_{23})\}\,\Psi'\Phi' + \{c\Lambda\,[s\Phi c\Phi\,(I_{11} - I_{22}) - c2\Phi\, I_{12}] + s\Lambda\,(c\Phi\, I_{13} - s\Phi\, I_{23})\}\,\Psi'' + [s\Lambda c\Lambda\,(s^2\Phi\, I_{11} + c^2\Phi\, I_{22} - I_{33} - s2\Phi\, I_{12}) - c2\Lambda\,(s\Phi\, I_{13} + c\Phi\, I_{23})]\,(\Psi')^2$$

$$+ \{ c\Lambda\, s\Phi\, c\Phi\, [(I_{11}' - 2e_1 I_{11}) - (I_{22}' - 2e_1 I_{22})] - c\Lambda\, c2\Phi\, (I_{12}' - 2e_1 I_{12}) + s\Lambda\, [c\Phi\, (I_{13}' - 2e_1 I_{13}) - s\Phi\, (I_{23}' - 2e_1 I_{23})] + s\Lambda\, (s\Phi\, h_1 + c\Phi\, h_2) + c\Lambda\, h_3 + c\Psi\, [c2\Lambda\, (I_{33} - s^2\Phi\, I_{11} - c^2\Phi\, I_{22}) - (c^2\Phi\, I_{11} + s^2\Phi\, I_{22}) - [c\Psi\, s2\Phi\, (1 + s^2\Lambda) - 2 s\Psi\, s\Lambda\, c2\Phi]\, I_{12} - s\Psi\, s\Lambda\, s2\Phi\, (I_{11} - I_{22}) - 2\, c\Psi\, s2\Lambda\, (s\Phi\, I_{13} + c\Phi\, I_{23}) + 2\, s\Psi\, c\Lambda\, (c\Phi\, I_{13} - s\Phi\, I_{23})\} \Psi'$$

$$+ \{ c\Psi\, s\Lambda\, s\Phi\, c\Phi\, [(I_{11}' - 2e_1 I_{11}) - (I_{22}' - 2e_1 I_{22}) - c\Psi\, s\Lambda\, c2\Phi\, (I_{12}' - 2e_1 I_{12}) - s\Psi\, [c^2\Phi\, (I_{11}' - 2e_1 I_{11}) + s^2\Phi\, (I_{22}' - 2e_1 I_{22}) + s2\Phi\, (I_{12}' - 2e_1 I_{12})] - c\Psi\, c\Lambda\, [c\Phi\, (I_{13}' - 2e_1 I_{13}) - s\Phi\, (I_{23}' - 2e_1 I_{23})] + c\Psi\, c\Lambda\, (s\Phi\, h_1 - c\Phi\, h_2) + c\Psi\, s\Lambda\, h_3 + c\Psi\, s\Psi\, c\Lambda\, [s\Phi\, c\Phi\, (I_{11} - I_{22}) - c2\Phi\, I_{12}] - c^2\Psi\, s\Lambda\, c\Lambda\, (s^2\Phi\, I_{11} + c^2\Phi\, I_{22} + I_{33} - s2\Phi\, I_{12}) + c^2\Psi\, c2\Lambda\, (s\Phi\, I_{13} + c\Phi\, I_{23}) + c\Psi\, s\Psi\, s\Lambda\, (c\Phi\, I_{13} - s\Phi\, I_{23})\}$$

$$= \mathcal{Q}_\Lambda(\theta)\ ; \qquad \text{(I.1b)}$$

Φ Degree of Freedom (Pitch, Spin)

$$I_{33}\Phi'' + (I_{33}' - 2e_1 I_{33})\Phi' + [3/(1+e\,c\theta)]\{c_2\Phi[s\Psi c\Psi s\Lambda(I_{11}-I_{22}) + (c^2\Psi - s^2\Psi s^2\Lambda)I_{12}] + s\Phi c\Phi[(c^2\Psi - s^2\Psi s^2\Lambda)(I_{22}-I_{11}) + 2s2\Psi s\Lambda I_{12}] + s\Psi c\Lambda[s\Phi(c\Psi I_{13} + s\Psi s\Lambda I_{23}) - c\Phi(s\Psi s\Lambda I_{13} - c\Psi I_{23})]\} + f_3 - 2e_1 h_3 - [s\Lambda I_{33} + c\Lambda(s\Phi I_{13} + c\Phi I_{23})]\Psi'' + \{c^2\Lambda[s\Phi c\Phi(I_{22}-I_{11}) + c2\Phi I_{12}] - s\Lambda c\Lambda(c\Phi I_{13} - s\Phi I_{23})\}(\Psi')^2 + \{-s\Lambda(I_{33}' - 2e_1 I_{33}) - c\Lambda[s\Phi(I_{12}' - 2e_1 I_{12}) + c\Phi(I_{23}' - 2e_1 I_{23})] - c\Lambda(c\Phi h_1 - s\Phi h_2) + c\Lambda[(c\Psi s\Lambda s2\Phi - s\Psi c2\Phi)(I_{22}-I_{11}) - s\Psi I_{33}] + (c\Psi s2\Lambda c2\Phi + 2s\Psi c\Lambda s2\Phi)I_{12} + 2c\Psi c^2\Lambda(c\Phi I_{13} - s\Phi I_{23})\}\Psi' + \{c\Lambda[c2\Phi(I_{22}-I_{11}) - I_{33} - 2s2\Phi I_{12}] + 2s\Lambda(s\Phi I_{13} + c\Phi I_{23})\}\Lambda'\Psi' - (c\Phi I_{13} - s\Phi I_{23})\Lambda'' + [s\Phi c\Phi(I_{11}-I_{22}) - c2\Phi I_{12}](\Lambda')^2 + \{-c\Phi(I_{13}' - 2e_1 I_{13}) + s\Phi(I_{23}' - 2e_1 I_{23}) + s\Phi h_1 + c\Phi h_2$$

$$+ c\Psi s\Lambda \left[c2\Phi \left(I_{22} - I_{11} \right) - I_{33} \right] - 2 \left(c\Psi s\Lambda s2\Phi \right.$$

$$\left. - s\Psi c2\Phi \right) I_{12} - 2 c\Psi c\Lambda \left(s\Phi I_{13} + c\Phi I_{23} \right) \} \Lambda'$$

$$+ \{ c\Psi c\Lambda \left(I'_{33} - 2e_1 I_{33} \right) - \left(c\Psi s\Lambda s\Phi - s\Psi c\Phi \right)$$

$$\left(I'_{13} - 2e_1 I_{13} - h_2 \right) - \left(c\Psi s\Lambda c\Phi + s\Psi s\Phi \right) \left(I'_{23} - 2e_1 \right.$$

$$\left. I_{23} + h_1 \right) - \left(s^2\Psi - c^2\Psi s^2\Lambda \right) \left[s\Phi c\Phi \left(I_{22} - I_{11} \right) + c2\Phi \right.$$

$$I_{12} - s\Psi c\Psi s\Lambda \left[c2\Phi \left(I_{22} - I_{11} \right) - 2 s2\Phi I_{12} \right] + c\Lambda$$

$$\left[c^2\Psi s\Lambda \left(c\Phi I_{13} - s\Phi I_{23} \right) + c\Psi s\Psi \left(s\Phi I_{13} + c\Phi I_{23} \right) \right] \}$$

$$= \Omega_\Phi (\theta) \, . \qquad \text{(I.1c)}$$

APPENDIX II

SYSTEM MOMENTS OF INERTIA

II.1 Arbitrary Appendage

Moments of inertia are calculated with respect to the instantaneous center of mass of the satellite (O_c) but are expressed in terms of local appendage coordinates. Pertinent system geometry is given in Figure II-1.

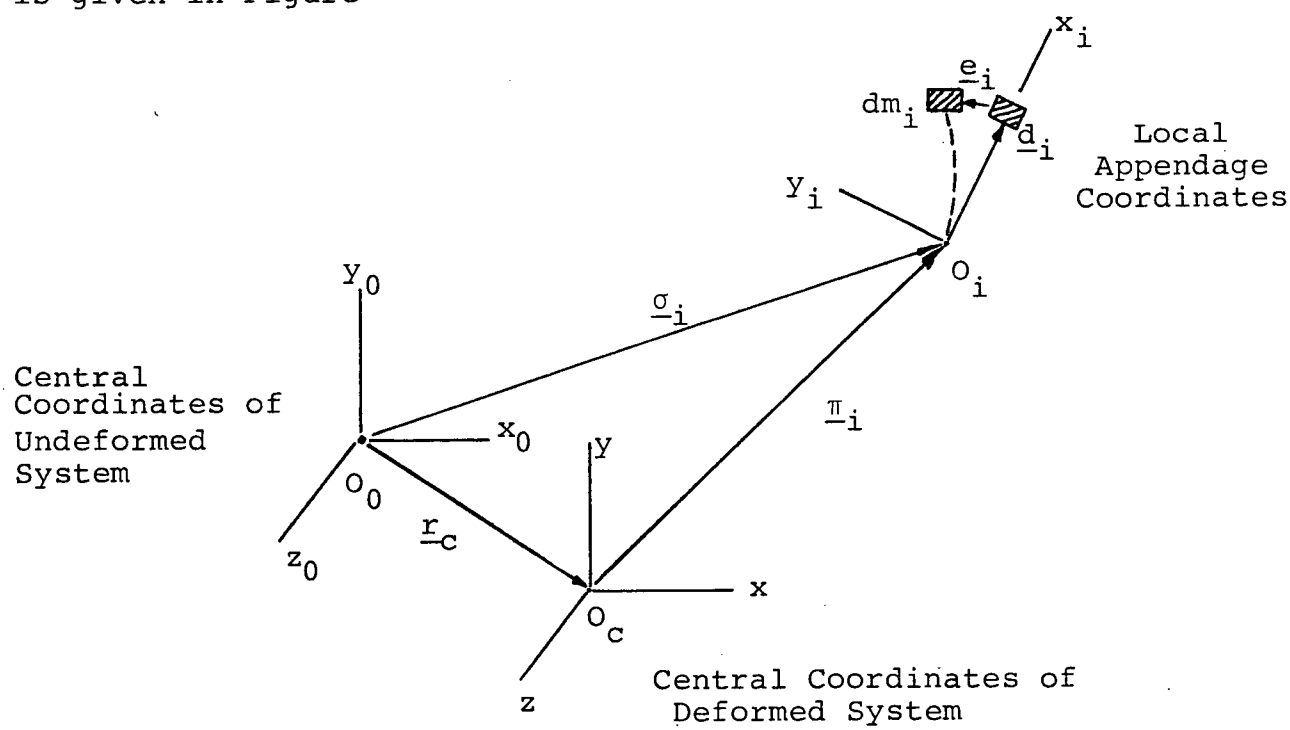

Figure II-1 General displacement of a mass element in the presence of flexibility ($\underline{e}_i$), geometric offset ($\underline{\sigma}_i$) and a shifting center of mass ($\underline{r}_c$).

Neglecting subscript i, the location of any mass element dm of the i^{th} appendage can be expressed:

$$\underline{r}_d = \underline{d} + \underline{b} + \underline{e} - \underline{r}_c = \underline{d} + \underline{\pi} + \underline{e} \quad ;$$

$$= \begin{Bmatrix} r_{d1} \\ r_{d2} \\ r_{d3} \end{Bmatrix} = \begin{Bmatrix} \pi_1 + x + u \\ \pi_2 + y + v \\ \pi_3 + z + w \end{Bmatrix} \quad ; \qquad \text{(II.1)}$$

where:

π_j = j^{th} component of net offset vector along the local axes.

Based on this description of the displacement field with respect to the instantaneous center of mass, one can evaluate appendage contributions to the inertia tensor of the overall system:

$$I_{11} = \int (r_{d2}^2 + r_{d3}^2)\, dm \;^{\dagger} \quad ;$$

$$= m(b_2^2 + b_3^2) + \int [y^2 + z^2 + 2(b_2 y$$

---

† $\int (-)\, dm = \int_m (-)\, dm$

$$+ b_3 z)]\,dm + m(y_c^2 + z_c^2) - 2\int[(y + b_2)y_c + (z + b_3)z_c]\,dm - 2\int(y_c v + z_c w)dm + \int[v^2 + w^2 + 2(y + b_2)v + 2(z + b_3)w]\,dm ;$$

$$I_{22} = \int (r_{d1}^2 + r_{d3}^2)\,dm ;$$

$$= m(b_1^2 + b_3^2) + \int[x^2 + z^2 + 2(b_1 x + b_3 z)]\,dm + m(x_c^2 + z_c^2) - 2\int[(x + b_1)x_c + (z + b_3)z_c]\,dm - 2\int(x_c u + z_c w)\,dm + \int[u^2 + w^2 + 2(x + b_1)u + 2(z + b_3)w]\,dm ;$$

$$I_{33} = \int (r_{d1}^2 + r_{d2}^2)\,dm ;$$

$$= m(b_1^2 + b_2^2) + \int[x^2 + y^2 + 2(b_1 x + b_2 y)]\,dm + m(x_c^2 + y_c^2) - 2\int[(x + b_1)x_c + (y + b_2)y_c]\,dm - 2\int(x_c u + y_c v)\,dm + \int[u^2 + v^2 + 2(x + b_1)u + 2(y$$

$$+ b_2) r] dm \quad ;$$

$$I_{12} = \int r_{d1} r_{d2} \, dm \; ;$$

$$= \int (xy + x b_2 + y b_1 + b_1 b_2) \, dm + m$$

$$x_c y_c - \int [(y + b_2) x_c + (x + b_1) y_c] dm$$

$$- \int (y_c u + x_c v) \, dm + \int [(y + b_2) u + (x$$

$$+ b_1) v + u v] dm \quad ;$$

Similarly;

$$I_{13} = \int r_{d1} r_{d3} \, dm \quad ;$$

$$= \int (xz + x b_3 + z b_1 + b_1 b_3) \, dm + m$$

$$x_c z_c - \int [(z + b_3) x_c + (x + b_1) z_c] dm$$

$$- \int (z_c u + x_c w) \, dm + \int [(z + b_3) u + (x$$

$$+ b_1) w + u w] dm \quad ;$$

$$I_{23} = \int r_{d2} r_{d3} \, dm \quad ;$$

$$= \int (yz + y b_3 + z b_2 + b_2 b_3) \, dm + m$$

$$y_c z_c - \int [(y + b_2) z_c + (z + b_3) y_c] dm$$

$$-\int (z_c v + y_c w)\, dm + \int [(z + b_3) v + (y + b_2) w + v w]\, dm \quad . \qquad \text{(II.2)}$$

It is seen that the resulting expressions are made up of terms associated with the undeformed configuration, flexibility, and net offset.

II.2 Beam-Type Appendage

Considering the beam to be slender, $y \simeq z \simeq 0$. For a uniform cross section $dm = \rho dx$ thus allowing some of the integrals of equation (II.2) to be evaluated explicitly. The net contribution (excluding $\underline{r}_c$) of a given appendage of this type to the overall inertia tensor is, using local coordinates:

$$I_{11} = m(b_2^2 + b_3^2) + \rho \int_0^l [v^2 + w^2 + 2(b_2 v + b_3 w)]\, dx ;$$

$$I_{22} = m(b_1^2 + b_3^2) + \rho l^2 (\tfrac{1}{3} l + b_1) + \rho \int_0^l [(u - u_{fs})^2 + w^2 + 2(x + b_1)(u - u_{fs}) + 2 b_3 w]\, dx ;$$

$$I_{33} = m(b_1^2 + b_2^2) + \rho l^2 (\tfrac{1}{3} l + b_1) + \rho \int_0^l [(u - u_{fs})^2 + v^2 + 2(x + b_1)(u - u_{fs}) + 2 b_2 v]\, dx ;$$

$$-I_{12} = -m b_1 b_2 - \tfrac{1}{2} \rho l^2 b_2 - \rho \int_0^l [b_2 (u - u_{fs}) + (x + b_1) v + (u - u_{fs}) v]\, dx ;$$

$$-I_{13} = -m b_1 b_3 - \tfrac{1}{2} \rho l^2 b_3 - \rho \int_0^l [b_3 (u - u_{fs})$$

$$+ (x+b_1)w + (u-u_{fs})\,w\,]\,dx \quad ;$$

$$-I_{23} = -m b_2 b_3 - \rho \int_0^{\ell} (b_3 v + b_2 w + v w)\,dx \; .$$

(II.3)

When differentiating such expressions, note that $\ell = \ell(t)$ but $\underline{\sigma}$ = constant.

Separating out the effects associated with geometric offset only:

$$
\begin{aligned}
{}_2I_{11} &= m(b_2^2 + b_3^2) \quad ; \quad {}_2I_{12} = m b_1 b_2 \quad ; \\
{}_2I_{22} &= m(b_1^2 + b_3^2) \quad ; \quad {}_2I_{13} = m b_1 b_3 \quad ; \\
{}_2I_{33} &= m(b_1^2 + b_2^2) \quad ; \quad {}_2I_{23} = m b_2 b_3 \quad ;
\end{aligned}
$$

(II.4a)

and the 'undeformed' beam:

$$
\begin{aligned}
{}_3I_{11} &= 0 \quad ; \quad {}_3I_{12} = \tfrac{1}{2}\rho\ell^2 b_2 \quad ; \\
{}_3I_{22} &= \rho\ell^2(\tfrac{1}{3}\ell + b_1) \quad ; \quad {}_3I_{13} = \tfrac{1}{2}\rho\ell^2 b_3 \quad ; \\
{}_3I_{33} &= \rho\ell^2(\tfrac{1}{3}\ell + b_1) \quad ; \quad {}_3I_{23} = 0 \quad .
\end{aligned}
$$

(II.4b)

In the derivation of vibration equations the inertia density ($\tilde{I}_{jk}$) is required as an explicit function of elastic deflections using the local coordinates. Equations (II.2) can be used in the

derivation. Those terms which are not explicit functions of u, v, w are not included in the following.

Generally

$$I_{jk} = \int_m \tilde{I}_{jk}\, dm \,. \tag{II.5}$$

For the beam-type appendage adopted here, which includes axial foreshortening and $\rho = \rho(x)$:

$$e\tilde{I}_{11} = \rho\,[\, v^2 + w^2 + 2(\pi_2 v + \pi_3 w)\,] \;;$$

$$e\tilde{I}_{22} = 2\rho\,[\,\pi_1(x+u) + \pi_3 w\,] + \rho(x+u)^2 + \rho w^2 - [\,\int_x^{\ell} 2\rho(\pi_1 + \alpha + u)\, d\alpha\,]\,[\,\tfrac{1}{2}(v_x^2 + w_x^2)\,] \;;$$

$$e\tilde{I}_{33} = 2\rho\,[\,\pi_1(x+u) + \pi_2 v\,] + \rho(x+u)^2 + \rho v^2 - [\,\int_x^{\ell} 2\rho(\pi_1 + \alpha + u)\, d\alpha\,]\,[\,\tfrac{1}{2}(v_x^2 + w_x^2)\,] \;;$$

$$e\tilde{I}_{12} = \rho\,[\,(\pi_2 + v)(x+u) + \pi_1 v\,] - [\,\int_x^{\ell} \rho(\pi_2 + v)\, d\alpha\,]\,[\,\tfrac{1}{2}(v_x^2 + w_x^2)\,] \;;$$

$$e\tilde{I}_{23} = \rho\,(\pi_3 v + \pi_2 w + v w) \;;$$

$$e\tilde{I}_{13} = \rho[(\pi_3 + w)(x+u) + \pi_1 w] - [\int_x^{\ell} \rho(\pi_3 + w)d\alpha][\tfrac{1}{2}(v_x^2 + w_x^2)] \quad . \tag{II.6}$$

The theorem of Appendix IV has been applied when dealing with u_{fs}. For example:

$$I_{22} = \cdots + \int_0^{\ell} \rho\{\cdots - 2(\pi_1 + x + u)\, u_{fs} \cdots\} dx + \cdots$$

$$\simeq \cdots + \int_0^{\ell} \{\cdots - [\int_x^{\ell} 2\rho(\pi_1 + \alpha + u)\, d\alpha][\tfrac{1}{2}(v_x^2 + w_x^2)]\} dx + \cdots \quad ;$$

since,

$$u_{fs} \simeq \tfrac{1}{2}\int_0^x (v_\alpha^2 + w_\alpha^2)\, d\alpha \quad .$$

II.3 Inertias of Spacecraft Having Arbitrary Appendages

Adding up the results of equation (II.2), overall satellite moments of inertia can be arrived at which separate out the effects of flexibility. The expression can be simplified by eliminating the appearance of $\underline{r}_c$ components in local coordinates. This is possible since, aside from deployment effects, variations in center of mass location are not independent but ultimately are functions of local appendage deflections. Total satellite mass moment of inertia, which includes the effects of flexibility, geometric off-

set of appendage root, center of mass shift, and deployment, can be put in the following useful form with respect to the central reference system x, y, z:

$$[I] = [{}_1I] + [{}_2I] + [{}_3I] + [{}_eI] + [{}_{cm}I];$$

$$= [{}_uI] + [{}_eI] + [{}_{cm}I];$$

$$= \begin{bmatrix} {}_uI_{11} - m_s(y_c^2+z_c^2) & -{}_uI_{12} + m_s x_c y_c & -{}_uI_{13} + m_s x_c z_c \\ \cdots & \cdots & \cdots \\ {}^{S}{}_{Y}{}_{M}{}_{M}{}_{E}{}_{T}{}_{R}{}_{I}{}_{C} & {}_uI_{22} - m_s(x_c^2+z_c^2) & -{}_uI_{23} + m_s y_c z_c \\ \cdots & \cdots & \cdots \\ & & {}_uI_{33} - m_s(x_c^2+y_c^2) \end{bmatrix}$$

$$+\sum_i \left[\chi_i\right]^T \begin{bmatrix} \int_{m_i}\left[v_i^2+w_i^2+2(y_i+b_{2,i})v_i+2(z_i+b_{3,i})w_i\right]dm_i & -\int_{m_i}\left[(y_i+b_{2,i})u_i+(x_i+b_{1,i})v_i+u_iv_i\right]dm_i & -\int_{m_i}\left[(z_i+b_{3,i})u_i+(x_i+b_{1,i})w_i+u_iw_i\right]dm_i \\ & \int_{m_i}\left[u_i^2+w_i^2+2(x_i+b_{1,i})u_i+2(z_i+b_{3,i})w_i\right]dm_i & -\int_{m_i}\left[(z_i+b_{3,i})v_i+(y_i+b_{2,i})w_i+v_iw_i\right]dm_i \\ & & \int_{m_i}\left[u_i^2+v_i^2+2(x_i+b_{1,i})u_i+2(y_i+b_{2,i})v_i\right]dm_i \end{bmatrix} \left[\chi_i\right]. \qquad \text{(II.7)}$$

SYMMETRIC

Note that axial foreshortening terms can be accommodated by replacing u_i by $(u_i - u_{fs,i})$ in this expression. Also the $[\chi_i]$ matrices are constant with respect to time in this analysis.

II.4 Inertias of Spacecraft With Beam-Type Appendages

II.4.1 Continuous coordinates

The effect on spacecraft moments of inertia of appendage flexibility is worked out in detail here for an arbitrary number of beam-type appendages. General relations converting components from local coordinates (equations II.2 and II.3) to central coordinates are presented. Then, based on the coordinate transformations defined in Chapter 6, the terms ${}_eI_{jk}$ are expanded out for the case of appendages restricted to the x-y and x-z planes as identified by subscripts p (planar) and o (out-of-plane) respectively.

Considering the i^{th} appendage to have an arbitrary, but fixed orientation:

$$I_{11} = \sum_i \left[\chi_{11,i}^2 I_{11,i}^{(i)} + \chi_{21,i}^2 I_{22,i}^{(i)} + \chi_{31,i}^2 I_{33,i}^{(i)} - 2\left(\chi_{11,i}\chi_{21,i} I_{12,i}^{(i)} + \chi_{11,i}\chi_{31,i} I_{13,i}^{(i)} + \chi_{23,i}\chi_{31,i} I_{23,i}^{(i)} \right) \right] ;$$

$$I_{22} = \sum_i \left[\chi_{12,i}^2 I_{11,i}^{(i)} + \chi_{22,i}^2 I_{22,i}^{(i)} + \chi_{32,i}^2 I_{33,i}^{(i)} - 2\left(\chi_{12,i}\chi_{22,i} I_{12,i}^{(i)} + \chi_{12,i}\chi_{32,i} I_{13,i}^{(i)} + \chi_{22,i}\chi_{32,i} I_{23,i}^{(i)} \right) \right] ;$$

$$I_{33} = \sum_i \left[\chi_{13,i}^2 I_{11,i}^{(i)} + \chi_{23,i}^2 I_{22,i}^{(i)} + \chi_{33,i}^2 I_{33,i}^{(i)} - 2 \left(\chi_{13,i} \chi_{23,i} I_{12,i}^{(i)} + \chi_{13,i} \chi_{33,i} I_{13,i}^{(i)} + \chi_{23,i} \chi_{33,i} I_{23,i}^{(i)} \right) \right] ;$$

$$-I_{12} = \sum_i \left[\chi_{11,i} \chi_{12,i} I_{11,i}^{(i)} + \chi_{21,i} \chi_{22,i} I_{22,i}^{(i)} + \chi_{31,i} \chi_{32,i} I_{33,i}^{(i)} - (\chi_{11,i} \chi_{22,i} + \chi_{12,i} \chi_{21,i}) I_{12,i}^{(i)} - (\chi_{11,i} \chi_{32,i} + \chi_{12,i} \chi_{31,i}) I_{13,i}^{(i)} - (\chi_{21,i} \chi_{32,i} + \chi_{22,i} \chi_{31,i}) I_{23,i}^{(i)} \right] ;$$

$$-I_{13} = \sum_i \left[\chi_{11,i} \chi_{13,i} I_{11,i}^{(i)} + \chi_{21,i} \chi_{23,i} I_{22,i}^{(i)} + \chi_{31,i} \chi_{33,i} I_{33,i}^{(i)} - (\chi_{11,i} \chi_{23,i} + \chi_{13,i} \chi_{21,i}) I_{12,i}^{(i)} - (\chi_{11,i} \chi_{33,i} + \chi_{13,i} \chi_{31,i}) I_{13,i}^{(i)} - (\chi_{21,i} \chi_{33,i} + \chi_{23,i} \chi_{31,i}) I_{23,i}^{(i)} \right] ;$$

$$-I_{23} = \sum_i \left[\chi_{12,i} \chi_{13,i} I_{11,i}^{(i)} + \chi_{22,i} \chi_{23,i} I_{22,i}^{(i)} + \chi_{32,i} \chi_{33,i} I_{33,i}^{(i)} - (\chi_{12,i} \chi_{23,i} + \chi_{13,i} \chi_{22,i}) I_{12,i}^{(i)} - (\chi_{12,i} \chi_{33,i} + \chi_{13,i} \chi_{32,i}) I_{13,i}^{(i)} - (\chi_{22,i} \chi_{33,i} + \chi_{23,i} \chi_{32,i}) I_{23,i}^{(i)} \right] .$$

(II.8)

Substituting the $[X_p]$, $[X_o]$ matrices of the configuration studied in Chapter 6 into equation (II.8), gives the following flexibility contributions:

$$
\begin{aligned}
{}_e I_{11} = \sum_p \Big[\rho_p \int_0^{\ell_p} \{ & c^2\varphi_p\, v_p^2 + w_p^2 + 2\, c^2\varphi_p\, b_{2,p}\, v_p \\
& + 2\, b_{3,p}\, w_p + s2\varphi_p\, (x_p + b_{1,p})\, v_p - \Big[s2\varphi_p \\
& \int_{x_p}^{\ell_p} v_p\, d\alpha + s^2\varphi_p\, (\ell_p^2 - x_p^2) + (s2\varphi_p\, b_{2,p} \\
& + 2\, s^2\varphi_p\, b_{1,p})\, (\ell_p - x_p) \Big] \left(\frac{v_{p,x}^2 + w_{p,x}^2}{2} \right) \} \, dx_p \Big] \\
+ \sum_o \Big[\rho_o \int_0^{\ell_o} \{ & v_o^2 + c^2\psi_o\, w_o^2 + 2\, b_{2,o}\, v_o + 2\, c^2\psi_o \\
& b_{3,o}\, w_o - s2\psi_o\, (x_o + b_{1,o})\, w_o - \Big[-s2\psi_o \int_{x_o}^{\ell_o} w_o\, d\alpha \\
& + s^2\psi_o\, (\ell_o^2 - x_o^2) + (-s2\psi_o\, b_{3,o} + 2\, s^2\psi_o\, b_{1,o}) \\
& (\ell_o - x_o) \Big] \left(\frac{v_{o,x}^2 + w_{o,x}^2}{2} \right) \} \, dx_o \Big] \quad ;
\end{aligned}
$$

$$
\begin{aligned}
{}_e I_{22} = \sum_p \Big[\rho_p \int_0^{\ell_p} & s^2\varphi_p\, v_p^2 + w_p^2 + 2\, s^2\varphi_p\, b_{2,p}\, v_p \\
& + 2\, b_{3,p}\, w_p - s2\varphi_p\, (x_p + b_{1,p})\, v_p - \Big[-s2\varphi_p \\
& \int_{x_p}^{\ell_p} v_p\, d\alpha + c^2\varphi_p\, (\ell_p^2 - x_p^2) + (-s2\varphi_p\, b_{2,p} \\
& + 2\, c^2\varphi_p\, b_{1,p})\, (\ell_p - x_p) \Big] \left(\frac{v_{p,x}^2 + w_{p,x}^2}{2} \right) \} \, dx_p \Big] \\
+ \sum_o \Big[\rho_o \int_0^{\ell_o} \{ & w_o^2 + 2\, b_{3,o}\, w_o - \Big[(\ell_o^2 - x_o^2) \\
& + 2\, b_{1,o}\, (\ell_o - x_o) \Big] \left(\frac{v_{o,x}^2 + w_{o,x}^2}{2} \right) \} \, dx_o \Big] \quad ;
\end{aligned}
$$

$$e I_{33} = \sum_{\rho} \Big[\rho_\rho \int_0^{l_\rho} \Big\{ v_\rho^2 + 2 b_{2,\rho} v_\rho - \big[(l_\rho^2 - x_\rho^2) + 2 b_{1,\rho} (l_\rho - x_\rho) \big] \Big(\frac{v_{\rho,x}^2 + w_{\rho,x}^2}{2} \Big) \Big\} dx_\rho \Big]$$

$$+ \sum_{o} \Big[\rho_o \int_0^{l_o} \Big\{ v_o^2 + s^2\psi_o \, w_o^2 + 2 b_{2,o} v_o + 2 s^2\psi_o \, b_{3,o} w_o + s2\psi_o (x_o + b_{1,o}) w_o - \big[s2\psi_o \int_{x_o}^{l_o} w_o \, d\alpha + c^2\psi_o (l_o^2 - x_o^2) + (s2\psi_o \, b_{3,o} + 2 c^2\psi_o \, b_{1,o}) (l_o - x_o) \big] \Big(\frac{v_{o,x}^2 + w_{o,x}^2}{2} \Big) \Big\} dx_o \Big] \quad ;$$

$$-e I_{12} = \sum_{\rho} \Big[\rho_\rho \int_0^{l_\rho} \Big\{ \tfrac{1}{2} s2\phi_\rho \, v_\rho^2 + \big[s2\phi_\rho \, b_{2,\rho} - c2\phi_\rho (x_\rho + b_{1,\rho}) \big] v_\rho + \big[\tfrac{1}{2} s2\phi_\rho (l_\rho^2 - x_\rho^2) + c2\phi_\rho \int_{x_\rho}^{l_\rho} v_\rho \, d\alpha + (s2\phi_\rho \, b_{1,\rho} + c2\phi_\rho \, b_{2,\rho}) (l_\rho - x_\rho) \big] \Big(\frac{v_{\rho,x}^2 + w_{\rho,x}^2}{2} \Big) \Big\} dx_\rho \Big]$$

$$+ \sum_{o} \Big[\rho_o \int_0^{l_o} \Big\{ \big[c\psi_o (x_o + b_{1,o}) + s\psi_o \, b_{3,o} \big] v_o + s\psi_o \, b_{2,o} w_o + s\psi_o \, v_o w_o - c\psi_o \big[\int_{x_o}^{l_o} v_o \, d\alpha + b_{2,o} (l_o - x_o) \big] \Big(\frac{v_{o,x}^2 + w_{o,x}}{2} \Big) \Big\} dx_o \Big] \; ;$$

$$-e I_{13} = \sum_{\rho} \Big[\rho_\rho \int_0^{l_\rho} \Big\{ s\phi_\rho \, b_{3,\rho} v_\rho + \big[s\phi_\rho \, b_{2,\rho} - c\phi_\rho (x_\rho + b_{1,\rho}) \big] w_\rho + s\phi_\rho \, v_\rho w_\rho + c\phi_\rho \big[\int_{x_\rho}^{l_\rho} w_\rho \, d\alpha$$

$$+ \; b_{3,\rho}\,(\ell_\rho - x_\rho)\Big]\left(\frac{v_{\rho,x}^2 + \omega_{\rho,x}^2}{2}\right)\Big\}\,dx_\rho\Big)$$

$$+\sum_0\Big(C_{\rho_0}\int_{x_0}^{\ell_0}\Big\{\tfrac{1}{2}\,s2\psi_0\,\omega_0^2 + \big[c2\psi_0\,(x_0 + b_{1,0})$$

$$+ s2\psi_0\,b_{3,0}\big]\omega_0 + \Big[-c2\psi_0\int_{x_0}^{\ell_0}\omega_0\,d\alpha$$

$$+ \tfrac{1}{2}\,s2\psi_0\,(\ell_0^2 - x_0^2) + (s2\psi_0\,b_{1,0} - c2\psi_0\,b_{3,0})$$

$$(\ell_0 - x_0)\Big]\left(\frac{v_{0,x}^2 + \omega_{0,x}^2}{2}\right)\Big\}\,dx_0\Big) \quad ;$$

$$-eI_{23} = \sum_\rho\Big(C_{\rho_\rho}\int_0^{\ell_\rho}\Big\{c\phi_\rho\,b_{3,\rho}\,v_\rho + \big[c\phi_\rho\,b_{2,\rho} + s\phi_\rho$$

$$(x_\rho + b_{1,\rho})\big]\omega_\rho + c\phi_\rho\,v_\rho\,\omega_\rho - s\phi_\rho\Big[\int_{x_\rho}^{\ell_\rho}\omega_\rho\,d\alpha$$

$$+ b_{3,\rho}\,(\ell_\rho - x_\rho)\Big]\left(\frac{v_{\rho,x}^2 + \omega_{\rho,x}^2}{2}\right)\Big\}\,dx_\rho\Big)$$

$$+\sum_0\Big(C_{\rho_0}\int_0^{\ell_0}\Big\{c\psi_0\,b_{3,0} - s\psi_0\,(x_0 + b_{1,0})\Big]v_0$$

$$+ c\psi_0\,b_{2,0}\,\omega_0 + c\psi_0\,v_0\,\omega_0 + s\psi_0$$

$$\Big[\int_{x_0}^{\ell_0} v_0\,d\alpha + b_{2,0}\,(\ell_0 - x_0)\Big]$$

$$\left(\frac{v_{0,x}^2 + \omega_{0,x}^2}{2}\right)\Big\}\,dx_0\Big) \quad .$$

(II.9)

II.4.2 Assumed-mode format

The solution for elastic displacement assumed in Chapter 4 is substituted into equations (II.9). Combining modal coefficients, simplifying, and rearranging yields the following working form for the inertia flexibility effects:

$$
\begin{aligned}
{}_{e}I_{II} = \sum_{\rho}\sum_{o}\Bigg[\sum_{m}\sum_{n}\Big\{ & B_{mn,1}\,\rho_{\rho}\,\ell_{\rho}^{3}\,(c^{2}\varphi_{\rho}\,\xi_{m}^{\rho}\,\xi_{n}^{\rho} + \zeta_{m}^{\rho}\,\zeta_{n}^{\rho}) \\
& + B_{mn,1}\,\rho_{o}\,\ell_{o}^{3}\,(\xi_{m}^{o}\,\xi_{n}^{o} + c^{2}\psi_{o}\,\zeta_{m}^{o}\,\zeta_{n}^{o}) \\
& - \tfrac{1}{2}\,\rho_{\rho}\,[s^{2}\varphi_{\rho}\,B_{mn,11}\,\ell_{\rho}^{3} + (s2\varphi_{\rho}\,b_{2,\rho} + 2s^{2}\varphi_{\rho} \\
& b_{1,\rho})\,\ell_{\rho}^{2}\,B_{mn,10}]\,(\xi_{m}^{\rho}\,\xi_{n}^{\rho} + \zeta_{m}^{\rho}\,\zeta_{n}^{\rho}) - \tfrac{1}{2}\rho_{o} \\
& [s^{2}\psi_{o}\,B_{mn,11}\,\ell_{o}^{3} - (s2\psi_{o}\,b_{3,o} + 2s^{2}\psi_{o}\,b_{1,o}) \\
& B_{mn,10}\,\ell_{o}^{2}]\,(\xi_{m}^{o}\,\xi_{n}^{o} + \zeta_{m}^{o}\,\zeta_{n}^{o})\Big\} \\
& + \sum_{m}\Big\{[C_{m,1}\,(2c^{2}\varphi_{\rho}\,b_{2,\rho} + s2\varphi_{\rho}\,b_{1,\rho}) + C_{m,4} \\
& \ell_{\rho}\,s2\varphi_{\rho}]\,\rho_{\rho}\,\ell_{\rho}^{2}\,\xi_{m}^{\rho} + 2C_{m,1}\,(\rho_{o}\,\ell_{o}^{2}\,b_{2,o} \\
& \xi_{m}^{o} + \rho_{\rho}\,\ell_{\rho}^{2}\,b_{3,\rho}\,\zeta_{m}^{\rho}) + [C_{m,1}\,(2c^{2}\psi_{o} \\
& b_{3,o} - s2\psi_{o}\,b_{1,o}) - C_{m,4}\,\ell_{o}\,s2\psi_{o}]\,\rho_{o}\,\ell_{o}^{2} \\
& \zeta_{m}^{o}\Big\}\Bigg] ;
\end{aligned}
$$

$$
\begin{aligned}
{}_eI_{22} = \sum_{\rho}\sum_{o}\Big[\sum_{m}\sum_{n}\Big\{ & B_{mn,1}\Big[\rho_\rho l_\rho^3\big(s^2\varphi_\rho\,\xi_m^\rho\,\xi_n^\rho \\
& + \zeta_m^\rho\,\zeta_n^\rho\big) + \rho_o l_o^3\,\zeta_m^o\,\zeta_n^o\Big] - \tfrac{1}{2}\rho_\rho\Big[c^2\varphi_\rho \\
& B_{mn,11}\,l_\rho^3 + \big(-s2\varphi_\rho\,b_{2,\rho} + 2c^2\varphi_\rho\,b_{1,\rho}\big) \\
& B_{mn,10}\,l_\rho^2\Big]\big(\xi_m^\rho\,\xi_n^\rho + \zeta_m^\rho\,\zeta_n^\rho\big) - \tfrac{1}{2}\rho_o\big(B_{mn,11} \\
& l_o^3 + 2\,b_{1,o}\,B_{mn,10}\,l_o^2\big)\big(\xi_m^o\,\xi_n^o + \zeta_m^o\,\zeta_n^o\big)\Big\} \\
+ \sum_{m}\Big(& \rho_\rho l_\rho^2\Big\{\Big[\big(2s^2\varphi_\rho\,b_{2,\rho} - s2\varphi_\rho\,b_{1,\rho}\big)C_{m,1} \\
& - s2\varphi_\rho\,C_{m,4}\,l_\rho\Big]\xi_m^\rho + 2\,b_{3,\rho}\,C_{m,1}\,\zeta_m^\rho\Big\} \\
& + \rho_o l_o^2\,b_{3,o}\,\zeta_m^o\Big)\Big] \;;
\end{aligned}
$$

$$
\begin{aligned}
{}_eI_{33} = \sum_{\rho}\sum_{o}\Big[\sum_{m}\sum_{n}\Big\{ & B_{mn,1}\Big[\rho_\rho l_\rho^3\,\xi_m^\rho\,\xi_n^\rho + \rho_o l_o^3 \\
& \big(\xi_m^o\,\xi_n^o + s^2\psi_o\,\zeta_m^o\,\zeta_n^o\big)\Big] - \tfrac{1}{2}\rho_\rho\big(B_{mn,11} \\
& l_\rho^3 + 2\,b_{1,\rho}\,B_{mn,10}\,l_\rho^2\big)\big(\xi_m^\rho\,\xi_n^\rho + \zeta_m^\rho\,\zeta_n^\rho\big) \\
& - \tfrac{1}{2}\rho_o l_o^2\Big[c^2\psi_o\,B_{mn,11}\,l_o + \big(s\psi_o\,b_{3,o} + 2 \\
& c^2\psi_o\,b_{1,o}\big)B_{mn,10}\Big]\big(\xi_m^o\,\xi_n^o + \zeta_m^o\,\zeta_n^o\big)\Big\} \\
+ \sum_{m}\Big(& 2\rho_\rho l_\rho^2\,b_{2,\rho}\,C_{m,1}\,\xi_m^\rho + \rho_o l_o^2\Big\{b_{2,o} \\
& \xi_m^o + \Big[\big(s2\psi_o\,b_{1,o} + 2s^2\psi_o\,b_{3,o}\big)C_{m,1} \\
& + l_o\,s2\psi_o\,C_{m,4}\Big]\zeta_m^o\Big\}\Big)\Big] \;;
\end{aligned}
$$

$$-eI_{12} = \sum_{\rho}\sum_{o}\Big(\sum_{m}\sum_{n}\Big\{B_{mn,1}\Big[\tfrac{1}{2}\rho_\rho l_\rho^3 s2\varphi_\rho \xi_m^\rho \xi_n^\rho + \rho_o l_o^3 s\psi_o \xi_m^o \zeta_n^o\Big] + \tfrac{1}{2}\rho_\rho l_\rho^2\Big[\tfrac{1}{2}s2\varphi_\rho B_{mn,11} l_\rho + (s2\varphi_\rho \delta_{1,\rho} + c2\varphi_\rho \delta_{2,\rho}) B_{mn,10}\Big](\xi_m^\rho \xi_n^\rho + \zeta_m^\rho \zeta_n^\rho) - \tfrac{1}{2}\rho_o l_o^2 \delta_{2,o} c\psi_o B_{mn,10}(\xi_m^o \xi_n^o + \zeta_m^o \zeta_n^o)\Big\} + \sum_{m}\Big(\rho_\rho l_\rho^2\Big[(s2\varphi_\rho \delta_{2,\rho} - c2\varphi_\rho \delta_{1,\rho}) C_{m,1} - c2\varphi_\rho C_{m,4} l_\rho\Big]\xi_m^\rho + \rho_o l_o^2\Big\{\Big[(c\psi_o \delta_{1,o} + s\psi_o \delta_{3,o}) C_{m,1} + c\psi_o C_{m,4} l_o\Big]\xi_m^o + s\psi_o \delta_{2,o} C_{m,1} \zeta_m^o\Big\}\Big)\Big] ;$$

$$-eI_{13} = \sum_{\rho}\sum_{o}\Big(\sum_{m}\sum_{n}\Big\{B_{mn,1}\Big(\rho_\rho l_\rho^3 s\varphi_\rho \xi_m^\rho \zeta_n^\rho - \tfrac{1}{2}\rho_o l_o^3 s2\psi_o \zeta_m^o \zeta_n^o\Big) + \tfrac{1}{2}\rho_\rho l_\rho^2 \delta_{3,\rho} c\varphi_\rho B_{mn,10}(\xi_m^\rho \xi_n^\rho + \zeta_m^\rho \zeta_n^\rho) - \tfrac{1}{2}\rho_o l_o^2\Big[\tfrac{1}{2}s2\psi_o B_{mn,11} l_o + (s2\psi_o \delta_{1,o} - c2\psi_o \delta_{3,o}) B_{mn,10}\Big](\xi_m^o \xi_n^o + \zeta_m^o \zeta_n^o)\Big\} + \sum_{m}\Big(\rho_\rho l_\rho^2\Big\{s\varphi_\rho \delta_{3,\rho} C_{m,1} \xi_m^\rho + \Big[(s\varphi_\rho \delta_{2,\rho} - c\varphi_\rho \delta_{1,\rho}) C_{m,1} - c\varphi_\rho C_{m,4} l_\rho\Big]\zeta_m^\rho\Big\} + \rho_o l_o^2\Big[(c2\psi_o \delta_{1,o} + s2\psi_o \delta_{3,o}) C_{m,1} + c2\psi_o C_{m,4} l_o\Big]\zeta_m^o\Big)\Big] ;$$

$$-{}_eI_{23} = \sum_{\rho}\sum_{o} C \sum_{m}\sum_{n} \{ B_{mn,1} (\rho_\rho l_\rho^3 c\phi_\rho \xi_m^\rho \xi_n^\rho + \rho_o l_o^3 c\psi_o \xi_m^o \zeta_n^o - B_{mn,10} [\tfrac{1}{2} \rho_\rho l_\rho^2 s\phi_\rho b_{3,\rho} (\xi_m^\rho \xi_n^\rho + \zeta_m^\rho \zeta_n^\rho) - \tfrac{1}{2} \rho_o l_o^2 s\psi_o b_{2,o} (\xi_m^o \xi_n^o + \zeta_m^o \zeta_n^o)] \} + \sum_{m} (\rho_\rho l_\rho^2 \{ c\phi_\rho b_{3,\rho} C_{m,1} \xi_m^\rho + [(c\phi_\rho b_{2,\rho} + s\phi_\rho b_{1,\rho}) C_{m,1} + s\phi_\rho C_{m,4} l_\rho] \zeta_m^\rho \} + \rho_o l_o^2 \{ c\psi_o b_{2,o} C_{m,1} \zeta_m^o + [(c\psi_o b_{3,o} - s\psi_o b_{1,o}) C_{m,1} - s\psi_o C_{m,4} l_o] \xi_m^o \})) . \qquad \text{(II.10)}$$

II.5 Time Rate of Change of Inertias for Spacecraft with Beam-Type Appendages

Not all elements comprising the spacecraft inertia tensor vary with time. $[{}_1I]$ and $[{}_2I]$, for example, are fixed. $[{}_3I]$, however, can vary during deployment by differentiating the local elements as given by equation (II.6), transforming to central coordinates, and summing over all appendages.

In terms of local coordinates these derivatives are:

$$
\begin{aligned}
{}_3\dot{I}_{11} &= 0 \quad ; \quad {}_3\dot{I}_{12} = \rho l \dot{l} \delta_2 \; ; \\
{}_3\dot{I}_{22} &= \rho l \dot{l} (l + 2\delta_1) \; ; \quad {}_3\dot{I}_{13} = \rho l \dot{l} \delta_3 \; ; \\
{}_3\dot{I}_{33} &= \rho l \dot{l} (l + 2\delta_1) \; ; \quad {}_3\dot{I}_{23} = 0 \; .
\end{aligned}
\tag{II.11}
$$

Contributions associated with the changing position of the center of mass (${}_{cm}I_{jk}$) can be found directly from equation (II.7):

$$
\begin{aligned}
{}_{cm}\dot{I}_{11} &= -2 m_s (y_c \dot{y}_c + z_c \dot{z}_c) \; ; \\
{}_{cm}\dot{I}_{22} &= -2 m_s (x_c \dot{x}_c + z_c \dot{z}_c) \; ; \\
{}_{cm}\dot{I}_{33} &= -2 m_s (x_c \dot{x}_c + y_c \dot{y}_c) \; ; \\
{}_{cm}\dot{I}_{12} &= m_s (x_c \dot{y}_c + \dot{x}_c y_c) \; ; \\
{}_{cm}\dot{I}_{13} &= m_s (x_c \dot{z}_c + \dot{x}_c z_c) \; ; \\
{}_{cm}\dot{I}_{23} &= m_s (y_c \dot{z}_c + \dot{y}_c z_c) \; .
\end{aligned}
\tag{II.12}
$$

The most involved expressions are associated with flexibility. They can be determined most efficiently by differentiating the assumed-mode form of ${}_eI_{jk}$ as given by equation (II.10). That is, the total effect from all appendages is:

$$
\begin{aligned}
e\dot{I}_{11} = {} & \sum_{\rho}\sum_{o}\Big[\sum_{m}\sum_{n}\Big(B_{mn,1}\Big\{ 2\rho_\rho l_\rho^3 \left(c^2\varphi_\rho \dot{\xi}_m^\rho \dot{\xi}_n^\rho + \dot{\zeta}_m^\rho \dot{\zeta}_n^\rho\right) \\
& + 2\rho_o l_o^3 \left(\dot{\xi}_m^o \dot{\xi}_n^o + \dot{\zeta}_m^o \dot{\zeta}_n^o\right) + 3\Big[\rho_\rho l_\rho^2 \dot{l}_\rho \left(c^2\varphi_\rho \xi_m^\rho \xi_n^\rho + \zeta_m^\rho \zeta_n^\rho\right) + \rho_o l_o^2 \dot{l}_o \left(\xi_m^o \xi_n^o + c^2\psi_o \zeta_m^o \zeta_n^o\right)\Big]\Big\} \\
& - \tfrac{1}{2}\rho_\rho l_\rho \Big\{ \dot{l}_\rho \Big[2\left(s2\varphi_\rho b_{2,\rho} + 2s^2\varphi_\rho b_{1,\rho}\right) B_{mn,10} \\
& + 3\, s^2\varphi_\rho B_{mn,11} l_\rho\Big]\left(\xi_m^\rho \xi_n^\rho + \zeta_m^\rho \zeta_n^\rho\right) + 2 l_\rho \Big[s^2\varphi_\rho B_{mn,11} l_\rho + \left(s2\varphi_\rho b_{2,\rho} + 2s^2\varphi_\rho b_{1,\rho}\right) B_{mn,10}\Big]\left(\dot{\xi}_m^\rho \xi_n^\rho \right. \\
& \left. + \dot{\zeta}_m^\rho \zeta_n^\rho\right)\Big\} - \tfrac{1}{2}\rho_o l_o \Big\{ \dot{l}_o \Big[-2\left(s2\psi_o b_{3,o} + 2s^2\psi_o b_{1,o}\right) B_{mn,10} + 3 s^2\psi_o B_{mn,11} l_o\Big]\left(\xi_m^o \xi_n^o + \zeta_m^o \zeta_n^o\right) + 2 l_o \\
& \Big[s^2\psi_o B_{mn,11} l_o - \left(s2\psi_o b_{3,o} + 2 s^2\psi_o b_{1,o}\right) B_{mn,10}\Big] \left(\dot{\xi}_m^o \xi_n^o + \dot{\zeta}_m^o \zeta_n^o\right)\Big\}\Big) + \sum_{m}\Big(\rho_\rho l_\rho \Big\{\Big[\left(2c^2\varphi_\rho b_{2,\rho}\right. \\
& \left. + s2\varphi_\rho b_{1,\rho}\right) C_{m,1} + s2\varphi_\rho C_{m,4} l_\rho\Big]\left(2\dot{l}_\rho \xi_m^\rho + l_\rho \dot{\xi}_m^\rho\right) + s2\varphi_\rho C_{m,4} l_\rho \dot{l}_\rho \xi_m^\rho + 2 b_{3,\rho} C_{m,1}\left(2\dot{l}_\rho \zeta_m^\rho + l_\rho \dot{\zeta}_m^\rho\right)\Big\} \\
& + \rho_o l_o \Big\{\Big[\left(2c^2\psi_o b_{3,o} - s2\psi_o b_{1,o}\right) C_{m,1} - s2\psi_o C_{m,4} l_o\Big]\left(2\dot{l}_o \zeta_m^o + l_o \dot{\zeta}_m^o\right) - s2\psi_o C_{m,4} l_o \dot{l}_o \zeta_m^o \\
& + 2 b_{2,o} C_{m,1}\left(2\dot{l}_o \xi_m^o + l_o \dot{\xi}_m^o\right)\Big\}\Big)\Big] ;
\end{aligned}
$$

$$e\dot{I}_{22} = \sum_{\rho}\sum_{o}\Big[\sum_{m}\sum_{n}\Big(B_{mn,1}\{2\rho_\rho l_\rho^3(s^2\varphi_\rho\dot{\xi}_m^\rho\xi_n^\rho+\dot{\zeta}_m^\rho\zeta_n^\rho)+2\rho_o l_o^3\dot{\zeta}_m^o\zeta_n^o+3[\rho_\rho l_\rho^2\dot{l}_\rho(s^2\varphi_\rho\xi_m^\rho\xi_n^\rho+\zeta_m^\rho\zeta_n^\rho)+\rho_o l_o^2\dot{l}_o\zeta_m^o\zeta_n^o]\}-\tfrac{1}{2}\rho_\rho l_\rho\{[3c^2\varphi_\rho B_{mn,11}+2(-s2\varphi_\rho b_{2,\rho}+2c^2\varphi_\rho b_{1,\rho})B_{mn,10}]l_\rho\dot{l}_\rho(\xi_m^\rho\xi_n^\rho+\zeta_m^\rho\zeta_n^\rho)+2[c^2\varphi_\rho B_{mn,11}+(-s2\varphi_\rho b_{2,\rho}+2c^2\varphi_\rho b_{1,\rho})B_{mn,10}]l_\rho^2(\dot{\xi}_m^\rho\xi_n^\rho+\dot{\zeta}_m^\rho\zeta_n^\rho)\}-\tfrac{1}{2}\rho_o l_o[(3B_{mn,11}+2b_{1,o}B_{mn,10})l_o\dot{l}_o(\xi_m^o\xi_n^o+\zeta_m^o\zeta_n^o)+2(B_{mn,11}+2b_{1,o}B_{mn,10})l_o^2(\dot{\xi}_m^o\xi_n^o+\dot{\zeta}_m^o\zeta_n^o)]\Big)+\sum_{m}\Big(\rho_\rho l_\rho\{[2s^2\varphi_\rho b_{2,\rho}-s2\varphi_\rho b_{1,\rho})C_{m,1}-s2\varphi_\rho C_{m,4}l_\rho](2\dot{l}_\rho\xi_m^\rho+l_\rho\dot{\xi}_m^\rho)+2b_{3,\rho}C_{m,1}(2\dot{l}_\rho\zeta_m^\rho+l_\rho\dot{\zeta}_m^\rho)-s2\varphi_\rho C_{m,4}l_\rho\dot{l}_\rho\xi_m^\rho\}+2\rho_o l_o b_{3,o}C_{m,1}(2\dot{l}_o\zeta_m^o+l_o\dot{\zeta}_m^o)\Big)\Big];$$

$$e\dot{I}_{33} = \sum_{\rho}\sum_{o}\Big[\sum_{m}\sum_{n}\Big(B_{mn,1}\{2\rho_\rho l_\rho^3\dot{\xi}_m^\rho\xi_n^\rho+2\rho_o l_o^3(\dot{\xi}_m^o\xi_n^o+s^2\psi_o\dot{\zeta}_m^o\zeta_n^o)+3[\rho_\rho l_\rho^2\dot{l}_\rho\xi_m^\rho\xi_n^\rho+\rho_o l_o^2\dot{l}_o(\xi_m^o\xi_n^o+\zeta_m^o\zeta_n^o)]\}-\tfrac{1}{2}\rho_\rho l_\rho[(4b_{1,\rho}B_{mn,10}+3B_{mn,11}l_\rho)(\xi_m^\rho\xi_n^\rho+\zeta_m^\rho\zeta_n^\rho)$$

$$+ 2(2\beta_{1,\rho}\, B_{mn,10} + B_{mn,11}\, l_\rho)\, l_\rho\, (\dot{\xi}_m^\rho\, \xi_n^\rho + \dot{\zeta}_m^\rho\, \zeta_n^\rho)] - \tfrac{1}{2}\rho_0 l_0 \{[2(s2\psi_0\, \beta_{3,0} + 2c^2\psi_0\, \beta_{1,0})\, \dot{l}_0\, B_{mn,10} + 3c^2\psi_0\, B_{mn,11}\, l_0]\, (\xi_m^0\, \xi_n^0 + \zeta_m^0\, \zeta_n^0) + 2[(s2\psi_0\, \beta_{3,0} + 2c^2\psi_0\, \beta_{1,0})\, B_{mn,10} + c^2\psi_0\, B_{mn,11}\, l_0]\, l_0\, (\dot{\xi}_m^0\, \xi_n^0 + \dot{\zeta}_m^0\, \zeta_n^0)\}) + \sum_m (2\rho_\rho l_\rho\, \beta_{2,\rho}\, C_{m,1}\, (2\dot{l}_\rho\, \xi_m^\rho + l_\rho\, \dot{\xi}_m^\rho) + \rho_0 l_0 \{[(s2\psi_0\, \beta_{1,0} + 2s^2\psi_0\, \beta_{3,0})\, C_{m,1} + s2\psi_0\, C_{m,4}\, l_0]\, (2\dot{l}_0\, \zeta_m^0 + l_0\, \dot{\zeta}_m^0) + 2\beta_{2,0}\, C_{m,1}\, (2\dot{l}_0\, \xi_m^0 + l_0\, \dot{\xi}_m^0) + s2\psi_0\, C_{m,4}\, l_0 \dot{l}_0\, \zeta_m^0\})];$$

$$-e\dot{I}_{12} = \sum_\rho \sum_0 C \sum_m \sum_n (B_{mn,1}\, [\rho_\rho l_\rho^3\, s2\varphi_\rho\, \dot{\xi}_m^\rho\, \xi_n^\rho + \rho_0 l_0^3\, s\psi_0\, (\dot{\xi}_m^0\, \zeta_n^0 + \xi_m^0\, \dot{\zeta}_n^0) + 3(\tfrac{1}{2}\rho l_\rho^2 \dot{l}_\rho\, s\varphi_\rho\, \xi_m^\rho\, \xi_n^\rho + \rho_0 l_0^2\, \dot{l}_0\, s\psi_0\, \xi_m^0\, \zeta_n^0)] + \tfrac{1}{2}\rho_\rho l_\rho \{[2(s2\varphi_\rho\, \beta_{1,\rho} + c2\varphi_\rho\, \beta_{2,\rho})\, B_{mn,10} + \tfrac{3}{2}s\varphi_\rho\, B_{mn,11}\, l_\rho]\, \dot{l}_\rho\, (\xi_m^\rho\, \xi_n^\rho + \zeta_m^\rho\, \zeta_n^\rho) + 2[\tfrac{1}{2}s2\varphi_\rho\, B_{mn,11}\, l_\rho + (s2\varphi_\rho\, \beta_{1,\rho} + c2\varphi_\rho\, \beta_{2,\rho})\, B_{mn,10}]\, l_\rho\, (\dot{\xi}_m^\rho\, \xi_n^\rho + \dot{\zeta}_m^\rho\, \zeta_n^\rho)\} - \rho_0 l_0\, \beta_{2,0}\, c\psi_0\, B_{mn,10}\, [\dot{l}_0\, (\xi_m^0\, \xi_n^0 + \zeta_m^0\, \zeta_n^0)$$

$$+ l_o (\dot{\xi}^o_m \xi^o_n + \dot{\zeta}^o_m \zeta^o_n)]) + \sum_m (\rho_\rho l_\rho \{[$$

$$(s2\varphi_\rho b_{2,\rho} - c2\varphi_\rho b_{1,\rho}) C_{m,1} - c2\varphi_\rho C_{m,4} l_\rho](2\dot{l}_\rho$$

$$\xi^\rho_m + l_\rho \dot{\xi}^\rho_m) - c2\varphi_\rho C_{m,4} l_\rho \dot{l}_\rho \xi^\rho_m\} + \rho_o l_o \{[$$

$$(c\psi_o b_{1,o} + s\psi_o b_{3,o}) C_{m,1} + c\psi_o C_{m,4} l_o](2\dot{l}_o \xi^o_m$$

$$+ l_o \dot{\xi}^o_m) + s\psi_o C_{m,1} b_{2,o} (2\dot{l}_o \zeta^o_m + l_o \dot{\zeta}^o_m)$$

$$+ c\psi_o C_{m,4} l_o \dot{l}_o \xi^o_m\})] \quad ;$$

$$-\frac{\dot{I}_{13}}{e} = \sum_\rho \sum_o [\sum_m \sum_n (B_{mn,1} [\rho_\rho l_\rho^3 s\varphi_\rho (\dot{\xi}^\rho_m \zeta^\rho_n + \xi^\rho_m \dot{\zeta}^\rho_n)$$

$$- \rho_o l_o^3 s2\psi_o \dot{\zeta}^o_m \zeta^o_n + 3(\rho_\rho l_\rho^2 \dot{l}_\rho s\varphi_\rho \xi^\rho_m \zeta^\rho_n$$

$$- \tfrac{1}{2}\rho_o l_o^2 \dot{l}_o s2\psi_o \zeta^o_m \zeta^o_n) + \rho_\rho l_\rho b_{3,\rho} c\varphi_\rho$$

$$[\dot{l}_\rho (\xi^\rho_m \xi^\rho_n + \zeta^\rho_m \zeta^\rho_n) + l_\rho (\dot{\xi}^\rho_m \xi^\rho_n + \dot{\zeta}^\rho_m \zeta^\rho_n)]$$

$$- \tfrac{1}{2}\rho_o l_o \{[2(s2\psi_o b_{1,o} - c2\psi_o b_{3,o}) B_{mn,10}$$

$$+ \tfrac{3}{2} s2\psi_o B_{mn,11} l_o] \dot{l}_o (\xi^o_m \xi^o_n + \zeta^o_m \zeta^o_n)$$

$$+ 2[(s2\psi_o b_{1,o} - c2\psi_o b_{3,o}) B_{mn,10} + \tfrac{1}{2} s2\psi_o$$

$$B_{mn,11} l_o] l_o (\dot{\xi}^o_m \xi^o_n + \dot{\zeta}^o_m \zeta^o_n)\}) +$$

$$+ \sum_m (\rho_\rho l_\rho \{ s\varphi_\rho b_{3,\rho} C_{m,1} (2\dot{l}_\rho \xi^\rho_m + l_\rho \dot{\xi}^\rho_m)$$

$$+ [(s\varphi_\rho b_{2,\rho} - c\varphi_\rho b_{1,\rho}) C_{m,1} - c\varphi_\rho C_{m,4} l_\rho]$$

$$(2\dot{l}_\rho \zeta^\rho_m + l_\rho \dot{\zeta}^\rho_m) - c\varphi_\rho C_{m,4}\, l_\rho \dot{l}_\rho \xi^\rho_m \}$$

$$+ \rho_o l_o \{ [(c2\psi_o b_{1,o} + s2\psi_o b_{3,o}) C_{m,1} + c2\psi_o C_{m,4} l_o] (2\dot{l}_o \zeta^o_m + l_o \dot{\zeta}^o_m) + c2\psi_o C_{m,4} l_o \dot{l}_o \xi^o_m \})] \quad ;$$

$$-e\dot{I}_{23} = \sum_\rho \sum_o (\sum_m \sum_n \{ B_{mn,1} [2\rho_\rho l_\rho^3 c\varphi_\rho \dot{\xi}^\rho_m \xi^\rho_n + \rho_o l_o^3 c\psi_o (\dot{\xi}^o_m \zeta^o_n + \xi^o_m \dot{\zeta}^o_n) + 3(\rho_\rho l_\rho^2 \dot{l}_\rho c\varphi_\rho \xi^\rho_m \xi^\rho_n + \rho_o l_o^2 \dot{l}_o c\psi_o \xi^o_m \zeta^o_n) - \rho_\rho l_\rho \delta_{3,\rho} s\varphi_\rho B_{mn,10} [\dot{l}_\rho (\xi^\rho_m \xi^\rho_n + \zeta^\rho_m \zeta^\rho_n) + l_\rho (\dot{\xi}^\rho_m \xi^\rho_n + \dot{\zeta}^\rho_m \zeta^\rho_n)] + \rho_o l_o b_{2,o} s\psi_o B_{mn,10} [\dot{l}_o (\xi^o_m \xi^o_n + \zeta^o_m \zeta^o_n) + l_o (\dot{\xi}^o_m \xi^o_n + \dot{\zeta}^o_m \zeta^o_n)] \}$$

$$+ \sum_m (\rho_\rho l_\rho \{ b_{3,\rho} c\varphi_\rho C_{m,1} (2\dot{l}_\rho \xi^\rho_m + l_\rho \dot{\xi}^\rho_m) + [(c\varphi_\rho b_{2,\rho} + s\varphi_\rho b_{1,\rho}) C_{m,1} + s\varphi_\rho C_{m,4} l_\rho] (2\dot{l}_\rho \zeta^\rho_m + l_\rho \dot{\zeta}^\rho_m) + s\varphi_\rho C_{m,4} l_\rho \dot{l}_\rho \xi^\rho_m \} + \rho_o l_o [(c\psi_o b_{3,o} - s\psi_o b_{1,o}) C_{m,1} - s\psi_o C_{m,4} l_o] (2\dot{l}_o \xi^o_m + l_o \dot{\xi}^o_m) + c\psi_o b_{2,o} C_{m,1} (2\dot{l}_o \zeta^o_m + l_o \dot{\zeta}^o_m) - s\psi_o C_{m,4} l_o \dot{l}_o \xi^o_m \})] \quad . \qquad \text{(II.13)}$$

APPENDIX III

EVALUATION OF $\{r_c\}$, $\{h\}$, AND $\{\Gamma\}$ FOR BEAM-TYPE APPENDAGES

The general nonlinear attitude equations of Chapter 2 remain quite lengthy despite the compact form in which flexibility and deployment effects are represented. Evaluation of these effects in fact requires a major effort when dealing with the three dimensional case containing offset and arbitrary appendage orientation. Upon applying the definition, for $\{h\}$ and $\{\Gamma\}$ and in particular, to the configuration of Figure 2-2 one quickly loses any naiveté!

III.1 Shifting Center of Mass Location $\{r_c\}$ and Associated Time Derivatives

The expressions developed here are based on the definition of $\underline{r}_c$ given in Chapter 2 which allows for a change in center of mass location due to elastic motions or deployment. An arbitrary number of appendages lie in the x-y, x-z planes. Deformations are solved for as in Chapter 4.

$$x_c = (1/m_s)\{ \sum_p \rho_p [\tfrac{1}{2} c\varphi_p (l_p^b)^2 - s\varphi_p l_p^2 \sum_m (C_{m,1} \xi_m^p)] + \sum_o \rho_o [\tfrac{1}{2} c\psi_o (l_o^b)^2 + s\psi_o l_o^2 \sum_m (C_{m,1} \xi_m^o)] \} ;$$

$$y_c = (1/m_s)\{ \sum_p \rho_p [\tfrac{1}{2} s\varphi_p (l_p^b)^2 + c\varphi_p l_p^2 \sum_m (C_{m,1}$$

$$\xi_m^p + \sum_o [2\rho_o l_o^2 \sum_m (C_{m,1} \xi_m^o)] \} ;$$

$$z_c = (1/m_s) [\sum_p [\rho_p l_p^2 \sum_m (C_{m,1} \zeta_m^p)] + \sum_o \{ \rho_o [-\tfrac{1}{2} s\psi_o (l_o^b)^2 + c\psi_o l_o^2 \sum_m (C_{m,1} \zeta_m^o)] \}] .$$

(III.1)

$$\dot{x}_c = (1/m_s) \{ \sum_p \rho_p [c\varphi_p l_p^b \dot{l}_p - s\varphi_p \sum_m C_{m,1} l_p (l_p \dot{\xi}_m^p + 2 \dot{l}_p \xi_m^p)] + \sum_o \rho_o [c\psi_o l_o^b \dot{l}_o + s\psi_o \sum_m C_{m,1} l_o (l_o \dot{\zeta}_m^o + 2 \dot{l}_o \zeta_m^o)] \} ;$$

$$\dot{y}_c = (1/m_s) \{ \sum_p [\rho_p s\varphi_p l_p^b \dot{l}_p + c\varphi_p \sum_m C_{m,1} l_p (l_p \dot{\xi}_m^p + 2 \dot{l}_p \xi_m^p)] + \sum_o [2\rho_o \sum_m C_{m,1} l_o (l_o \dot{\xi}_m^o + 2 \dot{l}_o \xi_m^o)] \} ;$$

$$\dot{z}_c = (1/m_s) \{ \sum_p \rho_p [\sum_m C_{m,1} l_p (l_p \dot{\zeta}_m^p + 2 \dot{l}_p \zeta_m^p)] + \sum_o \rho_o [-s\psi_o l_o^b \dot{l}_o + c\psi_o l_o \sum_m C_{m,1} (l_o \dot{\zeta}_m^o + 2 \dot{l}_o \zeta_m^o)] \} .$$

(III.2)

$$\ddot{x}_c = (1/m_s)\Big[\sum_\rho \rho_\rho \{ c\varphi_\rho (\dot{l}_\rho^2 - l_\rho^b \ddot{l}_\rho) - s\varphi_\rho \sum_m c_{m,1} [l_\rho^2 \ddot{\xi}_m^\rho + 4 l_\rho \dot{l}_\rho \dot{\xi}_m^\rho + 2 (l_\rho \ddot{l}_\rho + \dot{l}_\rho^2) \xi_m^\rho] \} + \sum_o \rho_o \{ c\psi_o (\dot{l}_o^2 + l_o^b \ddot{l}) + s\psi_o \sum_m c_{m,1} [l_o^2 \ddot{\zeta}_m^o + 4 l_o \dot{l}_o \dot{\zeta}_m^o + 2 (l_o \ddot{l}_o + \dot{l}_o^2) \zeta_m^o] \} \Big] ;$$

$$\ddot{y}_c = (1/m_s)\Big[\sum_\rho \rho_\rho \{ s\varphi_\rho (\dot{l}_\rho^2 + l_\rho^b \ddot{l}_\rho) + c\varphi_\rho \sum_m c_{m,1} [l_\rho^2 \ddot{\xi}_m^\rho + 4 l_\rho \dot{l}_\rho \dot{\xi}_m^\rho + 2 (l_\rho \ddot{l}_\rho + \dot{l}_\rho^2) \xi_m^\rho] \} + \sum_o {}^2\rho_o \{ \sum_m c_{m,1} [l_o^2 \ddot{\xi}_m^o + 4 l_o \dot{l}_o \dot{\xi}_m^o + 2 (l_o \ddot{l}_o + \dot{l}_o^2) \xi_m^o] \} \Big] ;$$

$$\ddot{z}_c = (1/m_s)\Big[\sum_\rho \rho_\rho \{ \sum_m c_{m,1} [l_\rho^2 \ddot{\zeta}_m^\rho + 4 l_\rho \dot{l}_\rho \dot{\zeta}_m^\rho + 2 (l_\rho \ddot{l}_\rho + \dot{l}_\rho^2) \zeta_m^\rho] \} + \sum_o \rho_o \{ -s\psi_o (\dot{l}_o^2 + l_o^b \ddot{l}_o) + c\psi_o \sum_m c_{m,1} [l_o^2 \ddot{\zeta}_m^o + 4 l_o \dot{l}_o \dot{\zeta}_m^o + 2 (l_o \ddot{l}_o + \dot{l}_o^2) \zeta_m^o] \} \Big] . \qquad \text{(III.3)}$$

III.2 Local Angular Momentum {h}

A component matrix definition is given in Chapter 2 for angular momentum applied about the system instantaneous center of mass solely as a result of motion relative to the body-fixed axes x, y, z. In this case the relative motion referred to is caused by appendage vibration or deployment and does not include librational effects; hence the term 'local'.

III.2.1 Appendages with arbitrary orientation, continuous coordinates

Considered, is a beam-type appendage having an arbitrary orientation, undergoing transverse oscillations only, and also included is the effect of axial foreshortening. Components of momenta are evaluated along the central coordinate axes. However, appendage-related variables are based on coordinates x_i, y_i, z_i; for convenience the subscript i dropped. The contribution of the i^{th} appendage to {h} is demonstrated for the component along the x axis. The resultant h_2, h_3 terms are analogous.

$$h_1 = \rho \ell (\pi_2 \dot{\pi}_3 - \pi_3 \dot{\pi}_2) + \rho \int_0^{\ell} [[\chi_{33} \pi_1 - \chi_{22} \pi_3) + (\chi_{23} \chi_{12} - \chi_{22} \chi_{13}) x + (\chi_{23} \chi_{32} - \chi_{22} \chi_{33}) w] v_t + [(\chi_{33} \pi_2 - \chi_{32} \pi_3) + (\chi_{33} \chi_{12} - \chi_{32} \chi_{13}) x + (\chi_{33} \chi_{22} - \chi_{32} \chi_{13})$$

$$v\,]\,\omega_t + U\{(\chi_{13}\pi_2 - \chi_{12}\pi_3) + (\chi_{22}\chi_{13} - \chi_{23}\chi_{12})v + (\chi_{32}\chi_{13} - \chi_{33}\chi_{12})w + [(\chi_{23}\pi_2 - \chi_{22}\pi_3) + (\chi_{12}\chi_{23} - \chi_{13}\chi_{22})x + (\chi_{32}\chi_{23} - \chi_{33}\chi_{22})w\,]\,v_x + [(\chi_{33}\pi_2 - \chi_{32}\pi_3) + (\chi_{12}\chi_{33} - \chi_{13}\chi_{32})x + (\chi_{22}\chi_{33} - \chi_{23}\chi_{32})v\,]\,\omega_x\} + (\chi_{12}\dot{\pi}_3 - \chi_{13}\dot{\pi}_2)x + (\chi_{22}\dot{\pi}_3 - \chi_{23}\dot{\pi}_2)v + (\chi_{32}\dot{\pi}_3 - \chi_{33}\dot{\pi}_2)w - \{(\chi_{12}\dot{\pi}_3 - \chi_{13}\dot{\pi}_2)[\tfrac{1}{2}(v_x^2 + \omega_x^2)] + (\chi_{13}\pi_2 - \chi_{12}\pi_3)[v_x v_{xt} + \omega_x \omega_{xt} + U(v_x v_{xx} + \omega_x \omega_{xx})]\}(\ell - x)\,]\,dx\,. \tag{III.4}$$

III.2.2 Assumed-mode format for appendages in the x-y, x-z planes.

The more general results of the previous section are applied to the case of booms lying in the x-y or x-z planes only, using the coordinate transformations given in Chapter 6. Appendage deformations are replaced by the assumed series solutions of Chapter 4. Substituting into the expressions developed in the previous section and simplifying:

$$h_1 = \sum_{\rho}\sum_{o} < \rho_\rho l_\rho [\pi_{2,\rho}\dot{\pi}_{3,\rho} - \pi_{3,\rho}\dot{\pi}_{2,\rho} + s\varphi_\rho (\tfrac{1}{2} l_\rho \dot{\pi}_{3,\rho} - \pi_{3,\rho}\dot{l}_\rho)] + \rho_o l_o [\pi_{2,o}\dot{\pi}_{3,o} - \pi_{3,o}\dot{\pi}_{2,o} + s\psi_o (\tfrac{1}{2} l_o \dot{\pi}_{2,o} - \pi_{2,o}\dot{l}_o)]$$

$$+ \sum_m \{ \rho_\rho l_\rho [-C_{m,1} c\varphi_\rho \pi_{3,\rho} l_\rho \dot{\xi}^\rho_m + l_\rho (C_{m,1}\pi_{2,\rho} + s\varphi_\rho C_{m,4} l_\rho)\dot{\zeta}^\rho_m + c\varphi_\rho (C_{m,1}\dot{\pi}_{3,\rho} l_\rho - C_{m,10}\pi_{3,\rho}\dot{l}_\rho)\xi^\rho_m + (-C_{m,1}\dot{\pi}_{2,\rho} l_\rho + C_{m,10}\pi_{2,\rho}\dot{l}_\rho + C_{m,12} s\varphi_\rho l_\rho \dot{l}_\rho)\zeta^\rho_m]$$

$$+ \rho_o l_o [l_o (-C_{m,1}\pi_{3,o} + C_{m,4} s\psi_o l_o)\dot{\xi}^o_m + (C_{m,1}\dot{\pi}_{3,o} l_o - C_{m,10}\pi_{3,o}\dot{l}_o - s\psi_o C_{m,12} l_o \dot{l}_o)\xi^o_m + c\psi_o \pi_{2,o} C_{m,1} l_o \dot{\zeta}^o_m + c\psi_o (-C_{m,1}\dot{\pi}_{2,o} l_o + C_{m,10}\pi_{2,o}\dot{l}_o)\zeta^o_m] \}$$

$$+ \sum_m \sum_n \{ \rho_\rho l_\rho [B_{mn,10} s\varphi_\rho \pi_{3,\rho} l_\rho (\xi^\rho_m \dot{\xi}^\rho_n + \zeta^\rho_m \dot{\zeta}^\rho_n) + s\varphi_\rho (-\tfrac{1}{2} B_{mn,10}\dot{\pi}_{3,\rho} l_\rho + B_{mn,m}\pi_{3,\rho}\dot{l}_\rho)(\xi^\rho_m \xi^\rho_n + \zeta^\rho_m \zeta^\rho_n) + B_{mn,21} c\varphi_\rho l_\rho \dot{l}_\rho \xi^\rho_m \zeta^\rho_n] + \rho_o l_o [B_{mn,10} s\psi_o \pi_{2,o} l_o$$

$$(\xi^{\circ}_m \dot{\xi}^{\circ}_n + \zeta^{\circ}_m \dot{\zeta}^{\circ}_n) + s\psi_0 (-\tfrac{1}{2} B_{mn,10} \dot{\pi}_{2,0} l_0 + B_{mn,11} \pi_{2,0} \dot{l}_0 (\xi^{\circ}_m \xi^{\circ}_n + \zeta^{\circ}_m \zeta^{\circ}_n) + c\psi_0 l_0 (B_{mn,1} l_0 (\xi^{\circ}_m \dot{\zeta}^{\circ}_n - \dot{\xi}^{\circ}_m \zeta^{\circ}_n) + c\psi_0 l_0 B_{mn,21} \dot{l}_0 \xi^{\circ}_m \zeta^{\circ}_n]\} \rangle ;$$

$$h_2 = \sum_{\rho} \sum_{0} \langle \rho_\rho l_\rho [\pi_{3,\rho} \dot{\pi}_{1,\rho} - \pi_{1,\rho} \dot{\pi}_{3,\rho} + c\phi_\rho (\tfrac{1}{2} \dot{\pi}_{3,\rho} l_\rho - \pi_{3,\rho} \dot{l}_\rho)] + \rho_0 l_0 [\pi_{3,0} \dot{\pi}_{1,0} - \pi_{1,0} \dot{\pi}_{3,0} - \tfrac{1}{2} l_0 (s\psi_0 \dot{\pi}_{1,0} + c\psi_0 \dot{\pi}_{3,0}) + \dot{l}_0 (s\psi_0 \pi_{1,0} + c\psi_0 \pi_{3,0})] + \sum_{m} \{\rho_\rho l_\rho [C_{m,1} s\phi_\rho \pi_{3,\rho} l_\rho \dot{\xi}^{\rho}_m + l_\rho (C_{m,1} \pi_{1,\rho} + C_{m,4} c\phi_\rho l_\rho) \dot{\zeta}^{\rho}_m + s\phi_\rho (-C_{m,1} \dot{\pi}_{3,\rho} l_\rho + C_{m,10} \pi_{3,\rho} \dot{l}_\rho) \xi^{\rho}_m + (-C_{m,1} \dot{\pi}_{1,\rho} l_\rho + C_{m,10} \pi_{1,\rho} \dot{l}_\rho + C_{m,11} c\phi_\rho l_\rho \dot{l}_\rho) \zeta^{\rho}_m] + \rho_0 l_0 [l_0 (C_{m,1} s\psi_0 \pi_{3,0} - C_{m,1} c\psi_0 \pi_{1,0} - C_{m,4} l_0) \dot{\zeta}^{\circ}_m + ((s\psi_0 \pi_{3,0} - c\psi_0 \pi_{1,0}) C_{m,10} \dot{l}_0 - C_{m,12} \dot{l}_0 + (c\psi_0 \dot{\pi}_{1,0} - s\psi_0 \dot{\pi}_{3,0}) C_{m,1} l_0) \zeta^{\circ}_m]\}$$

$$+ \sum_m \sum_n \{ \rho_\rho \ell_\rho [B_{mn,10} \pi_{3,\rho} \ell_\rho (\xi_m^\rho \xi_n^\rho + \zeta_m^\rho \zeta_n^\rho) + (-\tfrac{1}{2} B_{mn,10} c\phi_\rho \pi_{3,\rho} \ell_\rho + B_{mn,17} \pi_{3,\rho} \dot{\ell}_\rho) (\xi_m^\rho \xi_n^\rho + \zeta_m^\rho \zeta_n^\rho) - B_{mn,21} s\phi_\rho \ell_\rho \dot{\ell}_\rho \xi_m^\rho \zeta_n^\rho] + \rho_o \ell_o [- B_{mn,10} (s\psi_o \dot{\pi}_{1,o} + c\psi_o \pi_{3,o}) \ell_o (\xi_m^o \dot{\xi}_n^o + \zeta_m^o \dot{\zeta}_n^o) + (\tfrac{1}{2} B_{mn,10} (s\psi_o \dot{\pi}_{1,o} + c\psi_o \dot{\pi}_{3,o}) \ell_o - B_{mn,17} (s\psi_o \pi_{1,o} + c\psi_o \pi_{3,o}) \dot{\ell}_o) (\xi_m^o \xi_n^o + \zeta_m^o \zeta_n^o)] \} \rangle ;$$

$$h_3 = \sum_\rho \sum_o \langle \rho_\rho \ell_\rho [\pi_{1,\rho} \dot{\pi}_{2,\rho} - \pi_{2,\rho} \dot{\pi}_{1,\rho} + (s\phi_\rho \pi_{1,\rho} - c\phi_\rho \pi_{2,\rho}) \dot{\ell}_\rho] + \rho_o \ell_o [\pi_{1,o} \dot{\pi}_{2,o} - \pi_{2,o} \dot{\pi}_{1,o} + c\psi_o (\tfrac{1}{2} \dot{\pi}_{2,o} \ell_o - \pi_{2,o} \dot{\ell}_o)]$$

$$+ \sum_m \{ \rho_\rho \ell_\rho [\ell_\rho (C_{m,1} c\phi_\rho \pi_{1,\rho} + C_{m,1} s\phi_\rho \pi_{2,\rho} + C_{m,4} \ell_\rho) \ddot{\xi}_m^\rho + (- C_{m,1} (c\phi_\rho \dot{\pi}_{1,\rho} + s\phi_\rho \dot{\pi}_{2,\rho}) + C_{m,10} (c\phi_\rho \pi_{1,\rho} + s\phi_\rho \pi_{2,\rho}) \dot{\ell}_\rho + C_{m,12} \ell_\rho \dot{\ell}_\rho) \dot{\xi}_m^\rho] + \rho_o \ell_o [\ell_o (C_{m,1} \pi_{1,o} + c\psi_o C_{m,4} \ell_o) \ddot{\xi}_m^o + (C_{m,10} \pi_{1,o} \dot{\ell}_o + C_{m,12} c\psi_o \ell_o \dot{\ell}_o - C_{m,1} \dot{\pi}_{1,o} \ell_o) \dot{\xi}_m^o$$

$$- C_{m,1}\, s\psi_0\, \pi_{2,0}\, l_0\, \dot{\zeta}^0_m + s\psi_0 \left(C_{m,1}\, \dot{\pi}_{2,0}\, l_0 - C_{m,10}\, \pi_{2,0}\, \dot{l}_0\right) \zeta^0_m \Big] \Big\} + \sum_m \sum_n \Big\{ \rho_\rho l_\rho \Big[- B_{mn,10} \left(s\phi_\rho \pi_{1,\rho} - c\phi_\rho \pi_{2,\rho}\right) l_\rho \left(\xi^\rho_m \dot{\xi}^\rho_n + \zeta^\rho_m \dot{\zeta}^\rho_n\right) + \left(\tfrac{1}{2} B_{mn,10} \left(s\phi_\rho \dot{\pi}_{1,\rho} - c\phi_\rho \dot{\pi}_{2,\rho}\right) l_\rho - B_{mn,17} \left(s\phi_\rho \pi_{1,\rho} - c\phi_\rho \pi_{2,\rho}\right) \dot{l}_\rho\right) \left(\xi^\rho_m \xi^\rho_n + \zeta^\rho_m \zeta^\rho_n\right) \Big] + \rho_0 l_0 \Big[B_{mn,10}\, c\psi_0\, \pi_{2,0}\, l_0 \left(\xi^0_m \dot{\xi}^0_n + \zeta^0_m \dot{\zeta}^0_n\right) + c\psi_0 \left(-\tfrac{1}{2} B_{mn,10}\, \dot{\pi}_{2,0}\, l_0 + B_{mn,17}\, \pi_{2,0} \dot{l}_0\right) \left(\xi^0_m \xi^0_n + \zeta^0_m \zeta^0_n\right) + s\psi_0 l_0 \Big(B_{mn,1}\, l_0 \left(\dot{\xi}^0_m \zeta^0_n - \xi^0_m \dot{\zeta}^0_n\right) - B_{mn,21}\, \dot{l}_0\, \xi^0_m \zeta^0_n \Big) \Big] \Big\} \Big\rangle \,. \tag{III.5}$$

III.3 Local Torque $\{\Gamma\}$

This section is analogous to section III.2. In this case, however, torques acting about the system center of mass as a result of flexibility and deployment are worked out in detail as opposed to momenta.

III.3.1 Appendages with arbitrary orientation, continuous coordinates

As in part III.2.1, the contribution of the i^{th} appendage to $\{\Gamma\}$ is demonstrated for the component along the x axis for the case of arbitrary boom orientation. Resultant Γ_2, Γ_3 terms are analogous.

$$\Gamma_1 = \rho \ell (\pi_2 \ddot{\pi}_3 - \pi_3 \ddot{\pi}_2) + \rho \int_0^\ell \langle [\chi_{23} \pi_2 - \chi_{22} \pi_3) + (\chi_{12} \chi_{23} - \chi_{13} \chi_{22}) x + (\chi_{32} \chi_{23} - \chi_{33} \chi_{22}) w] (v_{tt} + 2U v_{xt} + U^2 v_{xx} + U_t v_x) + [(\chi_{33} \pi_2 - \chi_{32} \pi_3) + (\chi_{12} \chi_{33} - \chi_{13} \chi_{32}) x + (\chi_{22} \chi_{33} - \chi_{23} \chi_{32}) v] (w_{tt} + 2U w_{xt} + U^2 w_{xx} + U_t w_x) + U_t [(\chi_{13} \pi_2 - \chi_{12} \pi_3) + (\chi_{22} \chi_{13} - \chi_{23} \chi_{12}) v + (\chi_{32} \chi_{13} - \chi_{33} \chi_{12}) w] + (\chi_{12} \ddot{\pi}_3 - \chi_{13} \ddot{\pi}_2) x + (\chi_{22} \ddot{\pi}_3 - \chi_{13} \ddot{\pi}_2) v + (\chi_{32} \ddot{\pi}_3 - \chi_{33} \ddot{\pi}_2) w - (\chi_{13} \pi_2 - \chi_{12} \pi_3) [U^2 (v_x v_{xx} + w_x w_{xx} + 2U (v_x v_{xt} + w_x w_{xt})] - (\ell - x) \{ [\ddot{\pi}_3 - \ddot{\pi}_2 + U_t (\chi_{13} - \chi_{12})] [\tfrac{1}{2} (v_x^2 + w_x^2)] + (\chi_{13} \pi_2 - \chi_{12} \pi_3) [v_x v_{xtt} + w_x w_{xtt} + (v_{xt})^2 + (w_{xt})^2 + U_t (v_x v_{xx} + w_x w_{xx})] \} \rangle dx . \quad \text{(III.6)}$$

III.3.2 Assumed mode format for appendages in the x-y, x-z planes

Proceeding as in section III.2.2, the general relative motion torque expressions can be applied to the case of appendages lying in the x-y and x-z planes.

$$
\begin{aligned}
\Gamma_1 = & \sum_{\rho} \sum_{o} < \rho_\rho l_\rho [\pi_{2,\rho} \ddot{\pi}_{3,\rho} - \pi_{3,\rho} \ddot{\pi}_{2,\rho} + s\phi_\rho \\
& (\tfrac{1}{2} \ddot{\pi}_{3,\rho} l_\rho - \pi_{3,\rho} \ddot{l}_\rho)] + \rho_o l_o [\pi_{2,o} \ddot{\pi}_{3,o} \\
& - \pi_{3,o} \ddot{\pi}_{2,o} + s\psi_o (\tfrac{1}{2} \ddot{\pi}_{2,o} l_o - \pi_{2,o} \ddot{l}_o)] \\
& + \sum_{m} \{ \rho_\rho l_\rho [-C_{m,1} c\phi_\rho \pi_{3,\rho} l_\rho \ddot{\xi}_1^\rho + l_\rho \\
& (C_{m,1} \pi_{2,\rho} + C_{m,4} s\phi_\rho l_\rho) \ddot{\zeta}_m^\rho - 2 C_{m,10} c\phi_\rho \pi_{3,\rho} \\
& \dot{l}_\rho \dot{\xi}_m^\rho + 2\dot{l}_\rho (C_{m,10} \pi_{2,\rho} + C_{m,11} s\phi_\rho l_\rho) \dot{\zeta}_m^\rho \\
& + c\phi_\rho (C_{m,1} \ddot{\pi}_{3,\rho} l_\rho - \pi_{3,\rho} (C_{m,10} \ddot{l}_\rho - C_{m,13} \\
& \dot{l}_\rho^2 / l_\rho)) \xi_m^\rho + (-C_{m,1} (\ddot{\pi}_{2,\rho} + s\phi_\rho \ddot{l}_\rho) l_\rho \\
& + \pi_{2,\rho} (C_{m,10} \ddot{l}_\rho - C_{m,13} \dot{l}_\rho^2 / l_\rho) + s\phi_\rho \\
& (C_{m,11} l_\rho \ddot{l}_\rho + C_{m,14} \dot{l}_\rho^2)) \zeta_m^\rho] \\
& + \rho_o l_o [(C_{m,4} s\psi_o l_o - C_{m,1} \pi_{3,o}) l_o \ddot{\xi}_m^o \\
& + 2 (-C_{m,10} \pi_{3,o} + C_{m,11} s\psi_o l_o) \dot{l}_o \dot{\xi}_m^o + (C_{m,1}
\end{aligned}
$$

$$\ddot{\pi}_{3,0} l_0 + (-C_{m,13}\pi_{3,0} + s\psi_0 C_{m,14} l_0)(\dot{l}_0^2/l_0) + (-C_{m,10}\pi_{3,0} + s\psi_0 C_{m,12} l_0)\ddot{l}_0)\xi_m^0 + c\psi_0 (C_{m,1}\pi_{2,0} l_0 \dot{\zeta}_m^0 + 2C_{m,10}\pi_{2,0}\dot{l}_0\dot{\xi}_m^0 + (C_{m,13}\pi_{2,0}\dot{l}_0^2/l_0 + C_{m,10}\pi_{2,0}\ddot{l}_0 - C_{m,1}\ddot{\pi}_{2,0} l_0)\zeta_m^0]\}$$

$$+ \sum_m \sum_n \{\rho_\rho l_\rho [B_{mn,10} s\phi_\rho \pi_{3,\rho} l_\rho (\ddot{\xi}_m^\rho \xi_n^\rho + \ddot{\zeta}_m^\rho \zeta_n^\rho + \dot{\xi}_m^\rho \dot{\xi}_n^\rho + \dot{\zeta}_m^\rho \dot{\zeta}_n^\rho) + s\phi_\rho \pi_{3,\rho}\dot{l}_\rho (B_{mn,23}(\dot{\xi}_m^\rho \xi_n^\rho + \dot{\zeta}_m^\rho \zeta_n) - B_{nm,12}(\xi_m^\rho \dot{\xi}_n^\rho + \zeta_m^\rho \dot{\zeta}_n^\rho)) + (\tfrac{1}{2} B_{mn,10}(\ddot{\pi}_{2,\rho} - \ddot{\pi}_{3,\rho} + s\phi_\rho \ddot{l}_\rho)\dot{l}_\rho + s\phi_\rho \pi_{3,\rho}(B_{mn,18}\ddot{l}_\rho + B_{mn,26}\dot{l}_\rho^2/l_\rho))(\xi_m^\rho \xi_n^\rho + \zeta_m^\rho \zeta_n^\rho) - B_{mn,1} c\phi_\rho l_\rho^2 (\ddot{\xi}_m^\rho \zeta_n^\rho + \xi_m^\rho \ddot{\zeta}_n^\rho) - 2c\phi_\rho l_\rho \dot{l}_\rho (B_{mn,19}\dot{\xi}_m^\rho \zeta_n^\rho - B_{mn,20}\xi_m^\rho \dot{\zeta}_n^\rho) + c\phi_\rho (B_{mn,21} l_\rho \ddot{l}_\rho + B_{mn,22}\dot{l}_\rho^2)\xi_m^\rho \zeta_n^\rho]$$

$$+ \rho_0 l_0 [B_{mn,10} s\psi_0 \pi_{2,0} l_0 (\ddot{\xi}_m^0 \xi_n^0 + \ddot{\zeta}_m^0 \zeta_n^0 + \dot{\xi}_m^0 \dot{\xi}_n^0 + \dot{\zeta}_m^0 \dot{\zeta}_n^0) + B_{mn,23} s\psi_0 \pi_{2,0}$$

$$\dot{l}_o\,(\xi^o_m\,\xi^o_n + \zeta^o_m\,\zeta^o_n) - B_{nm,12}\,s\psi_o\,\pi_{2,o}$$

$$\dot{l}_o\,(\xi^o_m\,\dot{\xi}^o_n + \zeta^o_m\,\dot{\zeta}^o_n) + (-\tfrac{1}{2}\,B_{mn,10}\,(\ddot{\pi}_{3,o}$$

$$- \ddot{\pi}_{2,o} - s\psi_o\,\ddot{l}_o)\,l_o + s\psi_o\,\pi_{2,o}\,(B_{mn,26}\,\dot{l}_o^2/l_o$$

$$+ B_{mn,18}\,\ddot{l}_o))\,(\xi^o_m\,\xi^o_n + \zeta^o_m\,\zeta^o_n) + B_{mn,1}\,c\psi_o$$

$$l_o^2\,(\xi^o_m\,\ddot{\zeta}^o_n - \ddot{\xi}^o_m\,\zeta^o_n) - 2\,B_{mn,19}\,c\psi_o\,l_o\,\dot{l}_o$$

$$\dot{\xi}^o_m\,\zeta^o_n + 2\,B_{mn,20}\,c\psi_o\,l_o\,\dot{l}_o\,\xi^o_m\,\dot{\zeta}^o_n + c\psi_o$$

$$(B_{mn,22}\,\dot{l}^2 + B_{mn,21}\,l\,\ddot{l})\,\xi^o_m\,\zeta^o_n\,]\,\}\,\rangle\,;$$

$$\Gamma_2 = \sum_\rho \sum_o \langle \rho_\rho\,l_\rho\,[\,\pi_{3,\rho}\,\ddot{\pi}_{1,\rho} - \pi_{1,\rho}\,\ddot{\pi}_{3,\rho} - c\phi_\rho$$

$$(\tfrac{1}{2}\,\ddot{\pi}_{3,\rho}\,l_\rho - \pi_{3,\rho}\,\ddot{l}_\rho)\,] + \rho_o\,l_o\,[\,\pi_{3,o}\,\ddot{\pi}_{1,o} - \pi_{1,o}$$

$$\ddot{\pi}_{3,o} - \tfrac{1}{2}\,(c\psi_o\,\ddot{\pi}_{3,o} + s\psi_o\,\ddot{\pi}_{1,o})\,l_o + (c\psi_o\,\pi_{3,o}$$

$$+ s\psi_o\,\pi_{1,o})\,\ddot{l}_o\,] + \sum_m \{\,\rho_\rho\,l_\rho\,[-C_{m,1}\,s\phi_\rho$$

$$\pi_{3,\rho}\,l_\rho\,\ddot{\xi}^\rho_m - l_\rho\,(C_{m,1}\,\pi_{1,\rho} + C_{m,4}\,c\phi_\rho\,l_\rho)\,\ddot{\zeta}^\rho_m$$

$$- 2C_{m,10}\,\pi_{3,\rho}\,\dot{l}_\rho\,\dot{\xi}^\rho_m - 2\,(C_{m,10}\,\pi_{1,\rho} + C_{m,11}$$

$$c\phi_\rho\,l_\rho)\,\dot{l}_\rho\,\dot{\zeta}^\rho_m - s\phi_\rho\,(C_{m,1}\,\ddot{\pi}_{3,\rho}\,l_\rho + \pi_{3,\rho}$$

$$(C_{m,10}\,\ddot{l}_\rho + C_{m,13}\,\dot{l}_\rho))\,\xi^\rho_m + (C_{m,1}\,(\ddot{\pi}_{1,\rho}$$

$$+ c\phi_\rho \ddot{l}_\rho) l_\rho - (\pi_{1,\rho} + c\phi_\rho l_\rho) (C_{m,10} \ddot{l}_\rho + C_{m,13} \dot{l}_\rho^2 / l_\rho)) \zeta_m^\rho] + \rho_o l_o [C_{m,1} (s\psi_o \pi_{3,o} - c\psi_o \pi_{1,o}) - C_{m,4} l_o) l_o \ddot{\xi}_m^o + (2 C_{m,10} (s\psi_o \pi_{3,o} - c\psi_o \pi_{1,o}) - C_{m,11} l_o) \dot{l}_o \dot{\xi}_m^o + ((s\psi_o \pi_{3,o} - c\psi_o \pi_{1,o}) (C_{m,10} l_o \ddot{l}_o + C_{m,13} \dot{l}^2 / l_o) - C_{m,12} l_o \ddot{l}_o - C_{m,14} \dot{l}_o^2 + C_{m,1} (c\psi_o \ddot{\pi}_{1,o} - s\psi_o \ddot{\pi}_{3,o}) l_o) \zeta_m^o] \}$$

$$+ \sum_m \sum_n \{ \rho_\rho l_\rho [B_{mn,10} c\phi_\rho \pi_{2,\rho} l_\rho (\ddot{\xi}_m^\rho \xi_n^\rho + \ddot{\zeta}_m^\rho \zeta_n^\rho + \dot{\xi}_m^\rho \dot{\xi}_n^\rho + \dot{\zeta}_m^\rho \dot{\zeta}_n^\rho) - c\phi_\rho \pi_{2,\rho} \dot{l}_\rho ((B_{mn,12} + 2 B_{nm,12}) (\dot{\xi}_m^\rho \xi_n^\rho + \dot{\zeta}_m^\rho \zeta_n^\rho) + B_{nm,12} (\xi_m^\rho \dot{\xi}_n^\rho + \zeta_m^\rho \dot{\zeta}_n^\rho)) + (-\tfrac{1}{2} B_{mn,10} l_\rho (\ddot{\pi}_{1,\rho} - \ddot{\pi}_{3,\rho} + c\phi_\rho l_\rho) + c\phi_\rho \pi_{2,\rho} (B_{mn,18} \ddot{l}_\rho + B_{mn,25} \dot{l}_\rho^2 / l_\rho)) (\xi_m^\rho \xi_n^\rho + \zeta_m^\rho \zeta_n^\rho) - B_{mn,1} s\phi_\rho l_\rho^2 (\ddot{\xi}_m^\rho \zeta_n^\rho + \xi_m^\rho \ddot{\zeta}_n^\rho) - 2 s\phi_\rho l_\rho \dot{l}_\rho (B_{mn,19} \dot{\xi}_m^\rho \zeta_n^\rho - B_{mn,20} \xi_m^\rho \dot{\zeta}_n^\rho) + s\phi_\rho (B_{mn,21} l_\rho \ddot{l}_\rho + B_{mn,22} \dot{l}_\rho^2) \xi_m^\rho \zeta_n^\rho]$$

$$+ \rho_o l_o \left[- B_{mn,10} \left(c\psi_o \pi_{3,o} + s\psi_o \pi_{1,o} \right) \dot{l}_o \right.$$

$$\left(\ddot{\xi}^o_m \xi^o_n + \ddot{\zeta}^o_m \zeta^o_n + \dot{\xi}^o_m \dot{\xi}^o_n + \dot{\zeta}^o_m \zeta^o_n \right)$$

$$- \left(c\psi_o \pi_{3,o} + s\psi_o \pi_{1,o} \right) \dot{l}_o \left(B_{mn,23} \left(\dot{\xi}^o_m \xi^o_n \right. \right.$$

$$\left. + \dot{\zeta}^o_m \zeta^o_n \right) - B_{nm,12} \left(\xi_m \dot{\xi}_n + \zeta_m \dot{\zeta}_n \right) \Big)$$

$$- \left(\tfrac{1}{2} B_{mn,10} \left(\ddot{\pi}_{1,o} - \ddot{\pi}_{3,o} + s\psi_o l_o + c\psi_o \ddot{l}_o \right) l_o \right.$$

$$+ \left(c\psi_o \pi_{3,o} + s\psi_o \pi_{1,o} \right) \left(B_{mn,26} \dot{l}_o^2 / l_o + B_{mn,18} \right.$$

$$\left. \left. \ddot{l}_o \right) \right) \left(\xi_m \xi_n + \zeta_m \zeta_n \right) \Big] \Big\} \Big\rangle \; ;$$

$$\Gamma_3 = \sum_m \sum_n \Big\langle \rho_\rho l_\rho \left[\pi_{1,\rho} \ddot{\pi}_{2,\rho} - \pi_{2,\rho} \ddot{\pi}_{1,\rho} - \tfrac{1}{2} \left(s\phi_\rho \right. \right.$$

$$\left. \ddot{\pi}_{1,\rho} - c\phi_\rho \ddot{\pi}_{2,\rho} \right) l_\rho + \left(s\phi_\rho \pi_{1,\rho} - c\phi_\rho \pi_{2,\rho} \right) \ddot{l}_\rho \Big]$$

$$+ \rho_o l_o \left[\pi_{1,o} \ddot{\pi}_{2,o} - \pi_{2,o} \ddot{\pi}_{1,o} + c\psi_o \left(\tfrac{1}{2} \ddot{\pi}_{2,o} l_o \right. \right.$$

$$\left. \left. - \pi_{2,o} \ddot{l}_o \right) \right] + \sum_m \Big\{ \rho_\rho l_\rho \Big[C_{m,1} \left(c\phi_\rho \pi_{1,\rho} \right.$$

$$\left. + s\phi_\rho \pi_{2,\rho} \right) + C_{m,4} l_\rho \Big) l_\rho \ddot{\xi}^\rho_m + 2 \dot{l}_\rho$$

$$\left(C_{m,10} \left(c\phi_\rho \pi_{1,\rho} + s\phi_\rho \pi_{2,\rho} \right) + C_{m,11} l_\rho \right) \dot{\xi}^\rho_m$$

$$+ \Big(- C_{m,1} l_\rho \left(c\phi_\rho \ddot{\pi}_{1,\rho} + s\phi_\rho \ddot{\pi}_{2,\rho} + \ddot{l}_\rho \right) + C_{m,11}$$

$$l_\rho \ddot{l}_\rho + C_{m,14} \dot{l}_\rho^2 + \left(c\phi_\rho \pi_{1,\rho} + s\phi_\rho \pi_{2,\rho} \right)$$

$$(C_{m,10}\ddot{l}_\rho + C_{m,13}\dot{l}_\rho^2/l_\rho))\xi_m^\rho] + \rho_o l_o$$

$$[(C_{m,1}\pi_{1,o} + c\psi_o C_{m,4} l_o) l_o \ddot{\xi}_m^o + 2(C_{m,10}$$

$$\pi_{1,o} + C_{m,11} c\psi_o l_o)\dot{l}_o \dot{\xi}_m^o + (-C_{m,1}\ddot{\pi}_{1,o}$$

$$l_o + (C_{m,10}\pi_{1,o} + C_{m,12} c\psi_o l_o)\ddot{l}_o + (C_{m,13}$$

$$\pi_{1,o} + C_{m,14} c\psi_o l_o)(\dot{l}_o^2/l_o)\xi_m^o - s\psi_o$$

$$(C_{m,1}\pi_{2,o} l_o \ddot{\zeta}_m^o + 2C_{m,10}\pi_{2,o}\dot{l}_o\dot{\zeta}_m^o + (C_{m,10}$$

$$\pi_{2,o}\ddot{l}_o + C_{m,13}\pi_{2,o}\dot{l}_o^2/l_o - C_{m,1}\ddot{\pi}_{2,o} l_o))\zeta_m^o]\}$$

$$+ \sum_m \sum_n \{\rho_\rho l_\rho [-B_{mn,10}(s\phi_\rho \pi_{1,\rho} - c\phi_\rho \pi_{2,\rho}) l_\rho$$

$$(\ddot{\xi}_m^\rho \xi_n^\rho + \ddot{\zeta}_m^\rho \zeta_n^\rho + \dot{\xi}_m^\rho \dot{\xi}_n^\rho + \dot{\zeta}_m^\rho \zeta_n^\rho) - (s\phi_\rho$$

$$\pi_{1,\rho} - c\phi_\rho \pi_{2,\rho})\dot{l}_\rho (B_{mn,23}(\dot{\xi}_m^\rho \xi_n^\rho + \dot{\zeta}_m^\rho \zeta_n^\rho)$$

$$- B_{nm,12}(\xi_m^\rho \dot{\xi}_n^\rho + \zeta_m^\rho \dot{\zeta}_n^\rho)) + (\tfrac{1}{2} B_{mn,10}$$

$$(\ddot{\pi}_{2,\rho} - \ddot{\pi}_{1,\rho} + s\phi_\rho \ddot{l}_\rho - c\phi_\rho \ddot{l}_\rho) l_\rho - (s\phi_\rho \pi_{1,\rho}$$

$$- c\phi_\rho \pi_{2,\rho}(B_{mn,18}\ddot{l}_\rho + B_{mn,26}\dot{l}_\rho^2/l_\rho))$$

$$(\xi_m^\rho \xi_n^\rho + \zeta_m^\rho \zeta_n^\rho)] + \rho_o l_o [B_{mn,10} c\psi_o$$

$$\pi_{2,o} l_o (\ddot{\xi}_m^o \xi_n^o + \ddot{\zeta}_m^o \zeta_n^o + \dot{\xi}_m^o \dot{\xi}_n^o + \dot{\zeta}_m^o \zeta_n^o)$$

$$+ c\psi_0 \pi_{2,0} \dot{l}_0 \left(B_{mn,23} \left(\dot{\xi}^0_m \xi^0_n + \dot{\zeta}^0_m \zeta^0_n \right) \right.$$

$$\left. - B_{nm,12} \left(\xi^0_m \dot{\xi}^0_n + \zeta^0_m \dot{\zeta}^0_n \right) \right) + \left(-\tfrac{1}{2} B_{mn,10} \right.$$

$$\left(\ddot{\pi}_{2,0} - \ddot{\pi}_{1,0} - c\psi_0 \ddot{l}_0 \right) l_0 + c\psi_0 \pi_{2,0}$$

$$\left. \left(B_{mn,26} \dot{l}_0^2 / l_0 + B_{mn,18} \ddot{l}_0 \right) \right) \left(\xi^0_m \xi^0_n \right.$$

$$\left. + \zeta^0_m \zeta^0_n \right) + B_{mn,1} s\psi_0 l_0^2 \left(\dddot{\xi}^0_m \zeta^0_n - \xi^0_m \dddot{\zeta}^0_n \right)$$

$$+ 2 s\psi_0 l_0 \dot{l}_0 \left(B_{mn,19} \ddot{\xi}^0_m \zeta^0_n - B_{mn,20} \xi^0_m \ddot{\zeta}^0_n \right)$$

$$\left. - s\psi_0 \left(B_{mn,21} l_0 \ddot{l}_0 + B_{mn,22} \dot{l}_0^2 \right) \xi^0_m \zeta^0_n \right] \Big\rangle .$$

(III.7)

APPENDIX IV

A USEFUL INTEGRAL THEOREM

THEOREM:

$$\int_0^{\ell} g(x)\left[\int_0^{x} f(\alpha)\,d\alpha\right]dx = \int_0^{\ell} f(x)\left[\int_x^{\ell} g(\alpha)\,d\alpha\right]dx . \tag{IV.1}$$

Proof:

For the purposes of this derivation consider u, v as arbitrary functions. Integrating by parts

$$\int_a^b u\,dv = uv\Big|_a^b - \int_a^b v\,du \quad . \tag{IV.2}$$

Consider:

$$u(x) = \int_0^x f(x)\,d\alpha \longrightarrow du = \frac{du}{dx}\,dx = f(x)\,dx \;;$$

$$v(x) = -\int_x^{\ell} g(\alpha)\,d\alpha \longrightarrow dv = g(x)\,dx \quad .$$

Then:

$$\int_0^{\ell} g(x)\left[\int_0^{x} f(\alpha)\,d\alpha\right]dx = -\int_0^{x} f(\alpha)\,d\alpha \int_x^{\ell} g(\alpha)\,d\alpha\Big|_{x=0}^{\ell}$$

$$+ \int_0^{\ell}\left(\int_x^{\ell} g(\alpha)\,d\alpha\right) f(x)\,dx \;;$$

$$= -\int_0^{\ell} f(\alpha)\,d\alpha \int_{\ell}^{\ell} g(\alpha)\,d\alpha + \int_0^{0} f(\alpha)\,d\alpha \cdot \int_0^{\ell} g(\alpha)\,d\alpha + \int_0^{\ell} f(x)\left[\int_x^{\ell} g(\alpha)\,d\alpha\right] dx \,. \tag{IV.3}$$

Q.E.D.

Discussion

When foreshortening is introduced explicitly as an additional axial displacement it remains as an integral function in the system kinetic energy for example. This theorem provides a method for transforming these terms into an effective axial load in the final equations of motion for beams with varying sectional properties.

APPENDIX V

APPLICATION OF HAMILTON'S PRINCIPLE TO A DEPLOYING CONTINUUM

The general form of Hamilton's Principle can be written (Meirovitch, 1970):[67]

$$\delta \int_{t_1}^{t_2} (\mathcal{L} + \mathcal{W}^{\circ}) \, dt = 0; \qquad \text{(V.1)}$$

where:

$\mathcal{L}$ = Lagrangian, which includes the potential energy of conservative forces;

$\mathcal{W}^{\circ}$ = generalized work function which can include nonconservative force contributions.

Note, for a given appendage spanning a region D,

$$\mathcal{L} = T - V = \int_D (\tilde{T} - \tilde{V}) \, dD = \int_D \tilde{\mathcal{L}} \, dD. \qquad \text{(V.2)}$$

For the case of a deploying beam-type appendage in the presence of a gravitational field, the Lagrange density function assumes the form of equation (3.20) when taken to 3rd degree:

$$\tilde{\mathcal{L}} = \tilde{\mathcal{L}}(x, \epsilon, \epsilon_x, \epsilon_{xx}, \epsilon_{xt}, \epsilon_t, t). \qquad \text{(V.3)}$$

Carrying out the variation on this functional as implied by equation (V.1):

$$\delta \int_{t_1}^{t_2} (\mathcal{L} + \mathcal{W}) dt$$

$$= \int_{t_1}^{t_2} \left[\int_{\mathcal{D}} \left(\frac{\partial \tilde{\mathcal{L}}}{\partial \epsilon} \delta\epsilon + \frac{\partial \tilde{\mathcal{L}}}{\partial \epsilon_x} \delta\epsilon_x + \frac{\partial \tilde{\mathcal{L}}}{\partial \epsilon_{xx}} \delta\epsilon_{xx} \right.\right.$$

$$\left.\left. + \frac{\partial \tilde{\mathcal{L}}}{\partial \epsilon_{xt}} \delta\epsilon_{xt} + \frac{\partial \tilde{\mathcal{L}}}{\partial \epsilon_t} \delta\epsilon_t + \delta \mathcal{W}) d\mathcal{D} \right] dt ; \qquad \text{(V.4)}$$

where:

$\delta \mathcal{W} = \mathcal{F}_\epsilon \delta\epsilon$;

$\delta \mathcal{D}$ = 0 for a continuum since $\mathcal{D} = \mathcal{D}(\underline{r}_i, t)$ only (Thus agreeing with the conclusion of Tabarrok et al. 1974).[222]

The system is taken to be deploying along the local x direction only, with velocity $U(x,t)$, so that:

$\frac{d(\,)}{dt}$ = total time derivative relative to the local appendage coordinates;

$$= \frac{\partial(\,)}{\partial t} + U \frac{\partial(\,)}{\partial x} . \qquad \text{(V.5)}$$

With this in mind the many terms of equation (V.4) can be evaluated by freely making use of integration by parts.

$$\int_{t_1}^{t_2} \left(\int_0^{\ell} \frac{\partial \tilde{\mathcal{L}}}{\partial \epsilon_x} \, \delta\epsilon_x \, dx \right) dt$$

$$= \int_{t_1}^{t_2} \left\{ \frac{\partial \tilde{\mathcal{L}}}{\partial \epsilon_x} \, \delta\epsilon \Big|_0^{\ell} - \int_0^{\ell} \left[\frac{\partial}{\partial x} \left(\frac{\partial \tilde{\mathcal{L}}}{\partial \epsilon_x} \right) \delta\epsilon \right] dx \right\} dt ;$$

(V.6a)

$$\int_{t_1}^{t_2} \left(\int_0^{\ell} \frac{\partial \tilde{\mathcal{L}}}{\partial \epsilon_{xx}} \, \delta\epsilon_{xx} \, dx \right) dt$$

$$= \int_{t_1}^{t_2} \left\{ \left[\frac{\partial \tilde{\mathcal{L}}}{\partial \epsilon_{xx}} \, \delta\epsilon_x - \frac{\partial}{\partial x} \left(\frac{\partial \tilde{\mathcal{L}}}{\partial \epsilon_{xx}} \right) \delta\epsilon \right]_0^{\ell} + \int_0^{\ell} \left[\frac{\partial^2}{\partial x^2} \left(\frac{\partial \tilde{\mathcal{L}}}{\partial \epsilon_{xx}} \right) \right] \delta\epsilon \, dx \right\} dt ;$$

(V.6b)

$$\int_{t_1}^{t_2} \left\{ \int_0^{\ell} \left[\frac{d}{dt} \left(\frac{\partial \tilde{\mathcal{L}}}{\partial \epsilon_t} \, \delta\epsilon \right) \right] dx \right\} dt$$

$$= \int_{t_1}^{t_2} \left\{ \int_0^{\ell} \left[\frac{\partial}{\partial t} \left(\frac{\partial \tilde{\mathcal{L}}}{\partial \epsilon_t} \cdot \delta\epsilon \right) + U \frac{\partial}{\partial x} \left(\frac{\partial \tilde{\mathcal{L}}}{\partial \epsilon_t} \, \delta\epsilon \right) \right] dx \right\} dt ;$$

$$= \int_{t_1}^{t_2} \left\{ \int_0^{\ell} \left[\frac{\partial}{\partial t} \left(\frac{\partial \tilde{\mathcal{L}}}{\partial \epsilon_t} \right) \right] \delta\epsilon \, dx + \int_0^{\ell} \left(\frac{\partial \tilde{\mathcal{L}}}{\partial \epsilon_t} \, \delta\epsilon_t \right) dx \right.$$

$$+ \; U \frac{\partial \tilde{\mathcal{L}}}{\partial \epsilon_t} \delta\epsilon \Big|_0^{\ell} - \int_0^{\ell} \left[\frac{\partial \tilde{\mathcal{L}}}{\partial \epsilon_t} \left(\delta\epsilon \frac{\partial U}{\partial x} \right) \right] dx \Big\} dt . \qquad \text{(V.6c)}$$

But:

$$\int_{t_1}^{t_2} \Big\{ \int_0^{\ell} \left[\frac{d}{dt} \left(\frac{\partial \tilde{\mathcal{L}}}{\partial \epsilon_t} \delta\epsilon \right) \right] dx \Big\} dt$$

$$= \int_0^{\ell} \Big\{ \int_{t_1}^{t_2} \left[\frac{d}{dt} \left(\frac{\partial \tilde{\mathcal{L}}}{\partial \epsilon_t} \delta\epsilon \right) \right] dt \Big\} dx ;$$

$$= \int_0^{\ell} \left(\frac{\partial \tilde{\mathcal{L}}}{\partial \epsilon_t} \delta\epsilon \Big|_{t_1}^{t_2} \right) dx = 0.$$

Therefore:

$$\int_{t_1}^{t_2} \left[\int_0^{\ell} \left(\frac{\partial \tilde{\mathcal{L}}}{\partial \epsilon_t} \delta\epsilon_t \right) dx \right] dt$$

$$= \int_{t_1}^{t_2} \Big\{ - U \frac{\partial \tilde{\mathcal{L}}}{\partial \epsilon_t} \delta\epsilon \Big|_0^{\ell}$$

$$+ \int_0^{\ell} \left[- \frac{\partial}{\partial t} \left(\frac{\partial \tilde{\mathcal{L}}}{\partial \epsilon_t} \right) + U_x \frac{\partial \tilde{\mathcal{L}}}{\partial \epsilon_t} \right] \delta\epsilon \, dx \Big\} dt ; \qquad \text{(V.7a)}$$

Similarly, it can be shown that:

$$\int_{t_1}^{t_2} \left\{ \int_0^{\ell} \left[\left(\frac{\partial \tilde{\mathcal{L}}}{\partial \epsilon_{xt}} \right) \delta \epsilon_{xt} \right] dx \right\} dt$$

$$= \int_{t_1}^{t_2} \left\{ \left[\frac{\partial}{\partial t} \left(\frac{\partial \tilde{\mathcal{L}}}{\partial \epsilon_{xt}} \right) - U_x \frac{\partial \tilde{\mathcal{L}}}{\partial \epsilon_{xt}} \right] \delta \epsilon \Big|_0^{\ell} \right.$$

$$- U \frac{\partial \tilde{\mathcal{L}}}{\partial \epsilon_{xt}} \delta \epsilon_x \Big|_0^{\ell}$$

$$\left. + \int_0^{\ell} \left[\frac{\partial^2}{\partial x \partial t} \left(\frac{\partial \tilde{\mathcal{L}}}{\partial \epsilon_{xt}} \right) - \frac{\partial}{\partial x} \left(U_x \frac{\partial \tilde{\mathcal{L}}}{\partial \epsilon_{xt}} \right) \right] \delta \epsilon \, dx \right\} dt. \qquad \text{(V.7b)}$$

Substituting equations (V.6) and (V.7) into (V.4), it is seen that a stationary value of the Hamilton functional demands that:

$$\frac{\partial}{\partial t} \left[\frac{\partial \tilde{\mathcal{L}}}{\partial \epsilon_t} - \frac{\partial}{\partial \epsilon_x} \left(\frac{\partial \tilde{\mathcal{L}}}{\partial \epsilon_{xt}} \right) \right] + \frac{\partial}{\partial x} \left(U_x \frac{\partial \tilde{\mathcal{L}}}{\partial \epsilon_{xt}} \right)$$

$$- U_x \frac{\partial \tilde{\mathcal{L}}}{\partial \epsilon_t} - \frac{\partial \tilde{\mathcal{L}}}{\partial \epsilon} + \frac{\partial}{\partial x} \left(\frac{\partial \tilde{\mathcal{L}}}{\partial \epsilon_x} \right) - \frac{\partial^2}{\partial x^2} \left(\frac{\partial \tilde{\mathcal{L}}}{\partial \epsilon_{xx}} \right)$$

$$= \mathcal{F}_{\epsilon} \; ; \qquad \text{(V.8a)}$$

and,

$$\left[\frac{\partial\tilde{\mathcal{L}}}{\partial\epsilon_x} - \frac{\partial}{\partial x}\left(\frac{\partial\tilde{\mathcal{L}}}{\partial\epsilon_{xx}}\right) - U\frac{\partial\tilde{\mathcal{L}}}{\partial\epsilon_t} - \frac{\partial}{\partial t}\left(\frac{\partial\tilde{\mathcal{L}}}{\partial\epsilon_{xt}}\right) + U_x\frac{\partial\tilde{\mathcal{L}}}{\partial\epsilon_{xt}}\right]\delta\epsilon = 0,$$

$$\left(\frac{\partial\tilde{\mathcal{L}}}{\partial\epsilon_{xx}} - U\frac{\partial\tilde{\mathcal{L}}}{\partial\epsilon_{xt}}\right)\delta\epsilon_x = 0,$$

at $x = 0, \ell.$ (V.8b)

(V.8a) represent the governing equations of motion defined in terms of the Lagrange density;

(V.8b) represent a complete set of boundary conditions, geometric and dynamic.

APPENDIX VI

MODAL INTEGRAL COEFFICIENTS

Defined here are a series of integrals associated with a chosen shape function $g_n(\hat{x})$. These integrals appear as coefficients in the solution of the governing equations of libration and vibration. In general, g_n can be any assumed function, such as a Galerkin polynomial [Jankovic (1980)[220]].

Modal Integral Coefficients $C_{n,j}$

$$C_{n,1} = \int_0^1 g_n \, d\hat{x} \quad ;$$

$$C_{n,2} = \int_0^1 g_n \hat{x} \, d\hat{x} \quad ;$$

$$C_{n,3} = \int_0^1 g_{n,\hat{x}\hat{x}} \, d\hat{x} \quad ;$$

$$C_{n,4} = \int_0^1 \hat{x} \, g_n \, d\hat{x} \quad ;$$

$$C_{n,5} = \int_0^1 \hat{x} \, g_{n,\hat{x}} \, d\hat{x} \quad ;$$

$$C_{n,6} = \int_0^1 \hat{x}^2 \, g_{n,\hat{x}} \, d\hat{x} \quad ;$$

$$C_{n,7} = \int_0^1 \hat{x} \, g_{n,\hat{x}\hat{x}} \, d\hat{x} \quad ;$$

$$C_{n,8} = \int_0^1 \hat{x}^2 g_{n,\hat{x}\hat{x}}\, d\hat{x} \quad ;$$

$$C_{n,9} = \int_0^1 \hat{x}^3 g_{n,\hat{x}\hat{x}}\, d\hat{x} \quad ;$$

$$C_{n,10} = C_{n,1} + C_{n,2} - C_{n,5} \quad ;$$

$$C_{n,11} = C_{n,4} + C_{n,5} - C_{n,6} \quad ;$$

$$C_{n,12} = C_{n,4} + C_{n,5} - C_{n,6} - C_{n,1} = C_{n,11} - C_{n,1} \quad ;$$

$$C_{n,13} = C_{n,3} - 2C_{n,7} + C_{n,8} \quad ;$$

$$C_{n,14} = C_{n,7} - 2C_{n,8} + C_{n,9} \quad . \qquad \text{(VI.1)}$$

Modal Integral Coefficients $B_{mn,j}$

$$B_{mn,0} = \int_0^1 g_m g_{n,\hat{x}\hat{x}\hat{x}\hat{x}}\, d\hat{x} \quad ;$$

$$B_{mn,1} = \int_0^1 g_m g_n\, d\hat{x} \quad ;$$

$$B_{mn,2} = \int_0^1 g_m g_{n,\hat{x}}\, d\hat{x} \quad ;$$

$$B_{mn,3} = \int_0^1 g_{m,\hat{x}} g_{n,\hat{x}}\, d\hat{x} \quad ;$$

$$B_{mn,4} = \int_0^1 g_{m,\hat{x}\hat{x}}\, g_n \, d\hat{x} \quad ;$$

$$B_{mn,5} = \int_0^1 g_{m,\hat{x}\hat{x}}\, g_{n,\hat{x}} \, d\hat{x} \quad ;$$

$$B_{mn,6} = \int_0^1 g_m\, \hat{x}\, g_{n,\hat{x}} \, d\hat{x} \quad ;$$

$$B_{mn,7} = \int_0^1 g_{m,\hat{x}\hat{x}}\, \hat{x}\, g_n \, d\hat{x} \quad ;$$

$$B_{mn,8} = \int_0^1 g_{m,\hat{x}\hat{x}}\, \hat{x}\, g_{n,\hat{x}} \, d\hat{x} \quad ;$$

$$B_{mn,9} = \int_0^1 g_{m,\hat{x}\hat{x}}\, \hat{x}^2 g_n \, d\hat{x} \quad ;$$

$$B_{mn,10} = \int_0^1 g_{m,\hat{x}}\, (1-\hat{x})\, g_{n,\hat{x}} \, d\hat{x} \quad ;$$

$$B_{mn,11} = \int_0^1 g_{m,\hat{x}}\, (1-\hat{x}^2)\, g_{n,\hat{x}} \, d\hat{x} \quad ;$$

$$B_{mn,12} = \int_0^1 g_{m,\hat{x}}\, (1-\hat{x})\, \hat{x}\, g_{n,\hat{x}\hat{x}} \, d\hat{x} \quad ;$$

$$B_{mn,13} = \int_0^1 g_{m,\hat{x}\hat{x}}\, (1-\hat{x})\, \hat{x}^2 g_{n,\hat{x}\hat{x}} \, d\hat{x} \quad ;$$

$$B_{mn,14} = \int_0^1 g_{m,\hat{x}\hat{x}\hat{x}}\, (1-\hat{x})\, \hat{x}^2 g_{n,\hat{x}} \, d\hat{x} \quad ;$$

$$B_{mn,15} = B_{mn,2} - B_{nm,2} \quad ;$$

$$B_{mn,16} = B_{nm,6} - B_{mn,6} \quad ;$$

$$B_{mn,17} = B_{nm,5} - B_{nm8} - B_{mn,12} \quad ;$$

$$B_{mn,18} = B_{nm,5} - B_{nm8} - B_{nm,12} \quad ;$$

$$B_{mn,19} = B_{mn,1} + B_{nm,2} - B_{nm,6} \quad ;$$

$$B_{mn,20} = B_{mn,1} + B_{mn,2} - B_{mn,6} \quad ;$$

$$B_{mn,21} = B_{mn,15} + B_{mn,16} \quad ;$$

$$B_{mn,22} = -(B_{mn,4} - B_{nm,4} + 2(B_{mn,7} - B_{nm,7}) - (B_{mn,9} - B_{nm,9}) \quad ;$$

$$B_{mn,23} = 2(B_{mn,3} - B_{nm,12} - B_{mn,12} \quad ;$$

$$B_{mn,24} = 2(B_{mn,3} + B_{nm,12}) + B_{mn,12} \quad ;$$

$$B_{mn,25} = 2\,B_{nm,12} + B_{nm,13} + B_{mn,14} \quad ;$$

$$B_{mn,26} = B_{nm,5} - 2B_{mn,8} + 2B_{nm,12} + B_{mn,13} + B_{mn,14} ;$$

$$B_{mn,27} = B_{nm,5} - 2B_{mn,8} - 2B_{nm,12} - 2B_{mn,13} - B_{mn,14} ;$$

$$B_{mn,28} = B_{mn,2} - B_{mn,6} ;$$

$$B_{mn,29} = 2(B_{mn,2} - B_{mn,6} - B_{mn,10}) + B_{mn,11} ;$$

$$B_{mn,30} = B_{mn,1} - B_{nm,6} ;$$

$$B_{mn,31} = B_{mn,20} - B_{mn,10} ;$$

$$B_{mn,32} = B_{mn,30} - B_{mn,10} .$$

(VI.2)

APPENDIX VII

A METHOD FOR ISOLATING SECOND DERIVATIVES OF COMPLEX COUPLED SECOND ORDER SYSTEMS

A common approach adopted when integrating a system of second order equations numerically is to transform them to a system of first order equations. An essential element in the strategy involves expressing the second order derivative of each independent variable in terms of lower order derivatives only. Such a requirement is easily met for uncoupled systems. For more complex fully coupled systems, as represented by the librational and vibrational motions dealt with in this thesis, one is faced with a considerable amount of algebraic manipulation. The effort needed is alleviated somewhat by taking advantage of numerical techniques where appropriate.

VII.1 Analysis

All second order derivatives appearing in the librational equations are to be expressed explicitly in terms of attitude degrees of freedom. To begin with the general result of Chapter 2 can be written:

$$\ddot{q}_k = \alpha_0^{q_k} + \alpha_r^{q_k} + \alpha_{q_\ell}^{q_k}; \qquad \text{(VII.1)}$$

$$q_k = \Psi, \Lambda, \Phi$$

$$\neq q_\ell$$

where:

$\alpha_0^{q_k}$ = terms in the governing equation for q_k lower than second order;

$\alpha_r^{q_k}$ = contribution to the equations q_k due to the combined effect of the relative motion torques;

$\alpha_{q_l}^{q_k}$ = contribution of the second order terms of the q_l degree of freedom to the q_k equation; but not including the $\alpha_r^{q_k}$ effect.

e.g. $q_k = \Psi$:

$$\ddot{\Psi} = \alpha_0^{\Psi} + \alpha_r^{\Psi} + \alpha_{\Lambda}^{\Psi}\ddot{\Lambda} + \alpha_{\Phi}^{\Psi}\ddot{\Phi}.$$

As indicated in Figure VII-1, the relative motion torque effect is ultimately a function of the $\ddot{q}_k$. The various coefficients necessary to describe this relationship quantitatively are developed as follows:

$$\alpha_r^{q_k} = \alpha_r^{q_k}\left[\Gamma_j(\ddot{\xi}_m^i, \ddot{\zeta}_n^i)\right] = \alpha_{r,0}^{q_k} + \alpha_{r,q_l}^{q_k}\ddot{q}_l ; \qquad \text{(VII.2)}$$

where:

$\alpha_{r,0}^{q_k}$ contains all terms having derivatives less than second order;

$\alpha_{r,q_l}^{q_k}$ = contributions of second order terms of the q_l degree of freedom to the $\alpha_r^{q_k}$ effect.

For the attitude equations considered here:

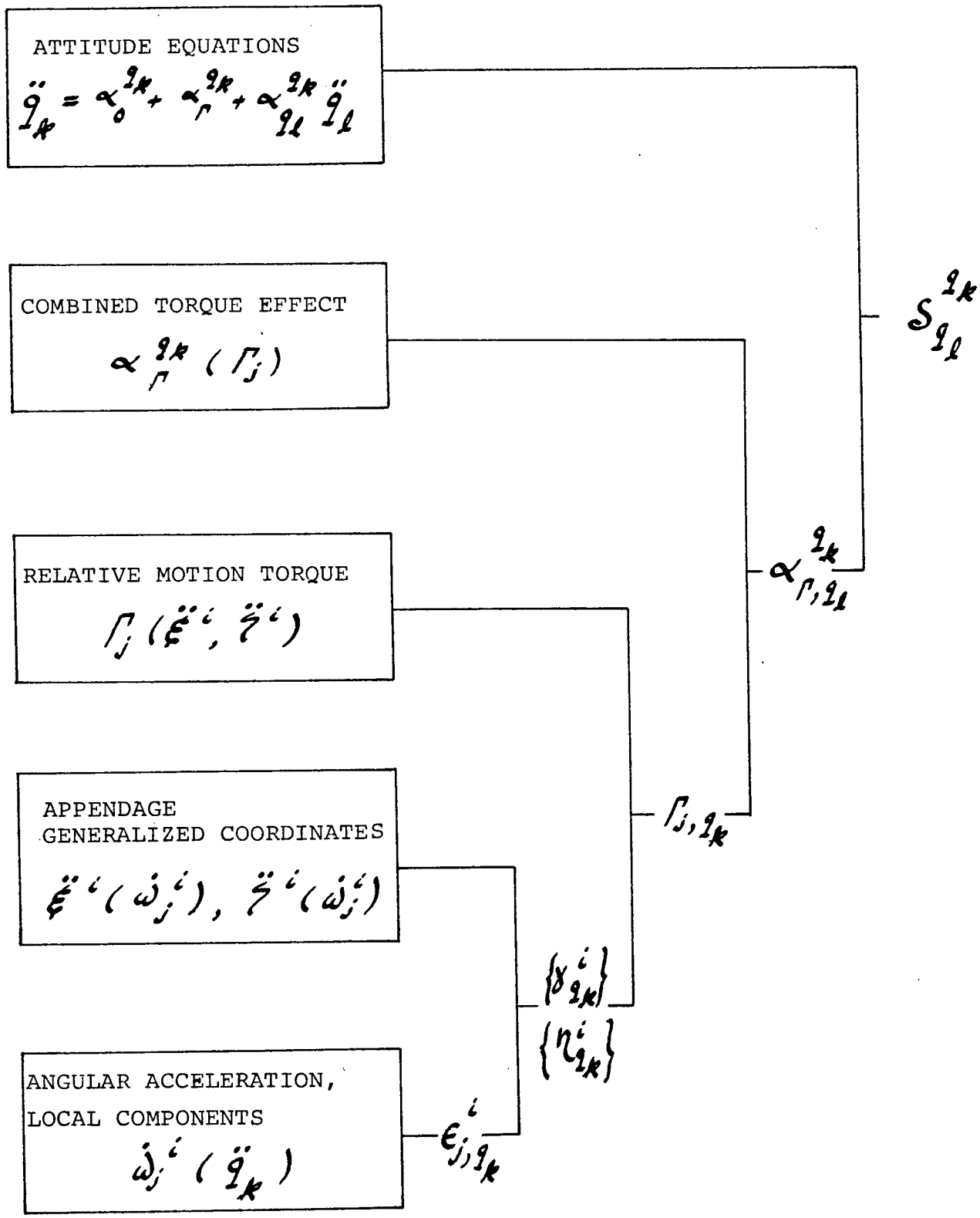

Figure VII-1 Functional dependence of terms used in the description of system equations.

$$\alpha^{\Psi}_{\Gamma,\Psi} = c\Lambda\,(s\Phi\,\Gamma_{1,\Psi} + c\Phi\,\Gamma_{2,\Psi}) - s\Lambda\,\Gamma_{3,\Psi};$$

$$\alpha^{\Psi}_{\Gamma,\Lambda} = c\Lambda\,(s\Phi\,\Gamma_{1,\Lambda} + c\Phi\,\Gamma_{2,\Lambda}) - s\Lambda\,\Gamma_{3,\Lambda};$$

$$\alpha^{\Psi}_{\Gamma,\Phi} = c\Lambda\,(s\Phi\,\Gamma_{1,\Phi} + c\Phi\,\Gamma_{2,\Phi}) - s\Lambda\,\Gamma_{3,\Phi};$$

$$\alpha^{\Lambda}_{\Gamma,\Psi} = c\Phi\,\Gamma_{1,\Psi} - s\Phi\,\Gamma_{2,\Psi};$$

$$\alpha^{\Lambda}_{\Gamma,\Lambda} = c\Phi\,\Gamma_{1,\Lambda} - s\Phi\,\Gamma_{2,\Lambda};$$

$$\alpha^{\Lambda}_{\Gamma,\Phi} = c\Phi\,\Gamma_{1,\Phi} - s\Phi\,\Gamma_{2,\Phi};$$

$$\alpha^{\Phi}_{\Gamma,\Psi} = \Gamma_{3,\Psi};$$

$$\alpha^{\Phi}_{\Gamma,\Lambda} = \Gamma_{3,\Lambda};$$

$$\alpha^{\Phi}_{\Gamma,\Phi} = \Gamma_{3,\Phi}. \qquad \text{(VII.3)}$$

Thus the $\alpha^{q_k}_{\Gamma,q_l}$ coefficients are in turn functions of the Γ_{j,q_k} coefficients where it can be shown:

$$\Gamma_j = \Gamma_j\,[\,\ddot{\xi}_m^{\,i}(\dot{\omega}_j^{\,i}),\ \ddot{\zeta}_n^{\,i}(\dot{\omega}_j^{\,i})\,];$$

$$= \Gamma_{j,0} + \Gamma_{j,q_k}\,\ddot{q}_k; \qquad \text{(VII.4)}$$

where:

$\Gamma_{j,0}$ contains all terms having derivatives less than second order;

Γ_{j,q_k} = contributions of second order terms of the q_k degree of freedom to the Γ_j effect.

Consider the case of appendages in the x-y plane only:

$$\Gamma_{1,q_k} = \sum_\rho \{ \rho_\rho \ell_\rho^2 \sum_m \sum_n [s\phi_\rho \pi_3^\rho B_{mn,10} (\gamma_{q_k,m}^\rho \xi_n^\rho + \eta_{q_k,m}^\rho \zeta_n^\rho) - c\phi_\rho \ell_\rho B_{mn,1} (\gamma_{q_k,m}^\rho \zeta_n^\rho + \xi_m^\rho \eta_{q_k,n}^\rho) - c\phi_\rho \pi_3^\rho C_{m,1} \gamma_{q_k,m}^\rho + (\pi_2^\rho C_{m,1} + s\phi_\rho \ell_\rho C_{m,4}) \eta_{q_k,m}^\rho] \} ;$$

$$\Gamma_{2,q_k} = \sum_\rho \{ \rho_\rho \ell_\rho^2 \sum_m \sum_n [c\phi_\rho \pi_2^\rho B_{mn,10} (\gamma_{q_k,m}^\rho \xi_n^\rho + \eta_{q_k,m}^\rho \zeta_n^\rho) - s\phi_\rho \ell_\rho B_{mn,1} (\gamma_{q_k,m}^\rho \zeta_n^\rho + \xi_m^\rho \eta_{q_k,n}^\rho) - s\phi_\rho \pi_3^\rho C_{m,1} \gamma_{q_k,m}^\rho - (\pi_1^\rho C_{m,1} + c\phi_\rho \ell_\rho C_{m,4}) \eta_{q_k,m}^\rho] \} ;$$

$$\Gamma_{3,q_k} = \sum_\rho \{ \rho_\rho \ell_\rho^2 \sum_m \sum_n [- (s\phi_\rho \pi_1^\rho - c\phi_\rho \pi_2^\rho) B_{mn,10} (\gamma_{q_k,m}^\rho \xi_n^\rho + \eta_{q_k,m}^\rho \zeta_n^\rho) + ((c\phi_\rho \pi_1^\rho$$

$$+ s\varphi_\rho \pi_2^\rho) C_{m,1} + \ell_\rho C_{m,4}) \gamma^\rho_{q_k,m}] \} .$$

(VII.5)

Derivatives for the generalized coordinates of the appendage vibrations can be put in the form:

$$\{\ddot{\xi}^i\} = \{\gamma_0^i\} + \{\gamma_{q_k}^i\} \ddot{q}_k ;$$

$$\{\ddot{\zeta}^i\} = \{\eta_0^i\} + \{\eta_{q_k}^i\} \ddot{q}_k ; \qquad \text{(VII.6)}$$

where:

$\{\gamma_0^i\}, \{\eta_0^i\}$ contain all terms having derivatives less than second order ;

$\{\gamma_{q_k}^i\}, \{\eta_{q_k}^i\}$ contributions of second order terms of the q_k degree of freedom to the $\ddot{\xi}^i, \ddot{\zeta}^i$ derivatives for the i^{th} appendage.

In particular:

$$\{\gamma_{q_k}^i\} = -(\epsilon^i_{3,q_k} \hat{\pi}_2^i + \epsilon^i_{2,q_k} \hat{\pi}_3^i) [B_{10}] \{\xi^i\}$$

$$+ \epsilon^i_{1,q_k} [B_1] \{\zeta^i\} - \epsilon^i_{3,q_k} \{c_4\}$$

$$- (\epsilon^i_{3,q_k} \hat{\pi}_1^i - \epsilon^i_{1,q_k} \hat{\pi}_3^i) \{c_1\} ;$$

$$\{\eta^{i}_{q_k}\} = -(\epsilon^{i}_{3,q_k}\hat{\pi}^{i}_{2} + \epsilon^{i}_{2,q_k}\hat{\pi}^{i}_{3})[B_{10}]\{\gamma^{i}\} - \epsilon^{i}_{1,q_k}[B_1]\{\xi^{i}\} + \epsilon^{i}_{2,q_k}\{C_4\} + (\epsilon^{i}_{2,q_k}\hat{\pi}^{i}_{1} - \epsilon^{i}_{1,q_k}\hat{\pi}^{i}_{2})\{C_1\}. \quad \text{(VII.7)}$$

Equation (VII.7) makes use of the coefficients ϵ^{i}_{j,q_k} appearing in expressions for components of angular accelerations taken along local appendage axes. That is:

$$\dot{\omega}^{i}_{j} = \dot{\omega}^{i}_{j,0} + \epsilon^{i}_{j,q_k}\ddot{q}_k; \quad \text{(VII.8)}$$

where:

$\dot{\omega}^{i}_{j,0}$ contains terms having derivatives less than second order;

ϵ^{i}_{j,q_k} = contributions of second order terms of the q_k degree of freedom to $\dot{\omega}^{i}_{j}$, determined by numerical methods.

Substituting back from equation (VII.8) through to (VII.1) yields:

$$\ddot{q}_k = \alpha^{q_k}_{0} + \beta^{q_k}_{q_l}\ddot{q}_l; \quad \text{(VII.9)}$$

where:

$S^{q_k}_{q_l}$ includes all contributions of the q_l degree of freedom to the q_k equation.

This system of three equations in three unknowns ($\ddot{\Psi}$, $\ddot{\Lambda}$, $\ddot{\Phi}$) can be solved using routine methods of elimination and substitution from the theory of equations:

$$\ddot{\Psi} = (1/\mu_6)\,(\mu_1 \alpha_\Psi + \mu_4 \alpha_\Lambda + \mu_5 \alpha_\Phi);$$

$$\ddot{\Lambda} = (1/\mu_1)\,[\mu_2 \ddot{\Psi} + (1 - S^{\Phi}_{\Phi})\,\alpha_\Lambda + S^{\Lambda}_{\Phi}\,\alpha_\Phi];$$

$$\ddot{\Phi} = [1/(1 - S^{\Phi}_{\Phi})]\,(\alpha_\Phi + S^{\Phi}_{\Phi}\,\ddot{\Psi} + S^{\Phi}_{\Lambda}\,\ddot{\Lambda});$$

(VII.10)

with:

$$\theta_1 = 1./[c^2\Lambda\,(s^2\Phi\,I_{11} + c^2\Phi\,I_{22} - s2\Phi\,I_{12}) + s^2\Lambda\,I_{33} + s2\Lambda\,(s\Phi\,I_{13} + c\Phi\,I_{23})];$$

$$\theta_2 = c\Lambda\,[s\Phi\,c\Phi\,(I_{11} - I_{22}) - c2\Phi\,I_{12}] + s\Lambda\,(c\Phi\,I_{13} - s\Phi\,I_{23});$$

$$\theta_3 = - s\Lambda\, I_{33} - c\Lambda\,(s\Phi\, I_{13} + c\Phi\, I_{23});$$

$$\theta_4 = 1./(c^2\Phi\, I_{11} + s^2\Phi\, I_{22} + s2\Phi\, I_{12});$$

$$\theta_5 = s\Phi\, I_{23} - c\Phi\, I_{13};$$

$$\theta_6 = c\Lambda\,[s\Phi c\Phi\,(I_{11} - I_{22}) - c2\Phi\, I_{12}] - s\Lambda\,\theta_5;$$

$$\theta_7 = 1./I_{33}.$$

$$\theta_8 = - s\Lambda\, I_{33} - c\Lambda\,(s\Phi\, I_{13} + c\Phi\, I_{23});$$

$$\theta_9 = s\Phi\, I_{23} - c\Phi\, I_{13};$$

$$S_{\Psi}^{\Psi} = - \theta_1[c\Lambda(s\Phi\, \Gamma_{1,\Psi} - c\Phi\, \Gamma_{2,\Psi}) - s\Lambda\, \Gamma_{3,\Psi}];$$

$$S_{\Lambda}^{\Psi} = - \theta_1[c\Lambda\,(s\Phi\, \Gamma_{1,\Lambda} + c\Phi\, \Gamma_{2,\Lambda}) - s\Lambda\, \Gamma_{3,\Lambda} + \theta_2];$$

$$S_{\Phi}^{\Psi} = - \theta_1[c\Lambda\,(s\Phi\, \Gamma_{1,\Phi} + c\Phi\, \Gamma_{2,\Phi}) - s\Lambda\, \Gamma_{3,\Phi} + \theta_3];$$

$$S_{\Psi}^{\Lambda} = - \theta_4\,(c\Phi\, \Gamma_{1,\Psi} - s\Phi\, \Gamma_{2,\Psi} + \theta_6);$$

$$S_{\Lambda}^{\Lambda} = - \theta_4\,(c\Phi\, \Gamma_{1,\Lambda} - s\Phi\, \Gamma_{2,\Lambda});$$

$$S_{\Phi}^{\Lambda} = -\theta_4 \left(c\Phi\, \Gamma_{1,\Phi} - s\Phi\, \Gamma_{2,\Phi} + \theta_5 \right);$$

$$S_{\Psi}^{\Phi} = -\theta_7 \left(\Gamma_{3,\Psi} + \theta_8 \right);$$

$$S_{\Lambda}^{\Phi} = -\theta_7 \left(\Gamma_{3,\Lambda} + \theta_9 \right);$$

$$S_{\Phi}^{\Phi} = -\theta_7 \Gamma_{3,\Phi};$$

$$\mu_1 = -S_{\Lambda}^{\Phi} S_{\Phi}^{\Lambda} + (1 - S_{\Lambda}^{\Lambda})(1 - S_{\Phi}^{\Phi});$$

$$\mu_2 = S_{\Phi}^{\Lambda} S_{\Psi}^{\Phi} + S_{\Psi}^{\Lambda} (1 - S_{\Phi}^{\Phi});$$

$$\mu_3 = S_{\Lambda}^{\Phi} S_{\Psi}^{\Lambda} + S_{\Psi}^{\Phi} (1 - S_{\Lambda}^{\Lambda});$$

$$\mu_4 = S_{\Phi}^{\Psi} S_{\Lambda}^{\Phi} + S_{\Lambda}^{\Psi} (1 - S_{\Phi}^{\Phi});$$

$$\mu_5 = S_{\Lambda}^{\Psi} S_{\Phi}^{\Lambda} + S_{\Phi}^{\Psi} (1 - S_{\Lambda}^{\Lambda});$$

$$\mu_6 = (1 - S_{\Psi}^{\Psi}) \mu_1 + S_{\Lambda}^{\Psi} \mu_2 - S_{\Phi}^{\Psi} \mu_3 . \qquad \text{(VII.11)}$$

VII.2 Application

The accuracy, and hence the ultimate success, of a numerical integration depends on use of the most 'current' information available when computing derivatives. For that class of problems analyzed in the preceding section where the state vector is a hybrid construction of two main groups of coordinates - librational and flexible - the calculations are organized as shown in Figure VII-2.

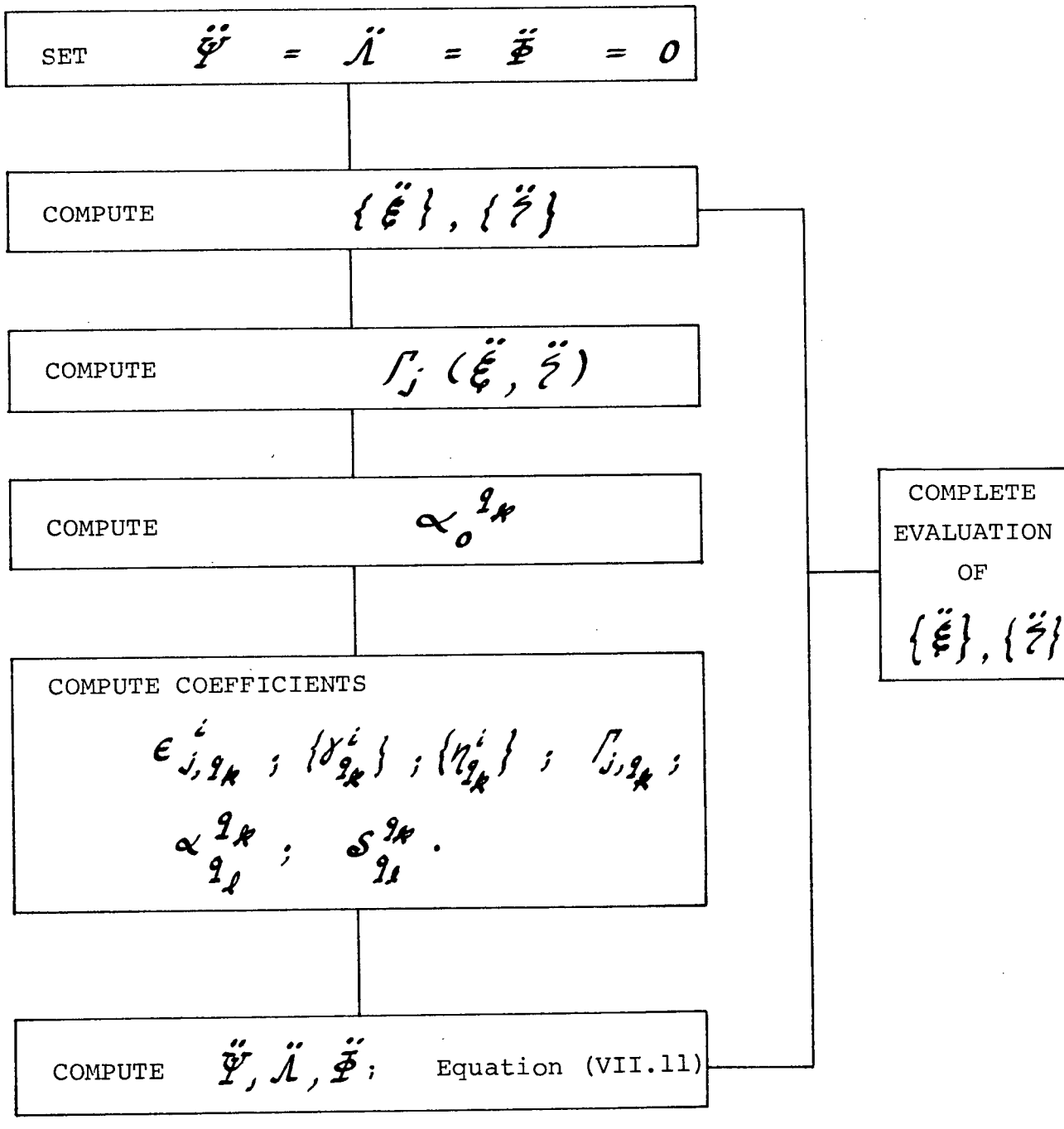

Figure VII-2 Computational procedure for updating system derivatives.